EDITE - ED 130

Doctorat ParisTech

T H È S E

pour obtenir le grade de docteur délivré par

TELECOM ParisTech

Spécialité « Communication et Electronique »

présentée et soutenue publiquement par

Yohan LEJOSNE

le 19 décembre 2014

Quelques Aspects des Réseaux Multi-Cellules Multi-Utilisateurs MIMO :

Délai, Conception d'Emetteur-Récepteur, Sélection d'Utilisateurs et Topologie

Directeur de thèse : **Dirk SLOCK**
Co-encadrement de la thèse : **Yi YUAN-WU**

Jury
M. Jean-Claude BELFIORE, Professeur, Telecom ParisTech   Président du jury
M. Constantinos PAPADIAS, Professeur, AIT   Rapporteur
M. Samson LASAULCE, Directeur de Recherche, CNRS, LSS Supelec   Rapporteur
M. Maxime GUILLAUD, Docteur, Huawei Technologies   Examinateur

TELECOM ParisTech
école de l'Institut Télécom - membre de ParisTech

T H È S E

DISSERTATION

In Partial Fulfillment of the Requirements

for the Degree of Doctor of Philosophy
from TELECOM ParisTech

Specialization: Communication and Electronics

Yohan Lejosne

Multi-Cell Multi-User MIMO Aspects: Delay, Transceiver Design, User Selection and Topology

Defended the 19th of December 2014 before a committee composed of:

Thesis Supervisor:		
Professor	Dirk Slock	EURECOM
Co-Supervisor:		
Doctor	Yi Yuan-Wu	Orange Labs
Reviewers:		
Professor	Constantinos Papadias	AIT
Director of Research	Samson Lasaulce	CNRS, LSS Supelec
Examiners:		
Professor	Jean-Claude Belfiore	Telecom ParisTech
Doctor	Maxime Guillaud	Huawei Technologies

THÈSE

présentée pour l'obtention du grade de
Docteur de TELECOM ParisTech

Spécialité: Communication et Electronique

Yohan Lejosne

Quelques Aspects des Réseaux Multi-Cellules Multi-Utilisateurs MIMO: Délai, Conception d'Emetteur-Récepteur, Sélection d'Utilisateurs et Topologie

Thèse soutenue le 19 décembre 2014 devant le jury composé de:

Directeur de Thèse:		
Professeur	Dirk Slock	EURECOM
Co-Encadrant:		
Docteur	Yi Yuan-Wu	Orange Labs
Rapporteurs:		
Professeur	Constantinos Papadias	AIT
Directeur de Recherche	Samson Lasaulce	CNRS, LSS Supelec
Examinateurs:		
Professeur	Jean-Claude Belfiore	Telecom ParisTech
Docteur	Maxime Guillaud	Huawei Technologies

Abstract

In order to meet ever-growing needs for capacity in wireless networks, transmission techniques and the system models used to study their performances have rapidly evolved. From single-user single-antenna point-to-point communications to modern multi-cell multi-antenna cellular networks there have been large advances in technology. Along the way, several assumptions are made in order to have either more realistic models, but also to allow simpler analysis. We analyze three aspects of actual networks and try to benefit from them when possible or conversely, to mitigate their negative impact. This sometimes corrects overly optimistic results, for instance when delay in the channel state information (CSI) acquisition is no longer neglected. However, this sometimes also corrects overly pessimistic results, for instance when in a broadcast channel (BC) the number of users is no longer limited to be equal to the number of transmit antennas or when partial connectivity is taken into account in cellular networks.

We first focus on the delay in the CSI acquisition because it greatly impairs the channel multiplexing gain if nothing is done to use the dead time during which the transmitters are not transmitting and do not yet have the CSI. We review and propose different schemes to use this dead time to improve the multiplexing gain in both the BC and the interference channel (IC). We evaluate the more relevant net multiplexing gain, taking into account the training and feedback overheads. Results are surprising because potential schemes to fight delay reveal to be burdened by impractical overheads in the BC. In the IC, an optimal scheme is proposed. It allows avoiding any loss of multiplexing gain even for significant feedback delay. Concerning the number of users, we propose a new criterion for the greedy user selection in a BC to benefit of the multi-user diversity, and two interference alignment schemes for the IC to benefit of having multiple users in each cell. Finally, partially connected cellular networks are considered and schemes to benefit from said partial connectivity to increase the multiplexing gain are proposed.

Résumé

Afin de répondre au besoin sans cesse croissant de capacité dans les réseaux sans fil, les techniques de transmission, et les modèles utilisés pour les étudier, ont évolués rapidement. De simples communications point à point avec une seule antenne nous sommes passé aux réseaux cellulaires de nos jours: de multiples cellules et de multiples antennes à l'émission et à la réception. Progressivement, plusieurs hypothèses ont été faites, soit afin d'avoir des modèles réalistes, mais aussi parfois pour permettre une analyse plus simple. Nous examinons et analysons l'impact de trois aspects des réseaux réels. Cela revient parfois à corriger des résultats trop optimistes, par exemple lorsque le délai dans l'acquisition des coefficients des canaux n'est plus négligé. Cela revient parfois à corriger des résultats trop pessimistes, par exemple, lorsque dans un canal de diffusion (BC) le nombre d'utilisateurs n'est plus limité au nombre d'antennes d'émission ou lorsque la connectivité partielle est prise en compte dans les réseaux cellulaires.

Plus précisément, dans cette thèse, nous nous concentrons sur le délai dans l'acquisition des coefficients des canaux par l'émetteur puisque sa prise en compte détériore grandement le gain de multiplexage du canal si rien n'est fait pour utiliser efficacement le temps mort au cours duquel les émetteurs ne transmettent pas et n'ont pas encore la connaissance du canal. Nous examinons et proposons des schémas de transmission pour utiliser efficacement ce temps mort afin d'améliorer le gain de multiplexage. Nous évaluons le gain de multiplexage net, plus pertinent, en tenant compte le temps passé à envoyer symboles d'apprentissage et à les renvoyer aux transmetteurs. Les résultats sont surprenant puisque les schémas contre le retard de connaissance de canal se révèle être impraticables à cause du cout du partage de la connaissance des canaux. Dans les réseaux multi-cellulaires, un schéma de transmission optimal est proposé et permet de n'avoir aucune perte de gain de multiplexage même en cas de retard important dans la connaissance de canal. En ce qui concerne le nombre d'utilisateurs, nous proposons un nouveau

critère pour la sélection des utilisateurs de les configurations à une seule cellule afin de bénéficier de la diversité multi-utilisateurs, et nous proposons deux schémas d'alignement d'interférence pour systèmes multi-cellulaires afin de bénéficier du fait qu'il y a généralement plusieurs utilisateurs dans chaque cellule. Enfin, les réseaux cellulaires partiellement connectés sont étudiés et des schémas bénéficiant de la connectivité partielle pour augmenter le gain de multiplexage sont proposés.

Acknowledgements

I would like to begin by thanking Yi Yuan-Wu and Dirk Slock who provided me with the exciting opportunity to carry out my PhD studies at Orange Labs and Eurecom.

I could not have completed this work without the precious guidance of my thesis director Dirk, whose numerous ideas were of invaluable help and whose quickness of mind never ceased to amaze me. This is also true of Yi who showed impressive dedication and zealously followed my progresses during these three years.

I would also like to thank everyone I met in Eurecom and in Orange Labs for they created a pleasant work environment, with special thanks to Paul who never tired of answering my questions and helped me work through the occasional issue.

I am truly indebted to all my friends for helping me going through these three intense years, with a special mention to Laurent who never defected on our weekly chilling hangouts.

I am also where I am thanks to my close family and their encouragement.

Last but not least, thank you to my wife, Leah, for your constant support, for believing in me and for making me a better person, one day at a time.

Contents

List of Figures

Acronyms

Here are the main acronyms used in this document. The meaning of an acronym is also indicated when it is first used.

AR	Autoregressive
BC	Broadcast Channel.
BS	Base Station.
BF	Beamforming.
CDF	Cumulative Density Function.
CSI	Channel State Information.
CSIT	Channel State Information at the Transmitter.
CSIR	Channel State Information at the Receiver.
DPC	Dirty Paper Coding.
e.g.	Exempli gratia.
FDD	Frequency Division Duplexing.
FRoI	Finite Rate of InnovationDivision Duplexing.
i.i.d.	Independent and identically distributed.
IA	Interference Alignment.
IBC	Interfering Broadcast Channel.
IC	Interference Channel.
LOS	Line Of Sight.
MIMO	multiple-Input multiple-Output.
MISO	multiple-Input single-Output.
MU-MIMO	Multi User multiple-Input multiple-Output.
MUI	Multi User Interference.
OCI	Other Cell Interference.
RX	Receiver(s).

SIMO	single-Input multiple-Output.
SNR	Signal-to-Noise Ratio.
SISO	Single-Input Single-Output.
STIA	Space-Time Interference Alignment
TDD	Time Division Duplex.
TDMA	Time Division Multiple Access.
TX	Transmitter(s).
ZF	Zero Forcing.
ZFBF	Zero Forcing BeamForming.
ZFDPC	Zero Forcing Dirty Paper Coding.

Chapter 1

Résumé Long [FR]

1.1 Motivation et Modèles

1.1.1 Introduction

Les communications sans fil sont devenues primordiales dans beaucoup d'aspects de nos vies. Que ce avec soit un utilisateur actif sur un ordinateur portable, sur une tablette ou sur un téléphone ou pour des usages automatiques comme le relevé de compteurs, les dimensions des réseaux sans fil ont augmenté drastiquement, à la fois par le nombre d'utilisateurs servis et par le volume de données transporté. Plus précisément, [1] prévoit une augmentation du trafic mobile mondial par un facteur 11 entre 2013 et 2018 et le nombre d'appareils mobiles connectés devrait atteindre 10 milliard en 2018. Avec l'augmentation exponentielle du trafic mobile les interférence sont devenues le problème limitant les performances des réseaux mobiles puisque le media sans fil est par essence partagé. Le méthodes d'orthogonalisation, que ce soit en temps ou en fréquence sont pratique et efficaces pour éviter les interférences mais diminuent drastiquement l'efficacité spectrale.

Il y a eu beaucoup de recherches, qui se sont révélées productives et variées dans le mais d'améliorer l'efficacité spectrale [2–4]. De nombreuse techniques permettent d'augmenter le gain de multiplexage dans les canaux a multiples récepteurs (broadcast channel, BC) et les canaux d'interférence à multiple émetteur et multiple récepteurs (interférence channel, IC). Dans un BC, les interférences proviennent toujours de la cellule et sont dues à la transmission de plusieurs flux de données qui sont destinées à plusieurs récepteurs par une seule station de base. Ce genre d'interférence peut être évité par de simples techniques comme le précodage forçant à zéro (zero forcing, ZF) ou des techniques plus complexes comme le codage papier sale (dirty paper coding, DPC) [5]. Beaucoup d'autres schémas de transmissions ont été proposés, par exemples [6–15]. Dans un IC, la situation

est plus compliquées car les interférences reçues par chaque récepteur viennent de cellules différentes. Néanmoins, différentes techniques, appelées alignement d'interférences (interference alignment, IA) peuvent être utilisées pour aligner les interférences dans un sous-espace de dimension réduite au niveau des différentes récepteurs. Certaines sont plus théoriques [4, 16, 17], d'autre sont plus pratiques [18–20]. Ces schémas alignent les interférences dans un sous-espace de manière qu'il reste suffisamment de dimension sans interférences pour le signal utile à chaque récepteur.

Cependant, la plupart de ces techniques reposent sur des hypothèses simplistes. Par exemple, en général dans un BC, le nombre d'utilisateurs est supposé être égal au nombre d'antennes de transmission. De la même manière, dans des configurations avec plusieurs cellules interférentes, ne considérer qu'il y a qu'un seul utilisateur par cellule se révèle être une grande simplification par rapport au modèle plus général qui comprend plusieurs BC qui s'interfèrent mutuellement (interfering broadcast channels, IBC). Pour la plupart des applications, le modèle IBS est plus adéquat que le IC et englobent également le modèle IC. La simplification qui fait une grande différence est que la plupart des techniques de transmissions ont besoin que le ou les émetteurs (et parfois les récepteurs) aient accès presque instantanément à une connaissance presque parfaite du canal de transmission (channel state information at the transmetteur, CSIT et channel state information at the récepteur, CSIR). En pratique, c'est surtout le CSIT qui pose problème, puisqu'il nécessite de faire du feedback ce qui cause irrémédiablement un délai qui peut être substantiel, et donc diminue les considérablement les performances. Se posent donc deux questions. Comment réduire le délai d'acquisition des CSIT. Comment mettre à profit les CSIT retardées (delayed CSIT, DCSIT), en d'autres termes, que faire pendant que l'acquisition des CSIT n'est pas terminée.

Dans cette thèse nous nous intéressons à une troisième différence entre réseaux théoriques et réseaux pratiques, la réseaux mobiles partiellement connecté. La connectivité partielle signifie que l'on prend en compte le fait que certain liens d'interférences dans un IBC sont suffisamment faibles pour être négligés. Si certaines solutions pour les IBC totalement connecté fonctionnent également sur les IBC partialement connecté, il se peut qu'elle ne bénéficie pas entièrement de la connectivité partielle si rien n'est fait pour. En effet, le gain de multiplexage doit augmenter avec le nombre de lien d'interférence qui sont négligés.

1.1.2 Résumé des Contributions

Cette thèse est divisé en deux parties. Dans la première partie, nous étudions ce qu'il est possible de faire quand il y a *plus* d'utilisateurs. Avoir plus d'utilisateurs dans un IC ou dans un IBC sont des choses très différentes. Dans un BC, avoir plus

d'utilisateurs que d'antennes d'émission n'augmente pas le gain de multiplexage donc, *plus* d'utilisateurs dans un BC, signifie plus d'utilisateurs que d'antennes d'émission. C'est intéressant de voir ce qu'il y a à faire avec plus d'utilisateurs que d'antennes d'émission car le nombre d'antennes d'émissions est fixé à la construction alors que le nombre d'utilisateurs évolue dans le temps et peut très bien être bien plus grand que le nombre d'antennes d'émission, d'autant plus que le nombre d'appareils mobiles connectés augmente considérablement chaque année [1].

Dans le Chapitre 3, nous proposons un schéma de sélection d'utilisateurs (greedy utilisateur selection, GUS) pour le MISO BC et pour le MIMO BC afin de bénéficier de la fameuse diversité multi-utilisateur et améliorer le débit total. Ces résultats sont publiés dans:

- Y. Lejosne, D. Slock, et Y. Yuan-Wu, "User Selection in MIMO BC," *in Proc. EUSIPCO*, Bucharest, Romania, Aug. 2012.

- Y. Lejosne, D. Slock, et Y. Yuan-Wu, "On Greedy Stream Selection in MIMO BC," *in Proc. WCNC*, Paris, France, Apr. 2012.

Dans un IC au contraire, avoir plus d'un utilisateur par cellule peut augmenter le gain de multiplexage; cela transforme le IC en IBC et dans un IBC, le gain de multiplexage augmente avec le nombre d'utilisateurs. Dans le Chapitre 4, nous proposons deux schémas pour le IBC afin de transmettre plus d'un utilisateur dans chaque cellule à la fois pour augmenter le gain de multiplexage. Les résultats concernant le premier algorithme sont publiés dans:

- Y. Lejosne, D. Slock, et Y. Yuan-Wu, "Ergodic Interference Alignment for the SIMO/MIMO Interference Channel, *in Proc. ICASSP*," Firenze, Italy, May 2014.

Le second algorithme a été breveté et les résultats soumis pour publication dans:

- Y. Lejosne, Y. Yuan-Wu, and D. Slock, "Procédé itératif d'évaluation de filtres numériques destinés à être utilisés dans un système de communication," FR Patent 1 462 878, Dec. 12, 2014.

- Y. Lejosne, Y. Yuan-Wu et D. Slock, "Interference Alignment Scheme for Fully or Partially Connected Interfering Broadcast Channels with Finite Symbol Extension," *submitted for publication in IEEE Transactions on Wireless Communications*.

Ensuite, dans le Chapitre 5, nous nous concentrons sur les IBC partiellement connectés car il est raisonnable de supposer que dans certains cas, seulement certains liens d'interférences doivent être pris en compte. Nous proposons un nouvel

algorithme pour certaines configurations pour lesquelles nous séparons d'abord le réseau en deux sous-réseaux indépendants. Nous évaluons également les performances d'un des algorithmes pour les IBC présenté dans le Chapitre 4 dans ces configurations. Les résultats sur la méthode de séparation on été breveté et soumis pour publication dans:

- Y. Lejosne, Y. Yuan-Wu et D. Slock, "Stratégie de transmission à deux niveaux pour certains réseaux de cellules interférées et servant chacun des utilisateurs asymétriques et pour certains réseaux hétérogènes," FR Patent FR 1 456 224, Jun. 30, 2014.

- Y. Lejosne, Y. Yuan-Wu et D. Slock, "A two-level transmission strategy for certain asymmetric interfering broadcast channels and heterogeneous networks," *submitted for publication in IEEE Transactions on Vehicular Technology*.

Dans la seconde partie de cette thèse nous nous intéressons aux DCSIT. Il faut toujours prendre du temps et des efforts pour permettre aux transmetteur de recevoir les CSI: envoie de séquence d'apprentissage et feedback pour les systèmes à duplex par séparation fréquentielle (frequency division duplexing, FDD). Afin d'évaluer les pertes dues aux DCSIT, on peut commencer par considérer un délai abstrait dans l'acquisition des CSI et tenter de limiter les pertes en terme de gain de multiplexage. Ensuite, une approche plus réaliste est de prendre en compte non seulement les pertes de gain de multiplexage dues au délai mais aussi les surcoût en transmission nécessaires afin d'obtenir une métrique plus équitable: le *gain de multiplexage net*.

Dans le chapitre 6, différents modèles de canal sont passée en revue et une modèle général est proposé. Dans ce modèle, un nouveau schéma de feedback est proposé pour être robuste au délai au prix d'une fréquence d'apprentissage et de feedback plus importante. Ces résultats sont publiés dans:

- Y. Lejosne, D. Slock, et Y. Yuan-Wu, "Finite Rate of Innovation Channel Models and DoF of MIMO Multi-User Systems with Delayed CSIT Feedback," *in Proc. ITA*, San Diego, CA, USA, Feb. 2013.

Ensuite, dans le Chapitre 7, nous proposons et évaluons le gain de multiplexage net de différent schéma de transmission. Il y a toujours une perte de gain de multiplexage due au délai dans l'acquisition des CSIT dans le BC et des techniques qui semblaient prometteuses en terme de gain de multiplexage se révèlent moins intéressantes quand tous les coûts sont pris en compte. Ces résultats sont publiés dans:

- Y. Lejosne, D. Slock, et Y. Yuan-Wu, "Foresighted Delayed CSIT Feedback for Finite Rate of Innovation Channel Models and Attainable netDoFs of the MIMO Interference Channel," *in Proc. WD*, Valencia, Spain, Nov. 2013.

- Y. Lejosne, D. Slock, et Y. Yuan-Wu, "NetDoFs of the MISO Broadcast Channel with Delayed CSIT Feedback for Finite Rate of Innovation Channel Models," *in Proc. ISIT*, Istanbul, Turkey, Jul. 2013.

- Y. Lejosne, D. Slock, et Y. Yuan-Wu, "Net Degrees of Freedom of Recent Schemes for the MISO BC with Delayed CSIT and Finite Coherence Time," *in Proc. WCNC*, Shanghai, China, Apr. 2013.

- Y. Lejosne, D. Slock, et Y. Yuan-Wu, "Degrees of Freedom in the MISO BC with Delayed CSIT and Finite Coherence Time: Optimization of the Number of User," *in Proc. NetGCooP*, Avignon, France, Nov. 2012.

- Y. Lejosne, D. Slock, et Y. Yuan-Wu, "Degrees of Freedom in the MISO BC with Delayed CSIT and Finite Coherence Time: a Simple Optimal Scheme," *in Proc. ICSPCC*, Hong Kong, China, Aug. 2012.

Dans le Chapitre 8, nous démontrons que le IC est plus robuste aux DCSIT que le BC en proposant un schéma de transmission qui résiste même à de longs délais, sans aucune perte de de gain de multiplexage et ne nécessitant aucun coût supplémentaire. Nous calculons également les gains de multiplexage de différents schémas de transmission pour le IC. Ces résultats sont publiés dans:

- Y. Lejosne, D. Slock, et Y. Yuan-Wu, "Achieving Full Sum DoF in the SISCO Interference Channel with Feedback Delay," *IEEE Communications Letters*, vol.18, no.7, July 2014.

- Y. Lejosne, D. Slock, et Y. Yuan-Wu, "Net Degrees of Freedom of Decomposition Schemes for the MIMO IC with Delayed CSIT," *in Proc. ISIT*, Honolulu, HI, USA Jun. 2014.

- Y. Lejosne, D. Slock, et Y. Yuan-Wu, "Space Time Interference Alignment Scheme for the MISO BC and IC with Delayed CSIT and Finite Coherence Time," *in Proc. ICASSP*, Vancouver, Canada, May 2013.

Dans d'autres contributions, non présentées dans cette thèse, on essaie de réduire les CSIT nécessaires afin de réduire le feedback. Les résultats sur ce sujet sont publiés dans:

- Y. Lejosne, M. Bashar, D. Slock, et Y. Yuan-Wu, "From MU massive MISO to pathwise MU massive MIMO," *in Proc. SPAWC*, Toronto, Canada, Jun. 2014.

- Y. Lejosne, M. Bashar, D. Slock, et Y. Yuan-Wu, "Decoupled, rank reduced, massive and frequency-selective aspects in MIMO interfering broadcast channels," *in Proc. ISCCSP*, Athens, Greece, May 2014.

- Y. Lejosne, M. Bashar, D. Slock, et Y. Yuan-Wu, "MIMO interfering broadcast channels based on Local CSIT," *in Proc. EW*, Barcelona, Spain May 2014.

- M. Bashar, Y. Lejosne, D. Slock, et Y. Yuan-Wu, "MIMO Broadcast Channels with Gaussian CSIT and Application to Location based CSIT," *in Proc. ITA*, San Diego, CA, USA Feb. 2014.

1.1.3 Modèle du Système et Notations

Dans cette thèse, nous allons considérer différentes configurations système: BC, IC et IBC. Commençons par le IBC car c'est le modèle plus général et que les deux autres configurations considérées peuvent en fait être vues comme des cas spéciaux d'un IBC.

Un IBC général a G cellules avec un seul émetteur dans chaque cellule et K_i récepteurs dans la cellule i. Le transmetteur dans la cellule j (transmetteur j) a M_j antennes, le $k$ème récepteur dans la cellule i (récepteur i_k) a N_{i_k} antennes.

Un exemple de IBC avec $G = 3$ et $K_1 = K_2 = K_3 = 2$ est donnée dans Fig. 1.1. Les lignes pointillées représentent les liens croisés ne supportant que des interférences et lignes pleines représentent les liens supportant les données.

La réalisation de canal entre le transmetteur j et le récepteur i_k au temps t est notée $\mathbf{H}_{i_k j}(t)$. quand T extension de symboles sont considérées, la matrice de canal résultante de dimension $TN_{i_k} \times TM_j$ entre BS $j \in [1,G]$ et utilisateur i_k, $(i,k) \in [1,G] \times [1,K]$

$$
\mathbf{H}_{i_k j}[N] = \begin{bmatrix} \mathbf{H}_{i_k j}(NT+1) & 0 & \cdots & 0 \\ 0 & \mathbf{H}_{i_k j}(NT+2) & \cdots & 0 \\ \vdots & \vdots & \ddots & \vdots \\ 0 & 0 & \cdots & \mathbf{H}_{i_k j}((N+1)T) \end{bmatrix} \quad (1.1)
$$

est diagonale diagonale par bloc.

Quand aucune extension n'est considérée ($T = 1$), ou si aucune confusion n'est possible, l'indice temporel sera omis.

A partir de ce modèle, on peut considéré qu'un BC est un cas particulier avec $G = 1$ et un IC est un cas particulier avec $K = 1$. quand une seule cellule est considérée, i.e., un BC, les notations seront simplifiées en $\mathbf{H}_k(t) = \mathbf{H}_{i_k 1}(t)$.
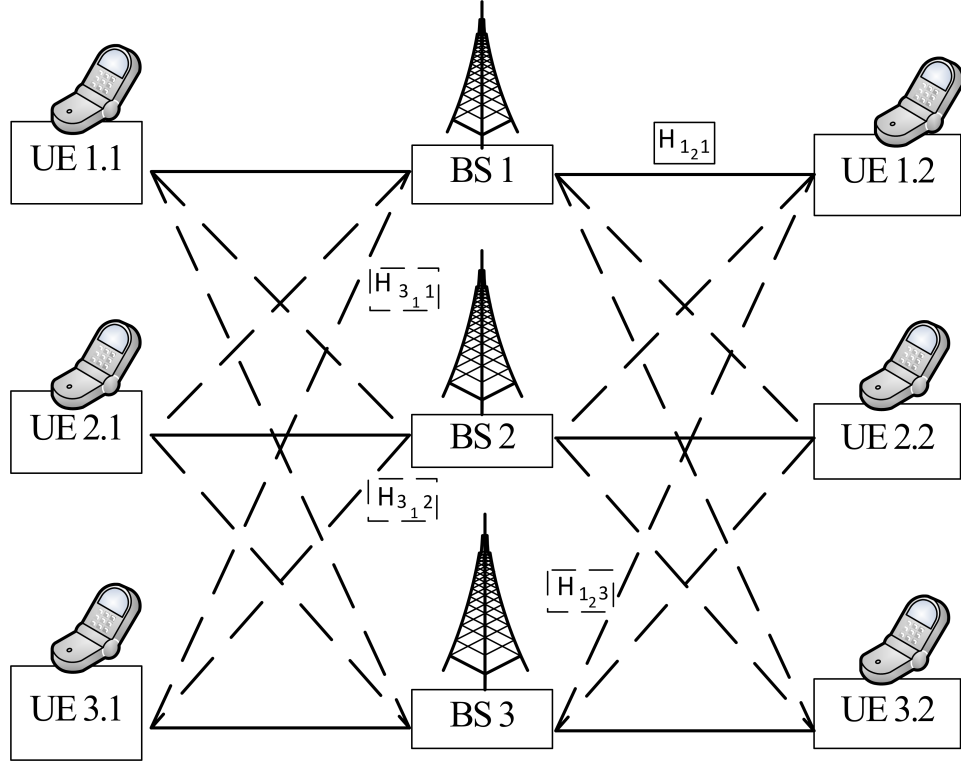
Figure 1.1: Exemple IBC avec $G = 3$ et $K_1 = K_2 = K_3 = 2$.

quand un seul utilisateur par cellule est considéré, i.e., un IC, les notations seront simplifiées en $\mathbf{H}_{ij}(t) = \mathbf{H}_{i_1j}(t)$.

Des exemples de BC avec $K = 3$ et de IC avec $G = 3$ sont donnés dans Fig. 1.2. Les lignes pointillées représentent les liens croisés ne supportant que des interférences et lignes pleines représentent les liens supportant les données.

Les filtres linéaires utilisés aux transmetteurs et aux récepteurs seront respectivement dénotés $\mathbf{V}_j$ et $\mathbf{U}_{i_k}$. Le signal reçu à l'utilisateur i_k est une combinaison linéaire bruité combinaison des entrées des différents transmetteurs

$$\mathbf{y}_{i_k} = \sum_{j=1}^{G} \mathbf{H}_{i_kj}\mathbf{V}_j\mathbf{x}_j + \mathbf{n}_j \tag{1.2}$$

où

$$\mathbf{V}_j = [\mathbf{V}_{j_1}, \mathbf{V}_{j_2}, \cdots, \mathbf{V}_{j_K}] \tag{1.3}$$

est la matrice de précodage du transmetteur j, et est composée de la concaténation

7

(a) Exemple de BC avec $K = 3$. (b) Exemple de IC avec $G = 3$.
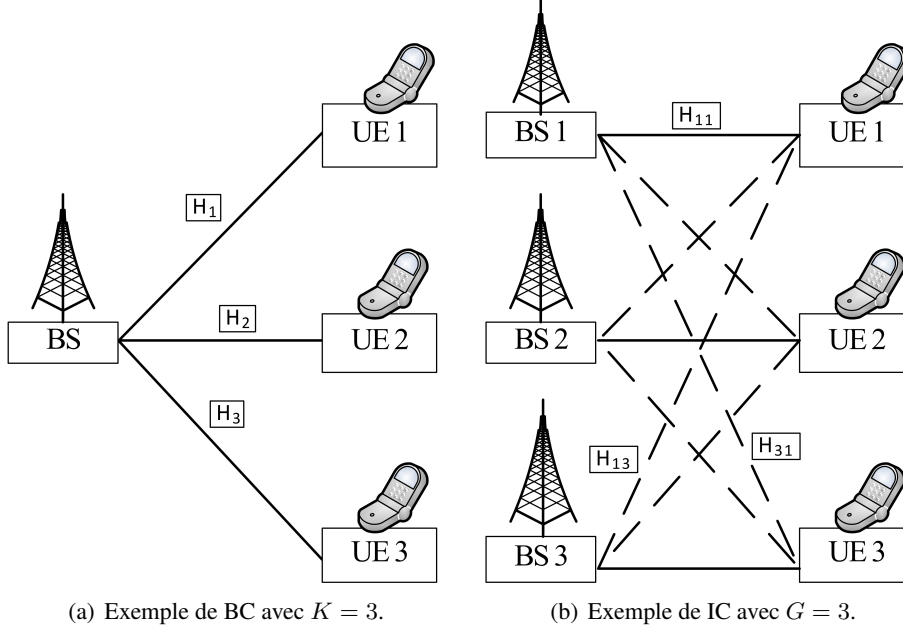
Figure 1.2: Exemples de BC et IC.

des matrices de précodages pour chacun de ses K_i utilisateurs, $\mathbf{x}_j$ est le symbole transmis et $\mathbf{n}_j$ le bruit blanc gaussien additif de variance $\sigma^2 = 1$ au récepteur.

Le signal est décodé au récepteur i_k par le filtre d réception $\mathbf{U}_{i_k}$, ce qui donne

$$\mathbf{z}_{i_k} = \mathbf{U}_{i_k}\mathbf{y}_{i_k} = \sum_{j=1}^{G} \mathbf{U}_{i_k}\mathbf{H}_{i_k j}\mathbf{V}_j\mathbf{x}_j + \mathbf{U}_{i_k}\mathbf{n}_j. \tag{1.4}$$

Le débit total atteint par l'ensemble des utilisateurs du système est une métrique sensée. Si on considère des symboles gaussiens, i.e., des symboles qui sont i.i.d. selon $\mathcal{CN}(0,1)$, alors le débit de l'utilisateur i est

$$R_i = \log \det(\mathbf{I}_{N_i} + (\sigma^2\mathbf{I}_{N_i} + \mathbf{Q}_{i_k}^{int})^{-1}\mathbf{Q}_{i_k}^{dir}) \tag{1.5}$$

où

$$\mathbf{Q}_{i_k}^{int} = \sum_{i \neq j \text{ ou } k \neq l} \mathbf{H}_{i_k j}\mathbf{V}_{j_l}\mathbf{V}_{j_l}^{H}\mathbf{H}_{i_k j}^{H} \tag{1.6}$$

est la matrice de covariance des interférences, *à la fois* des interférences des autres cellules (autres cellule interférence, OCI), i.e., $i \neq j$ *et* des interférences multi-

utilisateur (multi-utilisateur interférence, MUI) i.e., $i = j, k \neq l$ et

$$\mathbf{Q}_{i_k i}^{dir} = \mathbf{H}_{i_k i} \mathbf{V}_{i_k} \mathbf{V}_{i_k}^{H} \mathbf{H}_{i_k i}^{H} \tag{1.7}$$

est la matrice de covariance du signal désiré.

Le débit total est alors

$$\text{SR} = \sum_{i=1}^{K} R_i. \tag{1.8}$$

Dans certains cas, les résultats sont seulement obtenus en termes de degré de liberté (degrees of freedom, DoF), et sont valides à haut rapport signal à bruit (signal-to-noise ratio, SNR). La métrique DoF, qui est un autre nom du gain de multiplexage est le terme prelog du débit total, c'est dont la pente du débit total quand elle est tracée en fonction du logarithme du SNR. Avec $R_j(P)$ comme débit co-atteignable pour l'utilisateur j avec une puissance d'émission P, le DoF atteignable par l'utilisateur j est,

$$d_i = \lim_{P \to \infty} \frac{R_i(P)}{\log_2(P)} \tag{1.9}$$

et le DoF total du système est alors

$$\text{DoF} = \sum_{i=1}^{K} d_i. \tag{1.10}$$

quand on s'intéresse uniquement aux DoF, on peut omettre le bruit gaussien dans un souci de clarté.

Dans la seconde partie, on utilisera également le net DoF comme métrique, c'est à dire, le DoF qui reste après avoir pris en compte les séquences d'apprentissage et le feedback. Afin de prendre en compte les coût de feedback, on définit le volume de feedback. Soit $F(P)$ le débit de feedback total d'un système avec puissance d'émission P alors

$$\text{DoF}_{FB} = \lim_{P \to \infty} \frac{F(P)}{\log_2(P)}. \tag{1.11}$$

1.2 Plus d'Utilisateurs

1.2.1 GUS

Nous considérons ici un BC, ou en d'autres termes, la liaison descendante multi-utilisateur (MU) dans une cellule avec une seule station de base et des terminaux

mobile possiblement équipé de multiple antennes. S'il y a suffisamment d'utilisateurs, le fait d'avoir des récepteurs avec de multiples antennes n'améliore pas le gain de multiplexage. Cependant, la sélection d'utilisateurs apporte non seulement de la diversité multi-utilisateur mais également un diminution de la suboptimalité des simples techniques BF comparé à l'optimal DPC.

La sélection d'utilisateur par recherche exhaustive peut-être simplifiée en des approches que l'on qualifie de *greedy*, dans lesquelles des utilisateurs sont ajoutés à la sélection un par un. Nous proposons un critère pour la sélection d'utilisateurs MISO BF-style qui maximise une approximation du gain de débit attendu par l'ajout d'un utilisateur à la sélection actuelle.

La principale contribution sur ce sujet est la dérivation d'une approximation du gain de débit attendu par l'ajout d'un utilisateur à la sélection actuelle. Une extension pour le MIMO BC ainsi que le design des filtres de réception sont également proposés.

Nous montrons que la contribution du flux *i* peut-être approximée par

$$
\begin{aligned}
\|P^{\perp}_{h_{k_{1:i-1}}} h_{k_i}\|^2 \prod_{j=1}^{i-1} \sin^2 \phi_{ij} & \approx & \|P^{\perp}_{h_{k_{1:i-1}}} h_{k_i}\|^2 \sin^2 \phi_i \\
& = & \|h_{k_i}\|^2 \sin^4 \phi_i \\
& = & \|P^{\perp}_{h_{k_{1:i-1}}} h_{k_i}\|^4 / \|h_{k_i}\|^2 .
\end{aligned}
\tag{1.12}
$$

Le gain DPC est $\|P^{\perp}_{h_{k_{1:i-1}}} h_{k_i}\|^2 = \|h_{k_i}\|^2 \sin^2 \phi_i$ ce qui représente un certain compromis entre $\|h_{k_i}\|^2$ et $\cos^2 \phi_i$.

Dans le cas BF, $\|h_{k_i}\|^2 \sin^4 \phi_i$ conduit à un compromis similaire, mais avec une importance de l'orthogonalité plus importante.

L'équation (1.12) n'est pas exacte quand elle est évaluée pour un nombre arbitraire de canaux candidats h_k. Cependant, Pour un nombre de candidats K suffisant, qui conduit à des choix assez orthogonaux, l'approximation devient arbitrairement précise.

Cette analyse montre également que lorsque les canaux sont suffisamment orthogonaux, comme lorsqu'ils ont été choisis par un procédé de sélection d'utilisateur, alors la perte du au BF par rapport à DPC est égale à la perte de DPC par rapport au cas de canaux qui seraient réellement orthogonaux car $\log \sin^4 \phi_i = 2 \log \sin^2 \phi_i$.

Critère MISO BF-Style GUS

A l'étape *i* on utilise (1.12) pour sélectionner l'utilisateur qui donne le plus grand gain de débit (approximé)

$$
k_i = \arg \max_k \|P^{\perp}_{h_{k_{1:i-1}}} h_k\|^4 / \|h_k\|^2 .
\tag{1.13}
$$

Le premier utilisateur sélectionné, pour $i = 1$, est simplement l'utilisateur dont le canal a la plus grande norme. Contrairement au cas ZF-DPC, la sélection d'utilisateur optimale pour ZF-BF peut être de cardinalité inférieure à M. C'est pourquoi lorsque l'on sélectionne un utilisateur avec le critère (1.13), on ne l'ajoute à la sélection seulement si cela ne dégrade pas le débit total et le cas échéant la procédure de sélection est arrêtée.

1.2.2 IBC

lorsque l'on considère des configurations multi-cellule il n'y a jamais *trop* d'utilisateurs, en effet le DoF augmente avec le nombre d'utilisateurs.

Les schémas de transmission pour le IC peuvent être divisé en deux catégories en fonction de la borne qu'ils essaient d'approcher. La première catégorie vise à approcher la borne supérieure appelée borne DoF propre [21], qui n'est pas toujours atteignable, en utilisant la dimension spatiale (multi antenne), ou des des extensions de symboles *finies* en temps ou en fréquence. La deuxième catégorie vise la borne dite de *décomposition*, qui elle est toujours atteignable [4].

La techniques IA asymptotique est proposée dans [4] et atteint la borne de décomposition, $\frac{G}{2}$ DoF dans un SISO IC avec G utilisateurs dont les canaux varient dans le temps. En utilisant des extensions de symboles, le schéma aligne partiellement les interférences au récepteur de manière que plus de dimensions soit disponible pour la transmission de donnée sans interférences. En utilisant des extensions de symboles de plus en plus longues, la partie non alignée des symboles devient négligeable et on peut approcher le DoF optimal de $\frac{G}{2}$. L'extension de cette technique aux MIMO IC carrés est triviale. Le cas général du MIMO IC est étudié dans [22] et les auteurs prouvent que l'on peut atteindre $G\frac{MN}{M+N}$ DoF, ce qui croit également linéairement avec le nombre de cellules G. La borne de décomposition est directement transposable aux IBC symétriques avec K utilisateurs par cellule et devient $GK\frac{MN}{M+KN}$. On montre facilement qu'elle est atteignable puisque le schéma IA IC ne nécessite aucune coopération aux niveaux des antennes et est donc directement applicable dans les IBC [23].

La borne propre n'est pas toujours atteignable et elle est obtenue en comptant le nombre d'équations à satisfaire et le nombre de variables disponibles. Dans l'IC, cette borne vaut $G\frac{M+N}{G+1}$ et $GK\frac{M+N}{GK+1}$ dans un IBC symétrique [24].

Utiliser des extensions de symboles permet d'atteindre des DoF décimaux DoF mais ne change pas la borne propre. En effet, si on considère la borne propre avec T extensions, le nombre de variables devient $GK[d(TM - d) + d(TN - d)]$ et le nombre de contraintes ZF reste $GK(GK - 1)d^2$, et la borne propre est donc inchangée $\frac{d}{T} \leq \frac{M+N}{GK+1}$. Cependant, lorsque l'on considère des extensions de symboles, la borne propre n'est plus une borne supérieure sur le DoF puisque le

11

canal est maintenant structuré, en effet, les matrices de canaux sont diagonales ou diagonales par blocs ce qui fait que le canal n'est plus générique, alors que c'était une hypothèse nécessaire pour faire de la borne propre une borne supérieure sur le DoF.

Avec la borne propre, le DoF par cellule diminue avec G alors qu'il est constant dans la borne de décomposition. C'est pourquoi, si les deux bornes se croisent, la borne propre est optimale pour les petits G. quand la borne propre est plus grande, le DoF du IC ou IBC est entre la borne de décomposition et la borne propre [23,25] sans extension de symbole. Cependant, quand la borne de décomposition est plus grande, le DoF du canal est connu puisque cette borne est toujours atteignable avec IA ergodique [16], IA réel [17] ou IA asymptotique avec extension de symbole infinie [4].

Nous proposons en premier un schéma de décomposition. Dans la Section 4.2, nous étendons le schéma d'IA ergodique aux MIMO IC et aux MIMO IBC. L'IA ergodique est un outil conceptuellement simplet mais très puissant qui non seulement atteint le DoF optimal de $G/2$ DoF du SISO IC avec G utilisateurs, mais aussi, permet à chaque user d'atteindre au moins la moitié du débit qu'il aurait s'il n'y avait aucune interférence à n'importe quel SNR. En considérant des ensembles de messages plus généraux, Nazer et al. ont aussi couvert le cas MISO. Nous considérons d'abord un SIMO IC et étendons la technique d'IA ergodique à cette configuration avec N antennes de réception. Notre schéma atteint $GN/(N+1)$, ce qui est le DoF atteint par l'IA asymptotique et aussi le DoF du canal quand $G > N$. De plus, cette technique est invariante par redimensionnement spatial (multiplication du nombre d'antennes à l'émission et à la réception). En combinant les résultats MISO et SIMO, on peut maintenant couvrir le cas MIMO avec M antennes d'émission pour les cas où soit M/N soit N/M est un entier R, et on atteint DoF $= \min(M,N)GR/(R+1)$, ce qui est optimal pour $G > R$.

Nous proposons un second schéma qui vise a atteindre la borne propre. Dans la Section 4.3, nous étendons le schéma IA pour canaux structurés (avec symbole extension) aux MIMO IBC. De nombreuses techniques permettent d'améliorer le gain de multiplexage des réseaux sans fils en présence d'interférences. Si certaines de ces techniques sont suffisamment détaillées pour construire les filtres d'émission et de réception, la plupart des résultats ne concernent que le gain de multiplexage dans le IC et ne sont pas constructifs. De plus, pour atteindre le gain de multiplexage optimal il faut en général utiliser des extensions de symbole, ce qui donne une structure spéciale aux matrices de canal. Des progrès ont été fait pour le IC avec des extensions de symboles finies mais peu de résultats sont disponibles pour le IBC, alors que c'est en général un modèle plus adéquat pour représenter les réseaux mobiles actuels. Nous proposons un algorithme d'IA spécialement conçu

pour les IBC avec extension de symbole. Avoir plus d'un utilisateur par cellule complique la transmission mais permet d'augmenter le gain de multiplexage. Des simulations numériques sont également effectuées et confirment que l'algorithme proposé atteint les DoF ciblés.

1.2.3 IBC Partiellement Connectés

Les deux catégories de techniques IA, IA asymptotique et IA linéaire peuvent être adaptés pour être utilisé dans les réseaux partiellement connectés IBC mais pas de manière optimale. Par exemple, l'IA asymptotique ne nécessite pas de traitement joint aux antennes, donc les techniques d'IA asymptotique peuvent être directement utilisées dans les IBC [22]; cependant, il n'est pas simple de prendre en compte et bénéficier de la connectivité partielle. De plus, l'IA asymptotique nécessite de longues extensions de symboles, qui augmentent exponentiellement avec le nombre d'antennes, afin d'atteindre des gains de multiplexage décents. Néanmoins, des efforts ont étés fait pour trouver des solutions d'IA linéaires qui bénéficient de la connectivité partielle [26,27]. Cependant, elle sont souvent basée sur une recherche heuristique d'un sous-système pour lequel une solution d'IA linéaire simple peut être déployée.

On s'intéresse particulièrement aux IBC qui peuvent apparaître avec les utilisateurs en bord de cellule. Pour être précis, on considère des BC qui s'interfèrent avec 2 antennes à l'émetteur et 2 utilisateurs par cellule, un avec de multiples antennes qui reçoivent des interférences des autres cellules et un second qui est isolé des OCI et et qui n'a qu'une antenne, ou peut-être de multiples antennes mais seulement un canal de rang un, du fait d'être en ligne de vue (line of sight, LOS) par exemple.

Le schéma IA classique [18] ne donne pas de bons résultats dans ce contexte, à la fois parce qu'il y a plusieurs utilisateurs par cellule [28] et à cause de l'utilisation d'extension de symbole [29].

La meilleure méthode connues pour ce type de réseau est une recherche heuristique pour trouver une allocation de flux qui est faisable de manière linéaire et ensuite d'utiliser cette IA linéaire sans extension de symbole comme dans [27]. Nous proposons d'utiliser à bon escient un premier niveau de filtres d'émission afin d'obtenir deux sous-réseaux isolés réseaux. D'un côté, les utilisateurs isolés serait non seulement isolés des OCI grâce à la connectivité partielle mais également isolés des interférences multi-utilisateur (multi-user interference, MUI) dans leur propre cellule qui sont normalement dues aux données transmises au deuxième utilisateur de la cellule. De l'autre côté, les utilisateurs interférés ne recevraient que l'OCI qui est due aux flux destinées aux autres utilisateurs interférés mais ne recevraient pas les interférences dues aux flux destinés aux utilisateurs isolés. Dans

d'autres termes, après séparation, on aurait deux réseaux isolés, G liens parallèles SISO et un SISO IC à G utilisateurs. Les deux sous-réseaux peuvent ensuite être traités séparément et nous observons que cela augmente le gain de multiplexage, i.e., qu'il est possible d'augmenter le nombre de flux transmis par rapport à l'état de l'art.

1.3 DCSIT

Dans le BC et dans le IC, les CSIT peuvent être utilisés pour aligner les interférences aux récepteurs, permettant ainsi de réduire, voire d'éliminer leur impact. Cependant, ces techniques ont besoin de CSIT instantanées et parfaites, ce qui est impossible. Les CSIT sont par nature retardées et imparfaites. Des résultats intéressant ont été trouvés en ce qui concerne les CSIT imparfaites [30]. Le délai de feedback est par contre toujours un problème, surtout si ce délai est similaire au temps de cohérence du canal. Dans le Chapitre 6, nous proposons un nouveau modèle de canal, qui généralise les modèles de canaux à évanouissement rapide et évanouissement par bloc, pour lesquels nous proposons également une nouvelle stratégie de feedback qui permet aux transmetteurs d'avoir constamment les CSIT. Ensuite dans le Chapitre 7 nous évaluons les performances de différents schémas de transmission pour les CSIT retardées dans le BC, en prenant en compte le feedback et les séquences d'apprentissage. Enfin, dans le Chapitre 8 le IC est étudié. Pour évaluer les performances de tels schémas pour DCSIT on peut d'abord considérer un délai abstrait dans l'acquisition des CSIT et essayer de mitiger les pertes en termes de gain de multiplexage. Une approche plus intéressante est ensuite de prendre en compte la perte de gain de multiplexage due au délai mais aussi les surcoûts (feedback et séquences d'apprentissage) afin d'évaluer de manière plus juste le gain de multiplexage net.

1.3.1 FRoI

Nous proposons d'utiliser des signaux linéaires à débit d'information finie (Finite Rate of Information, FRoI) pour modéliser les coefficients de canaux. L'approche FRoI est particulièrement adaptées pour les analyses de DoF. Les canaux a évanouissement par bloc et les canaux à évanouissement rapides sont des cas particuliers du modèle FRoI. Cependant, le fait que le modèle FRoI permette de représenter les canaux a évanouissement rapides permet d'exploiter un dimension supplémentaire: les décalage temporaires arbitraires. De cette manière, le modèle de canal FroI permet d'avoir les DoF insensibles au retard des CSIT, simplement en augmentant la fréquence de feedback. Nous appellerons cette technique feedback du canal prédit

(Foresighted Channel Feedback, FCFB).

1.3.2 DCSIT dans le BC

Si de nombreux résultats existent pour les CSIT imparfaites [30], le délai dans le feedback est toujours un problème. Néanmoins, le schéma MAT [31] a complètement changé la donne en fournissant un DoF plus grand que un en utilisant uniquement des CSIT retardés, permettant ainsi d'avoir un gain de multiplexage même si le canal change indépendamment plus rapidement que le délai de feedback. Les valeurs de temps de cohérence pour lesquels l'utilisation seule du schéma MAT apporte du gain de multiplexage est déterminée dans [32] et [33] mais en considérant uniquement le coût du feedback ou uniquement le coût des séquences d'apprentissage mais jamais les deux.

L'hypothèse de variation de canal indépendantes plus rapide que le délai de feedback est assez pessimiste pour de nombreux cas pratiques. C'est pourquoi un autre schéma a été proposé dans [34] pour le cas de canaux variant dans le temps, mais de manière corrélée, d'un MISO BC avec 2 utilisateurs. Ce schéma combine de manière optimale les CSIT retardées et les CSIT actuels, toutes les deux imparfaites. Ce schéma n'est pas généralisé pour un plus grand nombre d'utilisateurs. Un des schémas que nous proposons est de combiner les schémas ZF et MAT et atteindre le gain de multiplexage optimal en prenant en compte uniquement le délai des CSIT. Il s'agit simplement d'effectuer le schéma ZF et d'y ajouter le schéma MAT seulement pendant les temps morts de ZF. Nous verrons que ce schéma retrouve le résultat d'optimalité de [34] pour $K = 2$ mais MAT-ZF est valide et optimal en termes de DoF pour un nombre d'utilisateurs quelconque. Une autre stratégie de transmission similaire consiste à utiliser le schéma ZF et ajouter TDMA pendant les temps mort au lieu MAT, le DoF total est plus faible mais c'est plus simple et beaucoup moins coûteux car il n'y a pas de surcoût pour faire TDMA contrairement à MAT.

Il était généralement admis que n'importe quel délai dans le feedback causait forcément une perte de DoF. Cependant, dans [35], Lee et Heath proposent un schéma qui atteint M DoF dans le canal MISO BC à évanouissement par bloc sous-déterminé avec M antennes d'émission et $K = M + 1$ utilisateurs si le délai dans le feedback est assez petit ($\leq \frac{T_c}{K}$).

On compare les gains de multiplexage que ZF, MAT, MAT-ZF, TDMA-ZF, ST-ZF et ZF$_{FCFB}$ peuvent atteindre dans un système réel, en prenant en compte les séquences d'apprentissage ainsi que le DoF perdu à cause du feedback sur le lien montant. Contrairement à [33], dans le net DoF nous comptons également le DoF consommé dans le lien montant. De manière plus générale, on pourrait considéré les net DoF pondérés comme dans [36] en donnant des poids différents pour les

DoF consommés sur les liens montants et les liens descendants. Nous considérons ici des net DoF non pondérés, mais les net DoF pondérés pourraient très facilement être extrapolé des net DoF no pondérés. On remarque que le schéma ZF considéré dans [33] est différent et n'a pas de temps mort. Cependant, ce ZF BF décrit dans [33] utilise seulement des prévisions de CSIT, ce qui induit des pertes de DoF.

Dans Fig. 1.3 les approches DoF et net DoF sont illustrée dans le cas BC. L'approche DoF revient simplement à se poser la question de comment utiliser au mieux le temps *No CSIT*, i.e., avant que le transmetteur obtienne les CSI et est surtout intéressant d'un point de vue théorique. L'objectif de la deuxième approche est aussi de faire le meilleur usage du temps *No CSIT*, mais cette fois en prenant en compte les coûts liés aux séquences d'apprentissage et au feedback, et donne donc des résultats plus pratiques.

(a) Topologie d'un bloc pour étude de DoF.
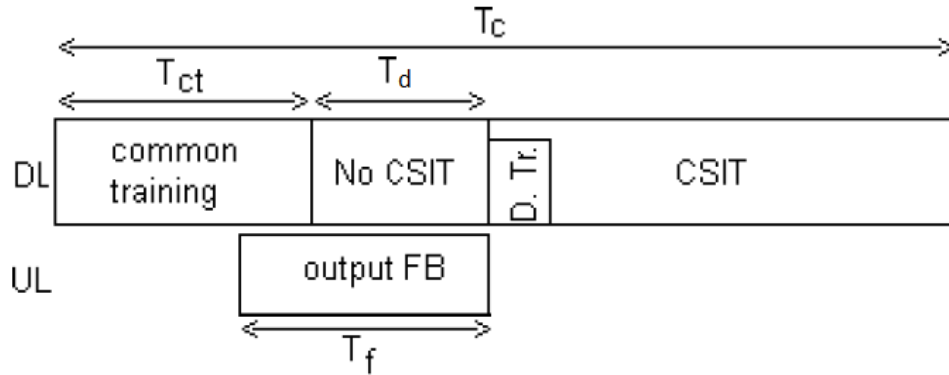
(b) Topologie d'un bloc pour étude de net DoF.

Figure 1.3: Topologie d'un bloc pour étude de DoF et de net DoF.

Dans ce chapitre, en rappelant et proposant des schémas de transmission pour limiter les pertes de DoF liées aux DCSIT. On remarquera rapidement qu'il est important de prendre en compte les coûts des séquences d'apprentissage et du feedback des différents schémas. En effet, la combinaison MAT-ZF, qui est optimale en termes de DoF, donne en fait de mauvais résultats dans la plupart des scénarios

quand les surcoûts sont pris en compte. De la même manière, le ZF$_{FCFB}$ était très prometteur en termes de DoF puisqu'il permettait de toujours avoir les CSIT et donc, aucun DCSIT se révèle en pratique être uniquement intéressant pour de très grand temps de cohérence quand on prend en compte les surcoût.

1.3.3 DCSIT dans le IC

Si de nombreuses techniques permettent d'augmenter le DoF, la plupart reposent sur des CSIT et CSIR précises et instantanées. Les CSIT posent plus particulièrement problème puisqu'en pratique elles ne peuvent être instantanées car pour les obtenir il faut faire du feedback, ce qui cause inexorablement un délai. En ce qui concerne le retard des CSIT, de nombreux progrès on été fait dans le BC comme on le voit dans le Chapitre 7 avec des schémas comme [31, 35, 37, 38].

On a remarqué que cette possibilité d'atteindre le DoF optimal pour des petits délais de feedback est au prix d'une légère augmentation du volume de feedback dans Chapitre 7. Il a aussi été démontré dans [41] que la fraction de temps minimale de CSIT parfaites nécessaire par utilisateur afin de pouvoir atteindre le DoF optimal de $\min(M,G)$ est donnée par $\min(M,G)/G$. On en déduit donc que, le manque de ponctualité des CSIT peut être compensé par le fait d'avoir les CSIT d'un plus grand nombre d'utilisateurs. En effet, le schéma donnant la borne inférieure dans [41] repose sur le fait d'avoir tout le temps les CSIT parfaites de M utilisateurs mais pas tout le temps celles des mêmes M utilisateurs. Dans le modèle classique d'évanouissement par bloc, cela nécessiterait aussi une augmentation du volume de feedback. Dans [42], le compromis entre feedback et performance est caractérisé en profondeur. Pour le cas carré, i.e., quand $G = M$, les auteurs confirment qu'avec un modèle de canal à évanouissement par bloc, n'importe quel délai dans le feedback cause une perte de DoF et que la simpliste combinaison: MAT, quand on a que les CSIT retardées, et ZF, quand les CSIT actuelles sont présentes, est optimale en termes de DoF.

Pour le SISO IC à trois utilisateurs, [43] propose de faire de l' *alignement d'interférence rétrospectif* et atteint un gain de multiplexage plus grand que un avec des CSIT complètement retardées. Ensuite, dans [44], un schéma général pour le SISO-IC à G utilisateurs avec des CSIT complètement retardées est proposé et atteint des DoF plus grands que un et qui augmentent avec G. Cepen-

Les résultats sur ce sujet pour le IC sont beaucoup plus rares, le schéma dans [38] est étendu au IC mais seulement pour le cas où il n'y a que deux utilisateurs dans [39] et le schéma dans [35] qui atteint M DoF dans MISO BC sous-déterminé avec M antennes d'émission et $G = M + 1$ utilisateurs si le délai de feedback est assez petit ($T_{fb} \leq T_c/G$) is aussi valide dans le MISO IC avec M antennes par transmetteur et $G = M + 1$ paires transmetteur-récepteur [40].

dant, ces DoF restent inférieurs à une borne supérieure qui vaut $\frac{4}{6\ln 2-1} \approx 1.266$. Dans [45], un schéma basé sur l'IA ergodique est proposé et atteint des DoF qui augmentent avec G et tendent vers 2 dans le G-utilisateur SISO IC avec des CSIT complètement retardées. Il n'y a pas de preuve d'optimalité pour aucun de ces DoF, mais les auteurs dans [44] conjecturent que les DoF du SISO IC avec des CSIT complètement retardées est borné par une constante. Ceci est donc très loin de l'optimal DoF de $\frac{G}{2}$ dans le SISO IC avec CSIT actuelles [4].

Nous allons démontrer que le DoF optimal du SISO IC à G utilisateurs est en fait toujours $\frac{G}{2}$ pour des délais de feedback jusqu'à $T_{fb} \leq T_c/2$ et nous allons proposer un schéma qui atteint ce DoF optimal pour ces délais. De plus, nous prouverons que ce délai de feedback que notre schéma supporte est le plus grand délai pour lequel il est toujours possible d'atteindre le DoF optimal de $G/2$ DoF pour tout G.

Notre approche est basée sur la technique d'*d'alignement d'interférence ergodique* schéma proposée dans [16], où les auteurs montrent que non seulement les $\frac{G}{2}$ DoF sont atteignable mais également que chaque utilisateur peut atteindre la moitié de son débit idéal (sans interférence) à n'importe quel SNR. Notre variante bénéficiera également de cette propriété.

En analyse DoF, T_{fb} représente un délai abstrait entre le début du bloc et le moment où les CSI sont disponibles à l'émetteur, cela représente donc le temps mort dans la transmission.

On étudie ensuite différents schémas pour le IC avec CSIT retardées, et on compare les netDoF des schémas car on a pu remarquer dans le Chapitre 7 que la prise en compte des surcoût pouvait faire une grande différence. Cependant, le nouveau schéma que l'on propose ne nécessite pas des surcoût et devrait donc se révéler intéressant en termes de netDoF également.

Résultat Principal

Notre résultat principal et le théorème suivant qui démontre la robustesse du DoF du IC contre le délai dans les CSIT.

Theorem 1 *Dans le SISO IC à G utilisateurs, tant que le délai de feedback $T_{fb} \leq \frac{T_c}{2}$,*

$$DoF(G) = \frac{G}{2} \ .$$

(1.14)

Résultat renforcé par l'optimalité de notre proposition:

Theorem 2 *S'il y a un schéma tel que*

$$\forall G, DoF = \frac{G}{2} \ pour \ T_{fb} = \alpha T_c$$

18

alors

$$\alpha \leq \frac{1}{2}.$$

La variante d'IA ergodique que l'on propose donne un résultat théorique très fort: le DoF optimal $G/2$ du SISO IC à G utilisateurs peut-être atteint pour des délais de feedback jusqu'à $\frac{T_c}{2}$. De plus on montre que ce délai est le maximum pour lequel on peut espérer toujours avoir le DoF optimal à $G/2$ pour tout G. La plupart des améliorations apportées à l'IA ergodique classique, par exemple pour réduire la latence, s'appliquent aussi à la variante que l'on propose. Le schéma permet aussi à chaque utilisateur d'atteindre la moitié du débit qu'il atteindrait en l'absence d'interférences. Une stratégie d'association de réalisation de canal différente pourrait également être utilisée pour atteindre le gain SNR optimal par rapport au schéma original comme proposé dans [46].

On observe que, contrairement au MISO BC, dans le SISO IC avec CSIT retardées le DoF optimal peut etre préservé sans avoir besoin d'utilisateurs supplémentaires [35, 41] et sans avoir de surcoût, ce qui se révèle particulièrement avantageux en termes de net DoF puisque l'IA ergodique surpasse à la fois l'IA asymptotique et, quand ils atteignent le même DoF, IA ergodique surpasse également les schémas visant la borne propre en termes de net DoF.

1.4 Conclusion et Perspectives

1.4.1 Conclusion

Le sujet principale de cette thèse est l'évaluation des des effets de certains aspects réalistes des réseaux sans fils.

Le premier aspect étudié est le nombre d'utilisateur. Que ce soit dans les configurations à une seule cellule ou à plusieurs cellules, nous avons proposé des solutions pour bénéficier du fait qu'en pratique il est possible d'améliorer les performances (débit ou gain de multiplexage) quand il y a *plus* d'utilisateurs. Dans le BC, nous avons proposé un nouveau critère GUS pour les configurations MISO et MIMO, en sélectionnant intelligemment les utilisateurs à qui la station de base transmets nous pouvons diminuer les pertes dues à la sous-optimalité de ZF BF par rapport à DPC et en adoptant des techniques plus simples que la recherche exhaustive nous avons su garder la complexité de calcul à un niveau raisonnable. Dans le IC, avoir plus d'utilisateur permet d'augmenter le gain de multiplexage et nous avons proposés deux algorithmes, pour bénéficier du fait d'avoir de multiples antennes quand on essaie d'atteindre la borne propre ou la borne de décomposition. Si l'algorithme visant à atteindre la borne de décomposition est assez théorique car

il a serait difficile à implémenter en pratique, l'algorithme pour la borne propre est facile à implémenter et s'est révélé efficace dans nos simulations numériques.

Ensuite, nous avons étudié comment la connectivité partielle influence le gain de multiplexage dans un IBC, i.e., dans un IBC ou certains lien d'interférence peuvent être négligés. On a proposé une première approche par séparation, qui permet d'obtenir un gain de multiplexage plus grand qu'avec les méthodes naïves. L'algorithme proposé pour les IBC entièrement connectés s'est révélé aussi efficace pour les IBC partiellement connectés. Il a en fait atteint des plus grands gains de multiplexages. L'approche par séparation garde tout de même un intérêt pour les cas où le temps de cohérence du canal est faible car elle nécessite moins de surcoût d'apprentissage et de feedback.

Dans la seconde partie de cette thèse on se concentre sur le problème des CSIT retardées, et au problème connexe des surcoûts d'apprentissage et de feedback. Nous avons d'abord proposé un modèle de canal général et une nouvelle méthode de feedback qui permet de passer outre le délai de feedback (et donc le retard des CSIT) au prix d'une augmentation de la fréquence de l'envoie de séquences d'apprentissage et de feedback. Ce modèle est aussi intéressant car il englobe les modèles de canaux à évanouissement par bloc et à évanouissement rapide, ce qui démontre qu'il n'y a pas de contradiction à comparer des résultats obtenues avec ces deux modèles. En ce qui concerne le retard des CSIT, la première question est de chercher quoi faire quand les canaux n'est pas encore connu par les transmetteurs. Pour le BC, nous avons proposé d'associer ZF et MAT, ce qui s'est révélé être optimal en termes de gain de multiplexage. Ensuite, les gains de multiplexage de différents schémas ont été dérivés, en prenant en compte les surcoût d'apprentissage et de feedback, ce qui a mis en évidence qu'il faut trouver un compromis et que différents schémas sont optimaux en fonction du délai de feedback et du temps de cohérence du canal. Pour le IC, nous avons proposé un schéma qui atteint le gain de multiplexage optimal du IC, et qui est robuste aux délais de feedback jusqu'à des délais de la moitié du temps de cohérence du canal et qui ne nécessite pas de surcoût d'apprentissage ou de feedback. Ce schéma de transmission surpasse donc également les autres schémas de transmission connus quand on prend en compte les surcoûts d'apprentissage et de feedback.

1.4.2 Perspectives

La suite la plus logique pour cette thèse serait de chercher à réduire les CSI nécessaire à l'émetteur. En effet, nous avons vu qu'avoir plus d'utilisateurs augmente les performances, mais quand tous les émetteurs doivent avoir tous les CSI comme c'est souvent supposé, cela devient irréaliste. C'est pourquoi il serait intéressant de chercher des schémas de transmission qui offrent de bonnes performances avec

des CSIT *partielles*. Il y a deux grands axes à explorer, on peut chercher à réduire le nombre de liens qui ont besoin d'être connus au niveau des émetteurs(partage incomplet des CSI), ou alors on peut chercher à réduire ce qui doit être connu sur chaque lien (par exemple CSIT sur la covariance du lien uniquement ou encore CSIT gaussien), ou encore mieux, combiner les deux réductions. Les bénéfices seraient doubles puisqu'à la fois le délai *et* le surcoût liés a l'acquisition des CSIT diminueraient.

Chapter 2

Motivation and Models

2.1 Introduction

Wireless communications are central to many aspects of our lives. With an active user on a laptop, a tablet or a cellphone or for automated use with smart metering for instance, wireless networks dimensions have increased dramatically, both in terms of data volumes and of number of users. Precisely, global mobile data traffic is forecast to increase nearly 11-fold between 2013 and 2018 and the number of connected mobile devices is expected to reach 10 billion in 2018 [1]. With the rapidly growing traffic, interference has become a major limitation in wireless networks as the wireless medium is inherently shared. Orthogonalization methods, in time or frequency are practical and efficient to avoid interferences but drastically degrade the spectral efficiency.

In order to improve the spectral efficiency, the search for efficient ways of transmitting has been productive and diversified [2–4]. Numerous techniques allow the increase of the multiplexing gain or the sum rate in broadcast channels (BC) or interference channels (IC). In a BC all the interference is intracell and is due to the transmission by a single base station (BS) of multiple streams intended to multiple users. This kind of interference can be taken care of by simple means of zero forcing (ZF) or by the more complex, but optimal, dirty paper coding (DPC) [5]. A lot of other schemes and variations were proposed e.g. [6–15]. In an IC, the situation is more complex as the interference at each receiver come from other cells. However, different techniques named interference alignment (IA) can be used to align the interference at the receivers in a subspace of reduced dimension. Some are more theoretical [4,16,17] others more practical [18–20]. These schemes align the interference in a subspace such that there remains enough dimensions free of interference for the useful signal at each receiver.

However, most techniques rely on overly simplistic assumptions. For instance in a BC the number of users is generally considered to be equal to the number of transmit antennas. Furthermore, in multi-cell configurations, considering an IC can be over simplifying compared to the more general interfering broadcast channel (IBC) i.e., interfering cells with multiple users in each cell. For most applications the IBC is a more realistic model than the IC and actually also encompasses the IC as a special case.

Another issue is that most transmission techniques rely on accurate and timely channel state information at the transmitter (CSIT) and at the receiver (CSIR). In actual networks especially CSIT is problematic because it requires feedback that inevitably causes a delay, which may be substantial, and considerably decrease the system performances. This raises two related questions. How to reduce the delay CSIT acquisition? How to make good use delayed CSIT (DCSIT), in other words, what to do while awaiting for the CSIT acquisition to be over?

A third discrepancy between models and actual networks is considered in this thesis, the partial connectivity in wireless networks. Partial connectivity means that we actually take into account the fact that some interference links in the IBC are attenuated enough to be neglected. While any solution for a fully connected IBC will still work if some interference links are negligible, it might not fully benefit from the partial connectivity if nothing is done to especially do so. Indeed, the multiplexing gain should increase with the number of interference links that are neglected.

2.2   Summary of Contributions

This thesis is divided in two parts. In Part I, we will study what is possible with *more* users. Having more users means really different things in a BC and in an IC. In a BC, having more users than transmit antennas does not increase the multiplexing gain so by, *more* users in a BC, we mean more users than transmit antennas. It is relevant to search for what to do with more users than transmit antennas because the number of transmit antennas is fixed by design whereas the number of users evolves in time and can very well be significantly higher than the number of transmit antennas, especially with the rapidly increasing number of connected mobile devices in the world [1].

In Chapter 3, we propose a greedy user selection (GUS) for the multiple-input single-output (MISO) BC and for the multiple-input multiple-output (MIMO) BC in order to benefit from the so-called multi-user diversity and improve the sum rate. These results are published in:

- Y. Lejosne, D. Slock, and Y. Yuan-Wu, "User Selection in MIMO BC," *in*

Proc. EUSIPCO, Bucharest, Romania, Aug. 2012.

- Y. Lejosne, D. Slock, and Y. Yuan-Wu, "On Greedy Stream Selection in MIMO BC," *in Proc. WCNC*, Paris, France, Apr. 2012.

On the contrary, in an IC, having more than one user in each cell can improve the multiplexing gain; it actually makes it an IBC and, in the IBC, the multiplexing gain increases with the number of users. In Chapter 4, we propose two schemes for the IBC to transmit to more than one user in each cell in order to improve the multiplexing gains. The results concerning the first algorithm are published in:

- Y. Lejosne, D. Slock, and Y. Yuan-Wu, "Ergodic Interference Alignment for the SIMO/MIMO Interference Channel, *in Proc. ICASSP*," Firenze, Italy, May 2014.

A patent was filed for the second algorithm and the corresponding results were submitted for publication in:

- Y. Lejosne, Y. Yuan-Wu, and D. Slock, "Procédé itératif d'évaluation de filtres numériques destinés à être utilisés dans un système de communication," FR Patent 1 462 878, Dec. 12, 2014.

- Y. Lejosne, Y. Yuan-Wu et D. Slock, "Interference Alignment Scheme for Fully or Partially Connected Interfering Broadcast Channels with Finite Symbol Extension," *submitted for publication in IEEE Transactions on Wireless Communications*.

Then, in Chapter 5, we consider partially connected IBC because it is reasonable to assume that in certain configurations only certain interference links need to be taken into account. We derive a new algorithm for certain configurations for which we first separate the network in two independent subnetworks. We also evaluate one of the general IBC algorithms proposed in Chapter 4 in these configurations. The results on the separation method have been patented and submitted for publication in:

- Y. Lejosne, Y. Yuan-Wu and D. Slock, "Stratégie de transmission à deux niveaux pour certains réseaux de cellules interférées et servant chacun des utilisateurs asymétriques et pour certains réseaux hétérogènes," FR Patent FR 1 456 224, Jun. 30, 2014.

- Y. Lejosne, Y. Yuan-Wu and D. Slock, "A two-level transmission strategy for certain asymmetric interfering broadcast channels and heterogeneous networks," *submitted for publication in IEEE Transactions on Wireless Communications*.

Another study on the partial connectivity was conducted. We extend a technique developed in [47] to partially connected IC. In [47] the authors proposed a heuristic algorithm to find reduced CSIT allocation that preserve IA feasibility in an IC. Our variant shows significant CSIT reduction by taking into account the partial connectivity of partially connected IC. This result is not presented in this thesis and has been submitted for publication in:

- Y. Lejosne, A. Ben Nasser, Y. Yuan-Wu and D. Slock, "CSIT allocation reduction for partially connected MIMO Interference Channels," *submitted for publication in ICASSP 2015*.

In Part II, the focus is on DCSIT. It always takes time and efforts for the transmitter to acquire the CSI: training, and feedback for frequency division duplexing (FDD). To evaluate the loss due to DCSIT, a first approach is to consider an abstract delay in the CSI acquisition and try to mitigate the loss in the multiplexing gain. A more accurate approach is to consider the loss in the multiplexing gain due to delay and the extra overheads in order to evaluate the fairer resulting *net multiplexing gain*.

First, in Chapter 6, different channel models are reviewed and a general model is proposed. In this model, a general feedback scheme is proposed to overcome feedback delay at the cost of an increased of feedback and training frequency. These results are published in:

- Y. Lejosne, D. Slock, and Y. Yuan-Wu, "Finite Rate of Innovation Channel Models and DoF of MIMO Multi-User Systems with Delayed CSIT Feedback," *in Proc. ITA*, San Diego, CA, USA, Feb. 2013.

Then, in Chapter 7, we propose and evaluate the net multiplexing gain of different transmission schemes. There is always a multiplexing gain loss due to the CSIT delay in the BC and some promising techniques in terms of multiplexing gain actually only show limited gains when taking into account the extra overheads. These results are published in:

- Y. Lejosne, D. Slock, and Y. Yuan-Wu, "Foresighted delayed CSIT feedback for finite rate of innovation channel models and attainable netDoFs of the MIMO interference channel," *in Proc. WD*, Valencia, Spain, Nov. 2013.

- Y. Lejosne, D. Slock, and Y. Yuan-Wu, "NetDoFs of the MISO Broadcast Channel with Delayed CSIT Feedback for Finite Rate of Innovation Channel Models," *in Proc. ISIT*, Istanbul, Turkey, Jul. 2013.

- Y. Lejosne, D. Slock, and Y. Yuan-Wu, "Net Degrees of Freedom of Recent Schemes for the MISO BC with Delayed CSIT and Finite Coherence Time," *in Proc. WCNC*, Shanghai, China, Apr. 2013.

- Y. Lejosne, D. Slock, and Y. Yuan-Wu, "Degrees of Freedom in the MISO BC with delayed-CSIT and Finite Coherence Time: Optimization of the number of users," *in Proc. NetGCooP*, Avignon, France, Nov. 2012.

- Y. Lejosne, D. Slock, and Y. Yuan-Wu, "Degrees of Freedom in the MISO BC with Delayed-CSIT and Finite Coherence Time: a Simple Optimal Scheme," *in Proc. ICSPCC*, Hong Kong, China, Aug. 2012.

Finally, in Chapter 8, we show that the IC is more robust than the BC when it comes to CSIT delay by proposing a transmission scheme coping with large delays, without any loss of multiplexing gain and without requiring any extra overhead. We also derive the net multiplexing gain of several transmission schemes for the IC. These results are published in:

- Y. Lejosne, D. Slock, and Y. Yuan-Wu, "Achieving full sum DoF in the SISO interference channel with feedback delay," *IEEE Communications Letters*, vol.18, no.7, July 2014.

- Y. Lejosne, D. Slock, and Y. Yuan-Wu, "Net degrees of freedom of decomposition schemes for the MIMO IC with delayed CSIT," *in Proc. ISIT*, Honolulu, HI, USA Jun. 2014.

- Y. Lejosne, D. Slock, and Y. Yuan-Wu, "Space Time Interference Alignment Scheme for the MISO BC and IC with Delayed CSIT and Finite Coherence Time," *in Proc. ICASSP*, Vancouver, Canada, May 2013.

Other contributions, that are not presented in this thesis, focus on reducing the CSIT requirement and hence feedback overheads. The results on this topic are published in:

- Y. Lejosne, M. Bashar, D. Slock, and Y. Yuan-Wu, "From MU massive MISO to pathwise MU massive MIMO," *in Proc. SPAWC*, Toronto, Canada, Jun. 2014.

- Y. Lejosne, M. Bashar, D. Slock, and Y. Yuan-Wu, "Decoupled, rank reduced, massive and frequency-selective aspects in MIMO interfering broadcast channels," *in Proc. ISCCSP*, Athens, Greece, May 2014.

- Y. Lejosne, M. Bashar, D. Slock, and Y. Yuan-Wu, "MIMO interfering broadcast channels based on Local CSIT," *in Proc. EW*, Barcelona, Spain May 2014.

- M. Bashar, Y. Lejosne, D. Slock, and Y. Yuan-Wu, "MIMO Broadcast Channels with Gaussian CSIT and Application to Location based CSIT," *in Proc. ITA*, San Diego, CA, USA Feb. 2014.
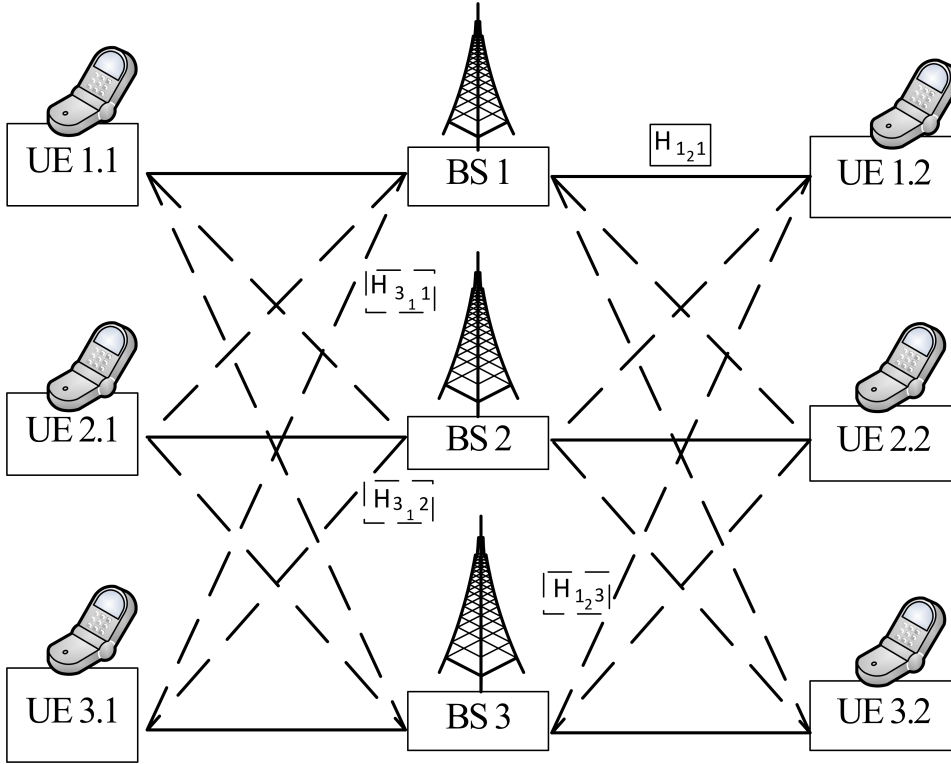
Figure 2.1: Example IBC with $G = 3$ and $K_1 = K_2 = K_3 = 2$.

2.3 System Model and Notations

In this thesis, we will be considering different system configurations: BC, IC, and IBC. Let us start with the IBC because it is the more general configuration and the two other configurations considered can be seen as special cases of IBC.

The general IBC has G cells with a single transmitter in each cell and K_i receivers in cell i. Transmitter in cell j (transmitter j) has M_j antennas, receiver k in cell i (receiver i_k) has N_{i_k} antennas.

An example of IBC with $G = 3$ and $K_1 = K_2 = K_3 = 2$ is given in Fig. 2.1. The dash lines represent the cross links carrying only interference and the full lines represent data bearing links.

The channel realization between transmitter j and receiver i_k at time index t is denoted by $\mathbf{H}_{i_k j}(t)$. When T symbol extensions are considered the resulting $TN_{i_k} \times TM_j$ channel matrix between BS $j \in [1,G]$ and user i_k, $(i,k) \in [1,G] \times$

28

(a) Example BC with $K = 3$.   (b) Example IC with $G = 3$.
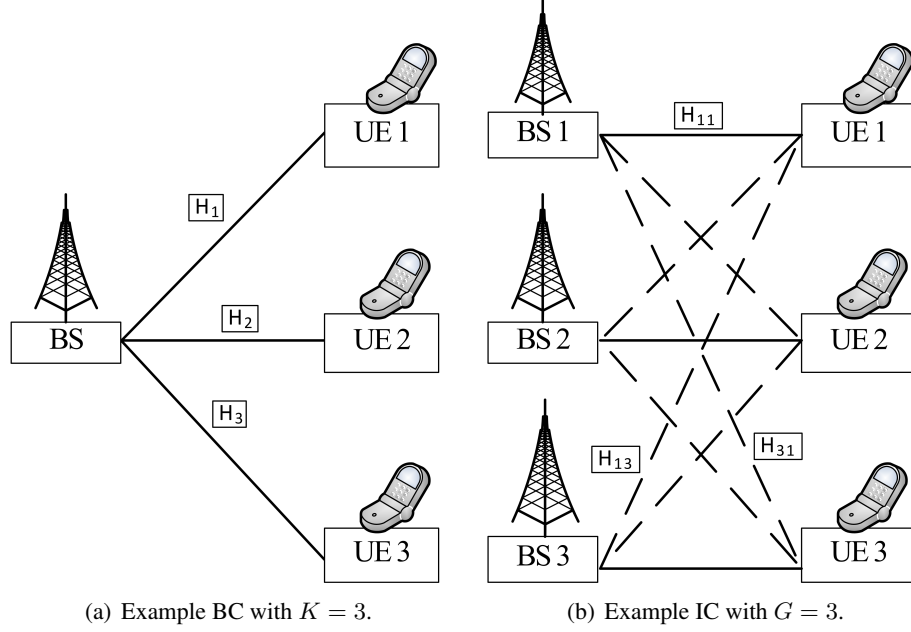
Figure 2.2: Example of BC and IC.

$[1,K]$

$$\mathbf{H}_{i_k j}[N] = \begin{bmatrix} \mathbf{H}_{i_k j}(NT+1) & 0 & \cdots & 0 \\ 0 & \mathbf{H}_{i_k j}(NT+2) & \cdots & 0 \\ \vdots & \vdots & \ddots & \vdots \\ 0 & 0 & \cdots & \mathbf{H}_{i_k j}((N+1)T) \end{bmatrix} \quad (2.1)$$

with a block diagonal structure.

When no extension is considered ($T = 1$) or if no confusion is possible, the time index will be omitted.

From this model, a BC can be seen as a special case for which $G = 1$ and an IC can be seen as a special case for which $K = 1$. When only one cell is considered, i.e., a BC, the notations will be shortened by using $\mathbf{H}_k(t) = \mathbf{H}_{i_k 1}(t)$. When only one user per cell is considered, i.e., an IC, the notations will be shortened by using $\mathbf{H}_{ij}(t) = \mathbf{H}_{i_1 j}(t)$.

Examples of BC with $K = 3$ and IC with $G = 3$ is given in Fig. 2.2. The dash lines represent the cross links carrying only interference and the full lines represent data bearing links.

The linear filters used at the transmitters and at the receivers will respectively

be denoted by $\mathbf{V}_j$ and $\mathbf{U}_{i_k}$. The received signal at user i_k is a noisy linear combination of the inputs of the different transmitters

$$\mathbf{y}_{i_k} = \sum_{j=1}^{G} \mathbf{H}_{i_k j} \mathbf{V}_j \mathbf{x}_j + \mathbf{n}_j \tag{2.2}$$

where

$$\mathbf{V}_j = [\mathbf{V}_{j_1}, \mathbf{V}_{j_2}, \cdots, \mathbf{V}_{j_K}] \tag{2.3}$$

is the precoding matrix of transmitter j, composed of the concatenation of the precoding matrices for each of its K_i users, $\mathbf{x}_j$ its transmitted symbol and $\mathbf{n}_j$ is the additive white Gaussian noise of variance $\sigma^2 = 1$ at the receiver.

The signal is then decoded at the receiver i_k with the receive filter $\mathbf{U}_{i_k}$ giving

$$\mathbf{z}_{i_k} = \mathbf{U}_{i_k} \mathbf{y}_{i_k} = \sum_{j=1}^{G} \mathbf{U}_{i_k} \mathbf{H}_{i_k j} \mathbf{V}_j \mathbf{x}_j + \mathbf{U}_{i_k} \mathbf{n}_j. \tag{2.4}$$

A meaningful metric is the sum of the rates reached by the users of the system. Assuming Gaussian signaling, i.e., data symbols being i.i.d. $\mathcal{CN}(0,1)$ the rate of user i is

$$R_i = \log \det(\mathbf{I}_{N_i} + (\sigma^2 \mathbf{I}_{N_i} + \mathbf{Q}_{i_k}^{int})^{-1} \mathbf{Q}_{i_k}^{dir}) \tag{2.5}$$

where

$$\mathbf{Q}_{i_k}^{int} = \sum_{i \neq j \text{ or } k \neq l} \mathbf{H}_{i_k j} \mathbf{V}_{j_l} \mathbf{V}_{j_l}^H \mathbf{H}_{i_k j}^H \tag{2.6}$$

is the interference covariance matrix of *both* the other cell interference (OCI), i.e., $i \neq j$ *and* the multi-user interference (MUI) i.e., $i = j, k \neq l$ and

$$\mathbf{Q}_{i_k}^{dir} = \mathbf{H}_{i_k i} \mathbf{V}_{i_k} \mathbf{V}_{i_k}^H \mathbf{H}_{i_k i}^H \tag{2.7}$$

is the covariance matrix of the desired signal.

The sum rate is then

$$\text{SR} = \sum_{i=1}^{K} R_i. \tag{2.8}$$

In some cases, results are only found in terms of degrees of freedom (DoF), and are valid at high signal-to-noise ratio (SNR). The DoF metric, which is also called multiplexing gain is the prelog of the sum rate, or, in other words, the slope

of the rate when plotted as a function of the logarithm of the SNR. Let $R_j(P)$ denote the achievable rate for user j with transmit power P, then the achievable DoF for user j is as follows,

$$d_i = \lim_{P \to \infty} \frac{R_i(P)}{\log_2(P)} \qquad (2.9)$$

and the sum DoF of a system is then

$$\text{DoF} = \sum_{i=1}^{K} d_i. \qquad (2.10)$$

When only the DoF are of interest, Gaussian noise will omitted for simplicity.

In Part II, we will also use the netDoF metric, i.e., the remaining DoF after accounting for training and feedback overheads. In order to take into account the feedback cost, we define the feedback overhead. Let $F(P)$ the total feedback rate of a MISO BC with M transmit antennas and K single-antenna receivers and transmit power P then

$$\text{DoF}_{FB} = \lim_{P \to \infty} \frac{F(P)}{\log_2(P)}. \qquad (2.11)$$

Part I

Benefits of Having Many/Too Many Users in a Cell

Chapter 3

Too many users in a BC: Multi-User Diversity

3.1 Introduction

The multi-user MIMO BC has been one a well investigated subject in wireless communications because of the high potential it offers in improving the system throughput. Information theory has shown that the capacity of MU-MIMO channels could be achieved through DPC [5, 48, 49]. However, DPC is difficult to implement and computationally complex. Suboptimal linear beamforming (BF) algorithms exist and can be divided into two main categories: the iterative [6–10] and the closed form (CF) solutions [11–15]. All the solutions can also be differentiated according to the number of streams allocated per user. In fact, there are precoders that cannot support more than one stream per user even if the system is not fully charged. Such precoders have been proposed and widely studied in [8, 9, 11–14]. Some multi-stream precoding solutions have also been proposed, for instance in [15, 50]. To the best of our knowledge, the best linear CF precoder in the literature is the so called ZFDPC-SUS (zero forcing DPC with successive user selection) that has been proposed in [15, 51]. This precoding technique is based on the selection of semi-orthogonal users based on the singular value decomposition of their respective channels. Another interesting multi-stream technique is the one presented in [50] based on the Signal to Leakage plus Noise Ratio (SLNR) maximization. This technique offers some advantages as e.g. the channel knowledge can be relaxed to only covariance matrix information. On the other hand the solution proposed in [50] imposes prefixing the stream distribution.

We consider a MIMO BC with M transmit antennas, K users with $N_k = N$ receiving antennas and assume perfect CSI. We also assume that in this setting

only one stream per user is assigned because there are many users to choose from.

Because there is only one transmitter in this configuration we have the following received signal: $\mathbf{y}_k = \mathbf{H}_k \mathbf{x} + \mathbf{z}_k = \mathbf{H}_k \sum_{i=1}^{K} \mathbf{V}_i \mathbf{s}_i + \mathbf{z}_k$ or hence

$$
\underbrace{\mathbf{U}_k}_{1 \times N} \underbrace{\mathbf{y}_k}_{N \times 1} = \underbrace{\mathbf{U}_k}_{1 \times N} \underbrace{\mathbf{H}_k}_{N \times M} \sum_{i=1}^{K} \underbrace{\mathbf{V}_i}_{M \times 1} \underbrace{\mathbf{x}_i}_{1 \times 1} + \underbrace{\mathbf{U}_k}_{1 \times N} \underbrace{\mathbf{n}_k}_{N \times 1}
$$

$$
= \underbrace{\mathbf{U}_k \mathbf{H}_k \mathbf{V}_k \mathbf{x}_k}_{\text{useful signal}} + \underbrace{\sum_{i=1,i \neq k}^{K} \mathbf{U}_k \mathbf{H}_k \mathbf{V}_i \mathbf{x}_i}_{\text{inter-user interference}} + \underbrace{\mathbf{U}_k \mathbf{n}_k}_{\text{noise}} . \qquad (3.1)
$$

Optimal MIMO BC design requires DPC, which is significantly more complicated than BF. User selection allows improvement of the rates of ZF-DPC and for the rates of ZF-BF to be closer to those of ZF-DPC. Optimal user selection requires the selection of the optimal combination of up to M users among K users and is often overly complex. Greedy user selection (GUS), selecting one user at a time, results in a complexity that is approximately M times the complexity of selecting one user ($K \gg M$). Multiple receive antennas cannot improve the sum rate prelog (spatial multiplexing gain) but they can be used to cancel interference from other transmitters (spatially colored noise). This, however, is out of the scope of this chapter because here, we focus on single-cell configurations.

Now consider ZF designs for BF, ZF-BF:

$$
\mathbf{U}_{1:i} \mathbf{H}_{1:i} \mathbf{V}_{1:i} = \begin{bmatrix} \mathbf{U}_1 & 0 & \cdots & 0 \\ 0 & \mathbf{U}_2 & \ddots & \vdots \\ \vdots & & \ddots & 0 \\ 0 & \cdots & 0 & \mathbf{U}_i \end{bmatrix} \begin{bmatrix} \mathbf{H}_1 \\ \mathbf{H}_2 \\ \vdots \\ \mathbf{H}_i \end{bmatrix} \begin{bmatrix} \mathbf{V}_1 & \mathbf{V}_2 & \cdots & \mathbf{V}_i \end{bmatrix}
$$

$$
= \begin{bmatrix} \mathbf{U}_1 \mathbf{H}_1 \mathbf{V}_1 & 0 & \cdots & 0 \\ 0 & \mathbf{U}_2 \mathbf{H}_2 \mathbf{V}_2 & & \vdots \\ \vdots & & \ddots & 0 \\ 0 & \cdots & 0 & \mathbf{U}_i \mathbf{H}_i \mathbf{V}_i \end{bmatrix}
$$

and for DPC (modulo reordering issues), ZF-DPC:

$$
\begin{aligned}
\mathbf{U}_{1:i}\mathbf{H}_{1:i}\mathbf{V}_{1:i} &=
\begin{bmatrix}
\mathbf{U}_1 & 0 & \cdots & 0 \\
0 & \mathbf{U}_2 & \ddots & \vdots \\
\vdots & & \ddots & 0 \\
0 & \cdots & 0 & \mathbf{U}_i
\end{bmatrix}
\begin{bmatrix}
\mathbf{H}_1 \\
\mathbf{H}_2 \\
\vdots \\
\mathbf{H}_i
\end{bmatrix}
[\mathbf{V}_1\ \mathbf{V}_2 \cdots \mathbf{V}_i] \\[2mm]
&=
\begin{bmatrix}
\mathbf{U}_1\mathbf{H}_1\mathbf{V}_1 & 0 & \cdots & 0 \\
* & \mathbf{U}_2\mathbf{H}_2\mathbf{V}_2 & & \vdots \\
\vdots & & \ddots & 0 \\
* & \cdots & * & \mathbf{U}_i\mathbf{H}_i\mathbf{V}_i
\end{bmatrix}
\end{aligned}
$$

where $*$ denotes an arbitrary non-zero entry. BF-style selection and DPC-style selection are selection process optimized for the use of the selected streams in ZF-BF and ZF-DPC respectively.

At high SNR, both optimized (MMSE style) filters instead of ZF filters or optimized instead of uniform power allocation only lead to $\frac{1}{\text{SNR}}$ terms in rates. At high SNR, the sum rate is of the form $M \log(\text{SNR}/M)$ plus the constant for the set of selected users S_I

$$\Delta(S_I) = \sum_{i \in S_I} \log \det(\mathbf{U}_i\mathbf{H}_i\mathbf{V}_i) \tag{3.2}$$

for properly normalized ZF receive filter $\mathbf{U}_i$ and ZF transmit filter $\mathbf{V}_i$. It is this constant term that we will maximize with our criterion.

3.1.1   State of the Art in GUS in the MIMO BC

MISO BC

The Gram-Schmidt channel orthogonalization with pivoting (DPC-style GUS) was introduced in [52]. In [53], a proper BF-style GUS, a large K analysis for DPC-style GUS and simulations were presented and the matrix inversion lemma for bordered matrices was used in order to lower the complexity of BF-style GUS. The BF with pseudo-BF-style GUS: SUS (semi-orthogonal) i.e., DPC-style GUS with inner product constraints limiting the size of pool of users for selection is analyzed in [51]. It is also shown that for BF-SUS, as for DPC-SUS,

$$\lim_{K \to \infty} \frac{SR}{M \log(1 + \frac{P}{M} \log K)} = 1 \tag{3.3}$$

In [54] a small refinement is proposed but with more constraints. A simplified at finite SNR, but otherwise exact, sum rate expression for MISO BF (regularized

ZF style) can be found in [55]. A suboptimal user selection with complexity of order K^2 and an interesting power loading algorithm, equating the correct sum rate gradient with that of an equivalent virtual parallel channel and performing WF on the virtual parallel channel are also proposed in [55].

MIMO BC

The transformation of the MIMO channel into a MISO channel, similarly to [54], is done in [15]. Pseudo-BF-style GUS (SUS) and analysis for use in DPC and in BF are carried out, the analysis only shows effect of antennas in higher-order terms. Single-stream MIMO BC and the use of receive antennas to minimize quantization error (for feedback) on resulting virtual channel particularly for partial CSIT (and CSIR) with (G)US are considered in [56]. In [57] the authors obtain the high SNR sum rate offset between BF and DPC without user selection. They extend the analysis of [58] from MISO to MIMO. It is also done in [59]. In [60] SESAM is introduced: proper DPC-style GUS for MIMO case (extension of [52] from MISO to MIMO). In [61] a BF-style GUS for MIMO-BC-BF is proposed. In the style of predecessors, only the receiver of the new stream to be added is adapted. They replace the proper geometric average of the stream channel powers by its harmonic average: $1/\mathrm{tr}\{diag((\mathbf{H}_i\mathbf{H}_i^H)^{-1})\}$, which leads to a generalized eigenvector solution for the receive filter, the min Frob algorithm. It can be simplified to a classical eigenvector problem: the LISA algorithm is equivalent to the SESAM algorithm. In [62] the same greedy approaches are proposed now for max WSR, without user selection. In [63] the authors prove that working per stream is equivalent to working per user.

3.2 GUS in the MISO BC

3.2.1 MISO DPC style GUS

In the MISO case, let $h_k = \mathbf{H}_k^H$, k_i denote the user selected at stage i, $H_i = h_{k_{1:i}}^H$, $S_i = \{k_1 \cdots k_i\}$ and $A(S_i) = H_i H_i^H$.
$h_{k_{1:i-1}\backslash k_j}$ denotes $[h_{k_1} \cdots h_{k_{j-1}} \; h_{k_{j+1}} \cdots h_{k_{i-1}}]$ and $P_{h_{k_{1:i}}}^{\perp}$ is the projector onto the orthogonal complement of the subspace spanned by $h_{k_{1:i}}$.
  Then,

$$\det(A(S_i)) = \prod_{j=1}^{i} \|P_{h_{k_{1:j-1}}}^{\perp} h_{k_j}\|^2 \qquad (3.4)$$

and, as described in [52], by selecting the user with the highest 2-norm projection on the complement of $h_{k_{1:i-1}}$ at stage i, one can assure the maximum increase of

sum rate. This corresponds to the following criterion selection

$$k_i = \arg\max_k \|P^{\perp}_{h_{k_{1:i-1}}} h_k\|^2 \tag{3.5}$$

3.2.2 MISO BF style GUS

When ZFBF is considered, the quantity of interest reads as

$$\Delta(S_I) = \sum_i^I \log \det(H_i G_i) = \sum_i^I \log(H_i G_i) = \log(\prod_i^I H_i G_i) \tag{3.6}$$

and the ZF-BF precoders are

$$G_i = (H_i^{\dagger})_i = \frac{(H_i^H (H_i H_i^H)^{-1})_i}{\|(H_i^H (H_i H_i^H)^{-1})_i\|^2} = \frac{(H_i^H (H_i H_i^H)^{-1})_i}{|((H_i H_i^H)^{-1})_{i,i}|} \tag{3.7}$$

yielding

$$\Delta(S_I) = \log(\prod_i^I \mathbf{H_i} H_i^{\dagger}{}_i) = \log(\prod_i^I \frac{\mathbf{H_i}(H_i^H (H_i H_i^H)^{-1})_i}{|((H_i H_i^H)^{-1})_{i,i}|}) \tag{3.8}$$

$$= \log(\prod_i^I \frac{1}{|((H_i H_i^H)^{-1})_{i,i}|}) \tag{3.9}$$

$$= \log(\det(diag\{(H_i H_i^H)^{-1}\}))^{-1} \tag{3.10}$$

The contribution of user i to the sum rate is then

$$\Delta(S_i) - \Delta(S_{i-1}) = \log(\det(diag\{(H_i H_i^H)^{-1}\}))^{-1}$$
$$-\log(\det(diag\{(H_{i-1} H_{i-1}^H)^{-1}\}))^{-1}$$
$$= \log \frac{(\det(diag\{(H_i H_i^H)^{-1}\}))^{-1}}{(\det(diag\{(H_{i-1} H_{i-1}^H)^{-1}\}))^{-1}} \tag{3.11}$$

which is maximized when

$$\frac{(\det(diag\{(H_i H_i^H)^{-1}\}))^{-1}}{(\det(diag\{(H_{i-1} H_{i-1}^H)^{-1}\}))^{-1}} \tag{3.12}$$

is maximized.

Proposition 1

$$\frac{\det(diag\{(H_i H_i^H)^{-1}\})^{-1}}{\det(diag\{(H_{i-1} H_{i-1}^H)^{-1}\})^{-1}}$$

$$= \|P_{h_{k_{1:i-1}}}^{\perp} h_{k_i}\|^2 \prod_{j=1}^{i-1} (1 - \frac{|h_{k_i}^H P_{h_{k_{1:i-1}\setminus k_j}}^{\perp} h_{k_j}|^2}{\|P_{h_{k_{1:i-1}\setminus k_j}}^{\perp} h_{k_i}\|^2 \|P_{h_{k_{1:i-1}\setminus k_j}}^{\perp} h_{k_j}\|^2}) \quad (3.13)$$

$$= \underbrace{\|P_{h_{k_{1:i-1}}}^{\perp} h_{k_i}\|^2}_{\textit{DPC gain}} \underbrace{\prod_{j=1}^{i-1} \sin^2 \phi_{ij}}_{\textit{further BF loss}} \quad (3.14)$$

where ϕ_{ij} is the angle between $P_{h_{k_{1:i-1}\setminus k_j}}^{\perp} h_{k_i}$ and $P_{h_{k_{1:i-1}\setminus k_j}}^{\perp} h_{k_j}$.

Proof. The proof of Proposition 1 is given in Appendix A.1.

To maximize the sum rate, one should the user that maximizes (3.13). However, we will show that this expression can be approximated in order to obtain a more computable criterion.

3.2.3 BF rate offset approximation

Let ϕ_i be the angle between h_{k_i} and $h_{k_{1:i-1}}$, then we can write $\|P_{h_{k_{1:i-1}}}^{\perp} h_{k_i}\|^2 = \|h_{k_i}\|^2 \sin^2 \phi_i$. For a sufficiently large K, the BF-style user selection process will lead to the selection of channel vectors that are close to being mutually orthogonal. We can then write up to first order

$$\frac{|h_{k_i}^H P_{h_{k_{1:i-1}\setminus k_j}}^{\perp} h_{k_j}|^2}{\|P_{h_{k_{1:i-1}\setminus k_j}}^{\perp} h_{k_i}\|^2 \|P_{h_{k_{1:i-1}\setminus k_j}}^{\perp} h_{k_j}\|^2} \approx \frac{|h_{k_i}^H h_{k_j}|^2}{\|h_{k_i}\|^2 \|h_{k_j}\|^2} \quad (3.15)$$

and also

$$\begin{aligned}
\prod_{j=1}^{i-1} \sin^2 \phi_{ij} &= \prod_{j=1}^{i-1} (1 - \cos^2 \phi_{ij}) \\
&\approx 1 - \sum_{j=1}^{i-1} \cos^2 \phi_{ij} \\
&\approx 1 - \sum_{j=1}^{i-1} \frac{|h_{k_i}^H h_{k_j}|^2}{\|h_{k_i}\|^2 \|h_{k_j}\|^2} \\
&\approx 1 - \|P_{h_{k_{1:i-1}}}^{\perp} h_{k_i}\|^2 / \|h_{k_i}\|^2 \\
&= \sin^2 \phi_i
\end{aligned} \quad (3.16)$$

As a result the contribution of stream i to the sum rate offset can be approximated by

$$
\begin{aligned}
\|P^{\perp}_{h_{k_{1:i-1}}} h_{k_i}\|^2 \prod_{j=1}^{i-1} \sin^2 \phi_{ij} &\approx \|P^{\perp}_{h_{k_{1:i-1}}} h_{k_i}\|^2 \sin^2 \phi_i \\
&= \|h_{k_i}\|^2 \sin^4 \phi_i \\
&= \|P^{\perp}_{h_{k_{1:i-1}}} h_{k_i}\|^4 / \|h_{k_i}\|^2. \quad (3.17)
\end{aligned}
$$

The DPC offset is $\|P^{\perp}_{h_{k_{1:i-1}}} h_{k_i}\|^2 = \|h_{k_i}\|^2 \sin^2 \phi_i$ which represents a certain compromise between max $\|h_{k_i}\|^2$ and min $\cos^2 \phi_i$.

In the case of BF, $\|h_{k_i}\|^2 \sin^4 \phi_i$ leads to a similar compromise, but with more emphasis on orthogonality.

Equation (3.17) is not the exact BF rate offset expression when evaluated for arbitrary candidate channels h_k. However, its optimization over sufficiently many candidates K lead to fairly orthogonal choices, in which case it becomes an arbitrarily good approximation of the BF rate offset.

This analysis also shows that when the channels vectors are close to being mutually orthogonal, such as resulting from user selection, then for a given user selection, the rate offset loss of BF compared to DPC is equal to the rate offset loss of DPC itself compared to DPC for the case of orthogonal channels (orthogonal hypothesis), because $\log \sin^4 \phi_i = 2 \log \sin^2 \phi_i$.

3.2.4 MISO BF-style GUS Criterion

At stage i we use (3.17) to select the user with the largest approximated rate offset

$$
k_i = \arg \max_k \|P^{\perp}_{h_{k_{1:i-1}}} h_k\|^4 / \|h_k\|^2. \quad (3.18)
$$

The first user selected, for $i = 1$, is simply the user whose channel has the largest norm. As opposed to ZF-DPC, the optimal user subset for ZF-BF may be of cardinality less than M. Therefore, we select a user according to (3.18), but we add it to the subset of previously selected users only if this does not decrease the sum rate, otherwise the selection process is stopped.

3.2.5 Complexity

In [53], the authors demonstrates a thorough complexity analysis of the ZF-BF true criterion user selection and of the ZF-DPC user selection. The evaluation of the complexity of the ZF-BF user selection with the approximate criterion can easily be deduced from their analysis.
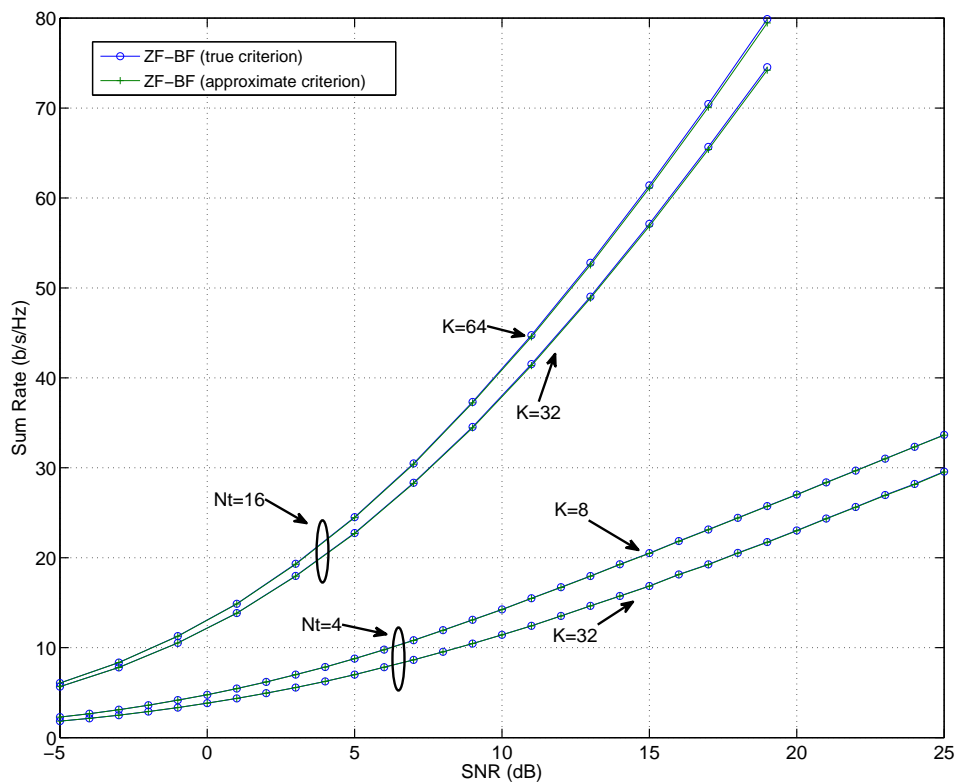
Figure 3.1: Average sum rate of MISO ZF-BF-GUS: true versus approximate criterion in the MISO BC with $M = 4$, $K \in \{8,32\}$ and $M = 16$, $K \in \{32,64\}$.
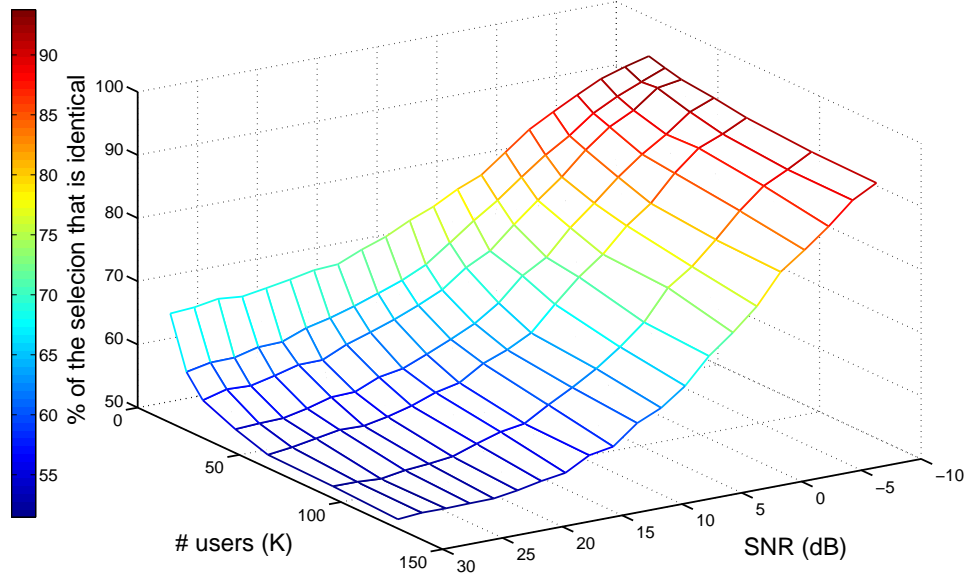
Figure 3.2: Similarity between the user subsets selected by the true and by the approximate criterion

Our algorithm will perform a maximum of M rate evaluations in order to determine whether to stop or continue selecting users. The evaluation of the rate is proved to be $O(M^2)$ in [53]. Finding the arg max in (3.18) requires K vector-matrix multiplications, for which complexity is $O(M^2)$. This is to be done at each stage; therefore, the complexity of our algorithm is $O(M^3) + O(M^3K) = O(M^3K)$, which is the same complexity as the original criterion found in [53].

3.2.6 Simulation Results

The comparison of throughput yielded by the ZF-BF algorithm with our approximate criterion (3.18) and with true criterion [53] (computation of the actual sum rate for each possible addition to the selection) for the MISO user selection is presented in Fig. 3.1 for $M = 4$, $K \in \{8,32\}$ and $M = 16$, $K \in \{32,64\}$. The simulation generates 10 000 independent Rayleigh fading channel realizations for each user and the average sum rate is plot as a function of the SNR. The use of the approximate criterion yields almost the same performances as the true criterion.

At high SNR and with a large pool of users, the algorithm can select users that
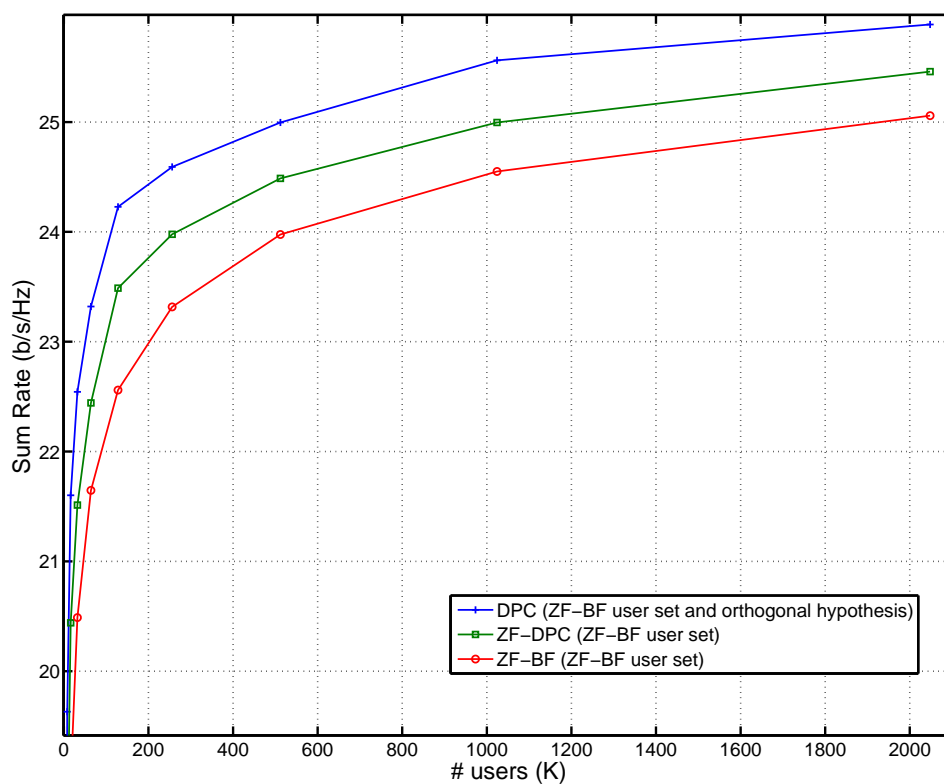
Figure 3.3: Sum rate offset between DPC (orthogonal hypothesis), ZF-DPC, ZF-BF for a given user subset selected for ZF-BF by the approximate criterion in the MISO BC with Nt=4, SNR=15 dB.

are close to being mutually orthogonal; therefore, the approximation is accurate. However, because of the large number of possible choices the user subset selected can differ from what would be selected by the exact criterion. In Fig. 3.2 the similarity between the selections from the true and the approximate criterion is evaluated, the percentage of the selections that are identical is plotted as a function of SNR and of the number of users K. We observe that the similarity between the selections decreases when K or the SNR increases, but because the approximation is accurate these different user subsets yield similar performances. When the user pool is small or at low SNR, the selection is smaller. Therefore, even though the approximation is less accurate we can see in Fig. 3.2 that the same users are selected by both criteria resulting in more similar performances for a small K or at low SNR.

Fig. 3.3 illustrates the rate offset loss between ZF-BF compared to ZF-DPC and the rate offset loss between ZF-DPC compared to DPC with orthogonal hypothesis, when the channel vectors are close to orthogonal. For that purpose, we find a user subset with the approximate criterion of the ZF-BF selection algorithm. Given this specific user subset we compute the sum rate achieved with the two different algorithms (ZF-BF and ZF-DPC) and the sum rate that DPC would yield if the channel vectors were orthogonal. We observe the expected equality: for large Ks, the rate offset loss between ZF-BF and ZF-DPC approaches the rate offset loss between ZF-DPC and DPC with orthogonal hypothesis. In other words, when compared to DPC with orthogonal hypothesis, the rate offset loss induced by the ZF-BF is twice the rate offset loss induced by ZF-DPC.

In Fig. 3.4 we observe that for the user subset selected either for ZF-BF or for ZF-DPC, ZF-DPC almost reaches the sum capacity. This also illustrates the loss one could expect from not matching the selection process and the ZF algorithm, namely performing ZF-BF with a user subset selected with ZF-DPC GUS or performing ZF-DPC with a user subset selected with ZF-BF GUS.

3.3   GUS in the MIMO BC

3.3.1   New MIMO BF-style GUS Criterion

We can obtain a straightforward extension to the MIMO case, in which, for GUS, only the receiver for each candidate user will be adapted to optimize the BF rate offset. Although, once k_i has been identified, it is useful while remaining at acceptable cost to reoptimize the receive filters for the various streams by alternating the receive filter optimization over the various streams.

In the MIMO case, we have the virtual channels $h_{k_i}^H = \mathbf{U}_i H_{k_i}$ (receiver-channel cascade per stream) and to evaluate the expected contribution of a user
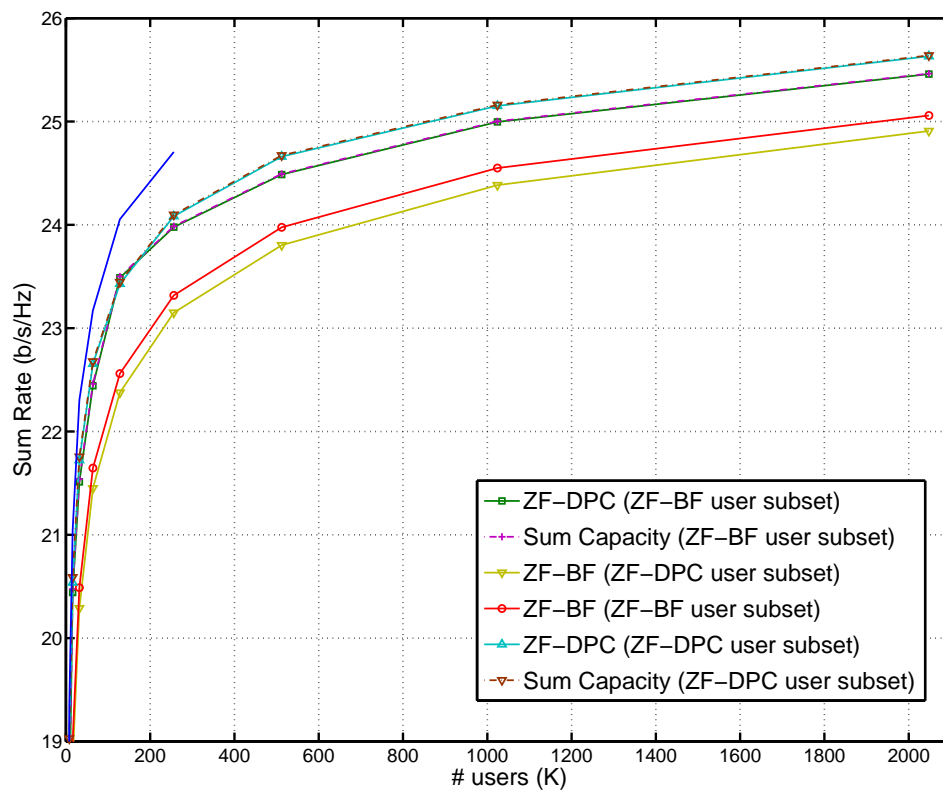
Figure 3.4: Sum rate offset between sum capacity, ZF-DPC, and ZF-BF for user subset selected for ZF-BF by the approximate criterion and ZF-DPC and ZF-BF for a user subset selected for ZF-DPC and the sum capacity for all users in the MISO BC with Nt=4, SNR=15 dB.

to the sum rate we first need to optimize its receive filter:

$$\max_{\mathbf{U}_i} \|P^{\perp}_{h_{k_{1:i-1}}} h_{k_i}\|^4 / \|h_{k_i}\|^2 \tag{3.19}$$

$$\text{s.t. } \mathbf{U}_i^H \mathbf{U}_i = 1$$

Because of the logarithm strict monotony this optimization problem is equivalent to:

$$\max_{\mathbf{U}_i} \left(2\ln\left(\|P^{\perp}_{h_{k_{1:i-1}}} H_{k_i}^H \mathbf{U}_i^H\|^2\right) - \ln\left(\|H_{k_i}^H \mathbf{U}_i^H\|^2\right)\right) \tag{3.20}$$

$$\text{s.t. } \mathbf{U}_i^H \mathbf{U}_i = 1$$

The Lagrangian of this problem is:

$$\begin{aligned} J(\mathbf{U}_i, \lambda_i) &= 2\ln\left(\|P^{\perp}_{h_{k_{1:i-1}}} H_{k_i}^H \mathbf{U}_i^H\|^2\right) \\ &\quad - \ln\left(\|H_{k_i}^H \mathbf{U}_i^H\|^2\right) - \lambda(\mathbf{U}_i^H \mathbf{U}_i - 1) \end{aligned} \tag{3.21}$$

and its partial derivative with respect to $\mathbf{U}_i^*$

$$\begin{aligned} \frac{\partial J(\mathbf{U}_i, \lambda_i)}{\partial \mathbf{U}_i^*} &= 2\frac{H_{k_i} P^{\perp}_{h_{k_{1:i-1}}} H_{k_i}^H}{\|P^{\perp}_{h_{k_{1:i-1}}} H_{k_i}^H \mathbf{U}_i^H\|^2} \mathbf{U}_i \\ &\quad - \frac{H_{k_i} H_{k_i}^H}{\|H_{k_i}^H \mathbf{U}_i^H\|^2} \mathbf{U}_i - \lambda \mathbf{U}_i \end{aligned} \tag{3.22}$$

At the optimum

$$\frac{\partial J(\mathbf{U}_i, \lambda_i)}{\partial \mathbf{U}_i^*} = 0$$

$$\Leftrightarrow \ 2\frac{H_{k_i} P^{\perp}_{h_{k_{1:i-1}}} H_{k_i}^H}{\|P^{\perp}_{h_{k_{1:i-1}}} H_{k_i}^H \mathbf{U}_i^H\|^2} \mathbf{U}_i - \frac{H_{k_i} H_{k_i}^H}{\|H_{k_i}^H \mathbf{U}_i^H\|^2} \mathbf{U}_i - \lambda \mathbf{U}_i = 0 \tag{3.23}$$

and $\mathbf{U}_i^H \frac{\partial J(\mathbf{U}_i, \lambda_i)}{\partial \mathbf{U}_i^*} = 0$ gives $\lambda = 1$.

Hence

$$2\frac{H_{k_i} P^{\perp}_{h_{k_{1:i-1}}} H_{k_i}^H}{\|P^{\perp}_{h_{k_{1:i-1}}} H_{k_i}^H \mathbf{U}_i^H\|^2} \mathbf{U}_i - \frac{H_{k_i} H_{k_i}^H}{\|H_{k_i}^H \mathbf{U}_i^H\|^2} \mathbf{U}_i - \mathbf{U}_i = 0 \tag{3.24}$$

$$\Leftrightarrow$$

$$H_{k_i} P^{\perp}_{h_{k_{1:i-1}}} H_{k_i}^H \mathbf{U}_i = \frac{\|P^{\perp}_{h_{k_{1:i-1}}} H_{k_i}^H \mathbf{U}_i^H\|^2}{2\|H_{k_i}^H \mathbf{U}_i^H\|^2} \left(H_{k_i} H_{k_i}^H + \|H_{k_i}^H \mathbf{U}_i^H\|^2 I\right) \mathbf{U}_i \tag{3.25}$$

and the fixed point equation can be seen as a generalized eigenvalue problem and can be solve iteratively via

$$\mathbf{U}_i^H = V_{max}(H_{k_i} P_{h_{k_{1:i-1}}}^{\perp} H_{k_i}^H, H_{k_i} H_{k_i}^H + ||\mathbf{U}_i H_{k_i}||^2 I) \qquad (3.26)$$

where $V_{max}(A,B)$ is the generalized eigenvector of matrices A and B corresponding to the maximum eigenvalue.

Our algorithm performs the greedy user selection and the receive filter optimization. At stage i, for each candidate user, it optimizes the corresponding receive filter iteratively according to (3.26) and evaluate its approximated rate offset (3.20). It adds the user yielding the largest contribution to the selection only if it increases the total sum rate otherwise the algorithm stops. When a user is added all the receive filters $j, j < i$ are reoptimized one or multiple times with the same approach:

$$\mathbf{U}_j^H = V_{max}(H_{k_j} P_{h_{k_{1:i\backslash j}}}^{\perp} H_{k_j}^H, H_{k_j} H_{k_j}^H + ||\mathbf{U}_j H_{k_j}||^2 I). \qquad (3.27)$$

We initialize with $\mathbf{U}_i = \frac{[1\cdots 1]}{\sqrt{N}}$ because we observed that different initializations yield almost the same results. Initializing with the min Frob of [61] increases the complexity but offers little improvement.

A detailed version of the algorithm is given in Appendix A.2.

3.3.2   Simulation Results

In Fig. 3.5 we compare the performances in terms of sum rate of our MIMO BF-style GUS criterion with those of the min Frob algorithm from [61]. In order to have a better differentiation, we plot the relative sum rate yield by the algorithm normalized to the Sato bound, the sum rate that would be achieved by DPC, computed according to [49]. We observe that our iterative algorithm brings some gains. For example, at SNR $= 10$dB, the min Frob algorithm reaches less than 89.5% of the Sato bound and our iterative algorithm more than 92.5%. Moreover, as we plot the curves for different number of iterations we notice that for $M = 8$, $N = 4$ and $K = 30$, 3 iterations per optimization are sufficient, and concerning the number of cycles of reoptimization going from 1 to 20 offers little improvement in regards to the increased complexity.

In Fig. 3.6 we plot the sum rates yielded by min Frob and by our iterative algorithm for $M = 8$, $K = 30$ as well as for different values of N, $N \in \{2,4,6\}$. We observe that our algorithm performs better for the different values of N even with few iterations and only one reoptimization cycle.

In Fig. 3.7 we plot the cumulative distribution function (CDF) of the sum rates yielded by min Frob, by our algorithm without reoptimization and by our algorithm
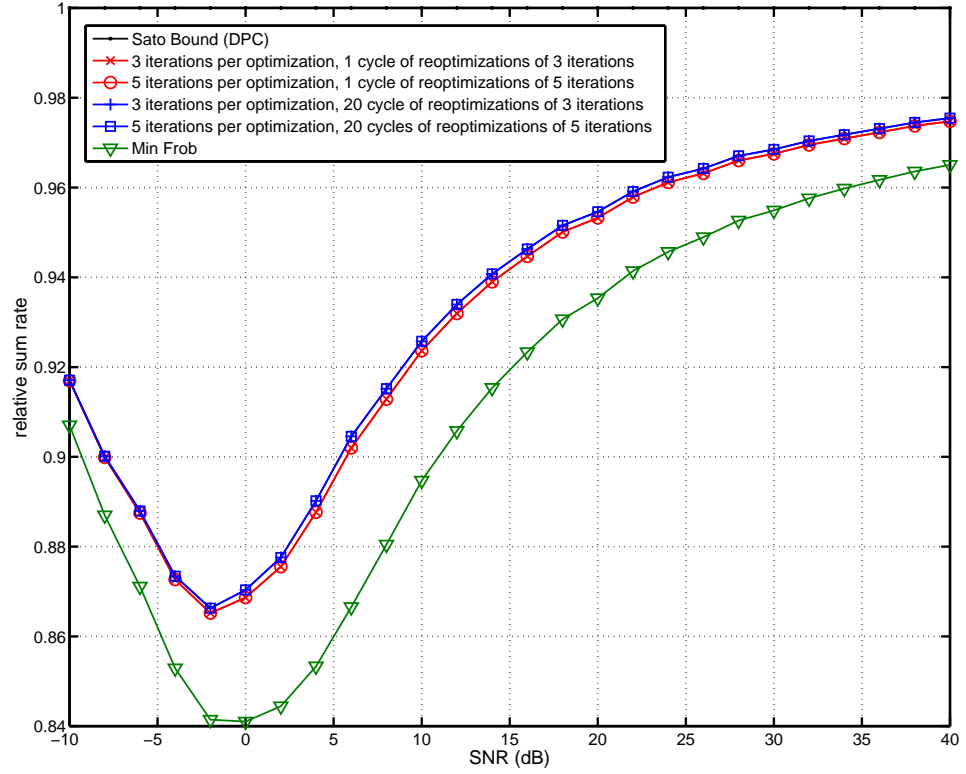
Figure 3.5: Average normalized sum rate of MIMO ZF-BF-GUS: Min Frob versus our iterative algorithm normalized to the Sato bound in the MIMO BC with $M = 8$, $N = 4$ and $K = 30$.
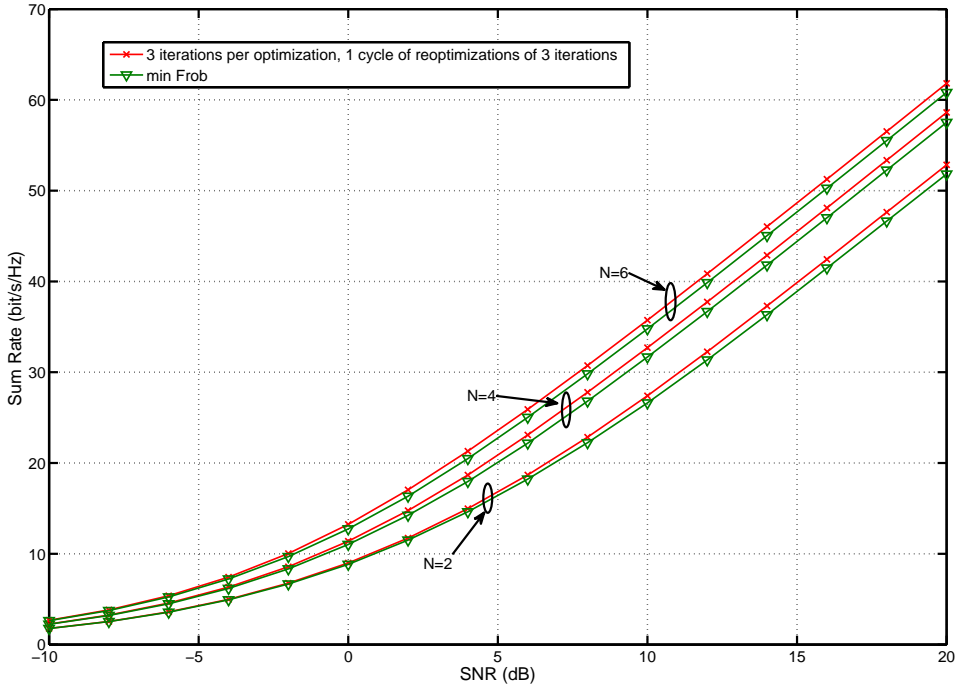
Figure 3.6: Average sum rate of MIMO ZF-BF-GUS: Min Frob versus our iterative algorithm in the MIMO BC with $M = 8$, $K = 30$ and $N \in \{2,4,6\}$.

we one cycle of reoptimization for SNR $= 10$dB for two different configurations. In the first configuration all the users experience the same Rayleigh fading, referred to as uniform configuration. In the second configuration all but two users experience an additional fading of 9 dB (non-uniform configuration). We observe that in the uniform configuration the gain are only because of the cycle of reoptimization whereas in the non uniform our algorithm brings some gain because it handles better different fading. Then, more gains are yielded by the cycle of reoptimization.

3.4 Conclusion

We introduced a new interpretation of the BF greedy user selection described in [53] and an approximate version of the selection criterion. For a sufficiently large K, this user selection process leads to a selection of channel vectors that are close to being mutually orthogonal. Therefore, the contribution of each stream added can be approximated using (3.17). Numerical simulations confirmed that
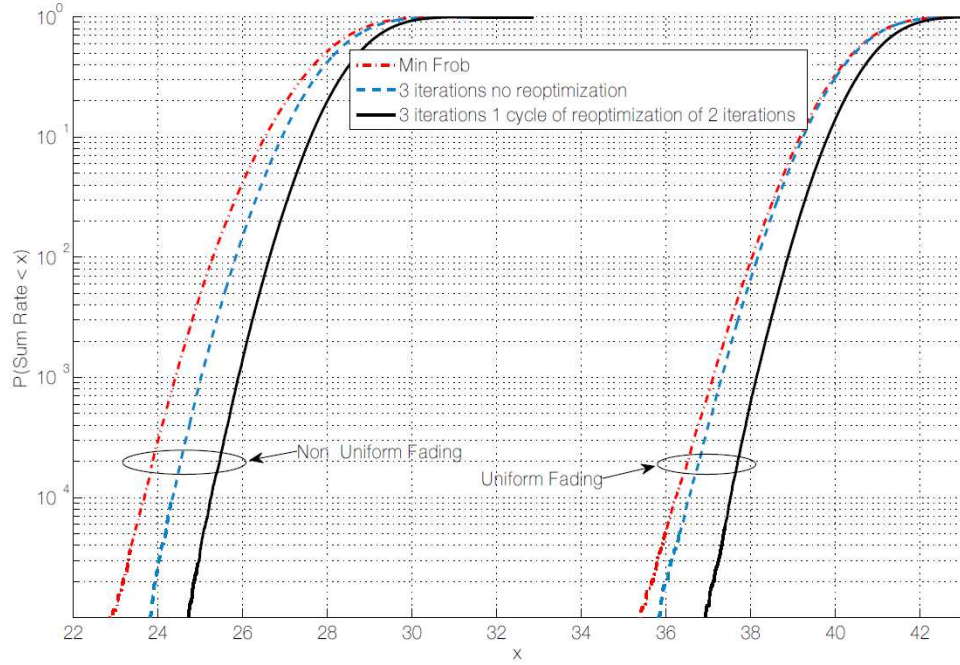
Figure 3.7: CDF of the sum rate of MIMO ZF-BF-GUS: Min Frob versus our iterative algorithm in the MIMO BC with $M = 8$, $K = 30$ and $N = 4$.

this approximation was accurate enough to result in either the same user selection as the original criteria, for small values of K or low SNR, or in the selection of streams that yield a similar sum rate, for large values of K and high SNR.

This also leads to the following result: for a specific, almost mutually orthogonal, user subset, when compared to DPC with orthogonal hypothesis, the rate offset loss induced by the ZF-BF is twice the rate offset loss induced by ZF-DPC.

We developed an extension of this criterion to the MIMO case, a MIMO BF-style GUS criterion with iterative receive filter optimization that we described and evaluated. The algorithm we propose proved to have better performances than the min Frob algorithm. Our algorithm is iterative but converges quickly. Being iterative also calls for a compromise between complexity and performance, empirically we found the tradeoff to be very good because the algorithm converges quickly with good performances. In fact, few iterations per optimization of receive filter are needed and few cycles of reoptimization are enough to obtain some gain in the sum rates.

Chapter 4

Multiple users in interfering cells: Interfering Broadcast Channels

4.1 Introduction

In this chapter, we will see that when considering multi-cell configurations there cannot be too many users, the more users there are in each cell the greater the sum DoF.

The transmission schemes for the IC can be divided into two main categories depending on what bound they aim at approaching. The first category aims at approaching the DoF proper bound [21], which is not always reachable, using spatial extension, or finite time/frequency extensions. The second category is concerned with the DoF decomposition bound, which is always approachable [4].

Asymptotic IA is introduced in [4] and achieves the decomposition bound, $\frac{G}{2}$ DoF in the G-user time-varying single-input single-output (SISO) IC. Using symbol extensions, the scheme partially aligns the interference at the receiver so that more signal dimensions can be used without interference. By using longer symbol extensions, the part of non-aligned symbols becomes negligible and the optimal $\frac{G}{2}$ DoF can be approached. The extension of this technique to square MIMO cases is straightforward. The general MIMO case is studied in [22] where the authors proves that one can attain $G\frac{MN}{M+N}$ DoF, where M and N are the number of transmit and receive antennas, which again increases linearly with G. The decomposition bound is directly transposed to the symmetric IBC with K users per cell and becomes $GK\frac{MN}{M+KN}$. Achievability follows because the asymptotic IA IC scheme does not require antenna cooperation. Therefore, it is also applicable in the IBC [23].

The proper bound is not always attainable and is obtained by counting the

number of equations to satisfy and the number of available variables. In the IC, it is $G\frac{M+N}{G+1}$ and $GK\frac{M+N}{GK+1}$ in the symmetric IBC [24].

Using symbol extensions helps reaching decimal DoF but does not change the proper bound. Indeed, consider the proper bound with T extensions, the number of variables becomes $GK[d(TM - d) + d(TN - d)]$ and the number of ZF constraints remains $GK(GK - 1)d^2$, hence the unchanged proper bound $\frac{d}{T} \leq \frac{M+N}{GK+1}$. However, when considering symbol extensions, the proper bound is no longer an upperbound on the DoF because there is structure in the channel, namely, the channel matrices are diagonal or block diagonal and it renders the channel not generic, which was an assumption used to make the proper bound an upperbound on the DoF.

In the proper bound, the DoF per cell decreases with G whereas it is constant in the decomposition bound. Therefore, if the two bounds intersect, the proper bound is optimal for smaller G. When the proper bound is larger, the DoF of the IC or IBC is between the decomposition bound and the proper bound [23, 25] without symbol extension. However, when the decomposition bound is larger, the DoF of the channel is known because this bound is always achievable by ergodic IA [16], real IA [17] or asymptotic IA with infinite symbol extension [4].

The first contribution in this chapter is a decomposition scheme. In Section 4.2, we extend the ergodic IA to MIMO IC and to MIMO IBC. Ergodic IA is a simple yet powerful tool that not only achieves the optimal $G/2$ DoF of the G-user SISO IC, but also allows each user to achieve at least half of its interference-free capacity at any SNR. By considering more general message sets, Nazer et al. also covered the MISO case. We first consider the single-input multiple-output (SIMO) IC and extend ergodic IA techniques to this setting with N receive antennas. Our scheme achieves $GN/(N + 1)$, which is the DoF yielded by (standard) IA and is also the DoF of the channel when $G > N$. Moreover, this technique exhibits spatial scale invariance. By combining the existing MISO and the new SIMO results, we can also cover MIMO with M transmit antennas for the cases where either M/N or N/M is an integer R, yielding DoF $= \min(M,N)GR/(R + 1)$, which is optimal for $G > R$.

The second contribution is a proper scheme. In Section 4.3, we extend an IA scheme for structured (symbol-extended) channels to MIMO IBC. Numerous techniques allow to increase the multiplexing gain of wireless networks in presence of interference. If some techniques are detailed enough to construct transmit and receive BF filters, most results on the multiplexing gain in the IC are not constructive. Moreover, reaching the optimal multiplexing gain usually require symbol extension, giving a special structure to the channel matrices. Some progress have been made in the IC even with finite symbol extensions but not much in the IBC,

which actually is a more adequate model for nowadays cellular networks. We propose an IA algorithm designed for IBC with symbol extension. Having more than one user per cell complicates the transmission but allows to increase the multiplexing gain. Numerical results confirming the algorithm ability to reach target multiplexing gains are provided.

4.2 A MIMO IBC Decomposition Scheme

4.2.1 Motivation

The idea of pairing complementary channel realizations, *ergodic interference alignment*, was first proposed by Nazer et al. in [16]. The scheme allows each user of an IC to achieve half of his interference free rate, i.e., half of the rate he would achieve if he had the channel for himself. It thereby reaches the optimal DoF $G/2$ of the G-user SISO IC that was first achieved by asymptotic IA [4].

Some improvements have been made to the original ergodic IA scheme, for instance the channel coefficient distribution does not need to be symmetric [46], the sum of channel matrices does not need to be the identity matrix but can be relaxed to an arbitrary diagonal matrix [46], and simple strategies can be deployed to reduce latency [64]. Other efforts were made to generalize the ergodic IA scheme to different networks, for instance for relay networks in [65]. Ergodic IA was also adapted to secrecy scenarios, in which the information leakage is to be minimized in [66]. A variant of ergodic IA for delayed feedback is proposed in Chapter 8, it shows that the full sum DoF $G/2$ of the SISO IC can be preserved for feedback delay as long as half the channel coherence time. Another variant, for completely outdated feedback, is developed in [45] and achieves larger DoF than retrospective alignment [43].

However, to the best of our knowledge, the ergodic alignment scheme and its variants do not cover the general symmetric MIMO IC. Indeed, both IA and ergodic IA schemes are also directly applicable to the MIMO symmetric square case, by decomposing each multi-antenna node in single-antenna nodes, but only asymptotic IA was also extended to SIMO and MISO symmetric configuration in [22] whereas only the MISO setting is covered by ergodic IA with the variant for "recovering more messages" proposed in [16].

We extend ergodic IA techniques to the SIMO IC and achieve the same DoF as asymptotic IA. Together with the existing MISO result we can also cover MIMO configurations with M transmit antennas and N receive antennas for the cases where either M/N or N/M is an integer R, yielding

$$\text{DoF} = \min(M,N)GR/(R+1) \qquad (4.1)$$

which is optimal for $G > R$ [4].

Even though different in terms of idea and complexity, asymptotic IA and ergodic IA schemes share certain characteristics. They both create a delay that roughly scales the same way and both have the property of decomposability: the antennas do not need to be collocated neither at the transmitter nor at the receiver. Therefore, the SIMO and MISO schemes are also directly applicable to interfering broadcast channels and interfering multiple access channels respectively.

Let us recall that the outer bound for the DoF IC depends on whether the ratio R is more or less than G [22]. Asymptotic IA is only needed for $G > R$ because when $G \leq R$ linear techniques usually yield better multiplexing gains. Ergodic IA is meant as an alternative to asymptotic IA; we will see that it achieves the same DoF as asymptotic IA. Therefore, it is only optimal for $G > R$.

4.2.2 System Model and Background

We consider a G-user SIMO IC. The transmitters are equipped with $M = 1$ antenna and the receivers with N antennas. $R = \max(\frac{M}{N}, \frac{N}{M})$ is equal to N in this case. Because our scheme is based on the idea of ergodic IA we have similar assumptions as [16]. Namely, the channel coefficients are drawn from a continuous distribution, their phases are uniformly distributed and are independent from their magnitude.

The channel realization at time index t is

$$
\begin{aligned}
\mathbf{H}(t) &= \{\mathbf{H}_{ji}(t)\} \in \mathbb{C}^{GN \times G} \\
&= \begin{bmatrix}
\mathbf{H}_{11}(t) & \cdots & \mathbf{H}_{g1}(t) & \cdots & \mathbf{H}_{G1}(t) \\
\vdots & \ddots & \vdots & \ddots & \vdots \\
\mathbf{H}_{1g}(t) & & \mathbf{H}_{gg}(t) & & \mathbf{H}_{Gg}(t) \\
\vdots & \ddots & \vdots & \ddots & \vdots \\
\mathbf{H}_{1G}(t) & \cdots & \mathbf{H}_{gG}(t) & \cdots & \mathbf{H}_{GG}(t)
\end{bmatrix}
\end{aligned}
\tag{4.2}
$$

where $\mathbf{H}_{ji}(t) = \{h_{j_a i}(t)\} \in \mathbb{C}^{N \times 1}$ and $h_{j_a i}(t)$ is the channel between transmitter i and receiver's j a^{th} antenna.

The channel output observed at antenna $a \in [1,N]$ of receiver $j \in [1,G]$ is a noisy linear combination of the inputs

$$
y_{j_a}(t) = \sum_{i=1}^{G} h_{j_a i}(t) x_i(t) + n_{j_a}(t)
\tag{4.3}
$$

where $x_i(t)$ is the transmitted symbol of transmitter i, $n_{j_a}(t)$ is the additive white Gaussian noise at antenna a of receiver j.

With

$$\mathbf{x}(t) = [x_1(t), \ldots, x_G(t)]^T, \tag{4.4}$$

$$\mathbf{y}(t) = [y_{1_1}(t), \ldots, y_{1_R}(t), \ldots, y_{G_R}(t)]^T, \tag{4.5}$$

$$\mathbf{n}(t) = [n_{1_1}(t), \ldots, n_{1_R}(t), \ldots, n_{G_R}(t)]^T, \tag{4.6}$$

we have our usual channel input output relationship without filter

$$\mathbf{y}(t) = \mathbf{H}(t)\mathbf{x}(t) + \mathbf{n}(t). \tag{4.7}$$

The performance metric is the sum DoF 2.10.

Ergodic IA

The main idea behind ergodic IA is to transmit the data a first time during channel realization at time t_1, then to wait for the complementary channel realization at times t_2 such that the sum of the two is the $G \times G$ identity matrix. It thereby allows each receiver to cancel all interference by simply adding the signals received at times t_1 and t_2.

The exact match will never happen when channel coefficients are drawn from a continuous distribution. However, it is still possible to match channel matrices up to an approximation error small enough to allow decoding [16]. This can be done through appropriately precise quantization. The authors of [16] prove that, by considering channel realization sequences that are long enough, it is possible to be sure with a sufficient probability that it will be possible to match up enough channel realizations to achieve a DoF that approaches $\frac{G}{2}$.

4.2.3 Main Results

Theorem 3 *In the G-user SIMO IC,*

$$G\frac{N}{(N+1)} \; DoF \tag{4.8}$$

are achievable through ergodic IA.

The theorem is proved in Section 4.2.4 by introducing an ergodic IA scheme that assures the transmission of N symbols between each transmitter-receiver pair over $N + 1$ symbol periods.

Corollary 1 *In the G-user MIMO IC where*

$$R = \max(\frac{M}{N}, \frac{N}{M}) \tag{4.9}$$
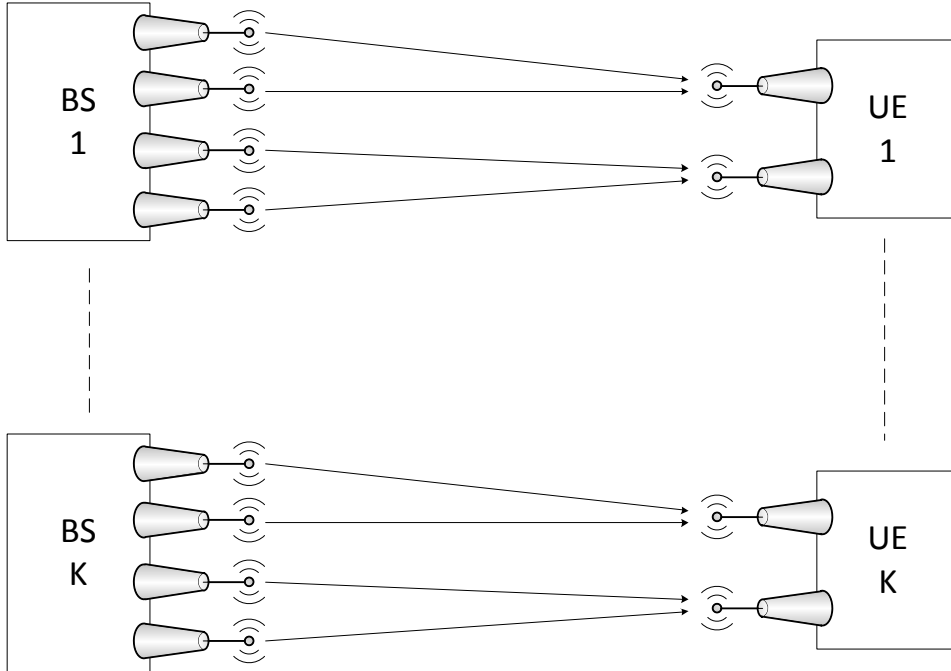
Figure 4.1: Decomposition of the G-user MIMO IC with $M = 4$ and $N = 2$, showing only links supporting intended messages between transmit and receive antennas.

is an integer,

$$\min(M,N)G\frac{R}{(R+1)} \, DoF \tag{4.10}$$

are achievable through ergodic IA.

Proof 1 *1. $R = \frac{M}{N}$: The scheme proposed in [16] for "recovering more messages" can be used. Indeed, by decomposing each node into single-antenna nodes, one obtains GM transmitters and GN receivers. Then, by making each single-antenna receiver ask for R different messages from the single-antenna transmitters, one falls into the framework of the scheme for "recovering more messages". It achieves $\frac{1}{(R+1)}$ DoF per message, which adds up to the $NG\frac{R}{(R+1)}$. An example of this kind of decomposition is given in Fig. 4.1 for the G-user MIMO IC with $M = 4$ and $N = 2$, showing only links supporting intended messages for clarity.*

2. $R = \frac{N}{M}$: By decomposing each transmitter in single-antenna transmitters and each receiver in M receivers with R antennas one obtains a GM-user SIMO

interference IC. According to Theorem 1, in this SIMO IC, $GM\frac{R}{(R+1)}$ are achievable through ergodic IA.

4.2.4 SIMO ergodic IA

Example

We start with an example for the SIMO IC with $G = 3$, $R = N = 2$. The scheme assures the transmission of 2 symbols between each transmitter-receiver pair in 3 symbol periods, over channel realizations t_1, t_2, t_3. Transmitter $i \in [1,3]$ has two messages for receiver i: $[s_1^i, s_2^i]$ and transmits $\mathbf{x}_i(t_n) = s_n^i$ during t_n, $n \in \{1,2\}$ then $\mathbf{x}_i(t_3) = s_1^i + s_2^i$ during t_3. We will see that, by picking channels realizations as below, the IA will be done by simply adding the signals received over the 3 channel realizations at each receiver.

Let the first channel realization be as follows:

$$
\mathbf{H}(t_1) = \begin{bmatrix}
-h_{11_1} & h_{21_1} & h_{31_1} \\
h_{11_2} & h_{21_2} & h_{31_2} \\
h_{12_1} & -h_{22_1} & h_{32_1} \\
h_{12_2} & h_{22_2} & h_{32_2} \\
h_{13_1} & h_{23_1} & -h_{33_1} \\
h_{13_2} & h_{23_2} & h_{33_2}
\end{bmatrix}.
\tag{4.11}
$$

Then, wait for t_2 such that

$$
\mathbf{H}(t_2) = \begin{bmatrix}
h_{11_1} & h_{21_1} & h_{31_1} \\
-h_{11_2} & h_{21_2} & h_{31_2} \\
h_{12_1} & h_{22_1} & h_{32_1} \\
h_{12_2} & -h_{22_2} & h_{32_2} \\
h_{13_1} & h_{23_1} & h_{33_1} \\
h_{13_2} & h_{23_2} & -h_{33_2}
\end{bmatrix}
\tag{4.12}
$$

and for t_3 such that

$$
\mathbf{H}(t_3) = \begin{bmatrix}
-h_{11_1} & -h_{21_1} & -h_{31_1} \\
-h_{11_2} & -h_{21_2} & -h_{31_2} \\
-h_{12_1} & -h_{22_1} & -h_{32_1} \\
-h_{12_2} & -h_{22_2} & -h_{32_2} \\
-h_{13_1} & -h_{23_1} & -h_{33_1} \\
-h_{13_2} & -h_{23_2} & -h_{33_2}
\end{bmatrix}.
\tag{4.13}
$$

First, we can notice that the cross links are chosen to be always the same when the transmitters are sending their symbols one by one, then the opposite when

the sum of the symbols are transmitted. This ensures that, by simply adding its received signals, each receiver cancels all inter cell interference. Then, for receiver i to get only its ath message on its ath antenna, the same rule is applied for the direct links, with the exception of the ath coefficient during t_a so that the intended signal is not canceled by the summation. Indeed, we have

$$\sum_{t=t_1}^{t_3} \mathbf{y}(t) \;=\; \sum_{t=t_1}^{t_3} \mathbf{H}(t)\mathbf{x}(t)$$

$$= \begin{bmatrix} h_{11_1} s_1^1 \\ h_{11_2} s_2^1 \\ h_{22_1} s_1^2 \\ h_{22_2} s_2^2 \\ h_{33_1} s_1^3 \\ h_{33_2} s_2^3 \end{bmatrix} \tag{4.14}$$

and, at each antenna, the intended message can be trivially retrieved. Transmitting 6 messages in 3 channel uses reaches the maximum DoF of $3\frac{2}{3} = 2$ of this SIMO IC.

Proof of Theorem 1.

Proof 2 *To achieve the $G\frac{N}{(N+1)}$ DoF in the G-user SIMO IC, we introduce an alignment scheme that assures the transmission of N symbols between each transmitter receiver pair in $R + 1 = N + 1$ symbol periods, over channel realizations $t_1, \ldots, t_{R+1}$. Transmitter $i \in [1,G]$ has R messages for receiver i: $[s_1^i, \ldots, s_R^i]$ and transmits $\boldsymbol{x}_i(t_n) = s_n^i$ during t_n, $n \in [1,R]$ and $\boldsymbol{x}_i(t_{R+1}) = \sum_{n=1}^R s_n^i$ during t_{R+1}.*

We start with t_{R+1} to simplify the formulas. During the first channel realization, $\boldsymbol{H}(t_{R+1}) = \{h_{j_a i}(t_{R+1})\}$, the sum of all messages is transmitted. Then channel realizations $\{\boldsymbol{H}(t_n)\}$, $n \in [1,R]$ are chosen so that

$$h_{j_a i}(t_n) \;=\; -h_{j_a i}(t_{R+1}) \, \text{for } j \neq i \text{ or } a \neq n \tag{4.15}$$

$$h_{i_a i}(t_n) \;=\; h_{j_a i}(t_{R+1}) \, \text{for } a \neq n. \tag{4.16}$$

By simply summing the signals received over the $N + 1$ symbols periods, each receivers gets one intended message at each of his N antennas, interference free, thereby achieving the $\frac{N}{(N+1)}$ DoF per user.

The certainty that enough pairings can be done to approach the DoF is formally established in [16].

4.2.5 Discussions

Decomposability

The ergodic IA scheme for SIMO IC does not require any joint receive antenna processing; therefore, they also can be used in interfering broadcast channels. With ergodic IA for the MIMO IC, this decomposability property is present at both transmitter and receiver side. This is also true of the asymptotic IA scheme [22] and make the 2 schemes also applicable to interfering multiple access channels.

Delay

For the SISO case, it was shown in [16] that both ergodic IA and standard asymptotic IA create a delay that roughly scales the same way, exponentially with G^2. This delay, needed to have a capacity that scales with $\frac{1}{2}\log P$, is the length of the symbol extension for asymptotic IA and the expected time before finding a channel realization sufficiently close to the exact complementary for ergodic IA. Going from SISO to SIMO, we have to match $N+1$ channel realizations. However, this does not influence the exponent in the delay, which is mainly influenced by the number of possible channel coefficients due to the quantization. Therefore, as a first approximation, the delay of the SIMO variant of ergodic IA should scale exponentially with RG^2. Which again, for large G, is roughly similar to the exponent $\Gamma = RG(G - R - 1)$ of the symbol extension in the SIMO case of asymptotic IA [22].

Improvements

It was shown that improvements could be made to the original SISO ergodic IA scheme; some of them could also be applied to the MIMO version. If the proposed scheme is DoF optimal, the SNR offset might be improved by finding better pairings as was done in [46]. Different pairing methods could also be considered to reduce the delay, with or without rate loss, as was investigated in [64] and [67]. In Chapter 8 we will prove that by slightly modifying the pairing these DoF can still be achieved with only DCSIT during the first transmission.

4.3 A MIMO IBC proper scheme

4.3.1 Motivation

Our focus in this section is on linear IA solutions that aim at approaching the proper bound. Limited symbol extensions are considered because it allows to reach

decimal DoF and can facilitate the enforcement of the alignment while remaining realistic. We consider the IBC because it is realistic to assume multiple receivers in a cell and because of the potential DoF gains compared to the IC [24].

Interesting results on linear IA were first on the DoF level in the IC [21, 68–71] where the authors try to settle the question of IA feasibility depending on the number of transmitter-receiver pairs, antennas and assuming generic channel realizations. Mainly, they indicate that it is sufficient to find a certain invertible Jacobian matrix, implicitly or explicitly, to prove the existence of an IA solution to a certain stream assignment, thereby proving the achievability of a certain sum DoF.

Actual filter design was then studied to approach these DoF. At first, using only the spatial capacity of the nodes, i.e., multiple antennas: [18, 72, 73], and minimizing different cost functions. Minimizing the interference leakage is useful to determine whether alignment is possible or not. Minimizing mean square error is likely to give better performance especially at low SNR. Then, in order to attain decimal DoF, filter design with the help of symbol extension, i.e., using supersymbols over extension in time and/or frequency were investigated. The main issue with symbol extensions is that channel matrices become structured, diagonal or block diagonal, and the previously mentioned algorithms may converge toward rank deficient solutions. In [19, 20] the authors tried to overcome this issue by incorporating the rank of the direct link in the optimization problem but the proposed algorithms still do not always provide acceptable solutions and sometimes suffer from numerical errors. To the best of our knowledge, the IA algorithm for structured channel that achieves the best results is described in [29]. By adding two constraints to the original interference leakage minimization problem, the authors obtain an algorithm that minimizes the interference leakage while preserving the direct links.

Here, we consider the interference minimization problem in the IBC with symbol extension and we add the same constraints as the authors in [29] because they proved to be efficient to yield the good results in the IC.

4.3.2   System Model and Problem Setup

As opposed to decomposition schemes, proper schemes usually are not decomposable; therefore we need to directly consider an IBC and not an IC.

We consider T symbol extensions and denote the resulting $TN_{i_k} \times TM_j$ channel matrix between BS $j \in [1,G]$ and user i_k, $(i,k) \in [1,G] \times [1,K]$.

The challenge of IA is then to find precoding and decoding matrices $\mathbf{V}_j = [\mathbf{V}_{j_1}, \mathbf{V}_{j_2}, \cdots, \mathbf{V}_{j_K}]$ and $\mathbf{U}_{i_k}$ such that the interference is aligned in a subspace at each receiver while the desired signal lay in a interference free subspace of large

enough dimension. Namely, it is required that

$$\text{rank}\,(\mathbf{U}_{i_k}\mathbf{H}_{i_k i}\mathbf{V}_{i_k}) = d_{i_k}, \forall i,k \tag{4.17}$$

$$\mathbf{U}_{i_k}\mathbf{H}_{i_k i}\mathbf{V}_{i_l} = 0, \forall k \neq l \tag{4.18}$$

$$\mathbf{U}_{i_k}\mathbf{H}_{i_k j}\mathbf{V}_j = 0, \forall i \neq j \tag{4.19}$$

where d_{i_k} is the number of streams intended for user i_k. (4.17) assures that the signal space is not collapsed, (4.18) assures that there is no MUI, i.e., interference between streams intended for users within the same cell and (4.19) assures there is no OCI.

The adopted approach here is to minimize the total interference leakage, MUI and OCI :

$$\min_{\mathbf{U},\mathbf{V}} \sum_{\substack{i,j,k,l \\ i \neq j \text{ or } k \neq l}} ||\mathbf{U}_{i_k}^H \mathbf{H}_{i_k j}\mathbf{V}_{j_l}|| \tag{4.20}$$

where $||.||$ is the Frobenius norm.

Without symbol extension, (4.17) is fulfilled with probability one if the channel realizations are generic and as long as full rank precoders and decoders are considered so there is no need to add constraints. However, with symbol extension, the channel matrices become structured and (4.17) may not be respected without adding constraints to the optimization problem. The tweaking of the optimization problem that gave the best results is in [29] for the IC, where the authors added two constraints to the optimization problem. One constraint on the direct links to protect the rank of the signal subspaces and another constraint on the norm of the precoders and decoders so that no normalization that could violate the first constraint will be needed

$$\mathbf{U}_{i_k}^H \mathbf{H}_{i_k i}\mathbf{V}_{i_k}(\mathbf{U}_{i_k}^H \mathbf{H}_{i_k i}\mathbf{V}_{i_k})^H \succeq \epsilon\mathbf{I} \tag{4.21}$$

$$\text{Tr}(\mathbf{U}_{i_k}^H \mathbf{U}_{i_k}) \leq 1 \tag{4.22}$$

$$\text{Tr}(\mathbf{V}_j^H \mathbf{V}_j) \leq 1 \tag{4.23}$$

for $j \in [1,G]$, $i \in [1,G]$ and $k \in [1,K]$, where $\text{Tr}(.)$ denotes the trace of a matrix, $\mathbf{A} \succeq \mathbf{B}$ means that $\mathbf{A} - \mathbf{B}$ is positive semidefinite and ϵ is a parameter that represents the strength of the direct links. Precisely, the smallest singular value of $\mathbf{U}_{i_k}^H \mathbf{H}_{i_k i}\mathbf{V}_{i_k}$ will be greater than $\sqrt{\epsilon}$.

4.3.3   Main Result

Algorithm

We propose an iterative algorithm to solve the optimization problem we defined

$$\min_{\mathbf{U},\mathbf{V}} \sum_{\substack{i,j,k,l \\ i\neq j \text{ or } k\neq l}} ||\mathbf{U}_{i_k}^H \mathbf{H}_{i_k j} \mathbf{V}_{j_l}|| \tag{4.24}$$

$$\text{subject to}$$

$$\mathbf{U}_{i_k}^H \mathbf{H}_{i_k i} \mathbf{V}_{i_k} (\mathbf{U}_{i_k}^H \mathbf{H}_{i_k i} \mathbf{V}_{i_k})^H \succeq \epsilon \mathbf{I}$$

$$\text{Tr}(\mathbf{U}_{i_k}^H \mathbf{U}_{i_k}) \leq 1$$

$$\text{Tr}(\mathbf{V}_j^H \mathbf{V}_j) \leq 1$$

Like many other interference leakage minimization algorithm for the IC our algorithm alternatively optimizes the transmit and the receive filters. The main differences is that in the IBC the MUI must be taken into account and also the transmit filters will be updated V_{j_l} by V_{j_l} and not the whole V_j at once.

First we consider the precoders V_j to be fixed and (4.24) is decomposed into $\sum_{i=1:G} K_i$ independent problems

$$\min_{\mathbf{U}_{i_k}} \quad \text{Tr}(\mathbf{U}_{i_k}^H \mathbf{Q}_{i_k}^{int} \mathbf{U}_{i_k}) \tag{4.25}$$

$$\text{subject to}$$

$$\mathbf{U}_{i_k}^H \mathbf{Q}_{i_k}^{dir} \mathbf{U}_{i_k} \succeq \epsilon \mathbf{I}$$

$$\text{Tr}(\mathbf{U}_{i_k}^H \mathbf{U}_{i_k}) \leq 1$$

where $\mathbf{Q}_{i_k}^{int} = \sum_{j\neq i \text{ or } l\neq k} \mathbf{H}_{i_k j} \mathbf{V}_{j_l} \mathbf{V}_{j_l}^H \mathbf{H}_{i_k j}^H$ is the interference covariance matrix of *both* the OCI from other cells ($i \neq j$) and the MUI from the cell ($i = j, k \neq l$) and $\mathbf{Q}_{i_k}^{dir} = \mathbf{H}_{i_k i} \mathbf{V}_{i_k} \mathbf{V}_{i_k}^H \mathbf{H}_{i_k i}^H$ is the covariance matrix of the desired signal.

A similar optimization problem is solved in [29], the solution is given by

$$\mathbf{U}_{i_k} = \sqrt{\epsilon} \mathbf{U}_{i_k}' (\mathbf{U}_{i_k}'^H \mathbf{Q}_{i_k}^{dir} \mathbf{U}_{i_k}')^{-\frac{1}{2}} \tag{4.26}$$

where $\mathbf{U}_{i_k}'$ is the matrix containing the generalized eigenvectors corresponding to the d_{i_k} smallest generalized eigenvalues of $(\mathbf{Q}_{i_k}^{int} + \mu_{i_k}\mathbf{I}, \mathbf{Q}_{i_k}^{dir})$ and μ_{i_k} is the Lagrange multiplier associated with the power constraint on receive filter $\mathbf{U}_{i_k}$. μ_{i_k} can be found by the bisection method when ensuring the power constraint is respected.

Then similarly, all receive filters $\mathbf{U}_{i_k}$ are considered fixed and the transmit filters $\mathbf{V}_j$ are updated. Contrary to the IC case, in the IBC the transmit filters will

carry messages intended for different receivers and we need to update each $\mathbf{V}_{j_l}$ separately. Again (4.24) is decomposed into $\sum_{i=1:G} K_i$ independent problems.

$$\min_{\mathbf{V}_{j_l}} \quad \mathrm{Tr}(\mathbf{V}_{j_l}^H \mathbf{R}_{j_l}^{int} \mathbf{V}_{j_l}) \tag{4.27}$$

$$\text{subject to}$$

$$\mathbf{V}_{j_l}^H \mathbf{R}_{j_l}^{dir} \mathbf{V}_{j_l} \succeq \epsilon \mathbf{I}$$

$$\mathrm{Tr}(\mathbf{V}_j^H \mathbf{V}_j) \leq 1$$

where $\mathbf{R}_{j_l}^{int} = \sum_{i \neq j \text{ or } k \neq l} \mathbf{H}_{i_k j}^H \mathbf{U}_{i_k} \mathbf{U}_{i_k}^H \mathbf{H}_{i_k j}$ is the interference covariance matrix of the interferences created by streams intended for user j_l received by *both* the users in other cells and the other users in the j cell and $\mathbf{R}_{j_l}^{dir} = \mathbf{H}_{j_l j}^H \mathbf{U}_{j_l} \mathbf{U}_{j_l}^H \mathbf{H}_{j_l j}$ is the signal covariance matrix.

Again the solution is given by

$$\mathbf{V}_{j_l} = \sqrt{\epsilon} \mathbf{V}'_{j_l} (\mathbf{V}'^H_{j_l} \mathbf{R}_{j_l}^{dir} \mathbf{V}'_{j_l})^{-\frac{1}{2}} \tag{4.28}$$

where $\mathbf{V}'_{j_l}$ is the matrix containing the generalized eigenvectors corresponding to the d_{j_l} smallest generalized eigenvalues of $(\mathbf{R}_{j_l}^{int} + \nu_{j_l} \mathbf{I}, \mathbf{R}_{j_l}^{dir})$, ν_{j_l} is the Lagrange multiplier associated with the power constraint on receive filter $\mathbf{V}_{i_k}$ and can be found by the bisection method.

A detailed version of the algorithm is given in Appendix A.3.

4.3.4 Comparison with IA in the IC

We review here the main difference with the algorithm proposed in [29] for the IC. The first difference is that each computation on each side needs to be made for each user. When computing receive filters it is quite logical: each receive filter update is calculated one by one. However, on the transmitter side, this means that we now need to decompose each transmit filter $\mathbf{V}_j = [\mathbf{V}_{j_1}, \mathbf{V}_{j_2}, \cdots, \mathbf{V}_{j_{K_j}}]$ in the concatenation of the precoding matrices for each of its K_i users and that each of this subfilter $\mathbf{V}_{j_k}$ is updated independently whereas in the IC case the whole filter $\mathbf{V}_j$ was updated at once.

This also means that there are more interference covariance and signal covariance matrices and that they need to be computed differently too. Indeed, now $\mathbf{Q}_{i_k}^{int} = \sum_{j \neq i \text{ or } l \neq k} \mathbf{H}_{i_k j} \mathbf{V}_{j_l} \mathbf{V}_{j_l}^H \mathbf{H}_{i_k j}^H$ is the interference covariance matrix of *both* the OCI from other cells ($i \neq j$) and the MUI from the cell ($i = j, k \neq l$) whereas in [29] we only had $\mathbf{Q}_i^{int} = \sum_{j \neq i} \mathbf{H}_{ij} \mathbf{V}_j \mathbf{V}_j^H \mathbf{H}_{ij}^H$. The difference is that on top of the OCI we added the MUI. Similarly for the direct link we now have $\mathbf{Q}_{i_k}^{dir} = \mathbf{H}_{i_k i} \mathbf{V}_{i_k} \mathbf{V}_{i_k}^H \mathbf{H}_{i_k i}^H$ when in the IC it was $\mathbf{Q}_i^{dir} = \mathbf{H}_{ii} \mathbf{V}_i \mathbf{V}_i^H \mathbf{H}_{ii}^H$ because now

we have to take into account that not everything coming from BS i is intended for user i_k but only what is sent along the kth component of the filter: $\mathbf{V}_{i_k}$.

These matrices being used to compute $\mathbf{U}'_{i_k}$ and $\mathbf{U}_{i_k}$ that are then different from [29] because the inputs are different.

Similarly on the transmitter side, for the interference covariance matrix we now have $\mathbf{R}^{int}_{jl} = \sum_{i \neq j \text{ or } k \neq l} \mathbf{H}^H_{i_k j} \mathbf{U}_{i_k} \mathbf{U}^H_{i_k} \mathbf{H}_{i_k j}$ instead of $\mathbf{R}^{int}_j = \sum_{i \neq j} \mathbf{H}^H_{ij} \mathbf{U}_i \mathbf{U}^H_i \mathbf{H}_{ij}$ because now not only the generated OCI needs to be taken into account but also the generated MUI.

Again this changes $\mathbf{V}'_{jl}$ because $\mathbf{R}^{int}_{jl}$ is changed and then is also changes $\mathbf{V}_j$ because only $\mathbf{V}'_{jl}$ is updated and not the whole $\mathbf{V}'_j$.

4.3.5 Numerical Results

In this section we provide numerical validation of the proposed algorithm. Being able to transmit in the IBC can provide some DoF gain and being able to use symbol extension should be advantageous especially with few antennas.

We focus on a symmetric IBC: $G = 4$, $K_i = K \in \{1,2,4\}$, $M_j = M = 1$ and $N_{i_k} = N = 1$. For $K_i = K \in \{1,2,4\}$ we assign $d_{i_k} = d \in \{4,2,1\}$ streams per user so that 4 DoF per BS are always assigned over the symbol extension. However, we use slightly different symbol extensions in order to increase the total DoF with K and benefit from having more than one user in the cells. Precisely, we use 11, 10 and 9 symbol extensions. Therefore, for $K = 1$ we assign a total of $16/11 \approx 1.4545$ DoF, for $K = 2$ a total of $16/10 = 1.6$ DoF and for $K = 4$ a total of $16/9 \approx 1.7778$ DoF. This values are chosen because they all represent about 90% of the proper bound, which, given by $GK\frac{M+N}{GK+1}$, is respectively 1.6, $16/9 \approx 1.778$ and $32/17 \approx 1.8823$ for our three configurations. Channel coefficients are zero mean Gaussian random variables with unit variance and we set $\epsilon = 10^{-3}$.

In Fig. 4.2 we plot the sum rate reached by the proposed algorithm and by a similar extension of min leakage [18] in the aforementioned configurations. It confirms that the target DoF are reached by the proposed algorithm but not by the IBC extension of the min leakage algorithm. It is especially interesting for $K = 4$ because considering this IBC with one stream per user and 9 symbol extension reaches a multiplexing gain of $16/9 \approx 1.7778$ strictly superior to the 1.6 upper bound of the four-user SISO IC and significantly more than the $16/11 \approx 1.4545$ DoF that we obtained using [29] (for $K = 1$).

In this section we have confirmed that the algorithms works, and that it significantly outperforms the IC version [29] that can serve only one user per cell. This is because with this IBC algorithm we are able to serve more users at the same time in a cell. Therefore, we are able to increase the multiplexing gain, which brings significant sum rate gains as shown on Fig. 4.2. It is interesting to notice that when
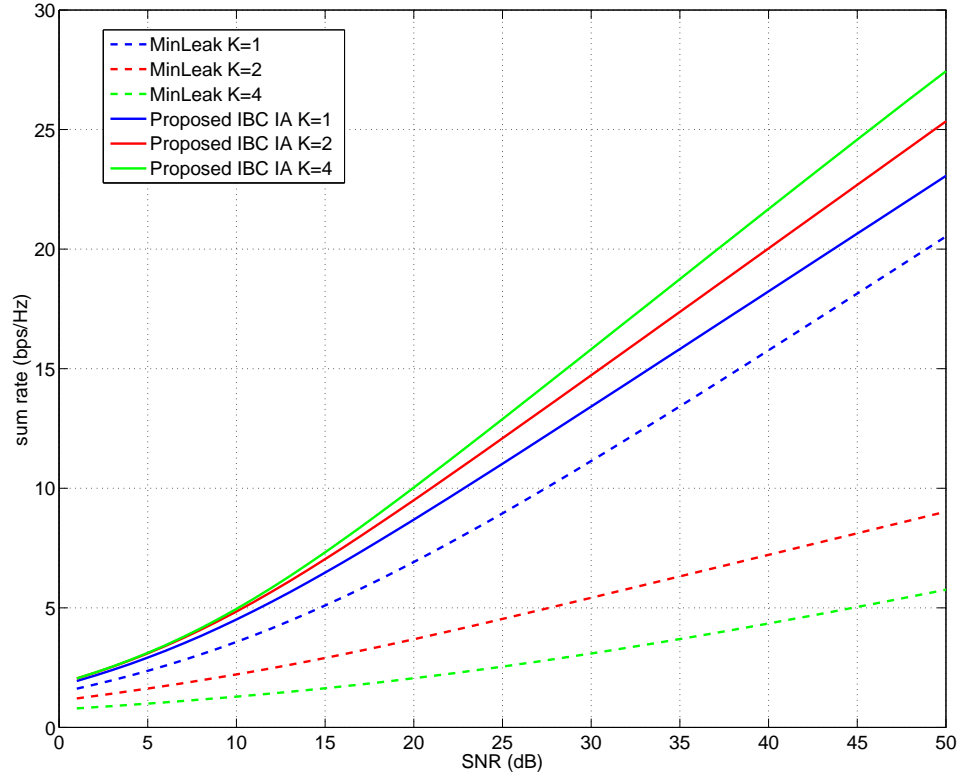
Figure 4.2: Sum rate of the 4-cell IBC with $K_i = K \in \{1,2,4\}$, $M_j = M = 1$ and $N_{i_k} = N = 1$.

extending the min leakage algorithm in a similar way it does not perform well for $K > 1$.

4.4 Conclusion

The DoF of an IBC grows with the number of users whether it is with decomposition or with proper bound. This has been illustrated and taken advantage of in this chapter with two contributions.

The first concerns the decomposition bound, we extended the ergodic IA technique to the SIMO IC. Because no joint antenna processing is needed, this technique trivially exhibits spatial scale invariance i.e., decomposability. Therefore, these SIMO results, combined with the existing MISO results, allow to cover the

symmetric MIMO configurations as well as IBC.

Concerning the proper bound, we have proposed an algorithm for the design of receive and transmit filters for the IBC with finite symbol extensions. It minimizes the interference leakage under two additional constraints that assure that the direct links will be preserved through the iterations. Having more than one user in each cell allows to increase the multiplexing gain. Using efficiently symbol extensions is useful to reach decimal multiplexing gains and, therefore, is especially useful in configurations with few antennas. The efficiency of the algorithm has been confirmed by numerical simulations that were conclusive.

Chapter 5

Partially Connected Interfering Broadcast Channels

5.1 Motivation

Both types of IA techniques, asymptotic and linear IA can be adapted to be used in partially connected IBC but only to a limited extent. For instance, asymptotic IA does not require joint processing at the antennas, so asymptotic IA techniques can directly be used in IBC [22]; however, it is not easy to take into account and benefit from the partial connectivity. Moreover, asymptotic IA requires long symbol extensions, which grow exponentially with the number of antennas, to yield decent multiplexing gains. On the other hand, some work have been done to find linear IA solutions that benefits from the partial connectivity [26, 27]. However, they often rely on a heuristic search for a sub system for which simple linear IA solution can be deployed.

We focus on a special class of IBC that may arise with small cells. Namely, we consider interfering BC with 2 antennas at the transmitter and 2 users per cell, one with multiple antennas that receives interference from the other cells and a second one that is isolated from the OCI and have only one antenna, or possibly multiple antennas but only a channel of rank one because of being in line of sight (LOS) for instance.

The classic IA scheme [18] does not perform well in this setting both because of the cellular framework [28] and because of the use of symbol extension [29].

The best known method for this kind of network would be to use a heuristic to find a stream assignment that is feasible with linear IA and then do linear IA without symbol extension as in [27]. What we propose is to make a wise use of a first level of precoders and decorrelators in order to obtain 2 isolated networks.

69

On one side, the isolated users would not only be isolated from the OCI because of the partial connectivity but also from the multi-user interference (MUI) within their cell that are due to data transmitted to the second user in the cell. On the other side, the interfered users would only receive OCI that are due to the streams intended for the other interfered user but would not get the interference due to streams meant for the isolated users. In other words, after separation, we will have 2 isolated networks, G parallel single-user SISO links and one G-user SISO IC. Then, they can be treated separately and we will observe that this leads to an improvement of the multiplexing gain, i.e., an increase of the number of streams that can be assigned, compared to the state of the art.

The proposed solution can also be used on the dual network. The dual network configuration is called interfering multiple access channels (several MAC [74], that are mutually interfering), and can be either the reverse link (uplink) of the IBC i.e., multiple cells comprising multiple mobile users that are transmitting to a single BS [75], or an heterogeneous network [76] on the contrary if we have multiple BSs (macro and small cell BSs for instance) in each cell, serving a single user. Any solution for the original problem can be used on the dual networks thanks to the IMAC-IBC duality [75]. Our partially connected configuration can model interfering macro cells that are transmitting to single users in their cell that are also in reach of small cells that do not interfere outside the small cell. The proposed solution can be used on both the uplink of the considered IBC and the heterogeneous network configuration we just described.

Within the IC (or IBC) framework, data sharing is usually not considered. Only CSI can be assumed to be available at all transmitters and not the data, which is assumed to be available at only one transmitter. However, the dual networks studied here are examples of heterogeneous networks and are usually considered within the framework of coordinated multipoint (CoMP) transmissions. CoMP techniques are separated into two categories depending on whether or not the data are shared between transmitters [77]. CoMP joint transmission (CoMP-JT) provides the highest sum rate gains by benefiting of the data sharing when CoMP coordinated BF (CoMP-CB) brings smaller gains but relies only on CSI sharing. The backhaul overhead needed for data sharing in CoMP-JT can quickly become prohibitive when the number of collaborating transmitters increases [3]. An intermediate solution is proposed in [78], in which the authors considered clustering to limit the need for data sharing to reasonably small clusters. Further improvement were made by jointly designing the clusters and the BF in [79] but are limited to a single beam per user transmissions. Then, in [80] the authors go back to CoMP-CB to reduce the cooperation overhead to its minimum and still achieve interesting results by jointly designing the cluster (i.e., the mobile-BS pairing) and the BF.
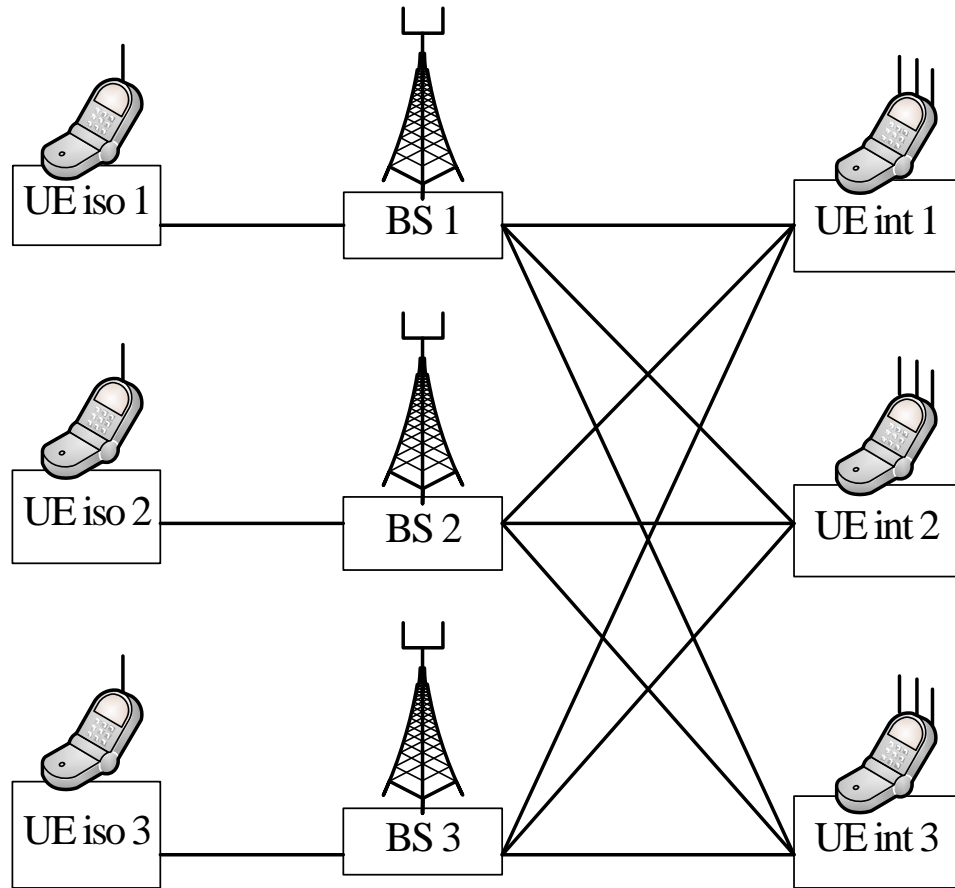
Figure 5.1: Considered configuration of partially connected IBC for $G = 3$.

However, in these techniques either the data is shared or the users are served only by one transmitter.

By using our approach on the dual network, we have an interesting transmission technique that falls into the CoMP-CB, i.e., it does not need any data sharing. Also, multiple transmitters can serve one user simultaneously with different data streams, which allows reaching larger multiplexing gains.

71
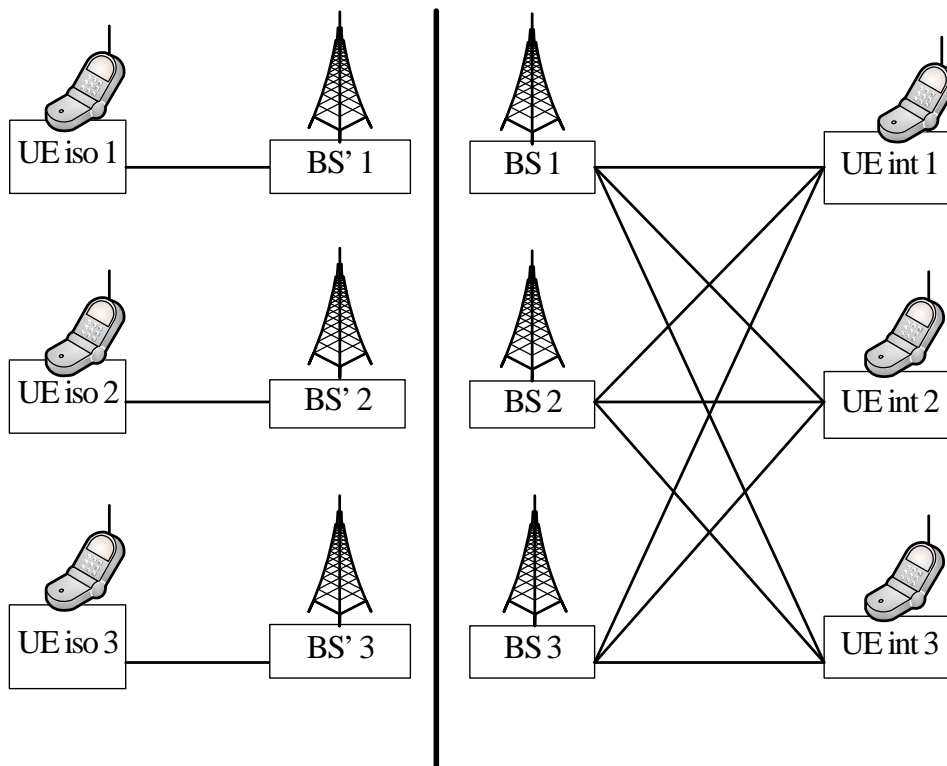
Figure 5.2: Considered configuration of partially connected IBC for $G = 3$ after separation.

5.2 IBC System Model and Background

5.2.1 System Model

We consider a G-cell two-user IBC, i.e., there are G cells, each with one transmitter and $K = 2$ receivers. In each cell, the transmitter has $M = 2$ antennas, one of the receivers has a single antenna and is isolated from the interference generated in the other cells, we call it the isolated receiver. The second receiver in each cell has G antennas at least and receives all the interference, we call it the interfered receiver. An example is illustrated in Fig. 5.1 for the 3-cell case.

$\mathbf{H}_{i_1 i}[t] \in \mathbb{C}^{1 \times 2}$ denotes the channel matrix at time t between the transmitter in cell i and its isolated receiver. $\mathbf{H}_{j_2 i}[t] \in \mathbb{C}^{G \times 2}$ denotes the channel matrix at time t between the transmitter in cell i and the interfered receiver in cell j. The partial connectivity means that $\forall i \neq j, \mathbf{H}_{i_1 j}[t] = 0$ so to avoid cumbersome notations $\mathbf{H}_{i_1 i}[t]$ is shortened to $\mathbf{H}_{i_1}[t]$.

The channel output observed at interfered receiver $j \in [1, G]$ is a noisy linear combination of the inputs of the different transmitters

$$\mathbf{y}_{j_2}[t] = \sum_{i=1}^{G} \mathbf{H}_{j_2 i}[t] \mathbf{x}_i[t] + \mathbf{n}_{j_2}[t] \tag{5.1}$$

where $\mathbf{x}_i[t]$ is the transmitted symbol of transmitter i, $\mathbf{n}_{j_2}[t]$ is the additive white Gaussian noise of variance σ^2 at interfered receiver in cell j.

The channel output observed at isolated receiver $j \in [1, G]$ is a noisy linear combination of the inputs of only its own transmitter

$$\mathbf{y}_{j_1}[t] = \mathbf{H}_{j_1}[t] \mathbf{x}_j[t] + \mathbf{n}_{j_1}[t] \tag{5.2}$$

where $\mathbf{n}_{j_1}[t]$ is the additive white Gaussian noise of variance σ^2 at the interfered receiver in cell j.

To avoid cumbersome notations the time index will be omitted when no confusion is possible.

The first performance metric is sum DoF 2.10

It is possible to use linear techniques to separate the network in 2 isolated networks, as illustrated in Fig. 5.2. For that purpose, we will use precoders $\mathbf{W}_i$, $i \in [1, G]$ and the algorithm to perform this separation is given in Section 5.3.1. In this chapter $\mathbf{U}$ and $\mathbf{V}$ will be used to denote the second level of precoders and decorrelators used within one of the isolated sub network.

5.2.2 Relevance

In numerous works, partial connectivity was considered to model systems that are larger than the span of interference [81–83]. One would consider G cells, but have

only overlapping subsets of $G' \leq G$ cells that are interfering one with another. For instance, cell g would be interfered only by cell $g-1$ and cell $g+1$. Our model of partial connectivity differs but can be an approximation of 3 different realistic scenarios that are described hereafter.

Cell Edge and Cell Center Users

Our system model can be a first approach to model an IBC in which some users are in the edge of the cell and, therefore, receiving interference from the other cells (interfered users) and some users are closer to the BS and not receiving interference from the other cells (isolated users). Moreover, a LOS component would justify the fact that even multiple-antennas users in the cell center have only a rank one channel.

Dense Small Cells

Small cells is another context in which configurations like ours arise. Indeed, higher BS density increases the possibility of having several users covered by multiple BSs; and the lessened height of the BS in small cells together with the topology of cities makes it possible to have isolated users. For instance, users in the middle of the street could only be covered by one BS thanks to the buildings whereas users at crossroads could be covered by multiple BSs. Again, a LOS component would justify the fact that some isolated users have only one effective antenna.

Dual Heterogeneous Networks

The dual heterogeneous network is also of interest. It corresponds to having G users with 2 antennas, served each by both a macro cell and a small cell with the macro cells generating interference but not the small cells because of their smaller power. The macro BS has at least G antennas but the small BS has only one antenna. The different number of antennas at the transmitters is also coherent because the small cells BS are likely to have fewer antennas or to be in LOS. Similar assumptions were made in [76, 84].

DoF analysis

A DoF analysis of fully IBC was conducted in Chapter 4 and known results about the DoF of symmetric fully connected IBC were reviewed. The partial connectivity and asymmetry considered here complicates the DoF analysis. However, by first separating the network into 2 independent subnetworks we transform the original

problem in 2 independent problems for which DoF optimal solutions are known. Though the approach may still be suboptimal, it proves to yield DoF gains.

5.3 Transmission Strategy

5.3.1 Separation

The idea is to first split the IBC in 2 isolated networks. The G isolated users are already quite isolated because of the partial connectivity. Indeed they receive no OCI, but only MUI from the streams intended to the other user in the cell. Each BS having 2 antennas and 2 users, simple ZF precoding can be used to make sure the isolated users do not receive any interference. By doing so we have an isolated network of G parallel SISO links.

The interfered users have $N = G$ antennas[1]. Because we intend to create a separate SISO IC, we only need to align the interference coming from streams assigned to isolated users and we do not take care of the other interference due to streams assigned to interfered users that are naturally present in an IC. Moreover, it is enough to align the interference over $G - 1$ dimensions at each receiver. Indeed, any interfered user receives interference from other cells on a $G - 1$ dimensional subspace and its BS then makes sure that the MUI at this interfered user will be aligned in this $G - 1$ dimensional subspace, which can then be zeroforced because the receiver has G antennas.

This way, the interfered users will still have one signaling dimension with their data and only the interference of the SISO IC. In other words, we need to find $\mathbf{W}_i = [\mathbf{W}_i(1)\mathbf{W}_i(2)], i \in [1,G]$ such that

$$\text{Rank}[\mathbf{H}_{1_21}\mathbf{W}_1(1) \ \mathbf{H}_{1_22}\mathbf{W}_2(1) \quad \cdots \quad \mathbf{H}_{1_2G}\mathbf{W}_G(1)] = G - 1$$
$$\text{Rank}[\mathbf{H}_{2_21}\mathbf{W}_1(1) \ \mathbf{H}_{2_22}\mathbf{W}_2(1) \quad \cdots \quad \mathbf{H}_{2_2G}\mathbf{W}_G(1)] = G - 1$$
$$\cdots$$
$$\text{Rank}[\mathbf{H}_{G_21}\mathbf{W}_1(1) \ \mathbf{H}_{G_22}\mathbf{W}_2(1) \quad \cdots \quad \mathbf{H}_{G_2G}\mathbf{W}_G(1)] = G - 1 \tag{5.3}$$

and

$$[\mathbf{H}_{1_1}\mathbf{W}_1(2) \ \mathbf{H}_{2_1}\mathbf{W}_2(2) \ \cdots \mathbf{H}_{G_1}\mathbf{W}_G(2)] = [0 \ 0 \ \cdots \ 0] \tag{5.4}$$

A simple iterative algorithm can be used to fulfill these conditions.

---

[1]We focus on the case $N = G$ even though a similar strategy could still be used when there are more than G receive antennas at the interfered receivers.

1. Generate one random virtual receive antenna at each interfered receiver: $\mathbf{a}_i \in \mathbb{C}^{1 \times G}$ that is then normalized, $\mathbf{a}_i = \frac{\mathbf{a}_i}{\mathbf{a}_i \mathbf{a}_i^H}$, and set the BF matrices as follows:

$$\forall i \in [1, G], \mathbf{W}_i = \begin{pmatrix} \mathbf{H}_{i_1} \\ \mathbf{a}_i \mathbf{H}_{i_2 i} \end{pmatrix}^{-1} \tag{5.5}$$

   Doing so assures condition (5.4) is satisfied and will actually be done at each iteration.

2. Iteratively fulfill each rank constraint in (5.3) by defining the new virtual antennas to belong in the appropriate null space[2]

$$\mathbf{a}_1 \in \text{null} \begin{bmatrix} (\mathbf{H}_{1_2 2} \mathbf{W}_2(1))^T \\ (\mathbf{H}_{1_2 3} \mathbf{W}_3(1))^T \\ \cdots \\ (\mathbf{H}_{1_2 G} \mathbf{W}_G(1))^T \end{bmatrix}, \mathbf{W}_1 = \begin{pmatrix} \mathbf{H}_{1_1} \\ \mathbf{a}_1 \mathbf{H}_{1_2 1} \end{pmatrix}^{-1} \tag{5.6}$$

$$\mathbf{a}_2 \in \text{null} \begin{bmatrix} (\mathbf{H}_{2_2 1} \mathbf{W}_1(1))^T \\ (\mathbf{H}_{2_2 3} \mathbf{W}_3(1))^T \\ \cdots \\ (\mathbf{H}_{2_2 G} \mathbf{W}_G(1))^T \end{bmatrix}, \mathbf{W}_2 = \begin{pmatrix} \mathbf{H}_{2_1} \\ \mathbf{a}_2 \mathbf{H}_{2_2 2} \end{pmatrix}^{-1} \tag{5.7}$$

$$\cdots$$

$$\mathbf{a}_G \in \text{null} \begin{bmatrix} (\mathbf{H}_{G_2 1} \mathbf{W}_1(1))^T \\ (\mathbf{H}_{G_2 2} \mathbf{W}_2(1))^T \\ \cdots \\ (\mathbf{H}_{G_2 (G-1)} \mathbf{W}_{G-1}(1))^T \end{bmatrix}, \mathbf{W}_G = \begin{pmatrix} \mathbf{H}_{G_1} \\ \mathbf{a}_G \mathbf{H}_{G_2 G} \end{pmatrix}^{-1} \tag{5.8}$$

3. Repeat 2) until (5.3) is satisfied. Then we should have (5.4) satisfied and also

$$\mathbf{a}_i \mathbf{H}_{i_2 j} \mathbf{W}_j(1) = 0 \quad \forall (i, j) \tag{5.9}$$

(5.4) and (5.9) are the mathematical formulations of the separation. (5.4) means that, in Fig. 5.2, the network on the left does not receive any interference

---

[2]The null space being of dimension one, this inclusion is an equality and can be used to define a vector.
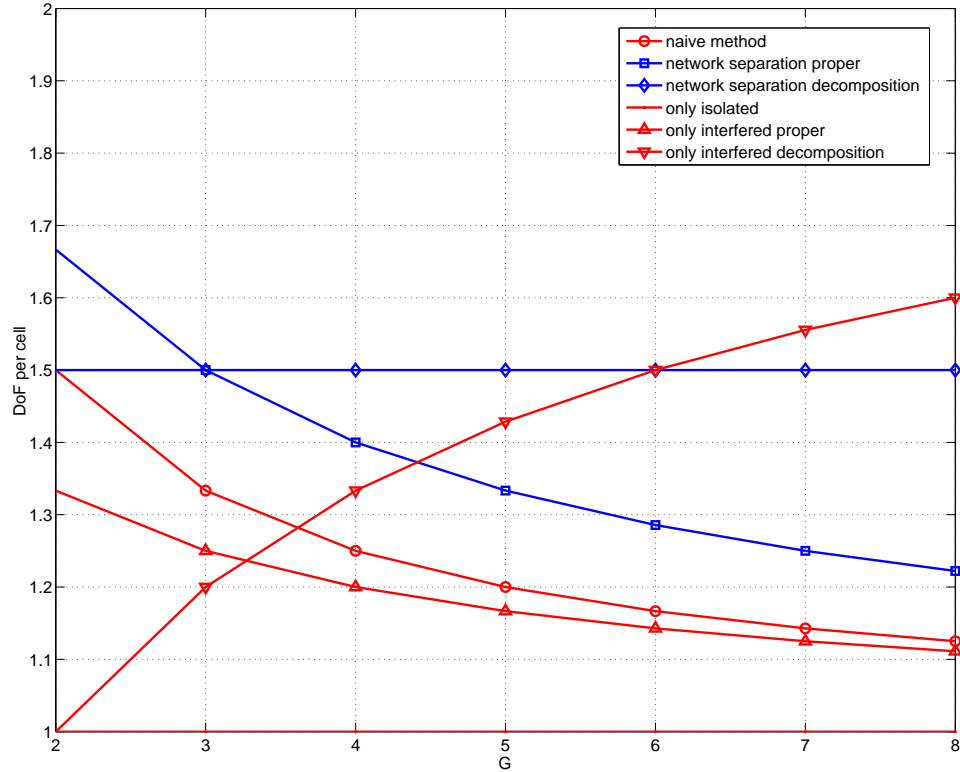
Figure 5.3: DoF per cell for different schemes.

from the network on the right; (5.9) means that the network on the right does not receive any interference from the network on the left.

Remarks: The exact alignment may not be reached within a finite number of iterations, it is not a problem as long as the remaining leakage is sufficiently small. Better chances of convergence can be secured by only partially updating the $\mathbf{a}_i$: instead of giving the new value to $\mathbf{a}_i$, having it updated to a weighted sum of its former value and the new value slightly slows the convergence down but make it more robust. If the minimum leakage is not reached within a reasonable number of iterations, reinitializing the $\mathbf{a}_i$ proves to be efficient.

A detailed version of algorithm is given in Appendix A.4.

5.3.2 DoF After Separation

By using the precoding matrices $\mathbf{W}_i$ and receive vectors $\mathbf{a}_i$, one obtains 2 separated SISO networks, one with G parallel links and another which is a G-user SISO IC.

The two networks are independent and do not generate interference towards one another as illustrated in Fig. 5.2.

Over the parallel links, one can achieve G DoF by simple means of G SISO point-to-point transmissions. Over the IC, one can try to approach either the decomposition bound, $\frac{G}{2}$, or the proper bound, $\frac{2G}{G+1}$. Overall, resorting to asymptotic IA allows to approach

$$\text{DoF(separation decomposition)} = \frac{3G}{2} \tag{5.10}$$

and linear IA

$$\text{DoF(separation proper)} = G + \frac{2G}{G+1} = \frac{G^2 + 3G}{G+1}. \tag{5.11}$$

5.3.3 Simple Strategies

Without performing the separation of the networks into 2 independent networks, one could resort to what we call the naive strategy: simply transmit G streams to the isolated users and one stream to one of the interfered users, for instance the interfered user of cell 1. This can be done by having each BS do zeroforcing between its isolated user and a virtual antenna at the first interfered user

$$\forall i \in [1,G], \mathbf{W}_i = \begin{pmatrix} \mathbf{H}_{i_1} \\ \mathbf{a}_1 \mathbf{H}_{1_2 i} \end{pmatrix}^{-1} \tag{5.12}$$

where $\mathbf{a}_1$ is the receive filter creating the virtual antenna at interfered user 1. Then, only the first BS transmits 2 streams, and the others only send one stream to their isolated user but without sending any interference on the virtual antenna of interfered user one. By doing so one would obtain

$$\text{DoF(naive)} = G + 1. \tag{5.13}$$

Two even simpler methods can be used by only considering a subset of receivers. Considering only the isolated receivers only yields

$$\text{DoF(only iso.)} = G \tag{5.14}$$

and is never interesting in a DoF perspective. On the other hand, considering only the interfered users results in treating a G-user MIMO IC with $M = 2$ and $N = G$ in the which the proper bound is

$$\text{DoF(only int. proper)} = \frac{G+2}{G+1}G = \frac{G^2 + 2G}{G+1} \tag{5.15}$$

and the decomposition bound is

$$\text{DoF(only int. decomposition)} = \frac{2G}{G+2}G. \tag{5.16}$$

We notice that, for large G, the decomposition scheme in (5.16), only treating the interfered users, could approach $2G$ DoF, which is more than the $3G/2$ obtained using decomposition scheme after separation. However, it is only for large G and even though the proposed scheme is valid for any G, G is usually considered not too large to keep the scenario representative and to keep the cooperation realistic. Moreover, when it comes to asymptotic IA schemes that can be used to approach the decomposition bound, the delay induced increases exponentially with G, but also with the number of antennas. Therefore, only schemes for small G and with few antennas may be considered to yield decent multiplexing gain with a reasonable number of symbol extensions. Some improvements have been made to require less extensions but usually then require only frequency extension [85] and remain unrealistic for large G. Another alternative is ergodic IA but it also induces unrealistic delays [16]. The third alternative is real IA. It is a constellation dependent scheme and its behavior in real system is difficult to forecast. Given the state of the art, there seem to be no asymptotic scheme available to bring decent multiplexing gain, with reasonably short symbol extensions.

Note that, the DoF obtained using the partial connectivity are equal to the DoF one would obtain by allowing user cooperation without using the partial connectivity. Indeed, in a G cell MIMO IC with 2 transmit antennas and $G + 1$ receive antennas, the proper bound is

$$\text{DoF(user cooperation proper)} = \frac{G+3}{G+1}G = \frac{G^2 + 3G}{G+1} \tag{5.17}$$

and is equal to (5.11). By using a feature of realistic networks (partial connectivity) we are able to have the same gain as by using the less realistic assumption of user cooperation.

In Fig. 5.3, we plot the DoF per cell bounds of the different strategies considered. As expected from the formulas, using a decomposition scheme only on the interfered users proves interesting for large G, precisely for $G \geq 7$. For more realistic values of G like $G \leq 6$, we observe that first separating the network as proposed provides larger DoF. These results justify the idea of first separating this kind of networks when it comes to maximizing the DoF, so it make sense for an high SNR analysis. In Section 5.5, we provide simulation results to demonstrate that this approach is also valid for reasonable values of SNR.
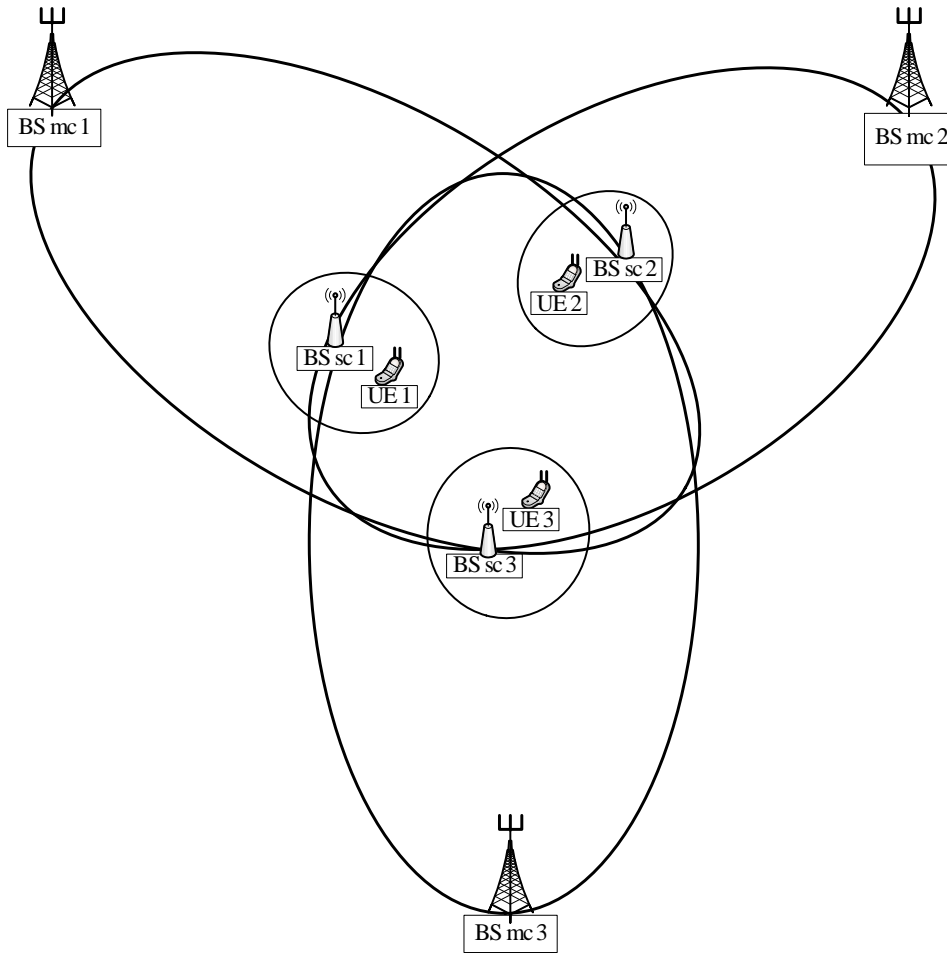
Figure 5.4: Considered dual configuration for $G = 3$.

G	N_{int}	naive	separation-proper	separation-decomp.
3	6	8	9	9
4	8	10	11.2	12
6	12	14	15.43	18

Table 5.1: DoF in different configurations for M=4.

5.3.4 Different Configurations

The two level strategy is presented here for the case of transmitters having $M = 2$ antennas but can be generalized to transmitter with more antennas. For instance if we have $G = 3$ transmitters with $M = 4$ antennas, each serving $K_{iso} = 2$ single-antenna isolated users and an $K_{int} = 1$ interfered user with $N_{int} = 6$ antennas, dimension-wise, it is still possible to isolate all the isolated users on one side, thereby creating six parallel SISO links, and a three-user MIMO IC with two antennas at each transmitter and each receiver on the other side. Doing so allows to reach 9 DoF instead of the 8 DoF that the naive approach would reach in this configuration. In the Table 5.1, we give some DoF values that can be reached when $M = 4$ and $K_{iso} = 2$ for different number of cells.

The same DoF can be obtained if we have one isolated user per cell ($K_{iso} = 1$) with two antennas per isolated user ($N_{iso} = 2$) instead of two isolated users with one antennas.

More generally with, any M, K_{iso} and N_{iso} such that $M > N_{iso}K_{iso}$ and

$$N_{int} = \underbrace{(G-1)N_{iso}K_{iso}}_{\text{interference}} + \underbrace{M - N_{iso}K_{iso}}_{\text{desired signal}}, \qquad (5.18)$$

after separation the isolated users can receive $GN_{iso}K_{iso}$ DoF and the interfered users $2G(M-N_{iso}K_{iso})/(G+1)$ with a proper approach and $G(M-N_{iso}K_{iso})/2$ with a decomposition approach.

The naive approach would only reach $GN_{iso}K_{iso} + (M - N_{iso}K_{iso})$, which is always less than the separation + proper approach, and less than the separation + decomposition approach for $G \geq 3$.

5.4 Dual Heterogeneous Networks

The two-level strategy we proposed can also be employed in the dual network which is an example of heterogeneous network. In more detail, we can consider G users with 2 antennas, each served by 2 transmitters, one in a macro cell that also generates interference to the other users and one in a small cell that does not

generate interference. An example is illustrated in Fig. 5.4 for $G = 3$ where BS mc denotes the macro cell BSs and BS sc the small cell BSs.

Let $\mathbf{H}_i^{\text{sc}}[t] \in \mathbb{C}^{2 \times 1}$ denote the channel matrix at time t between the small cell transmitter i and receiver i. $\mathbf{H}_{ji}^{\text{mc}}[t] \in \mathbb{C}^{2 \times G}$ denotes the channel matrix at time t between the macro cell transmitter i and receiver in cell j. As in the IBC, it will be possible to split the network into 2 isolated subnetworks. Denoting the receive filter at user i $\mathbf{B_i}$, the conditions to reach the separation are now

$$\text{Rank} \begin{bmatrix} \mathbf{B_1}(1)\mathbf{H}_{11}^{\text{mc}} \\ \mathbf{B_2}(1)\mathbf{H}_{12}^{\text{mc}} \\ \dots \\ \mathbf{B}_G(1)\mathbf{H}_{1G}^{\text{mc}} \end{bmatrix} = G - 1$$

$$\text{Rank} \begin{bmatrix} \mathbf{B_1}(1)\mathbf{H}_{21}^{\text{mc}} \\ \mathbf{B_2}(1)\mathbf{H}_{22}^{\text{mc}} \\ \dots \\ \mathbf{B}_G(1)\mathbf{H}_{2G}^{\text{mc}} \end{bmatrix} = G - 1$$

$$\dots$$

$$\text{Rank} \begin{bmatrix} \mathbf{B_1}(1)\mathbf{H}_{G1}^{\text{mc}} \\ \mathbf{B_2}(1)\mathbf{H}_{G2}^{\text{mc}} \\ \dots \\ \mathbf{B}_G(1)\mathbf{H}_{GG}^{\text{mc}} \end{bmatrix} = G - 1 \tag{5.19}$$

and

$$\begin{bmatrix} \mathbf{B_1}(2)\mathbf{H}_1^{\text{sc}} \\ \mathbf{B_2}(2)\mathbf{H}_2^{\text{sc}} \\ \dots \\ \mathbf{B}_G(2)\mathbf{H}_G^{\text{sc}} \end{bmatrix} = \begin{bmatrix} 0 \\ 0 \\ \dots \\ 0 \end{bmatrix}. \tag{5.20}$$

Denoting the transmit filters $\mathbf{B_i} \in \mathbb{C}^{\mathbf{G} \times \mathbf{1}}$, we also need

$$\mathbf{B}_j(1)\mathbf{H}_{ij}^{\text{mc}}\mathbf{B_i} = \mathbf{0} \quad \forall (\mathbf{i}, \mathbf{j}) \tag{5.21}$$

To solve this problem, one can use the algorithm already defined in Section 5.3.1, with $\overline{\mathbf{H}_{i_1}} = \mathbf{H}_i^{\text{sc}T}$, $\overline{\mathbf{H}_{i_2j}} = \mathbf{H}_{ij}^{\text{mc}T}$, $\mathbf{a}_i = \mathbf{B_i^T}$ and $\mathbf{W}_i = \mathbf{B}_i^T$ as the conditions (5.19), (5.20) and (5.21) are equivalent to conditions (5.3), (5.4) and (5.9). By doing so, the network is separated and each transmitter (macro cell transmitter BS mc i and

small cell transmitter BS sc i) can serve their common user (user i) at the same time independently. It is exactly as if the users had two independent antennas, one receiving only from its corresponding small cell BS thanks to (5.21) and one receiving only from the G macro BS thanks to (5.20).

Therefore, the DoF analysis in Section 5.3.2 also applies to this dual heterogeneous network. The focus here was on a special case of heterogeneous network but the remark in Section 5.3.4 is also valid and the algorithm can work on different configurations for example to work with BSs and receivers with more antennas. Consider, for instance, three users with four antennas, small cell BS with two antennas and macro cell BS with six antennas. It is the dual of the example network of Section 5.3.4 with the exception that there is only one small cell BS with two antennas, instead of two small cell BS with one antenna, serving each user. Nevertheless, as mentioned with Table 5.1, what can be done with antennas distributed over two BS can also be done with antennas collocated in one BS and again we can obtain 9 DoF in this heterogeneous network after separation when the naive method would only provide 8 DoF.

5.5 Finite SNR Performance Evaluation

The interest of separating the considered networks has been demonstrated in terms of DoF gain. In this Section, we perform Monte-Carlo simulations to confirm that the DoF increase we observed also results in sum rate gains at finite SNR. We simulate the naive method and the two-level transmission with separation. For the separation results, we first separate the network into 2 independent networks. Then, the isolated users are served in simple point-to-point transmission and the interfered users in the resulting IC are served with the IA scheme proposed in [29], which aims at approaching the proper bound with finite symbol extension. The transmit power is set to 1 at each BS and the power is divided equally among streams.

5.5.1 Naive Method

For the naive method, precoders are defined by (5.12), then each of their columns are normalized to satisfy the power constraint. At each BS transmitting only one stream, all the power is allocated to this stream. For the BS transmitting two streams, the power is equally split between the two streams. The sum-rate is then given by

$$\text{SR}_{naive}(SNR) = \sum_{i=2}^{G} \log_2 \left(1 + \frac{||\mathbf{H}_{i_1}\mathbf{W}_i(1)||^2}{\sigma^2} \right)$$

$$+ \log_2 \left(1 + .5\frac{||\mathbf{H}_{1_1}\mathbf{W}_1(1)||^2}{\sigma^2 + \text{Int}_1} \right)$$

$$+ \log_2 \left(1 + .5\frac{||\mathbf{a}_1\mathbf{H}_{1_21}\mathbf{W}_1(2)||^2}{\sigma^2 + \text{Int}_2} \right) \tag{5.22}$$

where $\text{Int}_1 = ||\mathbf{H}_{1_1}\mathbf{W}_1(2)||^2$, $\text{Int}_2 = \sum_{i=2}^{G}||\mathbf{a}_1\mathbf{H}_{1_2i}\mathbf{W}_i(1)||^2$ and $\sigma^2 = 10^{-\frac{SNR}{10}}$. In the first line are the contributions from isolated users whose BS is only serving them. Second and third lines terms are respectively the contribution of the isolated and interfered users of the first cell, in which the BS is transmitting 2 streams. Thanks to the choice of (5.12) for precoders, Int_1 and Int_2 are null and there are $G + 1$ log terms, hence the $G + 1$ DoF.

5.5.2 Separation

Once the separation procedure is done, the isolated users are served by simple point-to-point transmission. So if the separation reached a perfect alignment the sum rate of the isolated users would be

$$\text{SR}_{iso'}(SNR) = \sum_{i=1}^{G} \log_2 \left(1 + \frac{P_{iso}||\mathbf{H}_{i_1}\mathbf{W}_i(1)||^2}{\sigma^2} \right) \tag{5.23}$$

but because the separation algorithm may not reach perfect alignment we take into account the possible MUI

$$\text{SR}_{iso}(SNR) = \sum_{i=1}^{G} \log_2 \left(1 + \frac{P_{iso}||\mathbf{H}_{i_1}\mathbf{W}_i(1)||^2}{\sigma^2 + P_{int}||\mathbf{H}_{i_1}\mathbf{W}_i(2)||^2} \right) \tag{5.24}$$

where P_{iso} and P_{int} are respectively the power allocated to each streams aimed at the isolated users and at the interfered users. In the IBC we choose to share equally the power between streams: $P_{iso} = \frac{T}{T+d}$ and $P_{int} = \frac{d}{T+d}$, where T is the length of the symbol extension for the separated SISO IC and d is the number of streams allocated to an interfered user over the symbol extension.

In the dual heterogeneous network, P_{int} and P_{iso} are respectively replaced by P_{mc} and P_{sc}. The power allocation is largely simplified because each transmitter, in macro and small cells, only serves one user and can, therefore, devote all its power, respectively P_{mc} and P_{sc}, to this unique user.

By taking an extension over T symbols in the SISO IC coming from the separation algorithm, we obtain diagonal channel matrices. Let $H_{j,i}^e$ be the matrix of the extended channel between interfered receiver j and transmitter i after separation

$$\mathbf{H}e_{j,i} = \text{diag}\left(\mathbf{a}_j[1]\mathbf{H}_{j2i}[1]\mathbf{W}_i(2)[1], \cdots, \mathbf{a}_j[T]\mathbf{H}_{j2i}[T]\mathbf{W}_i(2)[T]\right). \qquad (5.25)$$

The IA algorithm then iteratively optimizes $\mathbf{V}_i$ and $\mathbf{U}_j$ the transmit and receive filters for this extended IC. The filters are then normalized. The sum rate is given by

$$\text{SR}_{IC}(SNR) = \sum_{i=1}^{K} \log_2 |\mathbf{I} + (\sigma^2\mathbf{I} + \mathbf{Q}_{I_i})^{-1}\mathbf{Q}_{D_i}| \qquad (5.26)$$

where $\mathbf{Q}_{I_i}$ and $\mathbf{Q}_{D_i}$ are respectively the interference covariance matrix and the signal covariance matrix. Namely, $\mathbf{Q}_{D_i} = P_{int}T\mathbf{H}e_{i,i}\mathbf{V}_i\mathbf{V}_i^H\mathbf{H}e_{i,i}^H$ and we would have

$$\mathbf{Q}_{I_i} = P_{int}T\sum_{i\neq j}\mathbf{H}e_{i,j}\mathbf{V}_j\mathbf{V}_j^H\mathbf{H}e_{i,j}^H \qquad (5.27)$$

if the alignment is perfectly reached in the separation. However, to include possible residual interference after separation we use

$$\mathbf{Q}_{I_i} = \sum_{j\neq i}\left(P_{int}T\mathbf{H}e_{i,j}\mathbf{V}_j\mathbf{V}_j^H\mathbf{H}e_{i,j}^H + P_{iso}\mathbf{H}i_{ij}\mathbf{H}i_{ij}^H\right)$$
$$+P_{iso}\mathbf{H}i_{ii}\mathbf{H}i_{ii}^H \qquad (5.28)$$

where $\mathbf{H}i_{ij}$ is the matrix of the residual interference between receiver i and transmitter j over the extended channel. Therefore,

$$\mathbf{H}i_{ij} = \text{diag}\left(\mathbf{a}_i[1]\mathbf{H}_{i2j}[1]\mathbf{W}_j(1)[1], \cdots, \mathbf{a}_i[T]\mathbf{H}_{i2j}[T]\mathbf{W}_j(1)[T]\right) \qquad (5.29)$$

is a diagonal matrix, which, for $i = j$, is the residual MUI and, for $i \neq j$, is the residual OCI caused by the stream intended for isolated user j.

The sum rate achieved after separation is then

$$\text{SR}_{separ}(SNR) = \text{SR}_{iso}(SNR) + \text{SR}_{IC}(SNR) \qquad (5.30)$$

5.5.3   Numerical Results

Both strategies, naive and separation, are evaluated in a 4-cell network IBC and in the dual heterogeneous network. The naive method should reach $G + 1 = 5$ DoF. For the two-level transmission strategy, after separation, the network of isolated
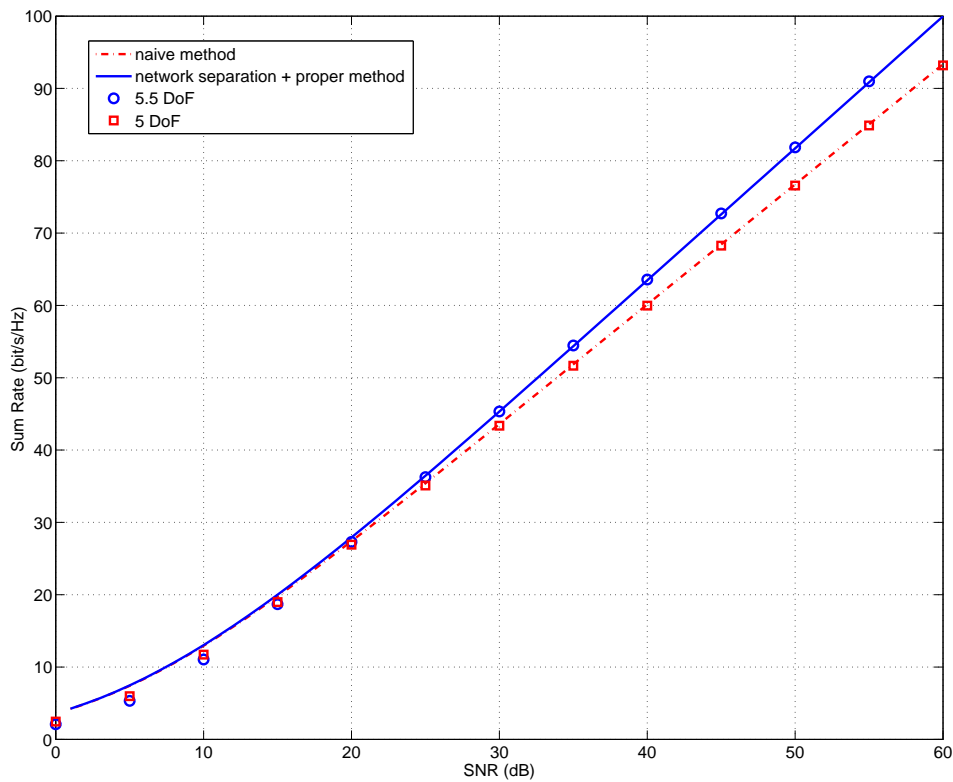
Figure 5.5: Sum rate reached by the naive method and the two-level transmission strategy as a function of the SNR in a 4-cell IBC.
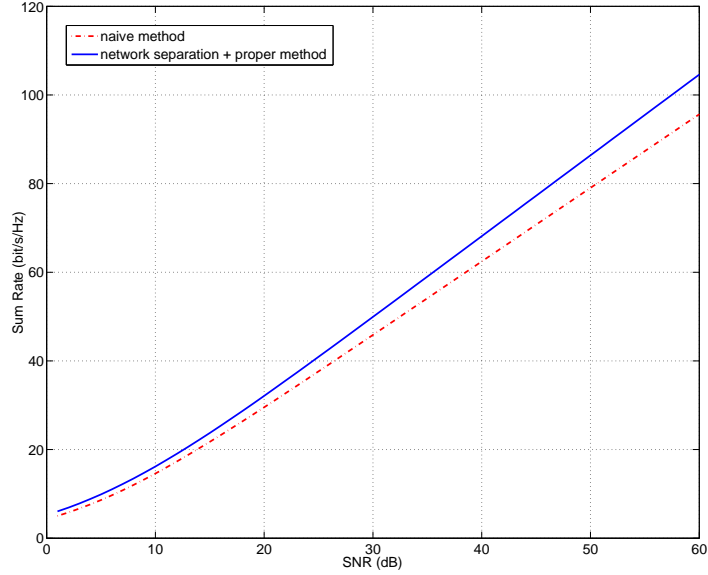
(a) With $P_{mc}/P_{sc} = 1$.
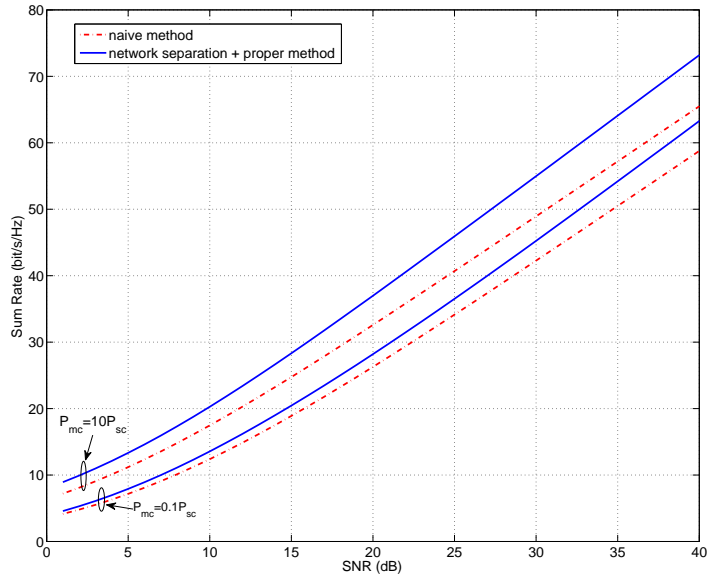
(b) With $P_{mc}/P_{sc} \in \{0.1, 10\}$.

Figure 5.6: Sum rate reached by the naive method and the two-level transmission strategy as a function of the SNR of the small cell link in a 4-cell heterogeneous network for different P_{mc}/P_{sc} ratios.

users should reach $G = 4$ DoF and, for the SISO IC, we assign 6 streams per user over a $T = 16$ symbol extension. This should reach $\frac{4 \times 6}{16} = 1.5$ DoF for a total of 5.5 DoF. In the SISO IC, we used the algorithm in [29] with $\epsilon = 10^{-3}$ for the direct links.

In Fig. 5.5, the sum rate reached by both methods in a 4-cell partially connected IBC, averaged over 500 channel realizations with *i.i.d.* channel coefficients generated from the zero-mean unit-variance complex Gaussian distribution, is plotted as well as two references curves of 5 and 5.5 DoF. We observe that the targeted DoF are reached for reasonably small SNR values. Similarly, the benefit of reaching more DoF thanks to the network separation also shows even for reasonable SNR values.

In Fig. 5.6(a), the sum rate reached by both methods in a heterogeneous network with 4 receivers, averaged over 500 channel realizations, is plotted as a function of the SNR of the small cell link. We used $P_{mc} = P_{sc} = 1$, which does not mean that the macro and small cell BS have the same transmit power but that, at the receiver, the incoming signal powers of the macro and small cell BS before receive filtering are the same. We observe that the two-level transmission strategy outperforms the naive strategy for any SNR in this configuration. This can be explained by the fact that our method, unlike the naive approach, uses all the power available at all the BS, hence the significantly improved sum rates.

In Fig. 5.6(b), the sum rate reached by the methods of Fig. 5.6(a) for different $\frac{P_{mc}}{P_{sc}}$ ratios. We used $P_{sc} = 1$ and $P_{mc} \in \{0.1, 10\}$, i.e., the power of received signal from the macro cell BS is either 10 dB less or 10 dB more than the power of received signal from the small cell BS. We notice that the improvement brought by the two-level transmission strategy increases with the ratio $\frac{P_{mc}}{P_{sc}}$, which was expected because the available power not used by the naive method increases with this ratio.

Another approach for the partially connected IBC is to actually used the algorithm we developed for the IBC in Section 4.3. The links that are negligible are automatically neglected when the matrices $\mathbf{Q}^{int}$, $\mathbf{Q}^{dir}$ and $\mathbf{R}^{int}$, $\mathbf{R}^{dir}$ are computed.

In the separation approach we first separate the network in two subnetworks. Then, for the case $G = 4$, we allocate one DoF per isolated user without symbol extension and six streams per interfered user over a $T = 16$ symbol extension. It gives $\frac{4 \times 6}{16} = 1.5$ DoF for the interfered users, thereby reaching a total of 5.5 DoF. We noticed that treating the network globally our algorithm was able to sustain this DoF assignment. If this DoF assignment is optimal after separation, it is not known if it is the case when treating the whole network globally; therefore, there is a chance larger DoF are reachable but at least 5.5 DoF are achievable. Actually,
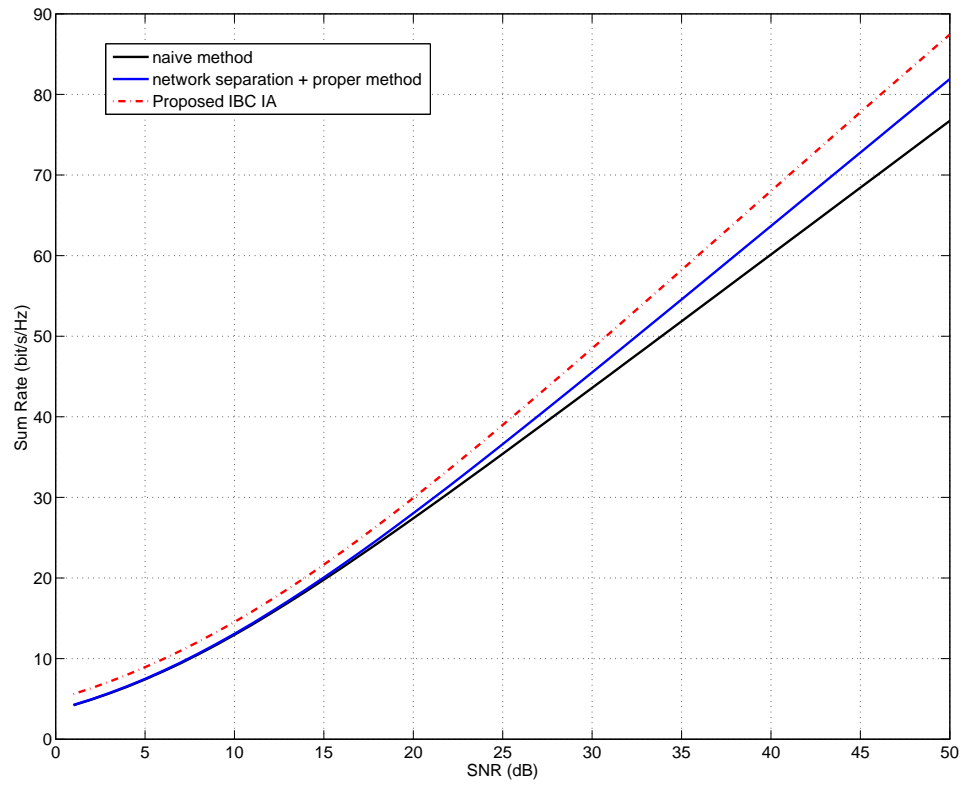
Figure 5.7: Sum rate of the 4-cell partially connected IBC.

with the algorithm we proposed, we are able to have good performance with a strictly larger DoF allocation. Namely, over $T = 8$ symbol extension, we allocate eight streams for each isolated user and four for each interfered user for a total of $\frac{4 \times (8+4)}{8} = 6$ DoF.

In Fig. 5.7 we plot the sum rate reached by the algorithm in the aforementioned configuration and by the separation method. It shows that the proposed algorithm outperforms the separation method with more than 6 bits/s/Hz of gain at SNR=50 dB the naive method with more than 10 bits/s/Hz of gain at SNR=50 dB. It also confirms that the 6 DoF are reached.

The separation method already outperformed the naive method; however, there was no way to know if the separation method was DoF optimal. Only the strategies deployed inside the two separated networks were DoF optimal. By treating the network globally we manage to achieve strictly larger DoF as illustrated on Fig. 5.7.

There is no inconsistency because there is no known upperbound for the partially connected IBC considered. If we start from the fully connected case, from Theorem 1 equation (3.b) in [24] we have the following upperbound in the fully connected case

$$
\sum_{j:(i,j)\in\mathcal{I}} (M_j - d_j)d_j + \sum_{i:(i,j)\in\mathcal{I}} \sum_{k\in\mathcal{K}_i} (N_{i_k} - d_{i_k})d_{i_k}
$$
$$
\geq \sum_{(i,j)\in\mathcal{I}} d_j \sum_{k\in\mathcal{K}_i} d_{i_k}, \quad \forall \mathcal{I} \subseteq \mathcal{J} \tag{5.31}
$$

which in our symmetric case gives

$$
G(M - d_1 - d_2)(d_1 + d_2) + G(N_1 - d_1)d_1 + G(N_2 - d_2)d_2
$$
$$
\geq (G^2 - G)(d_1 + d_2)^2. \tag{5.32}
$$

However, in our case user 1 is isolated and only user 2 is interfered so we actually have

$$
G(M - d_{iso} - d_{int})(d_{iso} + d_{int}) + G(N_{iso} - d_{iso})d_{iso}
$$
$$
+ G(N_{int} - d_{int})d_{int}
$$
$$
\geq (G^2 - G)(d_{iso} + d_{int})(d_{int}). \tag{5.33}
$$

We considered $N_{iso} = 1$ and because all users 1 are isolated it is reasonable to

allocate $d_{iso} = 1$. Therefore, we have

$$(M - 1 - d_{int})(1 + d_{int}) + (N_{int} - d_{int})d_{int}$$
$$\geq (G - 1)(1 + d_{int})(d_{int})$$
$$\Leftrightarrow$$
$$(G + 1)d_{int}^2 + (G + 1 - M - N_{int})d_{int} - (M - 1) \geq 0. \qquad (5.34)$$

Which, with the $G = 4$, $N_{int} = 4$ and $M = 2$ considered gives

$$5d_{int}^2 - d_{int} - 1 \leq 0 \qquad (5.35)$$

Therefore, we have $d_{int} \leq \frac{1}{10}(1 + \sqrt{21}) \approx 0.5583$ for the interfered user and a total of $4d_{iso} + 4d_{int} \leq 6.2330$, which is coherent with the 6 DoF obtain in Fig. 5.7.

Our IBC algorithm needs a predefined stream allocation for a given T. The proper bound in (5.34) can be used to guide the choice of the value d_{int}.

5.5.4 Comparison

Separation yields smaller DoF than the global approach; however, separation requires less feedback, so there is a tradeoff to find depending on the backhaul cost and most likely of the channel coherence time.

This is most clear for the isolated users. With the separation method, they do not need any information whereas with the algorithm using finite symbol extension, even with only one antenna, they need to use a temporal filter that need to be communicated to them unless they compute it themselves. Computing the filters requires global channel knowledge, so it is usually more interesting to have the filters communicated to the isolated users. For that, each isolated user needs to learn T coefficients that it will use over the T-symbol extension when it did not need any thing with the separation method.

5.6 Conclusion

We proposed a two-level algorithm to design the transmit and receive filters of a certain type of partially connected IBC. The relevance of such configurations was justified through 3 example networks in which this type of configuration may arise. The first level of separation allows to have two independent networks and provides the advantage of having then to treat 2 well known subnetworks independently, a G-user SISO IC and G parallel SISO links, which leads to DoF gains. The DoF metric being valid for high SNR, we conducted numerical simulations in an IBC to

evaluate our approach for small and medium SNR as well. The algorithm provided to separate the network proved to be efficient and the results shows that indeed it makes sense to use the DoF metric as a guideline even when concerned with performances at reasonably small SNR values. The same DoF gain is achieved in the heterogeneous network configuration and a more significant sum rate gain is brought by our scheme because, unlike the naive approach, it allows to use all the power available at all the macro BSs. Even more sum rate gain is obtained because the power received from the macro BS grows compared to the power received from the small cell BS.

Then, we have used the algorithm previously designed for fully connected IBC for the design of receive and transmit filters for the partially connected IBC with finite symbol extensions. It minimizes the interference leakage under two additional constraints that assure that the direct links will be preserved through the iterations. The efficiency of the algorithm has been confirmed by numerical simulations that were conclusive in a realistic partially connected configuration and that outperformed the separation approach. Nonetheless, as mentioned in the discussion in Section 5.5.4, the separation approach is still interesting in some settings because it requires less feedback.

Part II

Cost and Delay of CSIT Acquisition

Introduction

In the BC and in the IC, CSIT can be used to align the interferences at the receivers, thereby reducing or even eliminating their impact. However, these techniques rely on perfect current CSIT, which is not practical. CSIT is by nature delayed and imperfect. Though interesting results have been found concerning imperfect CSIT [30], feedback delay can still be an issue especially if it approaches the coherence time of the channel. In Chapter 6, we first introduce a new channel model, which generalize stationary and block fading models and for which we design a new feedback strategy that allows to have constant knowledge of the CSI at the transmitter. Then, in Chapter 7 we evaluate the performances of different schemes for delayed CSIT in the BC, accounting for feedback and training overheads. Finally, in Chapter 8 the IC case is studied. To evaluate the performances of such schemes for DCSIT one can first consider an abstract delay in the CSI acquisition and try to mitigate the loss in the multiplexing gain. A more accurate approach is to take into account the loss in the multiplexing gain due to delay and extra overheads in order to fairly evaluate the resulting net multiplexing gain.

Chapter 6

Finite Rate of Innovation and Foresighted Channel Feedback

In this chapter, we introduce the use of linear Finite Rate of Information (FRoI) signals to model time-selective channel coefficients. The FRoI dimension turns out to be well matched to DoF analysis because the FRoI channel model allows compressed feedback and captures the DoF of the channel coefficient time series. Both the block fading model and the stationary bandlimited channel model are special cases of the FRoI channel model. However, the fact that FRoI channel models model stationary channel evolutions allows to exploit one more dimension: arbitrary time shifts. In this way, the FroI channel model allows to maintain the DoF unaffected in the presence of CSIT feedback delay, by increasing the feedback rate. We call this Foresighted Channel FB (FCFB). FRoI channel model relates also to predictive filterbanks and we work out the optimization details in the biorthogonal case (different analysis and synthesis filters).

6.1   Introduction

Interference is undoubtedly the main limiting factor in multi-user wireless communication systems. Transmitter side or receiver side ZF BF or joint transmitter/receiver ZF BF (signal space IA) allow to obtain significant DoF. These technique require very good channel state information at transmitter and receiver, CSIT and CSIR. Especially CSIT is problematic because it requires feedback, which involves delay, which may be substantial. We shall remark here up front that these observations advocate the design of wireless systems in which the feedback delay is made as short as possible. In a Time Division Duplex (TDD) system this may be difficult but in a FDD system the feedback delay can be made as short as the

roundtrip delay. These considerations are independent of the fact that we can find ways to get around feedback delay, as we elaborate below, because a reduction in feedback delay always leads to improvements (be it in terms of DoF, or NetDoF or at finite SNR).

6.2   General Delayed CSIT State of the Art

It came as a surprise that with totally outdated CSIT, the MAT scheme [86] is still able to produce significant DoF gains for multi-antenna transmission compared to time division multiple access (TDMA). In the DCSIT setting, perfect CSIT is available only after a feedback delay T_{fb}. T_{fb} taken as the unit of time in number of the following schemes. The channel correlation over T_{fb} can be arbitrary, possibly zero. Perfect overall CSIR is assumed, which leads to significant NetDoF reduction due to CSIR distribution overhead [33]. The MISO BC case of [86] have been extended to some limited MIMO IC cases in [87].

Using a sophisticated variation of the MAT scheme, [38] was able to propose an improved scheme for the case where the feedback delay T_{fb} is less than the channel coherence time T_c, defined as the inverse of the Doppler bandwidth. We focus on the temporal correlation of one channel coefficient h. The channel feedback leads to an estimate and estimation error: $h = \widehat{\widehat{h}} + \widetilde{\widehat{h}}$ with feedback SNR $\dfrac{\sigma^2_{\widehat{\widehat{h}}}}{\sigma^2_{\widetilde{\widehat{h}}}} = \mathcal{O}(\rho)$

where ρ is the system SNR. At the transmitter, on the basis of $\widehat{\widehat{h}}$, channel prediction over a horizon T_{fb} leads to a prediction with error: $h = \widehat{h} + \widetilde{h}$ with prediction SNR $\dfrac{\sigma^2_{\widehat{h}}}{\sigma^2_{\widetilde{h}}} = \mathcal{O}(\rho^{1-\frac{T_{fb}}{T_c}})$. The scheme of [38] attains for MISO BC or IC with $K = 2$ users a sumDoF = $2(1 - \frac{T_{fb}}{3T_c}) = 2(\frac{2}{3}\frac{T_{fb}}{T_c} + 1 - \frac{T_{fb}}{T_c})$ using a sophisticated combination of analog and digital feedback. The scheme is limited to mostly MISO and to $K = 2$. They also consider: imperfect CSIT (apart from delayed) and the DoF region.

We introduce FRoI channel models and will exploit their approximately stationary character to propose simple ZF and IA schemes based on FCFB for the BC and IC in the following chapters. The DoF of FCFB ZF are insensitive to feedback delay.

6.3   Some Channel Model State of the Art

do not lead to interesting DoF results. These models are called regular in [88]. The two classical (nonregular) channel models that allow permanent perfect CSIT for Doppler rate perfect channel feedback are block fading and bandlimited stationary channels. The block fading model dates back to the time of GSM where it was quite an appropriate model for the case of frequency hopping. However, though this model is very convenient for very tractable analysis (e.g. for single-user MIMO [89]), it is inappropriate for DoF analysis, which works at infinite SNR and requires exact channel models. Now, whereas exact channel models do not exist, One category of popular channel models is the (first-order) autoregressive (Gauss-Markov) channel model, see e.g. [90]. However, these models (at finite and especially low order) do not allow perfect prediction and hence channel models for DoF analysis should at least be good approximations. Indeed, mobile speeds and Doppler shifts are finite. This leads to a strictly bandlimited Jakes Doppler spectrum. However, in the Jakes model, the mobile terminal has a certain speed without ever moving (attenuation, directions of arrival, path delays, speed vector etc. are all constant forever). In reality, the channel evolution constantly evolves from one temporarily bandlimited Doppler spectrum to another, leading to a possibly overall stationary process but that is not bandlimited.

Another aspect is that there is a difference between channel modeling for CSIR only and for CSIT. In the CSIR case, causality is not much of an issue and channel estimation can be done in a non-causal fashion. Hence block processing and associated channel models as in [90] and references therein are acceptable. However, in the CSIT case, the CSI needs to be fed back for adaptation of the transmitter. Due to the feedback delay, the channel estimation in the CSIT scenario is necessarily causal (case of prediction). Hence different channel models are required.

6.4   The Bandlimited Doppler Spectrum Case

In an optimal approach, all channel coefficients (in the channel impulse response) need to be treated jointly. However, if no deterministic relations exist between the channel coefficients, then for the purpose of DoF analysis, we may consider the case of i.i.d. channel coefficients. In what follows we consider one such generic channel coefficient h. Its temporal evolution is a stationary discrete-time process, at the sampling rate (channel uses) of the communications channel. We assume this sampling rate to be normalized to 1. We assume the Doppler spectrum $S_h(f)$, the spectrum of the process h, to be bandlimited to F_c, which is the total Doppler Bandwidth. Because the channel coefficients are complex, the position of
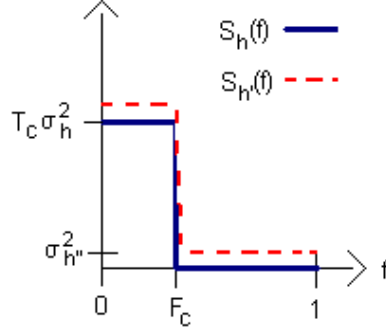
Figure 6.1: A bandlimited Doppler spectrum and its noisy version.

the Doppler spectrum with respect to the carrier frequency is less crucial, so we can assume the Doppler support to be $[0, F_c]$ as in Fig. 6.1; also, $S_h(f)$ is periodic in frequency f with period 1). We denote the coherence time as $T_c = 1/F_c$. Due to the (deterministic) estimation of the channel in the downlink, and its imperfect feedback to the transmitter, the transmitter has a noisy version $\widehat{\widehat{h}}$ with additive estimation noise $\widetilde{\widetilde{h}}$ (h', h'' in Fig. 6.1) because the use of a prior channel distribution in a Bayesian approach can be postponed until the prediction operation to follow. The noisy spectrum is

$$S_{\widehat{\widehat{h}}}(f) = S_h(f) + S_{\widetilde{\widetilde{h}}}(f) = S_h(f) + \sigma^2_{\widetilde{\widetilde{h}}} \tag{6.1}$$

assuming independent white noise $\widetilde{\widetilde{h}}$. Let T_{fb} be the delay with which the channel estimate $\widehat{\widehat{h}}$ arrives at the transmitter for instantaneous adaptation of the transmitter. That means that the transmitter has to perform channel prediction over a horizon of T_{fb}. Assuming a Gaussian channel and estimation noise, linear minimum mean squared error (LMMSE) prediction is optimal, if MMSE is the optimality criterion. Prediction over a horizon of T_{fb} samples will become prediction by one sample if we downsample the channel estimate signal by a factor T_{fb}. Downsampling in the time domain leads to a expansion of the spectrum support by a factor T_{fb} and prediction from a subsampled version is of a degraded quality in the noisy case. Considering Fig. 6.1, as long as $F_c T_{fb} < 1$, or $T_{fb} < T_c$, the downsampled channel signal remains bandlimited. Let $S(f)$ denote the downsampled version of $S_{\widehat{\widehat{h}}}(f)$. Then we get for the (infinite order) one sample ahead prediction MSE

$$\widetilde{\sigma}^2 = e^{\int_0^1 \ln S(f)\, df} \sim \sigma^{2(1-F_c T_{fb})}_{\widetilde{\widetilde{h}}} . \tag{6.2}$$

A similar behavior is obtained for the T_{fb} ahead prediction error from the original unsubsampled process. The prediction error $\widetilde{h}'$ considered in (6.2) is actually the

error in estimating $\widehat{\widetilde{h}}$ from its past. However, what we are really interested in is estimating h from the past of $\widehat{\widetilde{h}}$, with prediction error $\tilde{h}$. Now, because $\widetilde{\widetilde{h}}$ is white noise, we get in fact $\sigma_{\tilde{h}}^2 = \sigma_{h'}^2 - \sigma_{\widetilde{\widetilde{h}}}^2$. When $T_{fb} > 0$, the dominating term at high SNR is still $\sigma_{h'}^2$ though.

Let $P(f) = 1 - \sum_{n=1}^{\infty} p_n e^{-j2\pi f n}$ be the, one sample ahead, prediction error filter for $\widehat{\widetilde{h}}$ (monic: $p_0 = 1$). The $-p_k, k > 0$ are the coefficients for predicting both $\widehat{\widetilde{h}}$ or h. As infinite order prediction succeeds in whitening the prediction error, we have that

$$S_{\widehat{\widetilde{h}}}(f) = \frac{\widetilde{\sigma}^2}{|P(f)|^2} \tag{6.3}$$

which is the Kolmogorov representation, an infinite order autoregressive (AR(∞)) model. Because $|P(f)|$ is a scaled version of $1/\sqrt{S_{\widehat{\widetilde{h}}}(f)}$, it can easily be seen that $P(f)$ is a high-pass filter, and converges to an ideal high-pass filter as the SNR increases [91]. This has led a number of researchers (see [91] and references therein) to construct predictors for bandlimited signals simply by approximating ideal high-pass filters. These FIR filters are typically chosen to be linear phase and are made monic ($p_0 = 1$) by dividing the filter by its first coefficient. However, the prediction error filter $P(f)$ is not only monic but also minimum-phase.

6.4.1 The Noiseless bandlimited Case: two-time scale model

Now consider the noiseless case, $\sigma_{\widetilde{\widetilde{h}}}^2 = 0$. Then, the prediction errors become zero, $\sigma_{\tilde{h}}^2 = \sigma_{h'}^2 = 0$. Hence the signal can be perfectly predicted from its past. For simplicity let T_c be an integer. Let h_k denote the channel coefficient at discrete time k and consider one sample ahead prediction, then $h_k = \sum_{n=1}^{\infty} p_n h_{k-n}$. Note that the prediction error filter $P(f)$, which is an ideal high-pass filter, can be chosen to be independent of the actual Doppler spectrum $S_h(f)$ within its support, and can be chosen to be only a function of the Doppler spread $F_c = \frac{1}{T_c}$. Let us denote this spectrum independent prediction error filter as $P_{T_c}(f)$. Because we have perfect prediction, we can repeat the one sample ahead prediction recursively to perfectly predict multiple samples ahead. Can this be repeated indefinitely? Yes if we have all samples available to predict from, but no if T-ahead prediction is based on a T times downsampled version. In that case, when we hit prediction horizon T_c, T_c-ahead prediction being here, in terms of zero prediction error, equivalent to 1-ahead prediction on a T_c times downsampled signal, downsampling, hence stretching its support, $S_h(f)$ by a factor T_c makes it non-singular at all frequencies i.e., non bandlimited. Note also that because of the perfect predictibility over the

horizon $\{1, \ldots, T_c - 1\}$, linear estimation in terms of the complete past is equivalent to linear estimation in terms of a T_c times downsampled version of the past, because the samples in between can be filled up causally from a downsampled version. At prediction horizon T_c now, from a T_c times downsampled past, we are dealing with standard 1-ahead linear prediction of a non bandlimited stationary process, which under some regularity conditions can be considered as an AR(∞) process (Kolmogorov model). Let the infinite order prediction error filter for the T_c times downsampled process be $A(f)$. This reasoning allows us to formulate the following theorem.

Theorem 4 Two-Time Scale bandlimited Model *The prediction error filter for a stationary process h_k bandlimited to $1/T_c$ (T_c integer) can be modeled as*

$$P(f) = P_{T_c}(f)\, A(T_c f) \tag{6.4}$$

where $P_{T_c}(f)$ is the prediction error filter for a bandlimited process with flat Doppler spectrum and $A(f)$ is the prediction error filter for the downsampled h_{kT_c}.

Let $G(f) = 1/P_{T_c}(f) = \sum_{n=0}^{\infty} g_n\, e^{-j2\pi f n}$ which is like $P_{T_c}(f)$ again a minimum-phase monic causal filter. Note that $G(f)$ behaves like an ideal low-pass filter with bandwidth $1/T_c$, hence the T_c times downsampled version of its impulse response is a delta function: $g_{nT_c} = g_0\, \delta_{n0}$. Then the stationary bandlimited process h_k can be generated as

$$h_k \;=\; g_k \;*\; h_k^{\downarrow\uparrow} \tag{6.5}$$

where $h_k^{\downarrow\uparrow}$ is the T_c times downsampled and then T_c times upsampled (inserting $T_c - 1$ zeros between consecutive samples) version of h_k and $*$ denotes convolution. The block fading model is similar to (6.5) with g_k now a rectangle: $g_k = 1$, $k = 0, 1, \ldots, T_c - 1$ and zeros elsewhere. With this similarity, the block fading and bandlimited stationary case have in common that for every consecutive coherence period T_c, if the first sample (and the past) is known, then the remaining $T_c - 1$ samples of the current coherence period are known.

6.4.2   Back to the Noisy bandlimited Case

The prediction of a bandlimited process is not a stable operation [92] as can be seen from (6.2) where $\widetilde{\sigma}^2$ grows more rapidly than linear in $\sigma^2_{\underset{h}{\sim}}$ (assuming $\sigma^2_{\underset{h}{\sim}}$ is small). This is related to the fact that the (noiseless) prediction coefficients p_k are of infinite length and are not rapidly decaying. In [93], it was shown, for CSIR purposes, that the stationary bandlimited model and the block fading model

become equivalent as $F_c \rightarrow 0$. Such equivalence in the limit will also result for
CSIT purposes here. But we want to go beyond the limit of very small Doppler
spread.

Consider the infinite order autoregressive (Kolmogorov decomposition) and
moving-average (Wold decomposition) representations of a noisy bandlimited sta-
tionary process with spectrum as in Fig. 6.1 :

$$S(f) = \frac{\widetilde{\sigma}^2}{|P(f)|^2} = \widetilde{\sigma}^2 \, |G(f)|^2 \qquad (6.6)$$

with monic (first coefficient equal to 1) minimum-phase infinite order prediction
error filter $P(f)$ and spectral factor $G(f)$ and infinite order prediction error vari-
ance $\widetilde{\sigma}^2$ such that the prediction error SNR becomes at high SNR. In the rest of
this subsection $T = T_c$ and

$$\frac{\sigma_h^2}{\widetilde{\sigma}^2} = \sigma_h^2 \, e^{-\int \ln S(f)\,df} = T^{-1/T} \left(\frac{\sigma_h^2}{\sigma_{\widetilde{h}}^2} \right)^{1-1/T} . \qquad (6.7)$$

where the channel estimation/feedback SNR $\frac{\sigma_h^2}{\sigma_{\widetilde{h}}^2}$ is assumed to be proportional to
the system SNR ρ (even if only for large ρ) . It appears that analytical expressions
for $P(f)$ do not exist in the literature and the following may explain why. We get
straightforwardly

$$|P(f)|^2 = \frac{\widetilde{\sigma}^2}{S(f)} = \begin{cases} (\frac{T\sigma_h^2}{\sigma_{\widetilde{h}}^2})^{-(1-1/T)} & f \in [0,1/T] \\ (\frac{T\sigma_h^2}{\sigma_{\widetilde{h}}^2})^{1/T} & f \in [1/T,1] \end{cases} \qquad (6.8)$$

and hence we get for the energy in $P(f)$

$$||P||^2 = 1/T(\frac{T\sigma_h^2}{\sigma_{\widetilde{h}}^2})^{-(1-1/T)} + (1-1/T)(\frac{T\sigma_h^2}{\sigma_{\widetilde{h}}^2})^{1/T} \rightarrow \infty \qquad (6.9)$$

which explodes as $\rho \rightarrow \infty$. Similarly for the monic causal spectral factor $G(f) = 1/P(f)$ and hence its energy

$$||G||^2 = 1/T(\frac{T\sigma_h^2}{\sigma_{\widetilde{h}}^2})^{1-1/T} + (1-1/T)(\frac{T\sigma_h^2}{\sigma_{\widetilde{h}}^2})^{-1/T} \rightarrow \infty \qquad (6.10)$$

explodes also when we insist on monicity: $g_0 = 1$. It is possible to find a spectral
factor G with finite energy, but then $g_0 \rightarrow 0$.

6.4.3   No exact bandlimited model anywhere

In [38], the behavior of (6.2) is exploited to show the resulting DoF of the two-user MISO BC. However, what is not mentioned there is that these results correspond to a channel model that needs to be in a range between two extreme models. The one extreme model is block fading over blocks of length T_{fb}, with stationary F_c-bandlimited evolution of the value of the blocks, and channel feedback every T_{fb}. The other extreme is a genuine F_c-bandlimited stationary channel model, but then the channel needs to be fed back every sample, which is normally unacceptable in terms of NetDoF. In [33] still another approach is taken in which block fading over some T is assumed, plus bandlimited stationary evolution between blocks (such that one of the interpretations of [38] corresponds to this with $T = T_{fb}$).

The other popular model is the block fading model. In Chapter 7, we show that the DoFs of [38] can be reproduced very simply in the case of a block fading model, by the MAT-ZF scheme, a simple combination of MAT (during T_{fb}, while waiting for the channel feedback) and ZF for the rest of the coherence period. In [94] it was shown in an alternative fashion that the channel feedback rate could be reduced with respect to [38] by a factor T_c/T_{fb} (equivalent to feedback every T_c instead of every T_{fb}, as our FRoI approach also indicates, see Section 6.6). To reproduce these results for the stationary bandlimited case is not easy though, and the scheme of [38] is quite intricate, involving, as in MAT, feedback of residual interference, now necessarily digital, with superposition coding and sequential decoding.

The models we introduce next allow to retain the simplicity of block fading models and even go beyond them by exploiting stationarity.

6.5   Linear Finite Rate of Innovation (FRoI) Channel Models

FRoI signal models were introduced in [95]. Innovation here could be a somewhat misleading term because historically, in Kalman filter parlance, the term *innovations* has been used to refer to the infinite order prediction errors. In [95] and here, the rate of innovation could be considered to be the DoF of signals i.e., the source coding rate prelog. FRoI represents the time series case of sparse modeling. The FRoI signal models that have been considered in [95] could be in general non-linear. In other words, the FRoI represents the average number of parameters per time unit needed to describe the signal class and these parameters could enter the signal model in an arbitrary fashion. For instance, the signal could be a linear superposition of basis functions of which also the positions (delays, and in the channel modeling case e.g. also Doppler shifts) are parameterized. For the

purpose of channel modeling and feedback, with essentially stationary signals that need to be processed in a causal fashion, it would appear reasonable to stick to linear FRoI models, in which the parameters are just the linear combination coefficients of fixed, periodically appearing basis functions, commensurate with the Doppler bandwidth. This also corresponds exactly to so-called Basis Expansion Models (BEMs), which were probably introduced in [96] and used for estimating time-varying filters in the eighties and for channel modeling in [97].
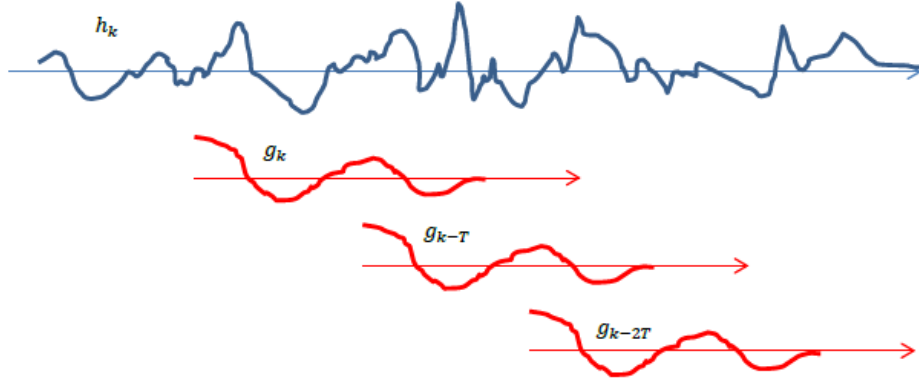
Figure 6.2: Finite Rate of Innovation time-varying channel modeling.

In the case of a single basis function, the FRoI channel model is similar to (6.5):

$$h_k = g_k \ * \ a_k^\uparrow \tag{6.11}$$

where $a_k^\uparrow$ is a T_c times upsampled discrete-time signal of which the non-zero samples (parameters) appear once every T_c sampling periods, and g_k is a basis function, see Fig. 6.2. The resulting FRoI model encompasses the following existing models:

- *block fading*: $g_k = \begin{cases} 1 & , \ k = 0,1,\ldots,T_c - 1 \\ 0 & , \ \text{elsewhere} \end{cases}$

- *stationary bandlimited* :

$$g_k = \text{sinc}(\pi k/T_c) = \frac{\sin(\pi k/T_c)}{\pi k/T_c} \ .$$

In our case, g_k is a causal FIR approximation to an ideal low-pass filter with overall bandwidth F_c. The length of the basis function g_k is intended to span several T_c.

However, by making the filter longer, a bandlimited characteristic can be better approximated. The bandlimited model (6.5) can be obtained by letting the filter length become infinite. Starting from a stationary sequence a_k, the process h_k generated by (6.11) is cyclostationary. By letting g_k better approximate a low-pass (or bandpass) filter, the cyclostationary process gets closer to stationary. In any case, at the start of each new coherence period T_c, knowing the past, the estimation of the sample h_k allows the estimation of the new parameter $a_k^{\uparrow}$ involved. And this in turn allows to determine the evolution of h_k for the next $T_c - 1$ samples.

In the presence of noise, it is desirable to have a first coefficient g_0 that is large, though any non-zero coefficient is sufficient for DoF analysis purposes. Due to the finite length and energy of the filter g_k, the effect of noise is limited and the prediction error variance over the coherence period will remain of the order of $\sigma^2_{\tilde{\tilde{h}}}$, the noise level in the channel feedback. As the sampling rate, and hence feedback frequency, of bandlimited signals increases, the horizon of perfect prediction increases proportionally, and becomes infinite as the continuous-time past signal becomes available [92].

However, for all real-world signals for which a bandlimited model seems plausible, e.g. the speech signal, this does not work because real-world signals are only approximately stationary and bandlimited over a limited time horizon. For instance, it is impossible to predict what a speaker is saying. In wireless communications, although Doppler shifts are finite because speed is finite, the Doppler spectrum becomes non-bandlimited because the Doppler shifts are time-varying. If the channel response would be a deterministic function of the mobile terminal position, prediction of the channel would correspond to prediction of the mobile position, which is impossible on a longer time scale. From this point of view, linear FRoI models, which are approximately bandlimited but with a finite memory, might be better approximations of approximately bandlimited real-world signals. A lot of work on estimating FRoI signals has focused on non-causal approaches [98]. However, what is needed for the application of FRoI to channel feedback is a design with prediction in mind.

The linear FroI model can also be considered as a filterbank with a single subband. The synthesis filter is g_k, and there is an analysis filter f_k. The analysis-synthesis cascade leads to

$$
\begin{aligned}
a_n &= \sum_k f_k \, h_{nT_c-k} \\
h_{nT_c+i} &= \sum_l a_{n-l} \, g_{lT_c+i} \;, \quad i = 0, 1, \ldots, T_c - 1 \;.
\end{aligned}
\tag{6.12}
$$

Perfect reconstruction for a strictly bandlimited process requires:

$$
g_k * f_k = \operatorname{sinc}(\pi k / T) \;.
\tag{6.13}
$$

This can be satisfied with e.g. $g_k = \text{sinc}(\pi k/T)$, $f_k = \delta_{k0}$ (Kronecker delta). In the case of an orthogonal filterbank with causal g_k, this requires $f_k = g_{-k}^*$, and $(g_k * g_{-k}^*)_{k=nT} = \delta_{n0}$, the convolution $g_k * g_{-k}^*$ (correlation sequence of g_k) should be a Nyquist pulse. In this case, if h_k is not a bandlimited signal, the reconstructed signal resulting from applying the FRoI model in (6.12) would produce the least-squares projection of the signal h_k on the subspace of F_c-bandlimited signals [99]. However, this requires $f_k = g_{-k}^*$ (matched filter) to be non-causal. As can be seen from Fig. 6.2, the optimal computation of coefficient a_n requires the correlation of the signal h_k that follows from the time instant $k = nT_c$ onwards with the basis function g_k. This is impractical for the channel feedback application in which both g_k and f_k should be causal, and, for optimal DoF considerations, the computation of a_n should be based on the first sample only of this correlation. Hence g_0 plays an important role and cannot be small.

For a number of applications, the use of FRoI models with multiple, N_b, basis functions might be desirable. In this case the FRoI model becomes

$$h_k = \sum_{n=1}^{N_b} g_k^{(n)} * a_k^{\uparrow (n)} \tag{6.14}$$

where the $a_k^{\uparrow (n)}$ are N_b sequences of parameters that are now $N_b T_c$ times upsampled, to preserve a RoI of F_c. As the $g_k^{(n)}$ represent N_b different basis functions that are essentially bandlimited and also time limited, there might be some connection with prolate spheroidal wave functions [90], [92]. However, to limit feedback delay, the first N_b coefficients of these basis functions play a particularly important role here.

Two basis function optimization approaches are presented in Appendix B.1.

6.6 Foresighted Channel Feedback

The main characteristic of FRoI channel models is that they are a close approximation of stationary bandlimited signals. *This means that if a FRoI channel model is a good model, so is an arbitrary time shift of the FRoI model.* This can be exploited to overcome the feedback delay as described in Fig. 6.3. Consider FRoI channel model with $N_b = 1$ basis function. While the current coherence period is running, as the Channel feedback (CFB) is going to take a delay of T_{fb}, instead of waiting for the end of the current T_c, we start the next coherence period T_{fb} samples early. This means jumping from the subsampling grid of the FRoI model to the shifted subsampling grid of another instance of the same FRoI model. This involves recalculating the finite number of past FRoI parameters $a_k^{\uparrow}$ for the new

grid from the past channel evolution on the old grid, plus a new channel estimate at the start of the T_c on the new grid. In this way the feedback sampling frequency increases from $\frac{1}{T_c}$ to $\frac{1}{T_c - T_{fb}}$. But the CSIT is available at the transmitter all the time, with a channel prediction error SNR proportional to the general SNR. This approach is applicable to any multi-user network.
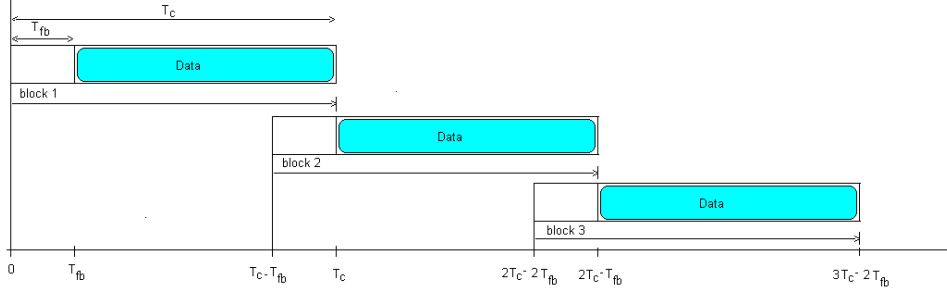
Figure 6.3: Foresighted Channel Feedback: DoF analysis.

By increasing N_b, the number of basis functions, this approach continues to work for any $T_{fb} < N_b T_c$, and hence for any T_{fb}. Related work appears in [41] where, to get full DoF in the presence of CSIT delay, instead of jumping from one subsampling phase to another for a given user, in [41] the authors propose to jump between users, for which the channels are modeled with different subsampling phases.

The proposed FCFB increases the feedback DoF consumed, hence, and in any case, it is of interest to consider the more relevant NetDoF. As illustrated in Fig. 6.4, we observe that in practice, feedback and training frequency has to be increased from $\frac{1}{T_c}$ to $\frac{1}{T_c - (T_d + T_{ct})}$ where T_d is the total dead time, the time where the transmitter is not sending training symbols and does not have the CSI yet. An analysis of the resulting NetDoF for the MISO BC is presented in Chapter 7 and for the MIMO IC is presented in Chapter 8.

6.7 Conclusion

In this chapter we unified the block fading and the stationary fading model, showing that they both are special cases of the more general FRoI channel model. Demonstrating at the same time that, with adequate training the CSI can be acquired at any time and be valid for the coherence time of the channel, allowing for a constant knowledge of the CSIT and the possibility to do ZF all the time at the cost of a slightly increased rate of training and feedback. The resulting net DoF
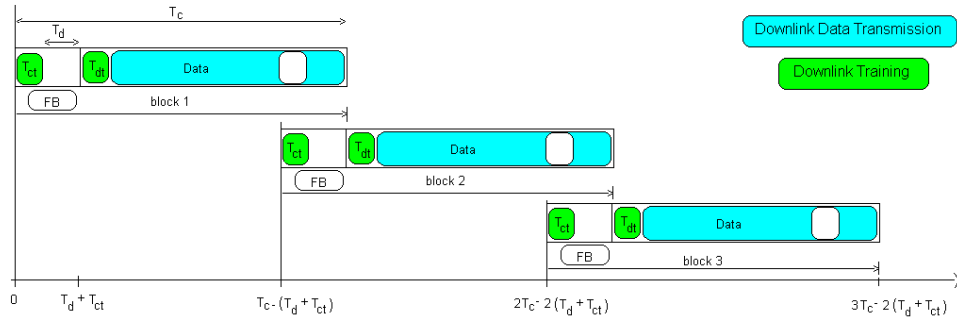
Figure 6.4: Foresighted Channel Feedback net DoF analysis.

are analyzed and compared to that of other schemes in the BC in Chapter 7 and in the IC in Chapter 8.

The FRoI channel model is just one way to get a certain rate, here the DoF, for a distortion of $O(\sigma_v^2)$ (noise level). More generally, the distortion in a predicted channel at the transmitter can contain a combination of approximation error and noise due to estimation and feedback. What is needed here is *predictive* rate-distortion theory. Such theory would e.g. allow to determine which estimation and feedback DoF are required to get the prediction distortion at the transmitter down to the level of the noise, with the channel distortion at the transmitter being reflected in an induced equivalent noise at the receiver. However, the proper evaluation of such rate-distortion theory depends heavily on the channel model, whereas all existing channel models are too approximate to allow a solid high SNR DoF analysis. Some related work appears in [100] where no causality is imposed and where the analysis filter f is not optimized (fixed), and in [101], where causal, but not predictive, rate-distortion theory is developed for the application of feedback in control systems.

Chapter 7

Delayed CSIT in the BC

In this chapter we review different schemes for the BC with delayed CSIT, propose some new schemes and evaluate their performances in terms on net DoF, i.e., accounting for training overhead as well as the DoF consumption due to the feedback on the reverse link. The proposed schemes are TDMA-ZF, MAT-ZF and ZF with FCFB described in Section 6.6. For comparisons, ZF, MAT, Space-Time IA Zero Forcing precoding (ST-ZF) from [35] are reviewed and their netDoF derived. We also extend the ST-ZF scheme to MIMO configurations.

7.1   Introduction

CSIT is by nature delayed and imperfect. Though interesting results have been found concerning imperfect CSIT [30], feedback delay can still be an issue especially if it approaches the coherence time of the channel. However, the MAT scheme [31] completely changed the paradigm by yielding DoF greater than one by relying solely on perfect but outdated CSIT, thus, allowing for some multiplexing gain even if the channel state changes independently over the feedback delay. The range of coherence time in which the sole use of MAT yields an increased multiplexing gain is determined in [32] and [33] but considering either only feedback or only training overheads and not both.

The assumption of totally independent channel variation is overly pessimistic for numerous practical scenarios. Therefore, another scheme was proposed in [34] for the time correlated MISO BC with 2 users. This scheme optimally combines delayed CSIT and current CSIT, both imperfect, but has not been generalized for a larger number of users. One of the schemes we propose combines ZF and MAT schemes to reach the optimal multiplexing gain accounting for CSIT delay only; we shall denote our scheme for the MISO BC with K users by MAT-ZF$_K$. It

essentially performs ZF and superposes MAT only during the dead times of ZF. We will show that the MAT-ZF scheme recovers the results of optimality of [34] for $K = 2$ but MAT-ZF is valid and optimal in terms of DoF for any number of users. The MAT-ZF scheme is based on a block fading model but we will show that stationary fading can be modeled exactly as a special block fading model as demonstrated in Chapter 6. Another similar transmission strategy is to do ZF and to perform TDMA during the dead time instead of MAT.

It was generally believed that any delay in the feedback necessarily causes a DoF loss. However, Lee and Heath in [35] proposed a scheme that achieves M (sum) DoF in the block fading underdetermined MISO BC with M transmit antennas and $K = M + 1$ users if the feedback delay is small enough ($\leq \frac{T_c}{K}$).

We will compare the multiplexing gains that ZF, MAT, MAT-ZF, TDMA-ZF, ST-ZF and ZF_{FCFB} can be expected to yield in actual systems, accounting for training overhead as well as the DoF loss due to the feedback on the reverse link. As opposed to [33], in the net DoF we also subtract the DoF consumed in the reverse link, as in [36]. In general, weighted net DoF could be considered as in [36] because forward and reverse link rates could have different weights. We consider here unweighted net DoF from which weighted net DoF can easily be extrapolated. Note that the ZF scheme considered in [33] is different and does not have any dead time. However, ZF BF in [33] is based on predicted CSIT only, leading to some DoF loss.

In Fig. 7.1 these DoF and netDoF approaches are illustrated in case of transmission over a BC, with output feedback of the same length as the training. The DoF approach simply asks what is the best use to make of the *No CSIT* time, i.e., before the transmitter gets the CSI and is especially interesting from a theoretical point of view. The question raised by the second approach is still what is the best use of the *No CSIT* time, but takes into account what is the cost in time and overheads to do so and is, therefore, more practical.

7.2 System Model

We consider a MISO BC with K single-antenna users and a transmitter equipped with M antennas. It is typically assumed that $K = M$ because having $K = M$ or $K > M$ single-antenna users results in the same maximum sum DoF. However, we will see that having an extra user $K = M + 1$ (underdetermination/overloading) becomes useful when there is some delay in the feedback because space-time precoding, as opposed to spatial only BF, can compensate for the delay in feedback in the MISO BC. We categorize this BC as underdetermined because there are more users than transmit antennas, which prevents purely spatial ZF.
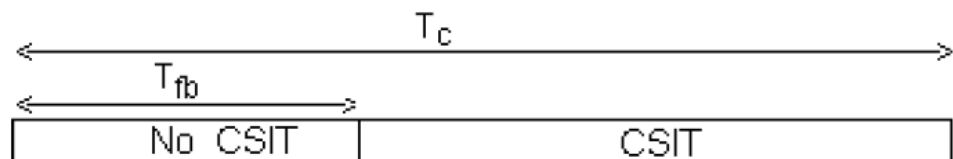
(a) Block topology for DoF analysis.
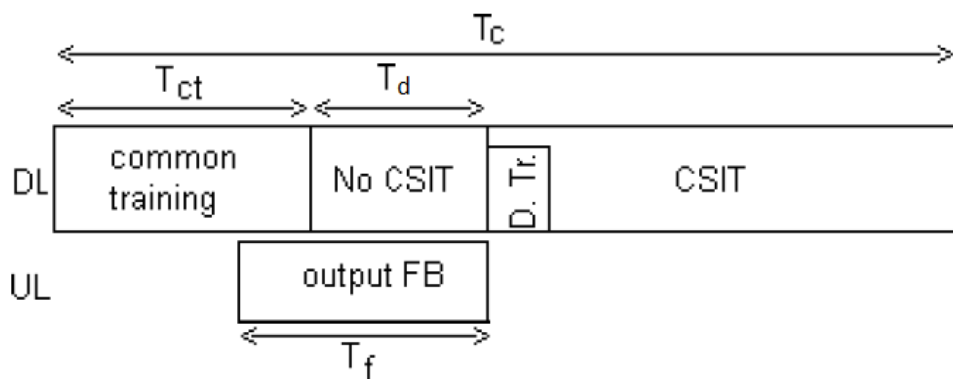
(b) Block topology for netDoF analysis.

Figure 7.1: Block topology for DoF and netDoF analysis.

We will consider $K = M$ or $K = M + 1$ depending on what is beneficial for each scheme.

The first performance metric is (sum) DoF 2.10 and then the netDoF, i.e., the remaining DoF after accounting for training and feedback overheads.

We consider a block fading model: the channel coefficients are constant for the channel coherence time T_c and change independently between blocks.

T_{fb} is the feedback delay. Precisely, when doing DoF analysis as in Fig. 7.1(a), T_{fb} is the abstract delay between the beginning of the block and the time CSI is available at the transmitter so it represent the dead time.

In order to compare the multiplexing gains that different schemes can be expected to obtain in actual systems, we derive their netDoFs, accounting for training overhead as well as the DoF loss due to the feedback on the reverse link. In other words, we evaluate how many DoF are available for data on the forward link, we account for delay and training, and subtract the DoF spent on the reverse link for the feedback. Note that for MAT, ZF, TDMA-ZF and MAT-ZF we consider the square case $K = M$ because adding one user would only increase the overhead and not the DoF whereas we consider $K = M + 1$ for STZF because it is actually designed to benefit from having one extra user.

113

When conducting net DoF analysis as in Fig. 7.1(b), this delay in the CSIT acquisition is not abstract anymore. It is composed of the training, but the during the training the transmitter is already sending training symbols, so it is not *dead time*. In this case, the dead time will be denoted T_d and will account for the delay du to the feedback transmission T_f and T_{fb} is kept in the equation to represent propagation and processing delay but is likely to be much smaller.

7.3 CSI Acquisition Overhead

7.3.1 Training and Feedback

In each block, a common training of length $T_{ct} \geq M$ is needed to estimate the channel as explained in [33]. To maximize the number of DoF we take $T_{ct} = M$. A dedicated training of 1 pilot is also needed to insure coherent reception whenever ZF is to be done according to [102].

Because we are interested in the DoF$_{FB}$, which is the scaling of the feedback rate with $\log_2(P)$ as $P \to \infty$, the noise in the fed back channel estimate can be ignored in the case of analog feedback or of digital feedback of equivalent rate because we are interested in the DoF consumed by the feedback. The feedback can be considered accurate, suffering only from the delay. We consider analog feedback and see two possible feedback strategies. First, channel feedback (CFB), the receivers estimate the channel state from the training sequences and feed back their channel estimate. Second, output feedback (OFB), the receivers directly feed back the training signals they receive and the transmitters perform the (downlink) channel estimation. We consider OFB because it minimizes the delay in the feedback and takes $T_f M$ time slots assuming joint detection at the transmitter. It is especially interesting in the BC because training and feedback take the same time; therefore, the dead time is just $T_d = T_{fb}$ with OFB whereas it would be $T_d = T_{fb} + T_f$ with CFB.

In Fig. 7.1(b) the shape of a block with feedback and training (common and dedicated) is presented, D. Tr. stands for dedicated training. The time slots available after accounting for training in each block are divided into two parts: a first one during which the transmitter does not have the current CSI a second during which there is CSIT.

7.3.2 MAT CSIR distribution

To perform the MAT scheme each receiver needs the channel of certain other receivers. As a first approximation on could consider that after the transmitter received the feedback from all the receivers it sends the CSI them to all the receivers.

We refer to this phase as the CSIR distribution. This could be done by broadcasting the channel states; however, it can be done in a slightly more efficient fashion because each receiver already knows its own channel.

Let us assume that all the K receivers need to know $\{\mathbf{H}_1, \mathbf{H}_2, \cdots, \mathbf{H}_K\}$ but receiver $k, k \in [1, K]$ already knows $\mathbf{H}_k$.

Multicasting all the coefficients $\{\mathbf{H}_1, \mathbf{H}_2, \cdots, \mathbf{H}_K\}$ would take K channel uses and receiver $k, k \in [1, K]$ would receive one message it did not need, $\mathbf{H}_k$ that it already has. Instead, we broadcast the $K - 1$ following messages $\{\mathbf{H}_1 + \mathbf{H}_2, \mathbf{H}_1 + \mathbf{H}_3, \cdots, \mathbf{H}_1 + \mathbf{H}_K\}$. Because receiver 1 already knows $\mathbf{H}_1$ it can subtract it from all the messages it received. Receiver 1 then has $\{\mathbf{H}_2, \mathbf{H}_3, \cdots, \mathbf{H}_K\}$ (and $\mathbf{H}_1$ it already had). Similarly receiver k gets $\mathbf{H}_1$ from the $k - 1$st message $\mathbf{H}_1 + \mathbf{H}_k$ by subtracting $\mathbf{H}_k$, and then can extract the other $\mathbf{H}_i$ for $i \notin \{1, k\}$. By doing so the CSIR distribution for K users can be done in $M(K - 1)$ channel uses instead of MK. The gain is limited for large k but significant for small values of K.

7.4 Net DoF Characterization

7.4.1 ZF

When CSI is available at the transmitter, the full multiplexing gain can be achieved with ZF [103]. Doing only ZF would allow to transmit 1 symbol per channel use to each user when the transmitter has CSIT and nothing otherwise. Without taking feedback and training into account it yields

$$\text{DoF}(\text{ZF}_M) = M\text{DoF}(\text{ZF}_1) = M\left(1 - \frac{T_{fb}}{T_c}\right). \tag{7.1}$$

The needed common and dedicated trainings occupy $M + 1$ time slots and the output feedback of M symbols per user results in a feedback overhead of

$$\text{DoF}_{FB}(\text{ZF}_M) = \frac{KM}{T_c} = \frac{M^2}{T_c}. \tag{7.2}$$

because for ZF the squared case $K = M$ is considered. The net multiplexing gain is then

$$\text{netDoF}(\text{ZF}_M) = M\left(1 - \frac{T_{fb}}{T_c} - \frac{\overbrace{2M + 1}^{\text{training and feedback}}}{T_c}\right). \tag{7.3}$$

7.4.2 TDMA-ZF

TDMA-ZF is a direct extension of ZF. The only difference being that while the transmitter is waiting for the CSI, and not sending training symbols it performs TDMA transmission because this does not require any CSIT, thereby yielding

$$\text{netDoF(TDMA-ZF}_M) = \text{netDoF(ZF}_M) + \frac{T_{fb}}{T_c}$$

$$= M \left(1 - \frac{M-1}{M} \frac{T_{fb}}{T_c} - \frac{2M+1}{T_c} \right) \tag{7.4}$$

7.4.3 MAT

The MAT scheme was proposed in [31]. The authors describe an original approach that yields a multiplexing gain of

$$\frac{M}{1 + \frac{1}{2} \cdots \frac{1}{M}} = \frac{MD}{Q} \tag{7.5}$$

with no *current* CSIT at all, without accounting for feedback and training overheads. Here $\{D,Q\} \in \mathbb{N}^2$ are such that $\frac{1}{1+\frac{1}{2}\cdots\frac{1}{M}} = \frac{D}{Q}$, where D is the least common multiple of $\{1,2,\cdots,M\}$ and $Q = DH_M$ with $H_M = \sum_{m=1}^{M} \frac{1}{m}$. This scheme allows the transmission of D symbols in Q time slots for each user as noted in [32].

The MAT scheme is composed of M phases, phase j is composed of $\frac{D}{j}$ slots. Multiple instances of the MAT scheme are performed in parallel, the first block is filled with first messages of as many instances of the MAT scheme as possible, then the second block is used for the second message of each instance of the MAT scheme and so on.

Only $M - j + 1$ antennas are active during phase j. Therefore, the length of the common training needed in each block depends on the phase: $M - j + 1$ for any block of phase j. This leads to an empty space of $j - 1$ time slots in each block of phase j.

Each block of phase j is dedicated to a subset of j users and the CSI needed from this block is the CSI of the $K - j$ other users that will be used to generate the messages for phase $j + 1$ resulting in a feedback overhead of $(K - j)(M - j + 1)$ per block of phase j

$$\text{DoF}_{FB}(MAT_M) = \frac{\sum_{j=1}^{K} \frac{D}{j}(K-j)(M-j+1)}{QT_c} \tag{7.6}$$

$$= \sum_{j=1}^{K} \frac{(K-j)(M-j+1)}{jH_MT_c} \tag{7.7}$$

With the details given in [31] we understand that these CSI of the $K - j$ users also need to be distributed to the j other users. So for a given block the users that need the CSI are not part of the subset of users whose CSI are to be distributed and our CSIR distribution method explained in 7.3.2 cannot be directly exploited. However, for symmetry reasons the total length of CSI to be sent is a multiple of the number of users K, for example equal to LK. Among these LK coefficients, L are already known at each receiver. Thus, by rearranging the CSI in groups of K in which each CSI is already known by a different user we can exploit the method described in 7.3.2 and reduce the total number of channel uses needed for the CSIR distribution by a factor $\frac{K-1}{K}$ compared to the one by one broadcasting strategy used in [33]. Using strategy in [33] the CSIR distribution length would be

$$\sum_{j=1}^{K} \frac{D(K - j)(M - j + 1)}{j} \tag{7.8}$$

and it becomes

$$\mathrm{L}_{CSIR}(MAT_M) = \frac{K - 1}{K} \sum_{j=1}^{K} \frac{D(K - j)(M - j + 1)}{j} \tag{7.9}$$

using the method we just described. This CSIR distribution can be partially taken care of in the empty space of $\sum_{j=1}^{K} \frac{D}{j}(j - 1) = D(K - H_K)$ time slots over the Q blocks because of the decreasing length of the common training in each phase. It leaves

$$\frac{K - 1}{K} \sum_{j=1}^{K} \frac{D(K - j)(M - j + 1)}{j} - D(K - H_K) =$$

$$D\left(\left(\frac{K - 1}{K} \sum_{j=1}^{K} \frac{(K - j)(M - j + 1)}{j}\right) + H_k - K\right) \tag{7.10}$$

remaining time slots to be used for the CSIR distribution. This is always greater than 0 for $K \geq 2$ and we note that there always is more CSIR to be distributed than empty space in any block because there is no empty space in the first phase, which takes D blocks. Because we assumed $K = M$ the resulting net multiplexing gain

is

$$\text{netDoF}(\text{MAT}_M) =$$

$$\frac{M(T_c - \overbrace{M}^{\text{training}}) - \overbrace{\sum_{j=1}^{K} \frac{1}{j}(K-j)(M-j+1)}^{\text{feedback}}}{H_K T_c + \left(\underbrace{\left(\frac{K-1}{K} \sum_{j=1}^{K} \frac{(K-j)(M-j+1)}{j} \right)}_{\text{CSIR distribution}} + \underbrace{H_k - K}_{\text{empty space}} \right)} \tag{7.11}$$

7.4.4 MAT-ZF

Let us first ignore the overhead. The idea behind the MAT-ZF scheme is essentially to perform ZF and superpose MAT only during the dead times of ZF. For that purpose we consider Q blocks of T_c symbol periods and split each block into two parts. The first part, the dead times of ZF, spans T_{fb} symbol periods and the second part, the $T_c - T_{fb}$ remaining symbols. We use the first part of each block to perform the MAT scheme T_{fb} times in parallel. During the second part of each block, ZF is performed.

The sum DoF for the MAT-ZF$_K$ scheme without accounting for the overhead is

$$\text{DoF}(\text{MAT-ZF}_M) = M \left(1 - \frac{(Q-D)T_{fb}}{QT_c} \right). \tag{7.12}$$

Indeed, per user, in QT_c channel uses, the ZF portion transmits $Q(T_c - T_{fb})$ symbols, whereas the MAT scheme transmits DT_{fb} symbols.

Now, we consider the overhead. In the MAT-ZF scheme ZF and MAT are performed. Because the training for ZF comprises the training needed for MAT, the training cost for MAT-ZF is the same as for ZF with a length of $M + 1$ time slots. But in order to perform MAT, the CSIR distribution is also required. The scheme was initially meant to be done over Q blocks to perform the MAT scheme but we add more blocks to do the CSIR distribution. We only use the dead times of the additional coherence blocks to do the CSIR distribution while we still perform ZF when the transmitter has CSI in order to avoid any degradation of the ZF DoF. The MAT part then requires $\Delta = \frac{L_{CSIR}(MAT_M)}{T_{fb}}$ additional blocks. The case of a non integer Δ can be dealt with by repeating the scheme until the total number of blocks to add is an integer. Let $\delta = \Delta/D$. Then, the netDoF of this scheme is

netDoF(ZF_M) + $MDT_{fb}/(T_c(Q + \Delta))$ or

$$\text{netDoF}(\text{MAT-ZF}_M) = \text{netDoF}(\text{ZF}_M) + \frac{T_{fb}}{T_c} \frac{M}{(H_M + \delta)} \qquad (7.13)$$

i.e., the netDoF of ZF plus an additional term, the DoF brought about by MAT but decreased by a factor because of the CSIR distribution.

7.4.5 ST-ZF

The scheme by Lee and Heath yields M DoF for $\alpha = \frac{T_{fb}}{T_c} = \frac{1}{K}$ with $K = M + 1$ users or for $\alpha < \frac{1}{K}$ by doing ZF the remaining time. We refer to this scheme as ST-ZF because it is a space-time precoding, which is combined with ZF for $\alpha < \frac{1}{K}$.

Simple ZF can only serve M users at a time and as mentioned earlier one channel use of dedicated training is needed for synchronization per subset of M users so instead of alternatively ZF to the K subsets of users $\{1, \cdots, i-1, i+1, \cdots, K\}$ in one block, it is less expensive to ZF to only one subset of $K-1$ out of K users per block and alternate over different blocks to assure fairness.

To allow the receivers to learn their channels, a common training sequence is needed so together with the dedicated training it takes $(M+1)$ time slots and $M + 1$ time slots for the output feedback (by choosing $K = M + 1$ times a different subset of $K-1$ users feeding back) resulting in a part without current CSIT of length $T_{fb} + 1$ instead of T_{fb}, thereby reducing the *with CSIT* part of one time slot too. This yields a feedback overhead of

$$\text{DoF}_{FB}(\text{ST-ZF}_M) = \frac{MK}{T_c} = \frac{M(M+1)}{T_c}. \qquad (7.14)$$

To decode its signal the receiver i needs to know $\mathbf{H}_{\text{eff}}^{(i)}$. The ST-ZF schemes spans over K blocks, but the different instances of the scheme overlap: the nth instance spans over blocks $n + 1$ to $n + K$, the $n + 1$th over blocks $n + 2$ to $n + K + 1$. So only the last line of $\mathbf{H}_{\text{eff}}$ is new in each instance. Therefore, each receiver actually only needs to get M coefficients of its $\mathbf{H}_{\text{eff}}^{(i)}$ (the last line). Using the CSIT part to transmit these coefficients takes $K = M + 1$ time slots by sending each time slot one message to each user of a different subset of $M = K - 1$ users. The net multiplexing gain is then

$$\text{netDoF}(\text{ST-ZF}_M) = M \frac{T_c - \overbrace{2(M+1)}^{\text{training and } \mathbf{H}_{\text{eff}}}}{T_c} - \frac{\overbrace{M(M+1)}^{\text{feedback}}}{T_c}$$

$$= M \left(1 - \frac{3(M+1)}{T_c} \right). \qquad (7.15)$$

119

It is valid as long as

$$\frac{T_{fb} + 1}{T_c - 2(M+1)} \leq \frac{1}{K}$$
$$\Leftrightarrow$$
$$T_c \geq K(T_{fb} + 3) \tag{7.16}$$

because ST-ZF needs a with CSIT part $K - 1 = M$ times longer than the no current CSIT part.

Another way of transmitting $\mathbf{H}_{\text{eff}}^{(i)}$ to the receivers is to do it in the following blocks in the no current CSIT part as presented for MAT-ZF. It assures a multiplexing gain always greater than that of ZF because it leaves the ZF part of each block untouched. It also enlarges the range of validity of the scheme because it does not reduce the part with CSIT. It takes KM time slots, therefore $\frac{KM}{T_{fb}+1}$ blocks because the dead time in ST-ZF is $T_{fb} + 1$ time slots long. We refer to this variant as ST-ZF 2. With this strategy the multiplexing gain is

$$\text{netDoF(ST-ZF2}_M) =$$

$$\frac{M\left(1 - \frac{\overbrace{2(M+1)}^{\text{training and feedback}}}{T_c}\right) + \text{netDoF(ZF}_M)\frac{KM}{T_{fb}+1}}{1 + \underbrace{\frac{KM}{T_{fb}+1}}_{\text{transmission of } \mathbf{H}_{\text{eff}}^{(i)}}} \tag{7.17}$$

as long as

$$\frac{T_{fb} + 1}{T_c - (M+1)} \leq \frac{1}{K}$$
$$\Leftrightarrow$$
$$T_c \geq K(T_{fb} + 2). \tag{7.18}$$

7.4.6 $\mathbf{ZF}_{FCFB}$

The training and feedback required to perform ZF_{FCFB} are the same as for classical ZF, the only difference is that to avoid any dead time the training/feedback frequency is increased from $\frac{1}{T_c}$ to $\frac{1}{T_c - (T_d + T_{ct})}$ as shown in 6.4. Here we considered OFB so $T_d = T_{fb}$.

With feedback every $T_c - (T_{fb} + Tct)$, the netDoF by performing ZF precoding is then

$$\text{netDoF(ZF}_M) = K\left(1 - \frac{2M + 1}{T_c - (T_{ct} + T_{fb})}\right)$$

$$= K\left(1 - \frac{\overbrace{2M + 1}^{\text{training and feedback}}}{T_c - (M + T_{fb})}\right) \tag{7.19}$$

because with full CSIT, the full DoF can be achieved with ZF.

7.5   Numerical Results and Discussion

In Fig. 7.2 and Fig. 7.3 we plot the netDoF provided by ZF, MAT, TDMA-ZF, MAT-ZF, TDMA, ST-ZF and ZF_{FCFB} for $M = 4$, as a function of T_c using (7.3) for ZF, (7.11) for MAT, (7.4) for TDMA-ZF, (7.13) for MAT-ZF, (7.15) for ST-ZF, (7.17) for ST-ZF 2 and (7.19) for ZF_{FCFB}. With $T_{fb} = 3$ in Fig. 7.2 and $T_{fb} = 10$ in Fig. 7.3. For TDMA we use $\frac{T_c - 1}{T_c}$, one pilot per coherence period being needed to insure coherent reception, by keeping the overhead to a minimum TDMA outperforms the other schemes for small T_c. We notice that even for $T_{fb} = 3$ and $T_c = 90$ the net DoF loss of the different schemes compared to the optimum $M = 4$ is significant. The DoF yielded by MAT and ST-ZF do not depend on T_{fb} except that ST-ZF is valid only for T_c greater or equal to a threshold, which grows with T_{fb}. We observe that the ST-ZF scheme performs better for larger values of T_{fb}, because the cost of the distribution of $\mathbf{H}_{\text{eff}}^{(i)}$ in the ST-ZF scheme can be compensated by not loosing any DoF on the no CSIT part of each block only if this part is long enough. If we compare analytically TDMA-ZF and ST-ZF we see that for $T_{fb} = M$ both schemes yield about the same multiplexing gain and the multiplexing gain of TDMA-ZF decreases below that of ST-ZF for T_{fb} sufficiently larger than M. The gain of ST-ZF over the other schemes becomes significant with larger values of T_{fb}. ST-ZF 2 is better than ST-ZF for small values of T_{fb}, so the best way to do the distribution of $\mathbf{H}_{\text{eff}}^{(i)}$ (in the CSIT part or in the DCSIT part) depends on T_{fb}. We notice that for small T_{fb} TDMA-ZF performs better than both variants of ST-ZF. However, by considering also a certain coherence in the frequency domain the relative cost of the transmission of the $\mathbf{H}_{\text{eff}}^{(i)}$ in the CSIT part should become negligible even for small values of T_{fb}. To summarize, for small T_c TDMA is the best, for large T_c TDMA-ZF or ST-ZF is better depending on T_{fb} and for intermediate T_c TDMA-ZF or MAT-ZF is better depending on T_{fb}.
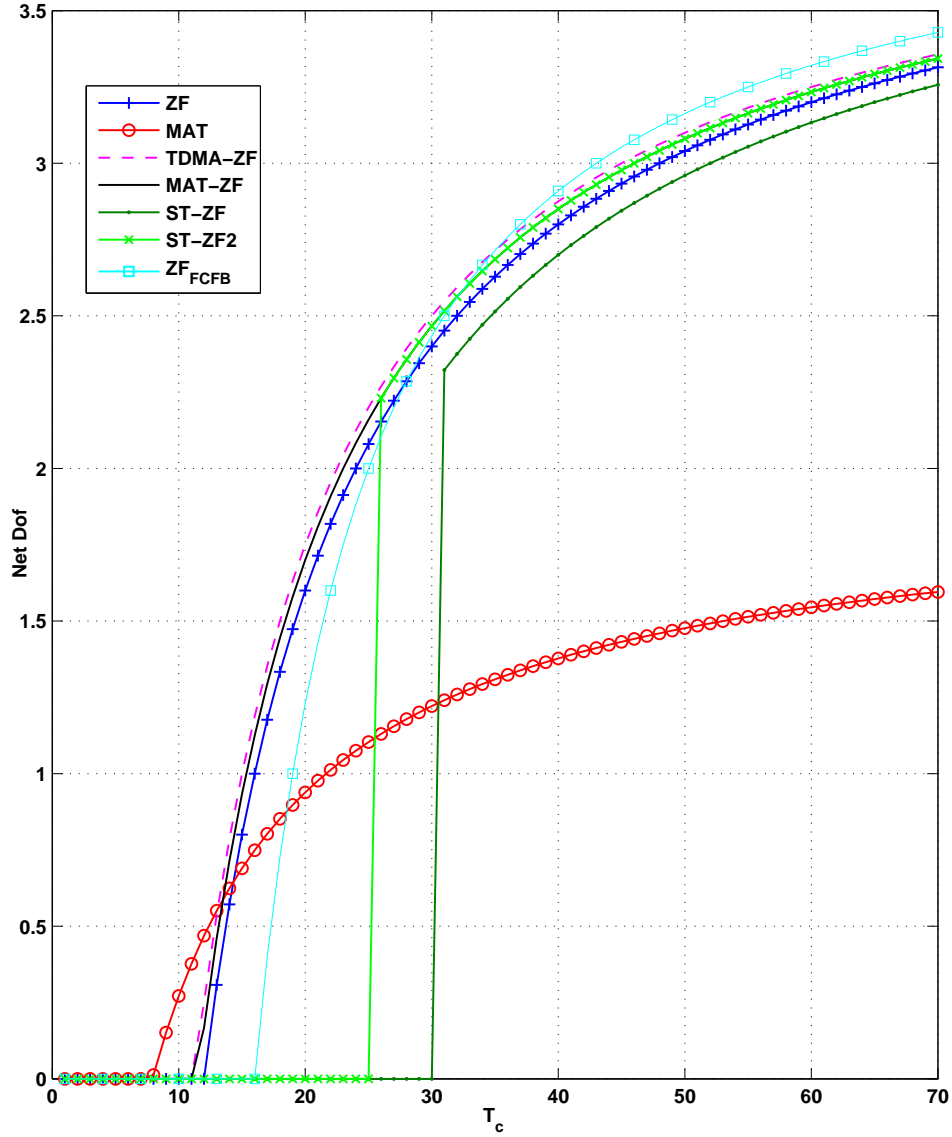
Figure 7.2: NetDoF of ZF_{FCFB}, ZF, MAT, TDMA-ZF, MAT-ZF, ST-ZF and TDMA in the MISO BC with $K = M = 4$ and $T_{fb} = 3$ as a function of T_c.

122
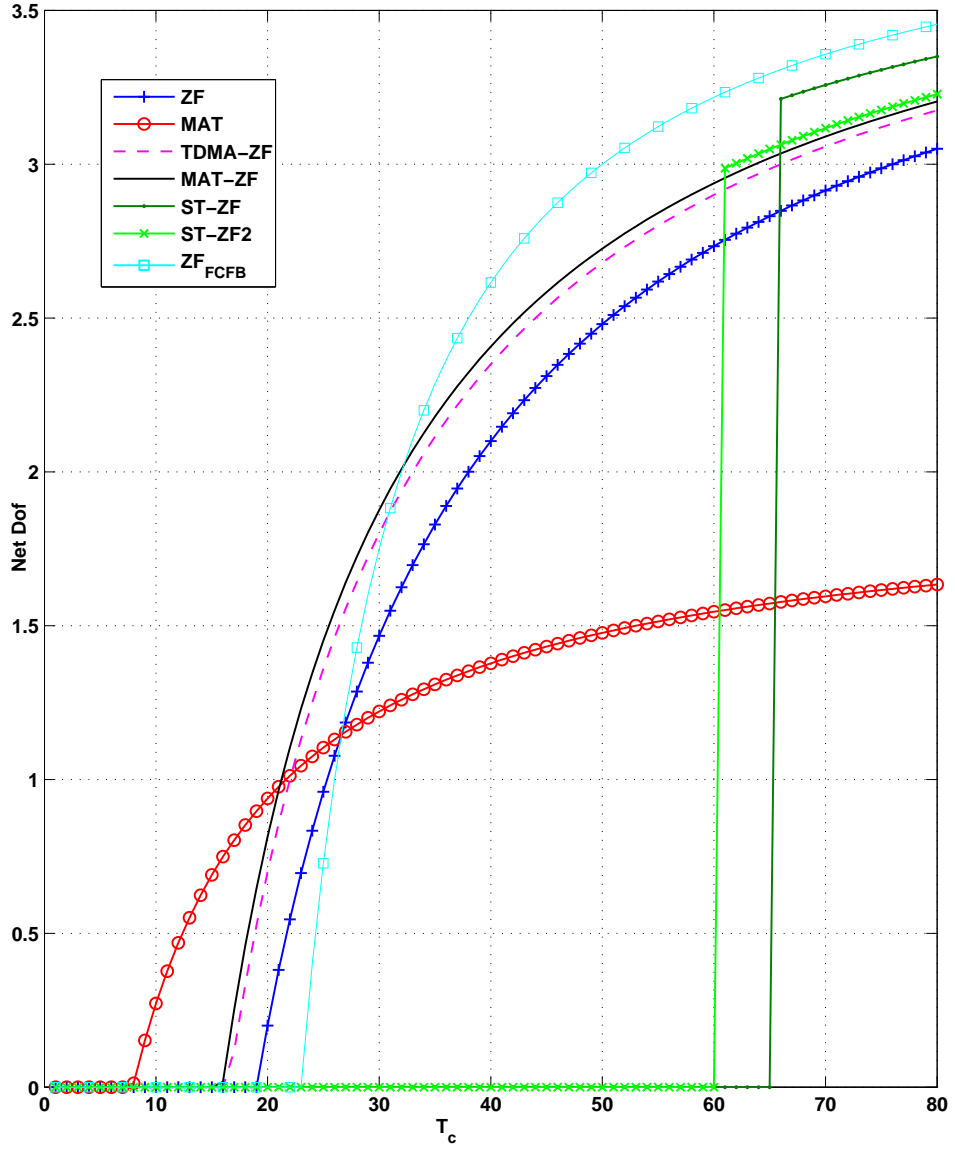
Figure 7.3: NetDoF of ZF_{FCFB}, ZF, MAT, TDMA-ZF, MAT-ZF, ST-ZF and TDMA in the MISO BC with $K = M = 4$ and $T_{fb} = 10$ as a function of T_c.
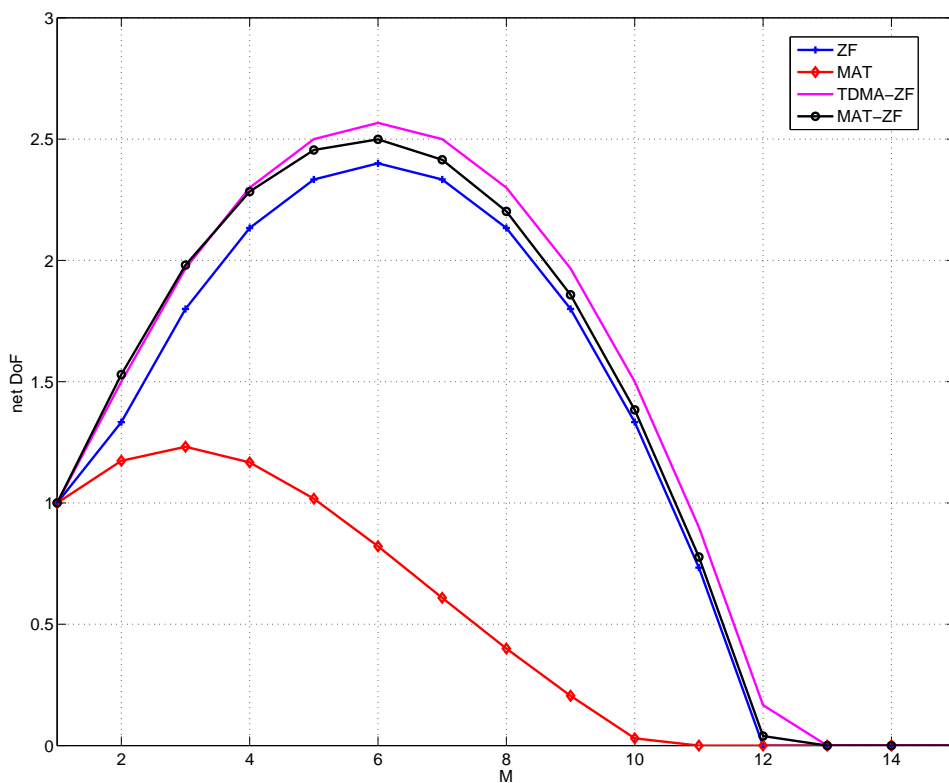
Figure 7.4: NetDoF of ZF, MAT, TDMA-ZF and MAT-ZF in the MISO BC with $T_c = 30, T_{fb} = 5$ as a function of $M = K$.

Finally, ZF_{FCFB} outperforms the other schemes but only for large T_c, in both case about $T_c > 33$ and the gap is larger for larger T_{fb}

7.5.1 Optimization of the number of users

In Fig. 7.4 the netDoFs of ZF, MAT, TDMA-ZF and MAT-ZF are plotted for $T_c = 30$, $T_{fb} = 5$ as a function of $M = K$. We notice that all the four schemes reach a maximum netDoF and then decrease. For each scheme there is an optimum number of users and active transmit antennas depending on the system parameters. Indeed first the DoF increases with M until a certain number beyond which the overhead becomes dominating. In this example the maximum netDoF is reached by TDMA-ZF with 6 active antennas (and 6 users).

The number of users K (and hence active antennas M) needs to be optimized
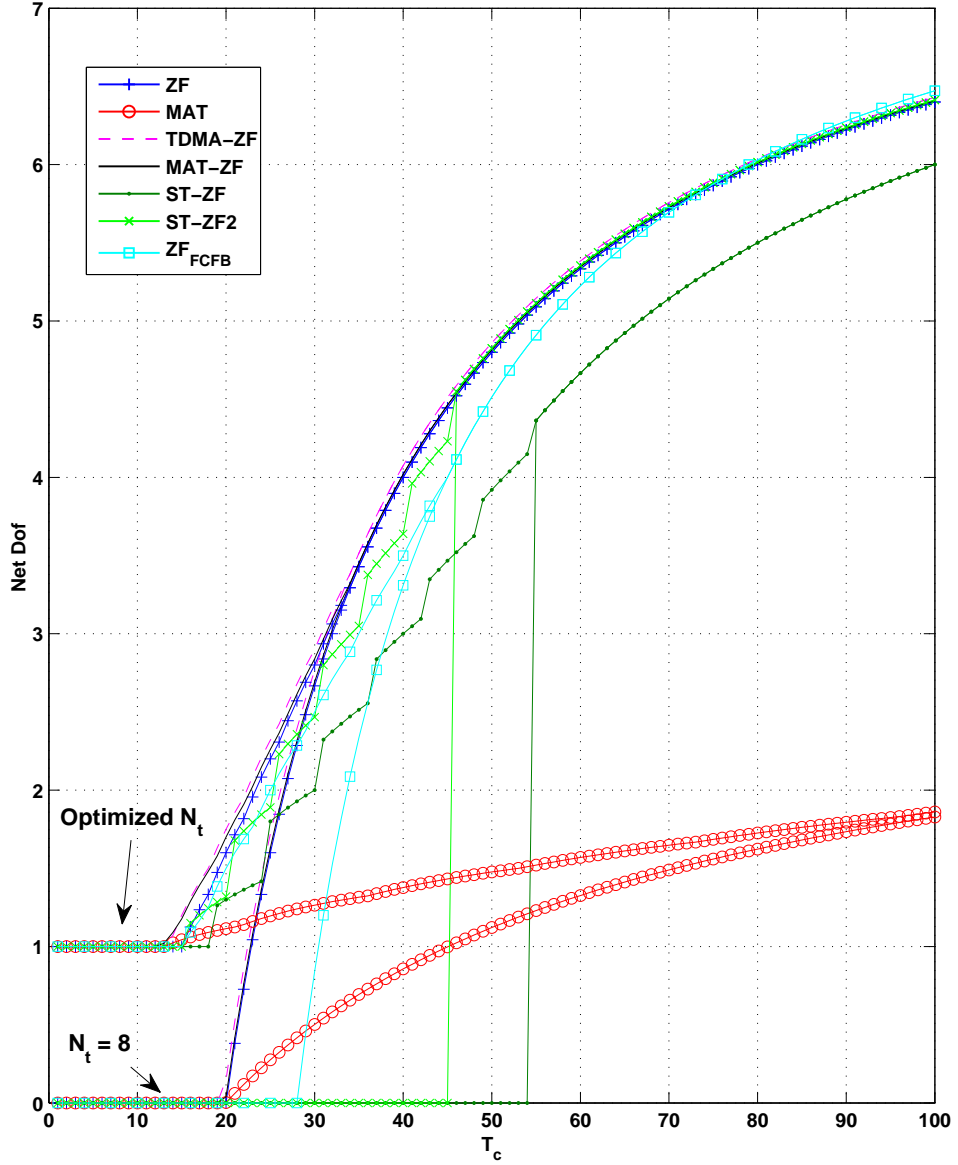
Figure 7.5: NetDoF of ZF$_{FCFB}$, ZF, MAT, TDMA-ZF, MAT-ZF, ST-ZF and TDMA and their optimized variants in the MISO BC with $M = 8$, $T_{fb} = 3$ as a function of T_c.

to find the right channel learning/using compromise because serving more users means a larger DoF but also larger overhead. All the net DoF of the schemes we reviewed reach a single maximum as a function of the number of antennas.

To each scheme we associate its optimized version, in which the number of active antennas is optimized, either analytically or empirically to maximize the net DoF.

In Fig. 7.5 we observe the net DoF of all considered schemes and of their optimized version for $K = 8$, $T_{fb} = 3$ as a function of T_c. We notice that if the optimization of the number antennas results in a gain for all schemes it also confirms that ZF_{FCFB} outperforms all the other schemes soon after having only one active antenna and one served user (simple TDMA) is not optimal anymore.

7.5.2 MAT

We proposed an improvement of the CSIR distribution but MAT still needs a very long coherence time for the CSIR distribution to be less penalizing. In Fig. 7.6 we plot the net DoF yielded by MAT with the CSIR distribution as in [33] (MAT1) and with our new CSIR distribution (MAT2) described in 7.3.2 for $T_c = 100$, $T_{fb} = 5$ as a function of $M = K$. We observe that especially for intermediate values of K the optimization of the CSIR distribution brings a limited but non negligible gain.

In Fig. 7.4 and Fig. 7.5 we notice that MAT barely outperforms simple TDMA transmission (1 DoF) for the parameters considered. In Fig. 7.7 we plot the net DoF obtained by MAT for $T_{fb} = 5$ and $T_c \in \{16,64,256,1024,4096,16384\}$ as a function of the number of users K as well as the asymptotic DoF of MAT, $\frac{K}{H_K}$. We observe that for example for $K = 5$, the asymptotic DoF of 2.19 is almost reached if $T_c \geq 1024$ but decreases by 8% for $T_c = 256$. For $K = 10$, $T_c = 1024$ only allows to reach 93% of the asymptotic DoF. The MAT scheme is impaired by the CSIR distribution overhead that grows quickly with the number of users, even with our optimized broadcast.

7.6 Multi-antennas receivers

Having noticed that ST-ZF for the MISO BC is interesting in terms of net DoF, especially for moderate vales of T_c and large T_{fb}, we now extend this scheme to the MIMO BC and make use of the multiple antennas at the receiver to widen the range of feedback delays for which the full sum DoF is preserved. We also propose an extension the MIMO IC. We consider now a MIMO BC with K users equipped with N antennas and a transmitter equipped with M antennas.
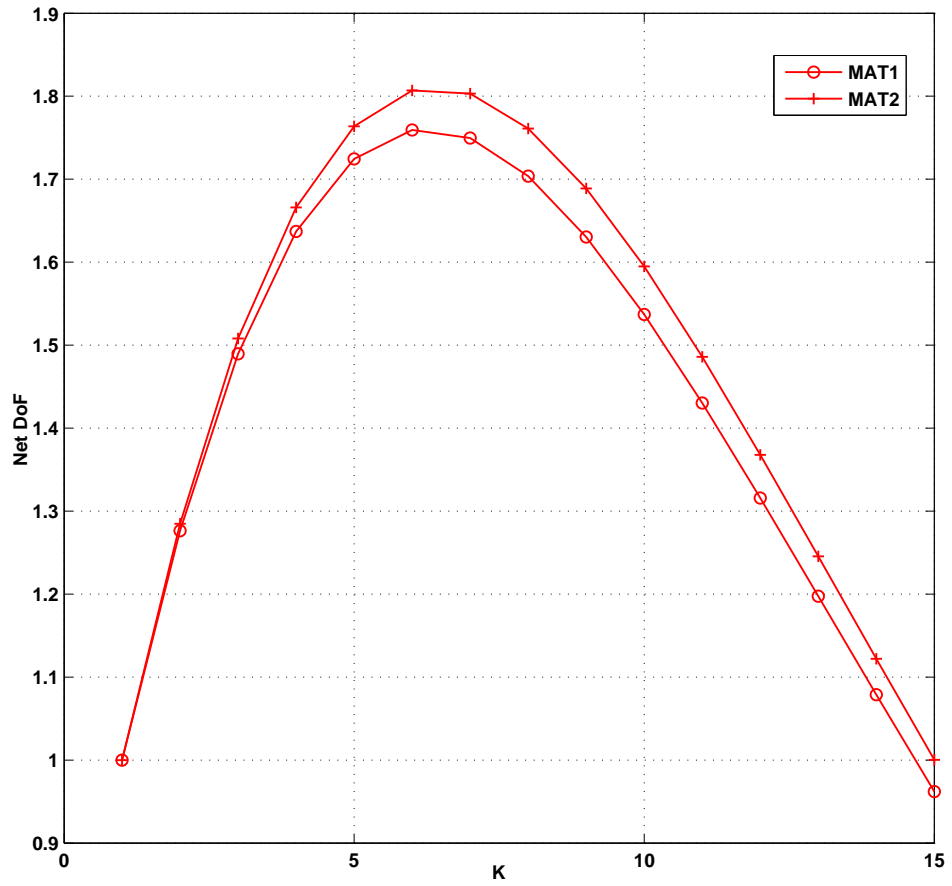
Figure 7.6: netDoFs provided by MAT as a function of $K = M$ for $T_{fb} = 5$ and $T_c = 100$.
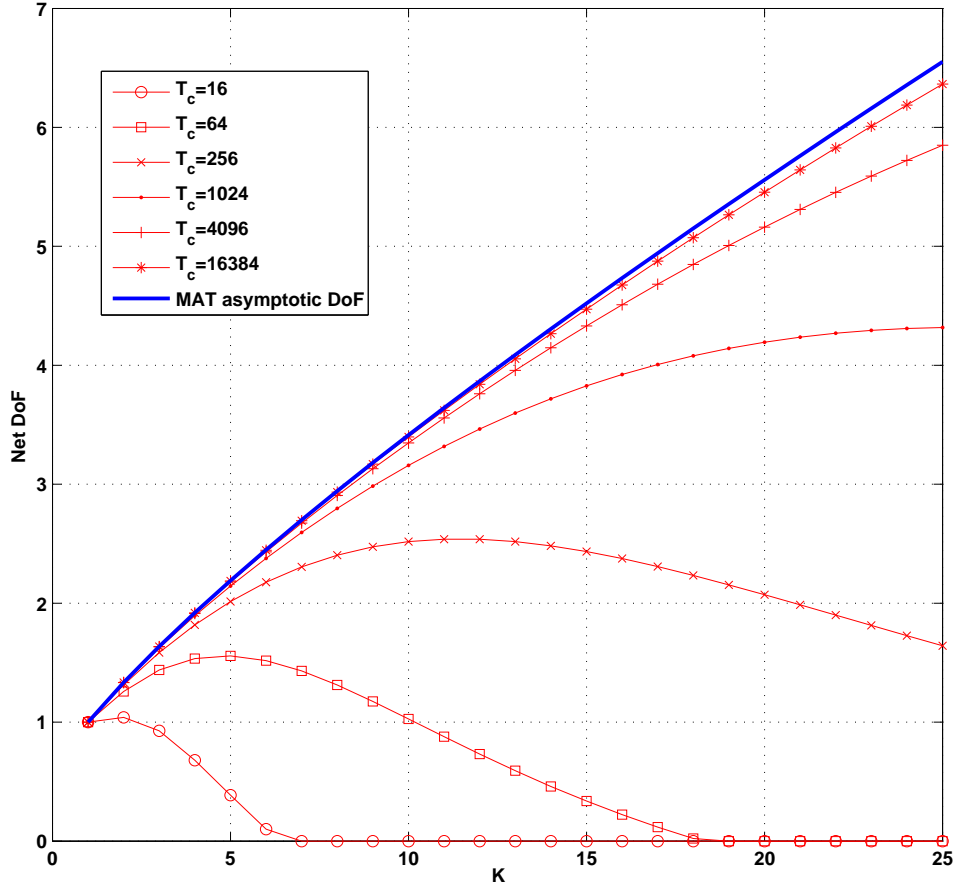
Figure 7.7: netDoFs provided by MAT as a function of $K = M$ for $T_{fb} = 5$ and $T_c \in \{16,64,256,1024,4096,16384\}$.

7.6.1 STIA-MIMO Scheme for the MIMO BC

The STIA-MIMO scheme we propose allows the transmission of M messages to each of the K users in K symbol periods scattered over K coherence blocks. More precisely, we use symbol periods $\{t_1, t_2, \cdots, t_K\}$ respectively in blocks $\{t + 1, t + 2, \cdots, t + K\}$. This results in a transient regime for the first K blocks after which we have KT_{fb} instances of the scheme in each block assuring the M DoF announced in the stationary state. We now focus on one instance of the STIA-MIMO scheme scattered over blocks $t + 1$ to $t + K$ for a $n \geq K$ so that we are in steady state. Only the symbol period t_1 in the first block corresponds to the transmitter not having the current CSI.

Messages $\mathbf{s}_k = \left[s_k^{(1)}, \cdots, s_k^{(M)} \right]^T \in \mathbb{C}^{M \times 1}$ are intended for user k, $k \in [1, K]$. $\mathbf{H}[n] = \left[\mathbf{H}_1[n]^T, \cdots, \mathbf{H}_K[n]^T \right]^T \in \mathbb{C}^{KN \times M}$ represents the channel matrix during block n and $\mathbf{y}[t_j] = \left[\mathbf{y}_1[t_j]^T, \cdots, \mathbf{y}_K[t_j]^T \right]^T \in \mathbb{C}^{KN \times 1}$ the concatenation of the received signals at the receivers during symbol period t_j. Because we are interested in the DoF provided by the scheme, we hereafter omit the noise variables to be concise. The transmitter always sends a combination of all symbols at each symbol period, always the same symbols for an instance of the scheme but with time-varying BF matrices $\mathbf{V}_k[t_j] \in \mathbb{C}^{M \times M}$

$$\mathbf{x}[t_j] = \sum_{k=1}^{K} \mathbf{V}_k[t_j] \mathbf{s}_k. \tag{7.20}$$

During the first symbol period t_1, the transmitter does not have any information on the current channel state, so for $k \in [1, K]$, $\mathbf{V}_k[t_1] = \mathbf{I}_M$, the M by M identity matrix, is as good as any other matrix of full rank. The transmission scheme is

summarized as follows

$$
\begin{bmatrix} \mathbf{y}[t_1] \\ \mathbf{y}[t_2] \\ \vdots \\ \mathbf{y}[t_K] \end{bmatrix} = \mathrm{diag}(\mathbf{H}[t+1], \mathbf{H}[t+2], \cdots, \mathbf{H}[t+K])
$$

$$
* \begin{bmatrix} \mathbf{I}_M & \cdots & \mathbf{I}_M \\ \mathbf{V}_1[t_2] & \cdots & \mathbf{V}_K[t_2] \\ \vdots & & \vdots \\ \mathbf{V}_1[t_K] & \cdots & \mathbf{V}_K[t_K] \end{bmatrix} \begin{bmatrix} \mathbf{s}_1 \\ \mathbf{s}_2 \\ \vdots \\ \mathbf{s}_K \end{bmatrix} =
$$

$$
\begin{bmatrix} \mathbf{H}[t+1] & \cdots & \mathbf{H}[t+1] \\ \mathbf{H}[t+2]\mathbf{V}_1[t_2] & \cdots & \mathbf{H}[t+2]\mathbf{V}_K[t_2] \\ \vdots & & \vdots \\ \mathbf{H}[t+K]\mathbf{V}_1[t_K] & \cdots & \mathbf{H}[t+K]\mathbf{V}_K[t_K] \end{bmatrix} \begin{bmatrix} \mathbf{s}_1 \\ \mathbf{s}_2 \\ \vdots \\ \mathbf{s}_K \end{bmatrix}
$$

The received signal at user i and time t_1 is

$$
\mathbf{y}_i[t_1] = \sum_{k=1}^{K} \mathbf{H}_i[t+1]\,\mathbf{s}_k = \mathbf{H}_i[t+1] \sum_{k=1}^{K} \mathbf{s}_k. \tag{7.21}
$$

The BF matrices are constructed so that the IA is simply done at each receiver by a subtraction of two received signal vectors: $\mathbf{y}_i[t_j] - \mathbf{y}_i[t_1], j \in [2,K]$. For user i, at time $t_j, j \in [2,K]$, we have

$$
\mathbf{y}_i[t_j] - \mathbf{y}_i[t_1] = \sum_{k=1}^{K} \left(\mathbf{H}_i[t+j]\mathbf{V}_k[t_j] - \mathbf{H}_i[t+1] \right) \mathbf{s}_k
$$

so the interferences are aligned if

$$
\mathbf{H}_i[t+j]\mathbf{V}_k[t_j] - \mathbf{H}_i[t+1] = \mathbf{0}_M, \forall i \neq k
$$

where $\mathbf{0}_M$ is the $M \times M$ null matrix. In other words, the BF matrices $\mathbf{V}_k[t_j]$ should transform the channel matrix $\mathbf{H}_i[t+j]$ in $\mathbf{H}_i[t+1]$ for $i \neq k$ so that the same interferences are received at any time $t_j, j \in [1,K]$. This is done by defining

the BF matrix for user k and time t_j as follows

$$
\mathbf{V}_k[t_j] = \begin{bmatrix} \mathbf{H}_1[t+j] \\ \vdots \\ \mathbf{H}_{k-1}[t+j] \\ \mathbf{H}_{k+1}[t+j] \\ \vdots \\ \mathbf{H}_k[t+j] \end{bmatrix}^{-1} \begin{bmatrix} \mathbf{H}_1[t+1] \\ \vdots \\ \mathbf{H}_{k-1}[t+1] \\ \mathbf{H}_{k+1}[t+1] \\ \vdots \\ \mathbf{H}_k[t+1] \end{bmatrix} \tag{7.22}
$$

for $j \in [2,K]$ which assures

$$
\begin{bmatrix} \mathbf{y}_i[t_2] - \mathbf{y}_i[t_1] \\ \mathbf{y}_i[t_3] - \mathbf{y}_i[t_1] \\ \vdots \\ \mathbf{y}_i[t_K] - \mathbf{y}_i[t_1] \end{bmatrix} = \underbrace{\begin{bmatrix} \mathbf{H}_i[t+2]\mathbf{V}_i[t_2] - \mathbf{H}_i[t+1] \\ \mathbf{H}_i[t+3]\mathbf{V}_i[t_3] - \mathbf{H}_i[t+1] \\ \vdots \\ \mathbf{H}_i[n+K]\mathbf{V}_i[t_K] - \mathbf{H}_i[n+1] \end{bmatrix}}_{\mathbf{H}_i^{\text{eff}}} \mathbf{s}_i
$$

and user i can decode $\mathbf{s}_i$ because the rank of the $M \times M$ matrix $\mathbf{H}_i^{\text{eff}}$ is almost surely M because all channel vectors are independent with a continuous distribution. This scheme allows to transmit a total of MK independent data symbols in K channels uses, thereby yielding M sum DoF.

7.6.2 Longer Feedback delays

Feedback delays longer than $\frac{N}{M+N}$ can simply be dealt with by doing time sharing between STIA and a scheme designed for completely outdated CSIT, MAT, as suggested in [35].

In Fig. 7.8 lower and upper bounds on the DoF region for $M = 8$ and different N as a function of α are given. We observe that increasing the number of receive antennas allows to win on both sides, preserving the full sum DoF on a wider range of α and also increasing the DoF reached by MAT. For $N = 4$ there is only one curve because the upper bound is $DoF^U(8,3,4) = 4\,DoF_1^U(2,3)$ and $DoF_1^U(2,3)$ is achievable according to Theorem 5 in [86]. For $N = 8$ there is only one curve because $DoF = \min\{M = 8, N = 8\} = 8$ is achievable without any CSIT.

The STIA scheme by Lee and Heath is very interesting because it proved that up to a certain delay in the feedback the full DoF of the MISO BC is still attainable. By extending this result to multi-antenna receivers (MIMO BC), we managed to widen the range of feedback delays for which the full sum DoF can be preserved. We also described an extension to a combination with MAT to cover all possible
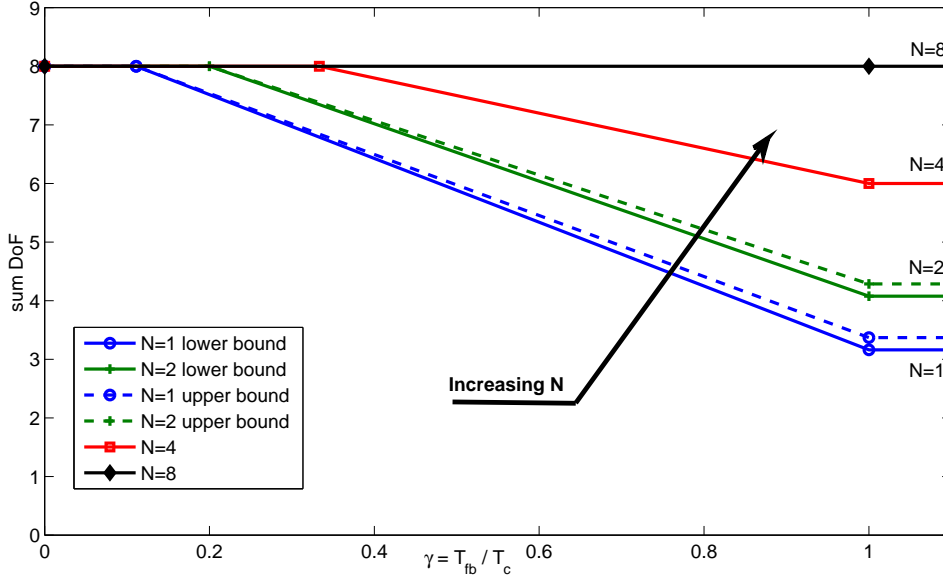
Figure 7.8: DoF reached by time sharing between STIA and MAT in the MIMO BC for $M = 8$ and $N \in \{1,2,4,8\}$.

feedback delays. Finally we provided a minor variation of the scheme to adapt it to the IC, allowing to maintain M DoF for the same range of feedback delays as in the BC.

7.7 Discussion

In this chapter we have reviewed and proposed several transmission scheme to mitigate the loss due to DCSIT. We quickly notice that it was important to take into account the training and feedback overhead of the different schemes. Indeed, the combination MAT-ZF, which is optimal in case of DCSIT in terms of DoF, underperforms in most scenarios when the overheads are accounted for. Similarly, the ZF_{FCFB} was very promising in terms of DoF because it allows to always have CSIT and, therefore, no DCSIT at all. However, it is only interesting for large T_c when we take into account the overheads.

Chapter 8

Delayed CSIT in the IC

8.1   Introduction

If numerous techniques allow the increase of the DoF, most of them rely on accurate and timely CSIT and CSIR. Especially CSIT cannot be assumed to be instantaneous because it requires feedback, which inexorably causes a delay. Concerning the issue of delayed CSIT, much progress has been made in the BC as detailed in Chapter 7 with schemes such as [31, 35, 37, 38].

Results for the IC are much sparser, the scheme in [38] is extended to the IC but only for the two-user case in [39] and the one in [35] that achieves M (sum) DoF in the block fading underdetermined MISO BC with M transmit antennas and $G = M + 1$ users if the feedback delay is small enough ($T_{fb} \leq T_c/G$) is also valid in the MISO IC with M antennas per transmitter and $G = M + 1$ transmitter-receiver pairs [40].

We noticed that this possibility of achieving the full sum DoF of the MISO BC with small feedback delays comes at the expense of a slight increase of the feedback overhead in Chapter 7. It was also demonstrated in [41] that the minimum fraction of time of perfect current CSIT required per user in order to achieve the optimal DoF of $\min(M,G)$ is given by $\min(M,G)/G$. Therefore, the lack of timeliness of CSIT can be compensated by having the CSIT of more users. Indeed, the achievability result in [41] relies on always having perfect current CSIT of M users at any time but not always of the same M users. In a classic block fading model, this would require an increase of the feedback overhead. In [42], the feedback versus performance trade-off is characterized extensively. For the square case, i.e., when $G = M$, the authors confirm that with a block fading model any feedback delay causes a DoF loss and that the basic combination of using MAT, when only delayed CSIT is available, and performing ZF, when current CSIT is

available, is optimal in terms of DoF.

Block fading and stationary bandlimited fading models are shown to be both special cases of the more general FRoI model in 6. Furthermore, we demonstrated that, with adequate training and foresighted feedback, the CSI can be acquired at any time and be valid for the coherence time of the channel T_c. It thereby allows for the permanent availability of CSIT and for the possibility of performing ZF without any dead time (ZF_{FCFB}), at the cost of an increased rate of training and feedback.

For the three-user SISO IC, [43] introduces *retrospective interference alignment* and reaches a DoF greater than one with outdated CSIT. Then, in [44], a general scheme for the G-user SISO IC with outdated CSIT was shown to reach a sum DoF that is greater than one and increases with G. However, these DoF are upper bounded by $\frac{4}{6\ln 2 - 1} \approx 1.266$. In [45], a scheme based on ergodic IA is shown to yield a DoF that increases with G and approaches 2 in the G-user SISO IC with outdated CSIT. There is no proof of optimality of these DoF, but it is conjectured that the DoF of the SISO IC with completely outdated CSIT is upper bounded by a constant in [44]. This is in sharp contrast with the optimal sum DoF of $\frac{G}{2}$ in the SISO IC with current CSIT [4].

We will demonstrate that the optimal sum DoF of the G-user SISO IC is still $\frac{G}{2}$ for feedback delay $T_{fb} \leq T_c/2$ and propose a scheme that achieves this optimal sum DoF. Moreover, this feedback delay supported here will be proved to be the longest for which the optimal $G/2$ DoF can still be obtained for all G.

The approach is based on a variation of the *ergodic interference alignment* scheme proposed in [16], where the authors show that not only $\frac{G}{2}$ DoF are attainable but also that each user can get half of its interference-free rate at any SNR. Our variation will conserve this property.

T_{fb} denotes an abstract delay between the beginning of the block and the time CSI is available at the transmitter so it represent the dead time.

Then, we will review different scheme for the IC with CSIT, and compare the netDoF of the schemes as we noticed in Chapter 7 that taking the overheads into account can make a significant difference. However, the newly proposed scheme does not require any extra overhead and should, therefore, also prove interesting in terms of netDoF.

8.2 System Model and Assumptions

We first consider a G-user SISO IC, i.e., there are G transmitter-receiver pairs, all equipped with a single-antenna so $\mathbf{H}[t] = [h_{ji}(t)] \in \mathbb{C}^{G \times G}$ denote the channel matrix at time t where $h_{ji}(t)$ is the frequency flat time-varying channel coefficient
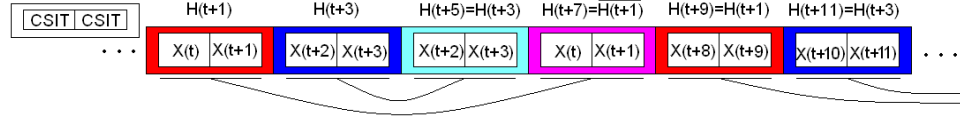
Figure 8.1: Example of ergodic IA with $T_c = 2$ and $T_{fb} = 0$.
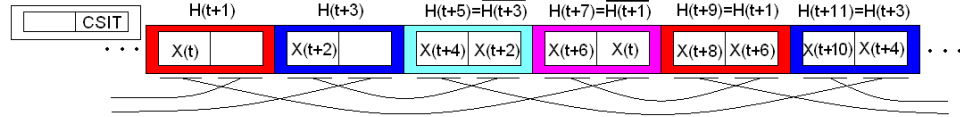
Figure 8.2: Example of ergodic IA variant for delayed CSIT with $T_c = 2$ and $T_{fb} = 1$.

between transmitter i and receiver j. We assume a block fading model, the channel coefficients are constant over blocks of length T_c and change independently between blocks. Furthermore, channel coefficients are drawn from a continuous distribution, their phases are uniformly distributed and are independent from their magnitude. It is assumed that, because of feedback delay, the transceivers possess the CSI only after a delay of T_{fb} channel uses.

Our starting point is the work on ergodic IA [16]; we use a similar system and channel model. Most of the remarks and improvements made to the original scheme could be applied also to our delayed CSIT version. For instance, the channel coefficient distribution does not need to be symmetric [46], the sum of channel matrices below can be relaxed to be an arbitrary diagonal matrix and not only the identity matrix [46], and simple strategies can be deployed to reduce latency [64].

8.3 Main Result

Our main result is the following theorem assessing the resilience of the IC sum DoF against the lack of timeliness of the CSIT.

Theorem 5 *In the G-user SISO IC, as long as feedback delay $T_{fb} \leq \frac{T_c}{2}$,*

$$DoF(G) = \frac{G}{2} \ . \tag{8.1}$$

To prove achievability, in Section 8.3.2, we introduce a variant of the ergodic IA scheme [16] that works in the block fading IC and does not require any CSIT before the second half of each block. The converse is trivial because $\frac{G}{2}$ is the DoF of the G-user SISO IC with instantaneous CSIT.

135

8.3.1 Ergodic IA

The main idea behind ergodic IA is to transmit the data a first time during channel realization $\mathbf{H}[t_1]$, then to wait for the complementary channel realization $\mathbf{H}[t_2]$ such that $\mathbf{H}[t_1] + \mathbf{H}[t_2] = I$, the $G \times G$ identity matrix. We shall denote this relation by $\mathbf{H}[t_2] = \overline{\mathbf{H}[t_1]}$. It allows each receiver to cancel all interference by simply adding the signals received at times t_1 and t_2.

As already concisely mentioned in Section 4.2, $\mathbf{H}[t_2] = \overline{\mathbf{H}[t_1]}$ will never happen in practice when channel coefficients are drawn from a continuous distribution. Nonetheless, through appropriately precise quantization, it is still possible to match up channel matrices to an approximation error that is small enough to allow decoding [16]. It is possible to match up enough channel realizations to yield $\mathrm{DoF}_{\mathrm{ErgoIA}}$ that approaches $\frac{G}{2}$ by using sequences of channel realizations that are long enough.

[16] assumes $T_c = 1$ and $T_{fb} = 0$, but the extension to larger T_c with $T_{fb} = 0$ is straightforward and is illustrated in Fig. 8.1 for $T_c = 2$. We will now prove that a similar strategy can be set up for any T_c and T_{fb} such that $T_{fb} \leq \frac{T_c}{2}$.

8.3.2 Ergodic IA with delayed CSIT

Assuming $T_{fb} = \frac{T_c}{2}$, we can divide each block in two parts of *equal* length: the beginning of the block, when there is no current CSIT and the end of the block, when current CSI is available at the transmitter. In this configuration, the original ergodic IA cannot be performed anymore, or at least not on the first part of each block. However, it is possible not to associate whole complementary blocks but only half blocks. For example, consider the case $T_c = 2$ and $T_{fb} = 1$. For all t: $\mathbf{H}[2t] = \mathbf{H}[2t+1]$ and current CSIT is only available on odd time indexes. Then, if $\mathbf{H}[2t_1] = \overline{\mathbf{H}[2t_2]}$ and $\mathbf{H}[2t_1+1] = \overline{\mathbf{H}[2t_2+1]}$, we can match the second channel use of the complementary channel realization, $\mathbf{H}[2t_2+1]$, with the first channel use of the first channel realization, $\mathbf{H}[2t_1]$, because, at time index $2t_2 + 1$, there is CSIT on both $\mathbf{H}[2t_1]$ and $\mathbf{H}[2t_2+1]$. This new pairing method is illustrated in Fig. 8.2.

In more detail, *new* data signals are sent during the first half of each block. As explained in [16], we quantize all possible channel realizations and can take blocks of channel realizations of length T coherence blocks such that the sequence of channel realizations will be γ-typical with probability $(1 - \epsilon)$. We refer to these blocks as meta-blocks here to indicate that, in our case, they are blocks of coherence blocks. This means that the number of occurrences $\#H_i$ of any channel realization H_i in a given meta-block is bounded as follows

$$T_c T \left(p(H_i) - \gamma \right) \leq \#H_i \leq T_c T \left(p(H_i) + \gamma \right)$$

with probability $(1-\epsilon)$. Because the coefficients are drawn i.i.d. from a distribution with uniform phase, the probability that the complement of a channel matrix occurs in a given time frame is the same as the probability that the original matrix occurs. However, this requirement on the distribution can be relaxed [46]. We can ensure it will be possible to pair enough channel realizations between two consecutive meta-blocks to approach $\frac{G}{2}$ DoFs in *steady state* by defining γ and ϵ as in [16]. Indeed, we notice that the second part of each block in the first meta-block will be wasted as well as the first part of each block of the last meta-block. However, by performing this scheme over a sequence of N meta-blocks, it is possible to transmit $(N-1)$ information blocks with the multiplexing gain of ergodic IA, thereby reaching DoF $= \frac{N-1}{N}\text{DoF}_{\text{ErgoIA}}$, which approaches $\text{DoF}_{\text{ErgoIA}}$ as N increases. It proves that $\text{DoF}_{\text{ErgoIA}}$ can be made arbitrarily close to $\frac{G}{2}$, which proves the achievability in Theorem 5 for the case $T_{fb} = \frac{T_c}{2}$. The case of smaller T_{fb} is trivially settled by still dividing each block in two parts of equal length, this time a fraction of the first part will correspond to the transmitter having current CSI instead of delayed CSI. However, what can be done with delayed CSIT can also be done with current CSIT and the proposed scheme is still applicable.

8.4 Feedback delay-DoF tradeoff

8.4.1 Time Sharing

The variant of ergodic IA described above works for $T_{fb} = \frac{T_c}{2}$ but also for any shorter feedback delay without any modification. The case of longer feedback delay can be dealt with by doing time sharing between the variant we propose and TDMA transmission or any technique designed for the SISO IC with completely delayed CSIT. To the best of our knowledge, in the IC, only two other schemes deal with non trivial feedback delays that remain smaller than the channel coherence time. In [40], for $G = 2$, the authors also obtain the full sum DoF of the SISO IC with feedback delays up to half the channel coherence time but this could also be obtained by simple TDMA transmission. Their scheme is generalized for larger G but requires more transmit antennas M and preserves the optimal sum DoF of $M = G - 1$ up to $T_{fb} = \frac{T_c}{G}$, which decreases with G. On the contrary, the scheme proposed here preserves the full sum DoF of the G-user SISO IC for $T_{fb} \leq \frac{T_c}{2}$ for any G. In the scheme proposed in Chapter 6, the full sum DoF can be preserved at the cost of an increase of the training and feedback frequency whereas the scheme proposed here does not. In Fig. 8.3, we plot the sum DoF that can be achieved (solid lines) in the G-user SISO IC as a function of $\frac{T_{fb}}{T_c}$. The dashed lines corresponds to time sharing between IA (when current CSIT is available) and
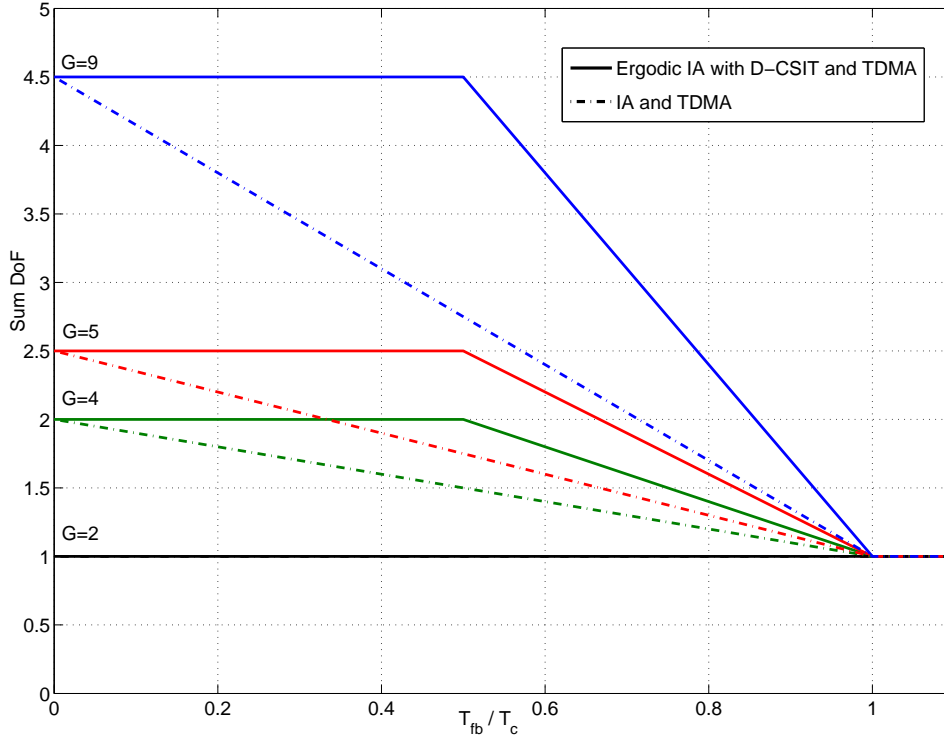
Figure 8.3: Feedback delay-DoF tradeoff in the SISO IC.

TDMA (otherwise). We observe that the proposed ergodic IA variant significantly improves the sum DoF.

8.4.2 Partial Optimality

The scheme described presents a partial optimality in the sense that the feedback delay of $T_{fb} = T_c/2$ supported here is the longest for which the optimal $G/2$ DoF can still be obtained for all G. The idea for proving this converse result is to use the DoF of the G-user MISO BC with G transmit antennas as an upper bound because splitting the transmit antennas can only decrease the capacity. In [42], the authors show that time sharing between MAT and ZF is optimal when dealing with delayed CSIT in the square MISO BC. This means that the DoF of the SISO IC with delayed CSIT, as a function of $\frac{T_{fb}}{T_c}$, is upperbounded by a line going from $(0,G)$ to $(1, \frac{G}{\sum_{k=1}^{G} \frac{1}{k}})$. For large G, this results in the DoF having to be less than $\frac{G}{2}$ at an abscissa increasingly closer to $\frac{1}{2}$ as illustrated in Fig. 8.4 for $G = 20$ and
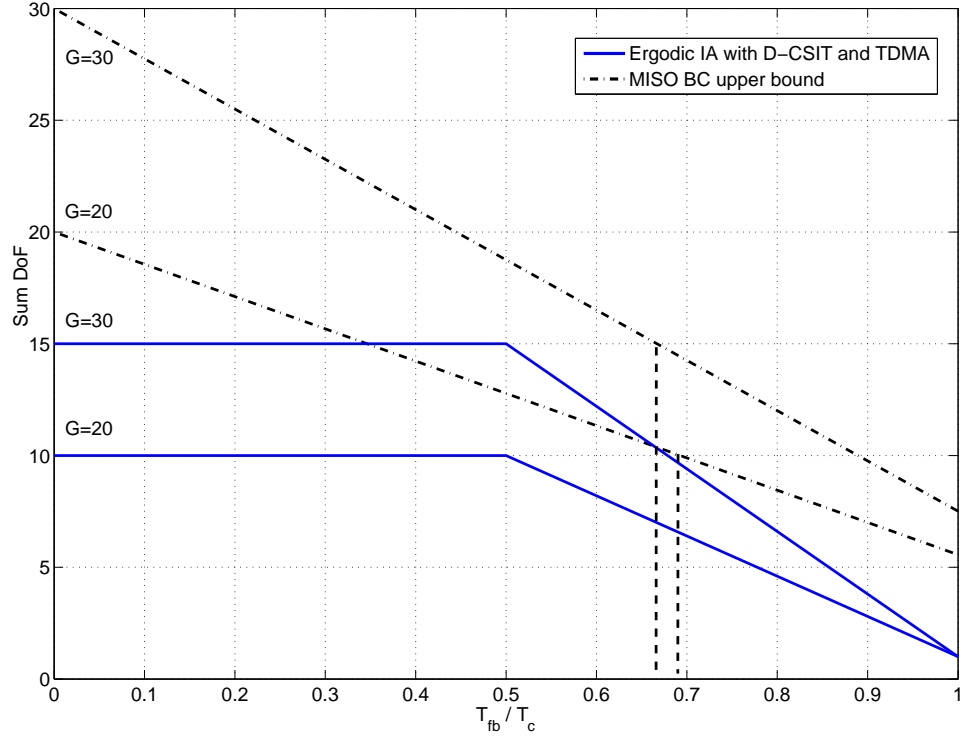
Figure 8.4: MISO BC upper bound.

$G = 30$. Formally, we have the following theorem,

Theorem 6 *If there is a scheme such that*

$$\forall G, DoF = \frac{G}{2} \text{ for } T_{fb} = \alpha T_c$$

then

$$\alpha \leq \frac{1}{2}.$$

Proof: According to [42], the DoF of the G-user MISO BC with $T_{fb} = \alpha T_c$ is reached by time sharing between MAT and ZF and is

$$(1 - \alpha)G + \alpha \frac{G}{\sum_{k=1}^{G} \frac{1}{k}}$$

which becomes less than $G/2$ for

$$\alpha > \frac{1}{2(1 - \frac{1}{\sum_{k=1}^{G} \frac{1}{k}})} \approx \frac{0.5}{1 - \frac{1}{\ln(G)}}$$

139

which approaches $\frac{1}{2}$ when G grows and makes it impossible to have a scheme that preserves the $G/2$ DoF for all G for any α strictly greater than $\frac{1}{2}$. $\qquad\square$

8.5 MIMO IC or IBC Configurations

8.5.1 Square MIMO Configurations

The exact same (SISO) scheme is applicable to the square MIMO IC, i.e., when there are $M = N$ transmit and receive antennas. Indeed, in this configuration, one can do at least as well as in the GM-user SISO IC and achieve $\frac{GM}{2}$ DoF with $T_{fb} \leq \frac{T_c}{2}$, which is the optimal sum DoF of the square MIMO IC according to [4].

8.5.2 Rectangular MIMO Configurations

The scheme proposed in [16] for "recovering more messages" can be used to reach the decomposition bound in the MISO case. In 4.2 we covered the SIMO case similarly. By combining the two, one can also cover MIMO configurations for the cases of either M/N or N/M being an integer R using the decomposability. In the SIMO and MISO variant, the CSI is not needed for the first transmission but only for the last R transmissions. Therefore, by doing the pairing in a similar fashion, it is possible to achieve the $\min(M,N)GR/(R + 1)$ DoF with feedback delay up to $\frac{1}{R+1}$ of the channel coherence time.

8.5.3 IBC Configurations

The ergodic IA scheme, and its variant proposed here, do not require any joint antenna processing and can, therefore, also be used in IBC or interfering multiple access channels.

8.6 Net DoF Characterization

The ergodic IA variant proposed here provides a strong theoretical result: the full sum DoF of the G-user SISO IC can be preserved with feedback delays up to $\frac{T_c}{2}$. Moreover, it is proved that this feedback delay supported here is the longest for which the optimal $G/2$ DoF can still be obtained for all G. Most improvements applicable to ergodic IA, for instance to reduce latency, can also be applied to the proposed variant. The scheme also assures that half the interference free rate can be reached at finite SNR [16]. A different pairing rule could be chosen to reach an optimal SNR offset over the original scheme as proposed in [46]. We observe that, contrary to the MISO BC, in the SISO IC with delayed CSIT the full sum DoF

can be preserved without requiring extra receivers [35, 41] or the extra overhead of the scheme presented in Chapter 6. We will now derive the net DoF in order to compare the multiplexing gains that asymptotic IA and ergodic IA can be expected to obtain in actual systems, we derive their net DoFs, accounting for training and feedback overhead. In other words, we evaluate how many DoF are available for data on the forward link (we account for delay and training) and subtract the DoF wasted on the reverse link for the feedback.

8.6.1 CSI Acquisition Overheads

For the G receivers to estimate their channel, a common training of length greater than or equal to M per transmitter is needed, resulting in a total training length $T_{ct} \geq GM$. To maximize the DoF we take the minimal $T_{ct} = GM$. According to [104], an additional dedicated training of d_k pilot is required in the end, to assure coherent reception at receiver k, resulting in $T_{tr_a} = GM + \sum_k d_k$ symbol periods per block devoted to training in order to perform asymptotic IA. For ergodic IA, the only difference is that there is no need for dedicated training because no precoding is done resulting in $T_{tr_e} = GM$ symbol periods per block devoted to training in order to perform ergodic IA.

As in the BC case, the noise in the fed back channel estimate can be ignored in the case of analog feedback or of digital feedback of equivalent rate. The feedback is accurate, suffering only from the delay. We consider analog feedback and two feedback strategies, CFB or OFB. In the BC, OFB is a lot better because the feedback length is the same as the training; however, this will not be case in the IC so the benefit of OFB compared to CFB is smaller in the IC. In any case, user k needs to feedback the coefficients of its G channels with transmitter $i,i \neq k$, i.e.; GMN coefficient to feedback per user. The total feedback is $GGMN$ symbols and consumes $T_{f_a} = GGN$ channel uses on the reverse link for both feedback strategies to do asymptotic IA.

A slight improvement could be made in case of ergodic IA. As was mentioned in [46], there exist an optimal pairing that maximizes the SNR offset that imposes a relation between coefficients of direct links, $\mathbf{H}[t_1](k,k)$ and $\mathbf{H}[t_2](k,k)$, in the two channel realizations. However, for DoF purposes, we only requires that coefficients of direct links are not additive inverses so that the intended signal is not canceled when received signals are added. Therefore, one bit feedback for the direct links is enough to do the pairing and it is null in terms of DoF so the feedback cost can be reduced to $T_{f_e} = G(G-1)N$ channel uses for ergodic IA.

The difference between CFB and OFB is the time it takes for the transmitter to have CSI after the training is done, with CFB it takes $T_{d,CFB} = T_f + T_{fb}$ where T_{fb} is the delay in the feedback because of processing and propagation. With OFB

the receivers do not have to wait for all the training to be done to start the feedback and we have $T_{d,OFB} = \max(T_f + T_{fb} - T_{tr}, T_{fb})$ because it cannot be less than T_{fb}. In order to have only one expression for the netDoF we will use the following notation, T_{d_a} and T_{d_e}, the DCSIT time. It is the total time between the end of training and the moment CSI available at the transmitters, which will be equal to $T_{d,CFB}$ or $T_{d,OFB}$ depending on the feedback strategy. In other words, it corresponds to the time spent with the forward link being free but with the transmitter not having CSI yet.

These feedback length values are obtained assuming a distributed model, each transmitter gets all the CSI from feedback without the need for a central unit. In Fig. 7.1(b) an illustration of a block is given for a better understanding of the different parts. The two parts available for downlink transmission are No CSIT and CSIT, they respectively correspond to the transmitter having only past CSI and past CSIT together with current CSI.

8.6.2   Asymptotic IA

Whit current CSIT, the full multiplexing gain can be achieved with asymptotic IA. Doing only asymptotic IA would allow to transmit an average of

$$D = \min(M,N)\frac{R}{R+1} \tag{8.2}$$

symbols per channel use to each user when the transmitter has CSIT and nothing otherwise (dead time). Taking feedback and training into account we obtain

$$\text{netDoF(aIA)} = D\left(1 - \frac{T_{\text{delay}_a} + GGN}{T_c}\right)$$

$$= D\left(1 - \frac{\overbrace{T_{d_a}}^{\text{dead time}} + \overbrace{GM + D}^{\text{training}} + \overbrace{GGN}^{\text{feedback}}}{T_c}\right) \tag{8.3}$$

where $T_{\text{delay}_a} = T_{d_a} + T_{tr_a}$ is the CSIT acquisition delay.

8.6.3   Ergodic IA

Whit current CSIT, the full multiplexing gain can be achieved with ergodic IA. The difference is that ergodic IA can also be performed over the DCSIT time T_{d_e} as long as it is not longer than the time with current CSIT 5, i.e., less than $T_c - T_{\text{delay}_e}$. Taking feedback and training into account we obtain

$$\text{netDoF(eIA)} =$$

$$D \left(1 - \frac{\overbrace{(T_{d_e} - (T_c - T_{\text{delay}_e}))^+}^{\text{dead time}} + \overbrace{GM}^{\text{training}} + \overbrace{G(G-1)N}^{\text{feedback}}}{T_c} \right) \tag{8.4}$$

indeed $T_c - T_{\text{delay}_e}$ is the number of channel uses available for transmission with CSIT and, with $(a)^+$ denoting $\max(0,a)$, $(T_{d_e} - (T_c - T_{\text{delay}_e}))^+$ is the part of DCSIT time that cannot be used with ergodic IA and is actually lost (dead time).

8.6.4 TDMA-IA

TDMA gives $\min(M,N)$ DoF and only require CSI at the receiver, which is available during the DCSIT time because the training has already been done. Therefore, doing TDMA over the DCSIT time that is not yet used is a simple way to improve the net DoF of asymptotic IA, and possibly of ergodic IA in case all the DCSIT time cannot be used to perform ergodic IA. We obtain

$$\text{netDoF(TDMA-aIA)} = \text{netDoF(aIA)} + \frac{\min(M,N)T_{d_e}}{T_c} \tag{8.5}$$

and

$$\begin{aligned}\text{netDoF(TDMA-eIA)} \quad &= \quad \text{netDoF(eIA)} + \\ &\frac{\min(M,N)(T_d - (T_c - T_{\text{delay}_e}))^+}{T_c}.\end{aligned} \tag{8.6}$$

More elaborate schemes could be used to benefit from the DCSIT time when TDMA could actually work even with no CSIT at all. However, unlike in the BC, the DCSIT schemes for IC have showed limited gain so far [43–45, 105].

We now derive the netDoF of a few proper schemes and of TDMA to be able to make broader comparisons for configurations for which the two bounds are the same. Because the STIA scheme for MIMO IC is closely related to the BC version, and will not be used for comparisons because it can not be used on configurations that yield both the same DoF for decomposition and proper schemes its description is given in Appendix B.2. The training is the same as for the two decomposition schemes and the feedback overhead is the same as for ergodic IA because the CSI on the direct links is not needed at the transmitter for DoF analysis of the proper IA schemes considered here.

8.6.5 IA$_{FCFB}$

With feedback every $T_c - T_d - T_{tr} = T_c - T_{\text{delay}}$ the transmitters always have the current CSI, which allows them to perform IA without any dead time. The DoF achieved by IA is $D = G\frac{M+N}{G+1}$, together with the augmented frequency of training and feedback it results in the following netDoF

$$\text{netDoF(IA}_{FCFB}) = \qquad\qquad (8.7)$$

$$D\left(1 - \frac{\overbrace{GM + D}^{\text{training}} + \overbrace{G(G-1)N}^{\text{feedback}}}{T_c - T_{\text{delay}}}\right)$$

as long as $T_c \geq T_{\text{delay}}$.

8.6.6 Classic IA

Waiting when CSIT is not available and performing IA only when CSIT is available achieves the following netDoF

$$\text{netDoF(IA)} = \qquad\qquad$$

$$\text{DoF(IA)}\left(1 - \frac{T_d + \overbrace{GM + D}^{\text{training}} + \overbrace{G(G-1)N}^{\text{feedback}}}{T_c}\right). \qquad (8.8)$$

8.6.7 TDMA-IA

TDMA-IA is a direct extension of IA. The only difference being that while the transmitter is waiting for the CSI, and not sending training symbols it performs TDMA transmission because this does not require any CSIT, thus achieving

$$\text{netDoF(TDMA-IA)} = \text{netDoF(IA)} + \min(M,N)\frac{T_d}{T_c}. \qquad (8.9)$$

8.6.8 TDMA

TDMA is the simplest strategy to avoid interferences and does not require CSIT, only one transmitter transmits at a time. This reaches a sum DoF of $\min(M,N)$ and only require CSIR, that can be obtained by the receiver after a training of $\min(M,N)$ channel uses thus achieving the following netDoF

$$\text{netDoF(TDMA)} = \min(M,N)\left(1 - \frac{\min(M,N)}{T_c}\right) \qquad (8.10)$$

144
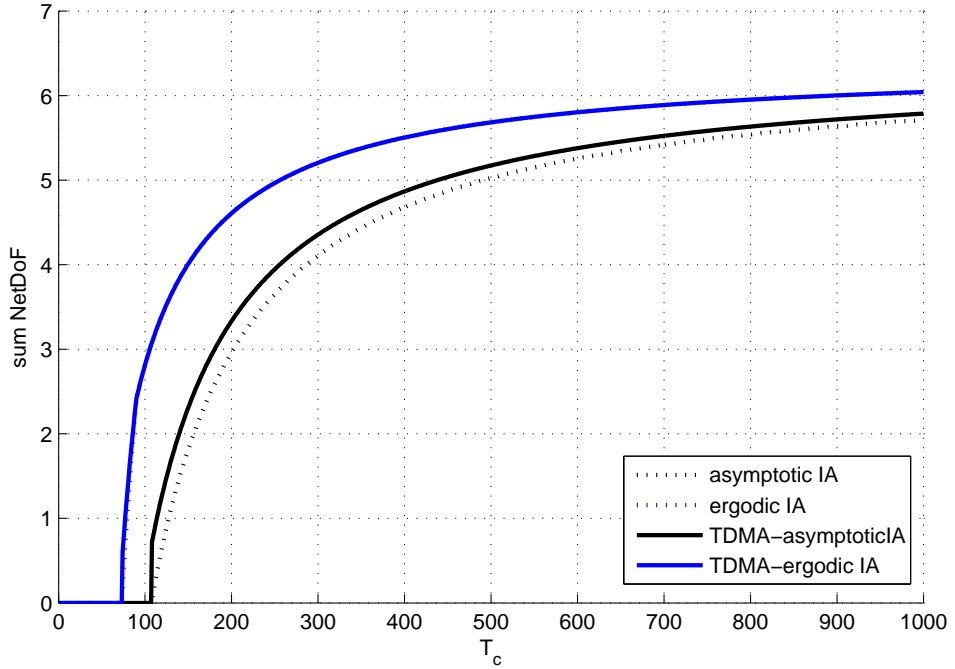
Figure 8.5: NetDoF of asymptotic IA, ergodic IA and their combination with TDMA for $G = 4$, $M = 8$, $N = 2$, $T_{fb} = 3$ as a function of T_c.

as long as $T_c \geq \min(M,N)$.

8.7 Numerical Results

8.7.1 Decomposition IA schemes

In Fig. 8.5 we plot the netDoF provided by asymptotic IA, ergodic IA and their combination with TDMA for $G = 4$, $M = 8$, $N = 2$, $T_{fb} = 3$ as a function of T_c, using (8.3) for asymptotic IA, (8.4) for ergodic IA, (8.5) for TDMA-asymptotic IA and (8.6) for TDMA-ergodic IA. OFB was chosen because it reduces the feedback delay. We notice that asymptotic IA is improved by the addition of TDMA but still is largely outperformed by ergodic IA, because the ergodic IA variant loses almost no DoF to feedback delay and does not require extra overheads. Because the DCSIT time is most of the time used to perform ergodic IA, the addition of TDMA is not significant.

In Fig. 8.6 the same observations can be made, this time in a square MIMO IC with $G = 4$, $M = N = 4$, $T_{fb} = 3$.
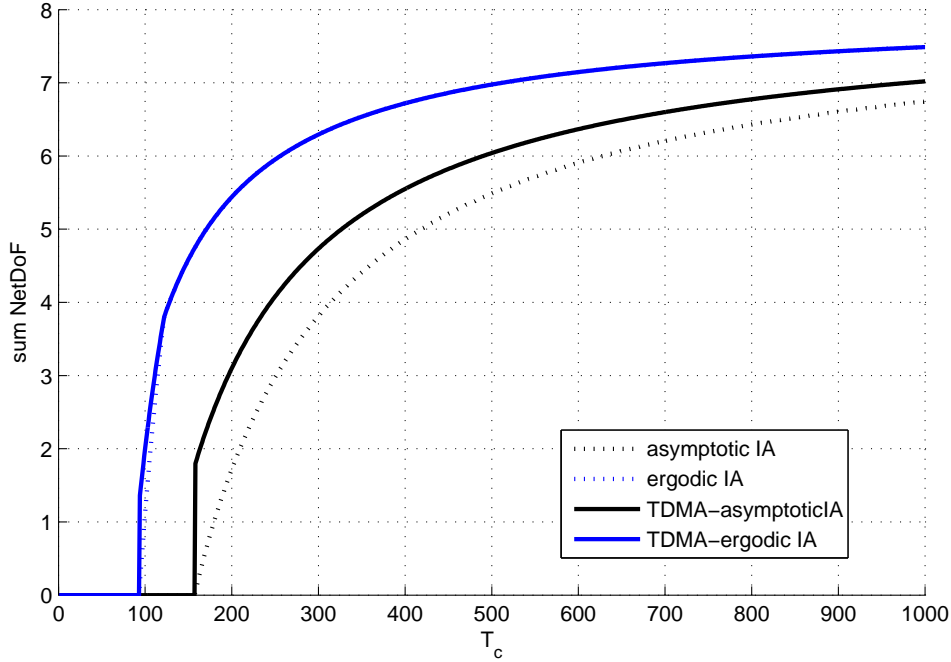
Figure 8.6: NetDoF of asymptotic IA, ergodic IA and their combination with TDMA for $G = 4$, $M = N = 4$, $T_{fb} = 3$ as a function of T_c.

8.7.2 Decomposition and proper IA schemes

In Fig. 8.7 we compare the netDoF of the decomposition schemes with proper schemes. To be fair, we consider a configuration where the proper bound and the decomposition bound are both equal to 1 DoF per user: $G = 3$ and $M = N = 2$. We notice that asymptotic IA has similar performances as the proper schemes, this is because it has the same DoF and similar losses due to feedback delay. On the contrary, thanks to its robustness to feedback delay, ergodic IA outperforms all the others schemes as soon as simple TDMA is not optimal anymore. However, it is worth mentioning that both asymptotic and ergodic IA induce similarly long decoding delays to approach the decomposition bound in comparison with proper schemes.

Similarly to what is mentioned in Chapter 7 for the BC case, in the IC the numbers of active cells and active antennas M and N need to be optimized to find the right channel learning/using compromise because serving more users (or having more active antennas) means a larger DoF but also larger overheads. This why for small T_c, TDMA, i.e., single-user MIMO, is optimal.

146
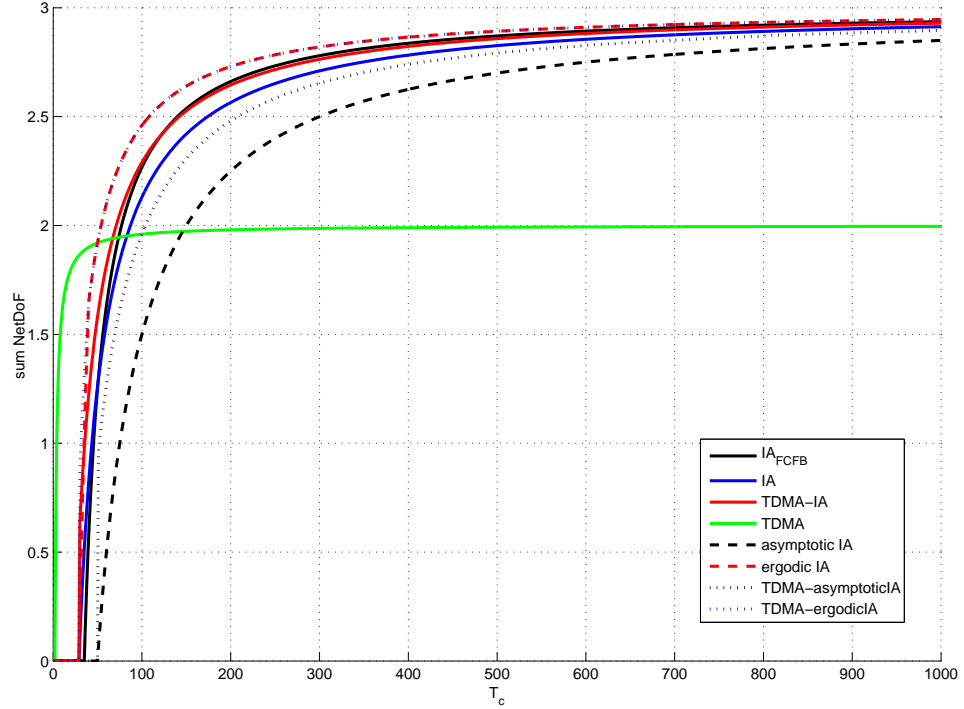
Figure 8.7: NetDoF comparison of decomposition schemes and linear schemes for $G = 3$, $M = N = 2$, $T_{fb} = 3$ as a function of T_c.

8.8 Conclusion

The ergodic IA variant proposed in this chapter provides a strong theoretical result: the full sum DoF of the G-user SISO IC can be preserved with feedback delays up to $\frac{T_c}{2}$. It was also proved that this feedback delay supported here is the longest for which the optimal $G/2$ DoF can still be obtained for all G. Most improvements applicable to ergodic IA, for instance to reduce latency, can also be applied to the proposed variant. The scheme also assures that half the interference free rate can be reached at finite SNR [16]. A different pairing rule could be chosen to reach an optimal SNR offset over the original scheme as proposed in [46].

We observe that, contrary to the MISO BC, in the SISO IC with delayed CSIT the full sum DoF can be preserved without requiring extra receivers [35, 41] or extra overhead, which proved to be especially advantageous in terms of net DoF because ergodic IA outperforms asymptotic IA, and, when they yield the same DoF, ergodic IA also outperforms the proper schemes in net DoF.

Chapter 9

Conclusion and Perspectives

9.1 Conclusion

The main focus of this thesis was the evaluation of the effect of a few realistic aspects of wireless networks.

The first aspect was the number of user. Both in single-cell and multi-cell configurations we have proposed solutions to benefit from having more users. For the BC, we proposed a GUS criterion for both MISO and MIMO configurations, by carefully selecting the user to which the BS transmits we were able to decrease the suboptimality of ZFBF compared to DPC and by resorting to a greedy approach we were able to keep a reasonable level of computational complexity. In the IC, having more user actually increases the multiplexing gain and we proposed two algorithms, to benefit from having multiple antennas when trying to approach the proper bound or the decomposition bound. While the algorithm for the decomposition bound is mostly theoretical because is has similar practical issues, the algorithm for the proper bound is easy to implement and proved to be efficient in numerical simulations.

Then, we studied what happen when there is partial connectivity in an IBC, in the sense that certain interference links can be neglected. We proposed a first approach called separation, which allows to increase the multiplexing gain compared to naive methods. The algorithm proposed for fully connected IBC also proved to perform well on partially connected IBC. It was actually able to achieve larger multiplexing gains. The separation approach remains interesting in certain cases because it requires less overheads.

The second part of this thesis was focused on the issue of delayed CSIT, to which the issue of overhead is closely related. We first proposed a general channel model and new feedback strategy to overcome feedback delay (and the de-

layed CSIT issue) at the cost of an increased training and feedback frequency. The model is also interesting because it encompasses both stationary fading and block fading, thereby proving that it makes sense to compare results derived using different (stationary or block fading). With actually delayed CSIT, the first question is what can be done when the channel is not yet known by the transmitters. In the BC, we proposed to associate ZF and MAT, which proved to be optimal in term of multiplexing gain. Then, the multiplexing gains of different schemes were reviewed, accounting for overheads, showing that a tradeoff to be found and different schemes are optimal depending on the delay and channel coherence time. In the IC, we proposed a scheme reaching the full sum multiplexing gain of the IC, robust to feedback delay up to half the channel coherence time and that does not require extra overheads. Therefore, the proposed scheme also outperforms other known schemes when accounting for overheads.

9.2 Perspectives

The most logical way to pursue this work would be to investigate ways of reducing CSI needed at the transmitter. Indeed, we saw that having more users is useful, but when global CSIT is assumed it quickly becomes less practical. Therefore, it would be interesting to find transmission schemes performing well with *partial* CSIT. There are two main axis, either reduce the number of links that need to be known at different nodes (incomplete CSI sharing), or reduce the information needed on each link (e.g. covariance or Gaussian CSIT), or ideally both. The benefits are twofold, because the overhead and the delay due to CSIT acquisition would decrease.

Appendices

Appendix A

More users

A.1 Proof of Proposition 1

In order to evaluate $\det(diag\{(H_i H_i^H)^{-1}\}))^{-1}$ we need to know

$$(H_i H_i^H)_{j,j}^{-1}, j = 1, \cdots, i.$$

For $j < i$ in order to compute $A(S_i)_{j,j}^{-1} = (H_i H_i^H)_{j,j}^{-1}$ easily, we move the jth row of H_i to the last position, meaning that we consider $\tilde{H}_i = h_{k_{1:j-1,j+1:i,j}}^H$. It can also be seen as the result of doing $i - j$ row permutations on H_i, $n \leftrightarrow n + 1$ for $j \leq n < i$. $\tilde{A}(S_i) = \tilde{H}_i \tilde{H}_i^H$ is the result of doing the same $i - j$ permutations on the rows and on the columns of $A(S_i)$, a total of $2(i - j)$ permutations, thus leaving the determinant unchanged. The Laplace expansion of $A(S_i)$ and $\tilde{A}(S_i)$ shows that the cofactors are also unchanged yielding $A(S_i)_{j,j}^{-1} = \tilde{A}(S_i)_{i,i}^{-1}$. We can decompose $\tilde{A}(S_i)$

$$\tilde{A}(S_i) \quad = \quad \left[\begin{array}{cc} A(S_{i-1} \backslash j) & B \\ B^H & A_r \end{array} \right]$$

where $A(S_{i-1} \backslash j) = h_{k_{1:i-1 \backslash j}}^H h_{k_{1:i-1 \backslash j}}$, $A_r = h_{k_{i,j}}^H h_{k_{i,j}}$ and $B = h_{k_{1:i-1 \backslash j}}^H h_{k_{i,j}}$. The matrix inversion lemma in block form yields

$$\tilde{A}(S_i)^{-1} \quad = \quad \left[\begin{array}{cc} X & Y \\ Z & U \end{array} \right]$$

where $U = (A_r - B^H A(S_{i-1} \backslash j)^{-1} B)^{-1}$. Therefore,

$$
\begin{aligned}
U^{-1} &= h_{k_{i,j}}^H h_{k_{i,j}} \\
&- (h_{k_{1:i-1}\backslash j}^H h_{k_{i,j}})^H (h_{k_{1:i-1}\backslash j}^H h_{k_{1:i-1}\backslash j})^{-1} h_{k_{1:i-1}\backslash j}^H h_{k_{i,j}} \\
&= \left[\begin{array}{cc}
h_{k_i}^H P_{h_{k_{1:i-1}\backslash k_j}}^\perp h_{k_i} & h_{k_i}^H P_{h_{k_{1:i-1}\backslash k_j}}^\perp h_{k_j} \\
h_{k_j}^H P_{h_{k_{1:i-1}\backslash k_j}}^\perp h_{k_i} & h_{k_j}^H P_{h_{k_{1:i-1}\backslash k_j}}^\perp h_{k_j}
\end{array} \right]
\end{aligned}
$$

and the 2×2 matrix inversion applied to U^{-1} yields

$$
\begin{aligned}
\frac{1}{U_{2,2}} &= \frac{\det(U^{-1})}{h_{k_i}^H P_{h_{k_{1:i-1}\backslash k_j}}^\perp h_{k_i}} \\
&= \frac{\|P_{h_{k_{1:i-1}\backslash k_j}}^\perp h_{k_j}\|^2 \|P_{h_{k_{1:i-1}\backslash k_j}}^\perp h_{k_i}\|^2}{\|P_{h_{k_{1:i-1}\backslash k_j}}^\perp h_{k_i}\|^2} \\
&- \frac{|h_{k_j}^H P_{h_{k_{1:i-1}\backslash k_j}}^\perp h_{k_i}|^2}{\|P_{h_{k_{1:i-1}\backslash k_j}}^\perp h_{k_i}\|^2} \\
&= \|P_{h_{k_{1:i-1}\backslash k_j}}^\perp h_{k_j}\|^2 - \frac{|h_{k_j}^H P_{h_{k_{1:i-1}\backslash k_j}}^\perp h_{k_i}|^2}{\|P_{h_{k_{1:i-1}\backslash k_j}}^\perp h_{k_i}\|^2} \qquad \text{(A.1)}
\end{aligned}
$$

giving the value of $(A(S_i)^{-1})_{(j,j)}$ for $j < i$. For $j = i$ we apply the matrix inversion lemma to $A(S_i)$ with a different decomposition

$$
A(S_i) = \left[\begin{array}{cc}
A(S_{i-1}) & h_{k_{1:i-1}}^H h_{k_i} \\
h_{k_i}^H h_{k_{1:i-1}} & h_{k_i}^H h_{k_i}
\end{array} \right]
$$

yielding

$$
\begin{aligned}
\frac{1}{A(S_i)_{i,i}^{-1}} &= h_{k_i}^H h_{k_i} - h_{k_i}^H h_{k_{1:i-1}} A(S_{i-1})^{-1} h_{k_{1:i-1}}^H h_{k_i} \\
&= h_{k_i}^H (I - h_{k_{1:i-1}} A(S_{i-1})^{-1} h_{k_{1:i-1}}^H) h_{k_i} \\
&= \|P_{h_{k_{1:i-1}}}^\perp h_{k_i}\|^2 \qquad \text{(A.2)}
\end{aligned}
$$

Combining (A.1) and (A.2) leads to $\det(\text{diag}\{(H_i H_i^H)^{-1}\}) =$

$$
\|P_{h_{k_{1:i-1}}}^\perp h_{k_i}\|^2 \prod_{j=1}^{i-1} (\|P_{h_{k_{1:i-1}\backslash k_j}}^\perp h_{k_j}\|^2 - \frac{|h_{k_i}^H P_{h_{k_{1:i-1}\backslash k_j}}^\perp h_{k_j}|^2}{\|P_{h_{k_{1:i-1}\backslash k_j}}^\perp h_{k_i}\|^2}).
$$

A similar reasoning applied to $\det(\text{diag}\{(H_{i-1}H_{i-1}^H)^{-1}\})$, moving the jth row and column to the last position and applying the matrix inversion lemma with A_r reduced to only one term, yields

$$\det(\text{diag}\{(H_{i-1}H_{i-1}^H)^{-1}\}) = \prod_{j=1}^{i-1} \|P^{\perp}_{h_{k_{1:i-1}\setminus k_j}} h_{k_j}\|^2.$$

These formulations allow us to have the gain due to the selection of user i decomposed into the DPC gain and the loss due to the BF

$$\frac{\det(\text{diag}\{(H_i H_i^H)^{-1}\})^{-1}}{\det(\text{diag}\{(H_{i-1}H_{i-1}^H)^{-1}\})^{-1}}$$

$$= \|P^{\perp}_{h_{k_{1:i-1}}} h_{k_i}\|^2 \prod_{j=1}^{i-1} \left(1 - \frac{|h_{k_i}^H P^{\perp}_{h_{k_{1:i-1}\setminus k_j}} h_{k_j}|^2}{\|P^{\perp}_{h_{k_{1:i-1}\setminus k_j}} h_{k_i}\|^2 \|P^{\perp}_{h_{k_{1:i-1}\setminus k_j}} h_{k_j}\|^2}\right)$$

$$= \underbrace{\|P^{\perp}_{h_{k_{1:i-1}}} h_{k_i}\|^2}_{\text{DPC gain}} \underbrace{\prod_{j=1}^{i-1} \sin^2 \phi_{ij}}_{\text{further BF loss}} \tag{A.3}$$

where ϕ_{ij} is the angle between $P^{\perp}_{h_{k_{1:i-1}\setminus k_j}} h_{k_i}$ and $P^{\perp}_{h_{k_{1:i-1}\setminus k_j}} h_{k_j}$.

A.2 GUS MIMO algorithm

We give here a detailed description of our algorithm for GUS in the MIMO BC:

Initialization:

- $G_i = []\ \forall i$, $H_{comp} = []$, $i = 2$
- $k_1 = \arg\max_k \|\text{Vmax}(H_k)H_k\|^2$
- $G_1 = \mathbf{U}_{k_1} = \text{Vmax}(H_k)H_k$
- $H_{comp}^H = [\text{Vmax}(H_{k_1})H_{k_1}]$

while $i \le N_t$: • Find the user with the largest approximated contribution to the sum rate:

- $k_i = \arg\max_k \|P^{\perp}_{h_{k_{1:i-1}}} h_k\|^4 / \|h_k\|^2$

where $h_k^H = \mathbf{U}_k H_k$ and $\mathbf{U}_k$ is iteratively approached using (3.26) and $P^{\perp}_{h_{k_{1:i-1}}}$ is the projection on the orthogonal complement of $h_{k_{1:i-1}}$.
• Update if there is an actual sum rate increase:
if $\text{SR}(H_{comp}^H) < \text{SR}([H_{comp}^H, \mathbf{U}_{k_i} H_{k_i}])$ **then**

- $H_{comp}^H = [H_{comp}^H, \mathbf{U}_{k_i} H_{k_i}]$
- $G_i = \mathbf{U}_{k_i}$
- $i = i + 1$

Receive filter reoptimization cycles:

repeat N_{cycle} times

- $j = 1$

while $j \leq i$

- $H_{reopt} = H_{comp,\backslash j}$ (H_{comp} without its jth row)
- Reoptimize the receive filter $\mathbf{U}_{k_j}$ by iterating:
  - $\mathbf{U}_{k_j}^H = V_{max}(H_{k_j} P_{h_{reopt}}^\perp H_{k_j}^H, H_{k_j} H_{k_j}^H + ||\mathbf{U}_{k_j} H_{k_j}||^2 I)$
- $H_{comp,j} = \mathbf{U}_{k_j} H_{k_j}$ (Update of H_{comp}'s jth row)
- $G_j = \mathbf{U}_{k_j}$
- $j = j + 1$

end while

end repeat

else

- break

end while

A.3 IA algorithm for IBC

We give here a detailed description of one iteration of our algorithm for IA in IBC:

for $i = 1 : G$ *(for each cell)*

    for $k = 1 : K_i$ *(for each user)*

        Computation of interference covariance matrix and the signal covariance matrix:

- $\mathbf{Q}_{i_k}^{int} = \sum_{j\neq i \text{ or } l\neq k} \mathbf{H}_{i_k j} \mathbf{V}_{j_l} \mathbf{V}_{j_l}^H \mathbf{H}_{i_k j}^H$
- $\mathbf{Q}_{i_k}^{dir} = \mathbf{H}_{i_k i} \mathbf{V}_{i_k} \mathbf{V}_{i_k}^H \mathbf{H}_{i_k i}^H$

        Iteration of the bisection method to respect the power constraint:

- $\mu = 0, p = 0$
- while(p<pmax)

            New receive filter:

  - $\mathbf{U}_{i_k}' = V_{min,d_{i_k}}(\mathbf{Q}_{i_k}^{int} + \mu_{i_k}\mathbf{I}, \mathbf{Q}_{i_k}^{dir})$
  - $\mathbf{U}_{i_k} = \sqrt{\epsilon}\mathbf{U}_{i_k}'(\mathbf{U}_{i_k}'^H \mathbf{Q}_{i_k}^{dir}\mathbf{U}_{i_k}')^{-\frac{1}{2}}$
  - power=Trace($\mathbf{U}_{i_k}^H\mathbf{U}_{i_k}$)
  - if power> 1: $\mu = \mu + 2^{-p}$
  - else: $\mu = \mu - 2^{-p}$
  - if $\mu \notin [0,1]$ break

- end while

    end for

end for

for $j = 1 : G$ *(for each cell)*

    for $l = 1 : K_j$ *(for each user)*

        Computation of interference covariance matrix and the signal covariance matrix:

- $\mathbf{R}_{j_l}^{int} = \sum_{i\neq j \text{ or } k\neq l} \mathbf{H}_{i_k j}^H \mathbf{U}_{i_k} \mathbf{U}_{i_k}^H \mathbf{H}_{i_k j}$
- $\mathbf{R}_{j_l}^{dir} = \mathbf{H}_{j_l j}^H \mathbf{U}_{j_l} \mathbf{U}_{j_l}^H \mathbf{H}_{j_l j}$

        Iteration of the bisection method to respect the power constraint:

- $\nu = 0, p = 0$
- while(p<pmax)

            New transmit subfilter:

- $\mathbf{V}'_{j_l} = V_{min,d_{j_l}}((\mathbf{R}^{int}_{j_l} + \nu_{j_l}\mathbf{I}, \mathbf{R}^{dir}_{j_l}))$
- $\mathbf{V}_{j_l} = \sqrt{\epsilon}\mathbf{V}'_{j_l}(\mathbf{V}'^{H}_{j_l}\mathbf{R}^{dir}_{j_l}\mathbf{V}'_{j_l})^{-\frac{1}{2}}$
- power=Trace$(\mathbf{V}^{H}_{j}\mathbf{V}_{j})$
- if power> 1: $\nu = \nu + 2^{-p}$
- else: $\nu = \nu - 2^{-p}$
- if $\nu \notin [0,1]$ break

• end while

end for

end for

A.4   Separation algorithm

We give here a detailed description of our separation algorithm for partially connected IBC:

Initialization:

- $\mathbf{a}_i = rand$, $\mathbf{a}_i = \mathbf{a}_i/\mathrm{norm}(\mathbf{a}_i)$ $\forall i \in [1,G]$

- $W_i = \begin{pmatrix} \mathbf{H}_i^{\mathrm{iso}} \\ \mathbf{a}_i\mathbf{H}_{ii}^{\mathrm{int}} \end{pmatrix}^{-1}$ $\forall i \in [1,G]$

while $it < itmax$:

- **for** $i = 1$ to G
  - find the new null space:
  $$n_i \in \mathrm{null} \begin{bmatrix} (\mathbf{H}_{i1}^{\mathrm{int}}W_1(1))^T \\ \cdots \\ (\mathbf{H}_{i(i-1)}^{\mathrm{int}}W_{i-1}(1))^T \\ (\mathbf{H}_{i(i+1)}^{\mathrm{int}}W_{i+1}(1))^T \\ \cdots \\ (\mathbf{H}_{iG}^{\mathrm{int}}W_G(1))^T \end{bmatrix}$$
  - partially update $\mathbf{a}_i$: $\mathbf{a}_i = \alpha\mathbf{a}_i + (1-\alpha)n_i$
  - $\mathbf{a}_i = \mathbf{a}_i/\mathrm{norm}(\mathbf{a}_i)$
  - $W_i = \begin{pmatrix} \mathbf{H}_i^{\mathrm{iso}} \\ \mathbf{a}_i\mathbf{H}_{ii}^{\mathrm{int}} \end{pmatrix}^{-1}$ $\forall i \in [1,G]$
  - $W_i(j) = W_i(j)/\mathrm{norm}(W_i(j))$ $\forall j \in \{1,2\}$
- $it = it + 1$

end while

- compute the residual interferences:
  $$int = \sum_{i=1}^{G} \sum_{j=1}^{G} \mathbf{a}_i\mathbf{H}_{ij}^{\mathrm{int}}W_j(2)(\mathbf{a}_i\mathbf{H}_{ij}^{\mathrm{int}}W_j(2))^H$$

if $int > tol$

- go back to initialization

Appendix B

Delayed CSIT

B.1 Basis Function Optimization

Although the true channel model cannot be strictly bandlimited, it is nevertheless reasonable to use a bandlimited model for the optimization of the FRoI model. Here we consider the FRoI model for a single generic channel coefficient. However, to be optimal, all (correlated) channel coefficients would have to be treated jointly.

B.1.1 Single Basis Function Case

Consider first the case $N_b = 1$. Let g_k span LT (we will denote $T = T_c$ in this section to simplify): g_k, $k = 0,1,\ldots,LT - 1$. Decompose discrete time as $k = nT + i$ where $i = k \mod T$, $n = \lfloor k/T \rfloor$. Then the FRoI or BEM channel model can be written as

$$h_k = \sum_{l=0}^{L-1} a_{n-l} g_{lT+i} \; , \;\; i = 0,1,\ldots,T - 1 \; . \tag{B.1}$$

B.1.2 Approach 1: FRoI model based Analysis

Receiver Side

Now assume that the user equipment (UE) disposes of a channel estimate

$$\widehat{h}_k = h_k + \tilde{h}_k \tag{B.2}$$

where we assume $\tilde{h}_k$ to be white noise with variance $\sigma_{\tilde{h}}^2$. (Net)DoF optimization requires to use minimal (just identifiable) data to estimate the basis expansion coefficients a_n. Hence, if we assume the BEM coefficients a_n to be estimated without delay, then they get estimated from one channel signal sample, as soon as their corresponding basis function starts. Hence a_n gets estimated from the following data model

$$
\begin{bmatrix}
\widehat{h}_{nT} \\
\widehat{h}_{nT-1} \\
\vdots \\
\widehat{h}_{(n-1)T} \\
\widehat{h}_{(n-1)T-1} \\
\vdots \\
\widehat{h}_{(n-2)T} \\
\vdots
\end{bmatrix}
=
\begin{bmatrix}
g_0 & g_T & g_{2T} & \cdots \\
0 & g_{T-1} & g_{2T-1} & \cdots \\
\vdots & \vdots & \vdots & \\
& g_0 & g_T & \cdots \\
& 0 & g_{T-1} & \cdots \\
& \vdots & \vdots & \\
& & g_0 & \cdots \\
& & & \ddots
\end{bmatrix}
\begin{bmatrix}
a_n \\
a_{n-1} \\
a_{n-2} \\
\vdots \\
\\
\\
\end{bmatrix}
+
\begin{bmatrix}
\tilde{h}_{nT} \\
\tilde{h}_{nT-1} \\
\vdots \\
\tilde{h}_{(n-1)T} \\
\tilde{h}_{(n-1)T-1} \\
\vdots \\
\tilde{h}_{(n-2)T} \\
\vdots
\end{bmatrix}
$$

$$\tag{B.3}$$

which can be rewritten compactly as

$$
\underline{\widehat{h}}_n = G \, \underline{a}_n + \underline{\tilde{h}}_n \ . \tag{B.4}
$$

The least-squares solution for $\underline{a}_n$ yields

$$
\underline{\widehat{a}}_n = (G^T G)^{-1} G^T \underline{\widehat{h}}_n \tag{B.5}
$$

and hence

$$
\hat{a}_n = \underline{f} \, \underline{\widehat{h}}_n \text{ with } \underline{f} = e_1^T (G^T G)^{-1} G^T \tag{B.6}
$$

where $e_1^T = [1 \ 0 \ 0 \cdots]$. The main characteristic of Approach 1 is that the analysis filter $\underline{f}$ is a function of the basis function (synthesis filter) g, and not of the actual channel h.

Transmitter Side

The feedback to the transmitter leads to the availability of

$$
\hat{\hat{a}}_n = \hat{a}_n + \tilde{\hat{a}}_n \tag{B.7}
$$

at the transmitter, on the basis of which the transmitter reconstructs the channel signal as

$$
\begin{bmatrix} \widehat{\widehat{h}}_{(n+1)T-1} \\ \vdots \\ \widehat{\widehat{h}}_{nT} \end{bmatrix} = \sum_{l=0}^{L-1} \begin{bmatrix} g_{(l+1)T-1} \\ \vdots \\ g_{lT} \end{bmatrix} \hat{\hat{a}}_{n-l} . \tag{B.8}
$$

At least, we shall consider this simple deterministic reconstruction for the purpose of optimizing the basis function g_k. (Alternatively the transmitter could account for the fact that the $\hat{\hat{a}}_n$ are noisy.)

Basis Function Optimization

Note that the matrix G is of the form

$$
G = \begin{bmatrix} g_0 & \underline{g}^T \\ 0 & G' \end{bmatrix} \tag{B.9}
$$

where $\underline{g}^T = [g_T \; g_{2T} \; g_{3T} \cdots]$. The optimization of the basis function g now follows by minimizing the MSE associated to (B.8) where the $\hat{\hat{a}}_n$ follow from (B.7) and (B.6). However, this leads to a quite nonlinear criterion. Now, the h_{nT} are used for the estimation of the a_n (and not for data transmission). Hence the $\underline{g}$ appears to be irrelevant for the reconstruction of h. Furthermore, having $\underline{g} \neq 0$ would seem to only deteriorate the estimation of the a_n. Hence we shall consider here a constrained optimization problem with $\underline{g} = 0$. This leads to the T-downsampled version of g_k to be a delta function. With $\underline{g} = 0$, we get

$$
\hat{a}_n = \widehat{h}_{nT} , \quad \hat{\hat{a}}_n = h_{nT} + \tilde{h}_{nT} + \tilde{\hat{a}}_n . \tag{B.10}
$$

For the design of the g_k, we consider the sum MSE over one coherence period in (B.8). This decouples to the MSE per sample

$$
h_{nT+i} - \widehat{\widehat{h}}_{nT+i} = h_{nT+i} - \sum_{l=0}^{L-1} g_{lT+i} \hat{\hat{a}}_{n-l} , \quad i = 0,1,\ldots,T-1 \tag{B.11}
$$

where we mentioned that we shall omit the consideration of $i = 0$ (or possibly even $i = 0,1,\ldots,T_{fb} - 1$ to account for feedback delay). Note that (B.11) corresponds to the prediction of h_{nT+i} on the basis of the L $\hat{\hat{a}}_{n-l}$. The MSE (for $i > 0$)

is dominated by approximation error at high SNR, hence we shall consider the noiseless case for the design of the g_k. Thus, we get the following MSE criterion

$$\text{MSE}_i = \text{E} \left| h_{nT+i} - \sum_{l=0}^{L-1} g_{lT+i} \, h_{(n-l)T} \right|^2 . \tag{B.12}$$

This leads to the following normal equations

$$R \, \underline{g}_i = \underline{r}_i \tag{B.13}$$

where we have a Toeplitz covariance matrix R

$$R = \begin{bmatrix} r_0 & r_T & \cdots & r_{(L-1)T} \\ r_T & r_0 & \ddots & \\ \vdots & \ddots & & \vdots \\ r_{(L-1)T} & r_{(L-2)T} & \cdots & r_0 \end{bmatrix} \tag{B.14}$$

and

$$\underline{r}_i = \begin{bmatrix} r_i \\ r_{i+T} \\ \vdots \\ r_{i+(L-1)T} \end{bmatrix} , \; \underline{g}_i = \begin{bmatrix} g_i \\ g_{i+T} \\ \vdots \\ g_{i+(L-1)T} \end{bmatrix} \tag{B.15}$$

with the correlation sequence $r_m = \text{E} \, h_{k+m} h_k$. For the case of an ideal low-pass Doppler spectrum, we have $r_m = \sigma_h^2 \, T \, \dfrac{\sin(\pi m / T)}{\pi m}$ (so $r_0 = \sigma_h^2$). The resulting MSE_i is

$$\text{MSE}_i = r_0 - \underline{r}_i^T R^{-1} \underline{r}_i . \tag{B.16}$$

The normalized average MSE (or inverse approximation SNR) is

$$\text{NMSE} = \frac{\sum_{i=t}^{T-1} \text{MSE}_i}{(T-t)\sigma_h^2} \tag{B.17}$$

where $t = T_{fb} \geq 1$. Another evaluation criterion is $|G(f)|^2 = |\sum_{k=0}^{LT-1} g_k e^{-j2\pi fk}|^2$ that should approximate an ideal low-pass filter. In particular the ratio of power outside and inside the frequency interval $\left[-\frac{1}{2T}, \frac{1}{2T}\right]$ can be considered.

B.1.3 Approach 2: Biorthogonal Approach with decoupled Analysis and Synthesis filters

Let $\mathbf{f} = [f_0 \, f_1 \cdots f_{M-1}]$ in $\hat{a}_n = \mathbf{f} \, \underline{\widehat{h}}_n$ be unconstrained, where now $\underline{\widehat{h}} = [\widehat{h}_{nT} \, \widehat{h}_{nT-1} \cdots]^T$ is of length M, not only to simplify the MSE cost function,

166

but to get a better approximation capability, in particular also to reduce pressure on g_0. The channel reconstruction (average) MSE criterion becomes

$$\text{MSE} = \frac{1}{T}\,\text{E}\left\|\underline{h}_n - \sum_{l=0}^{L-1} \mathbf{g}_l\,(\mathbf{f}\,\underline{\widehat{\underline{h}}}_{n-l} + \tilde{\underline{a}}_{n-l})\right\|^2 \tag{B.18}$$

which is now quadratic in $\mathbf{f}$ or $\mathbf{g}$ separately. This can be solved by alternating minimization, quite similar to joint transmitter/receiver design via MMSE.

Optimization with respect to g for a given f

We can rewrite the criterion (B.18) as

$$\text{E}\left\|\underline{h}_n - \mathbf{G}\,(\mathbf{F}\,\underline{\widehat{\underline{h}}}'_n + \tilde{\underline{a}}_n)\right\|^2 \tag{B.19}$$

where $\tilde{\underline{a}}_n = [\tilde{a}_n\ \tilde{a}_{n-1}\cdots\tilde{a}_{n-L+1}]^T$, $\underline{\widehat{\underline{h}}}'_n$ is an extended version of $\underline{\widehat{\underline{h}}}_n$ of length $J = M + L(L-1)$, $\mathbf{G} = [\mathbf{g}_0\ \mathbf{g}_1\cdots\mathbf{g}_{L-1}]$ and

$$\mathbf{F} = \mathcal{T}(\mathbf{f}) = \begin{bmatrix} \mathbf{f} & 0_{1\times L(L-1)} \\ 0_{1\times L} & \mathbf{f} & 0_{1\times L(L-2)} \\ & & \ddots \\ 0_{1\times L(L-1)} & & \mathbf{f} \end{bmatrix} \tag{B.20}$$

which is hence a banded block Toeplitz matrix (obtained by taking every L^{th} row of a banded Toeplitz matrix). With (B.19) we can rewrite (B.18) as

$$\text{MSE} = r_0 + \frac{1}{T}\text{Tr}\{\mathbf{G}(\mathbf{F}(R_{\underline{\widehat{\underline{h}}}'\underline{\widehat{\underline{h}}}'} + \sigma_{\tilde{h}}^2 I)\mathbf{F}^T + \sigma_{\tilde{a}}^2 I)\mathbf{G}^T - 2R_{\underline{h}\underline{\widehat{\underline{h}}}}\mathbf{F}^T\mathbf{G}^T\}. \tag{B.21}$$

Optimizing (B.21) leads to

$$\mathbf{G} = R_{\underline{h}\underline{\widehat{\underline{h}}}'}\mathbf{F}^T(\mathbf{F}(R_{\underline{\widehat{\underline{h}}}'\underline{\widehat{\underline{h}}}'} + \sigma_{\tilde{h}}^2 I)\mathbf{F}^T + \sigma_{\tilde{a}}^2 I)^{-1} \tag{B.22}$$

where we have $R_{\underline{\widehat{\underline{h}}}'\underline{\widehat{\underline{h}}}'} = R_J$ is a symmetric Toeplitz covariance matrix of the form (for arbitrary N_b)

$$R_{N_b} = \begin{bmatrix} r_0 & r_1 & \cdots & r_{N_b-1} \\ r_1 & r_0 & \ddots & \\ \vdots & \ddots & & \vdots \\ r_{N_b-1} & r_{N_b-2} & \cdots & r_0 \end{bmatrix} \tag{B.23}$$

167

and finally we have the Toeplitz matrix

$$
R_{\underline{h}\widehat{\underline{h}}'} = \begin{bmatrix} r_{T-1} & r_T & \cdots & r_{J+T-2} \\ \vdots & \vdots & \ddots & \vdots \\ r_1 & r_2 & \cdots & r_J \\ r_0 & r_1 & \cdots & r_{J-1} \end{bmatrix} \tag{B.24}
$$

where again $J = M + L(L-1)$.

Optimization with respect to f for a given g

Note that the feedback noise $\tilde{a}_n$ has no effect on the optimization of $\mathbf{f}$. Criterion (B.18) now becomes

$$
\mathrm{E} \sum_{k=0}^{T-1} |h_{nT+k} - \mathbf{f} \sum_{l=0}^{L-1} g_{k+lT}\widehat{\underline{h}}_{n-l}|^2 \tag{B.25}
$$

The optimal analysis filter $\mathbf{f}$ is solution to the following normal equations

$$
\mathbf{f}\,\mathbf{A} = \mathbf{b} \quad \Rightarrow \quad \mathbf{f} = \mathbf{b}\,\mathbf{A}^{-1} \tag{B.26}
$$

where

$$
\begin{aligned}
\mathbf{b} &= \sum_{k=0}^{T-1} \mathrm{E}\,h_{nT+k} \sum_{l=0}^{L-1} g_{k+lT}\widehat{\underline{h}}_{n-l}^{T} \\
&= \sum_{k=0}^{T-1} \sum_{l=0}^{L-1} g_{k+lT}\ \mathrm{E}\,h_{nT+lT+k}\,\widehat{\underline{h}}_{n}^{T} \\
&= \mathbf{g}\ \mathrm{E}\underline{h}'_n\widehat{\underline{h}}_{n}^{T} = \mathbf{g}\ \mathrm{E}\underline{h}'_n\underline{h}_{n}^{T} = \mathbf{g}\ R_{\underline{h}'\underline{h}}
\end{aligned} \tag{B.27}
$$

where $\underline{h}'_n = [h_{nT}\ h_{nT+1} \cdots h_{nT+LT-1}]^T$, we exploited the stationarity of h_k, $\mathbf{g} = [\mathbf{g}_0^T\ \mathbf{g}_1^T \cdots \mathbf{g}_{L-1}^T] = [g_0\ g_1 \cdots g_{LT-1}]$ and we have the Hankel matrix (constant along antidiagonals)

$$
R_{\underline{h}'\underline{h}} = \begin{bmatrix} r_0 & r_1 & \cdots & r_{M-1} \\ r_1 & r_2 & \cdots & r_M \\ \vdots & \vdots & \ddots & \vdots \\ r_{LT-1} & r_{LT} & \cdots & r_{M+LT-2} \end{bmatrix}. \tag{B.28}
$$

Finally

$$
\begin{aligned}
\mathbf{A} &= \sum_{k=0}^{T-1} \sum_{l=0}^{L-1} \sum_{m=0}^{L-1} g_{k+lT} g_{k+mT} \, \mathrm{E} \, \underline{\widehat{h}}_{n-l} \underline{\widehat{h}}_{n-m}^T \\
&= \sum_{l=0}^{L-1} \sum_{m=0}^{L-1} \mathbf{g}_l^T \mathbf{g}_m \, \mathrm{E} \, \underline{\widehat{h}}_{n-l} \underline{\widehat{h}}_{n-m}^T \\
&= \sum_{k=-(L-1)}^{L-1} r_{g,k} \left(R_{M,k} + \sigma_{\widetilde{h}}^2 I_{M,kT} \right) \\
&= r_{g,0} \left(R_M + \sigma_{\widetilde{h}}^2 I_M \right) \\
&\quad + \sum_{k=1}^{L-1} r_{g,k} \left(R_{M,k} + R_{M,-k} + \sigma_{\widetilde{h}}^2 (I_{M,kT} + I_{M,-kT}) \right)
\end{aligned}
\tag{B.29}
$$

where we have the $M \times M$ Toeplitz covariance matrix

$$
R_{M,k} = \begin{bmatrix}
r_{|kT|} & r_{|kT+1|} & \cdots & r_{|kT+M-1|} \\
r_{|kT-1|} & r_{|kT|} & \cdots & r_{|kT+M-2|} \\
\vdots & \vdots & \ddots & \vdots \\
r_{|kT-M+1|} & r_{|kT-M+2|} & \cdots & r_{|kT|}
\end{bmatrix},
\tag{B.30}
$$

the shifted $M \times M$ identity matrix $I_{M,n}$,

$$
[I_{M,n}]_{i,j} = \delta_{i-n,j}
\tag{B.31}
$$

where $\delta_{i,j}$ is the Kronecker delta, and

$$
r_{g,k} = \sum_{n=0}^{L-1-|k|} \mathbf{g}_{n+|k|}^T \mathbf{g}_n
\tag{B.32}
$$

which can be computed as

$$
[r_{g,0} \, r_{g,1} \cdots r_{g,L-1}] = [\mathbf{g} \, 0_{1 \times L(L-1)}] \, \mathcal{T}(\mathbf{g})^T
\tag{B.33}
$$

where the block Toeplitz function $\mathcal{T}(.)$ is defined in (B.20).

In the iterative MSE minimization, we iterate between solving for $\mathbf{g}$ from (B.22) and then for $\mathbf{f}$ from (B.26) until convergence. For initialization one can set the $\mathbf{g}$ to all ones. In the absence of noise, only the product of $\mathbf{g}$ and $\mathbf{f}$ counts (see (B.18)) and one could renormalize $g_0 = 1$ after each iteration.

Remark 1: Filter Banks

One may observe that the FRoI/BEM model introduced corresponds to modeling a signal by retaining only the first subband in a filterbank, see [99] and [106]. One can imagine a critically subsampled filterbank with T subbands, each subsampled by a factor T. Because the signal to be modeled is only expected to occupy the lowest fraction $1/T$ of the spectrum, only the first subband signal is retained. From the moment only a single subband is retained, the relation between subband bandwidth and subsampling factor becomes a little looser. In filterbank terminology, $\mathbf{f}$ is the analysis filter and $\mathbf{g}$ is the synthesis filter. Because both are different, the filterbank is biorthogonal. (Perfect reconstruction) filterbank design has been considered for reconstruction with a variable non-negative delay. Here, the delay needs to be negative though (prediction). Whereas the first approach for FRoI model optimization ($\mathbf{g}$ only) considered would correspond to orthogonal filterbanks in the noncausal case and in the absence of noise, we expect that the biorthogonal FRoI models of the second approach (involving $\mathbf{g}$ and $\mathbf{f}$) are much better suited for the prediction needed here. Furthermore, approach 2 allows to handle not only estimation error but also channel model approximation error.

Remark 2: Online Optimization

Here we considered the joint design of analysis and synthesis filters $\mathbf{f}$ and $\mathbf{g}$ in order to get an idea of the behavior of these filters and of their resulting performance. Note that because of the assumption of an (ideal) symmetric Doppler spectrum, channel correlations and optimal filters are real. In a real system, the UE could perform the joint optimization above, by assuming a certain feedback noise level $\sigma_{\tilde{a}}^2$. And the BS could optimize its synthesis filters by minimizing $\mathrm{E} \left\| \underline{h}_n - \sum_{l=0}^{L-1} \underline{g}_l \, \hat{\tilde{a}}_{n-l} \right\|^2$ or a sample average version hereof. However, the issue is that BS and UE need to use the same synthesis filter $\mathbf{g}$. One solution is to use an a priori design for $\mathbf{g}$, and then let the UE only adapt $\mathbf{f}$.

B.1.4 Multiple Basis Functions

Now consider $N_b > 1$. Compared to the $N_b = 1$ case, we can get to the $N_b > 1$ case straightforwardly by considering the "samples" h and a to represent $N_b \times 1$ consecutive samples, and the "samples" g become of size $N_b \times N_b$ in which the N_b rows represent N_b consecutive time samples and the N_b columns correspond to the coefficients of the N_b basis functions. T consecutive vector samples h_k now span in fact $N_b T$ sampling periods. We get similar normal equations in which the

correlation matrices r_m are Toeplitz, of size $N_b \times N_b$, and contain neighboring correlation values.

Note that in the case $N_b > 1$ an even higher noise sensitivity will exist due to the minimum delay estimation requirement for the a_n because the channel coefficient signal h_k will be heavily correlated over N_b consecutive samples if T is large, which will make the differentiation of the contributions of the N_b basis functions to the channel coefficient signal on the basis of only the first N_b samples ill conditioned.

In the filterbank interpretation, we are now splitting the original subband of bandwidth $1/T$ into N_b finer subbands, each subsampled by a factor N_bT.

For the case of rational $T = m/n$, a similar reasoning would lead to n basis functions (BEMs) in block length m. In case of multiple users with different T, the block length could be taken as their least common multiple and the number of BEMs would be different for different users.

B.2 STIA for MIMO BC

Because in the STIA scheme for MIMO BC, in Chapter 7, we always sent a combination of all symbols separately precoded, it can easily be extended to the MIMO IC with the following BF matrices

$$
\mathbf{V}^{(k)}[n_j] = \begin{bmatrix} \mathbf{H}^{(k,1)}[n+j] \\ \vdots \\ \mathbf{H}^{(k,k-1)}[n+j] \\ \mathbf{H}^{(k,k+1)}[n+j] \\ \vdots \\ \mathbf{H}^{(k,G)}[n+j] \end{bmatrix}^{-1} \begin{bmatrix} \mathbf{H}^{(k,1)}[n+1] \\ \vdots \\ \mathbf{H}^{(k,k-1)}[n+1] \\ \mathbf{H}^{(k,k+1)}[n+1] \\ \vdots \\ \mathbf{H}^{(k,G)}[n+1] \end{bmatrix}
$$

where $\mathbf{H}^{(i,j)}$ is the channel matrix between transmitter i and user j.

Using the same decoding strategy as in the BC yields M DoF with a feedback delay of $\frac{1}{\frac{M}{N}+1} = \frac{N}{M+N}$ of T_c.

Feedback delays longer than $\frac{N}{M+N}$ can simply be dealt with by doing time sharing between STIA and a scheme designed for completely outdated CSIT, for instance retrospective IA from [43].

With completely delayed CSIT, N DoF can be assured by TDMA transmission and for the cases with three or more users $\frac{6}{5}N$ DoF can be reached relying on delayed output feedback according to [43]. In Fig. B.1 lower bounds on the DoF
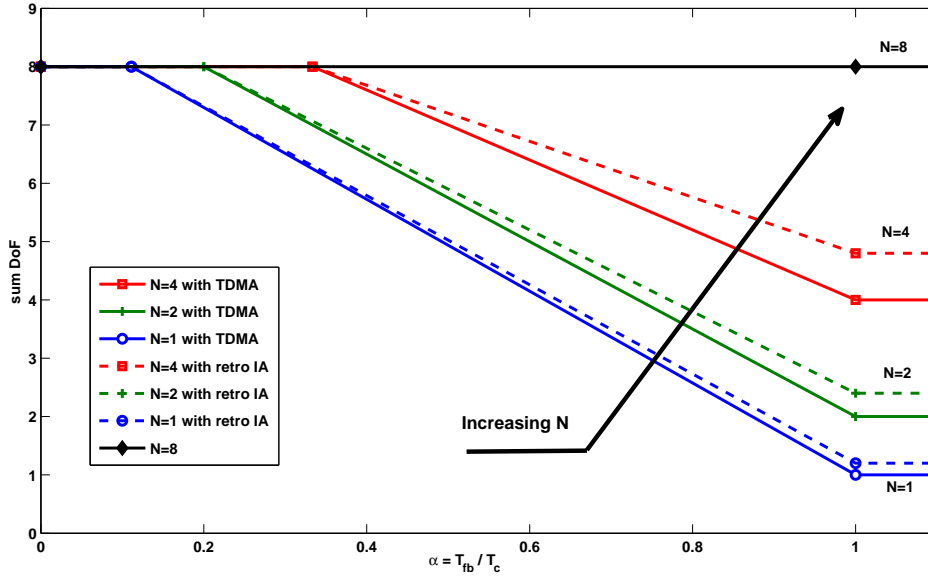
Figure B.1: Time sharing between STIA and TDMA or retrospective IA in the IC for $M = 8$.

region for $M = 8$ and different N as a function of α are given. Note that, for $\alpha \geq 1$, the scheme in [44] could be used because it yields a slightly larger DoF for large G, for example with $G = 9$, $\frac{573}{470} \approx 1.2191$ could be reached instead of the 1.2 of [43] that we used for $G \geq 3$. Again, increasing the number of receive antennas allows to preserve the full sum DoF on a wider range of α.

List of Publications

Journal Publications

- Y. Lejosne, D. Slock, and Y. Yuan-Wu, "Achieving full sum DoF in the SISO interference channel with feedback delay," *IEEE Communications Letters*, vol.18, no.7, July 2014.

- Y. Lejosne, Y. Yuan-Wu and D. Slock, "A two-level transmission strategy for certain asymmetric interfering broadcast channels and heterogeneous networks," *submitted for publication in IEEE Transactions on Vehicular Technology*.

- Y. Lejosne, Y. Yuan-Wu et D. Slock, "Interference Alignment Scheme for Fully or Partially Connected Interfering Broadcast Channels with Finite Symbol Extension," *submitted for publication in IEEE Transactions on Wireless Communications*.

Conference Publications

- Y. Lejosne, D. Slock, and Y. Yuan-Wu, "Net degrees of freedom of decomposition schemes for the MIMO IC with delayed CSIT," *in Proc. ISIT*, Honolulu, HI, USA Jun. 2014.

- Y. Lejosne, M. Bashar, D. Slock, and Y. Yuan-Wu, "From MU massive MISO to pathwise MU massive MIMO," *in Proc. SPAWC*, Toronto, Canada, Jun. 2014.

- Y. Lejosne, M. Bashar, D. Slock, and Y. Yuan-Wu, "Decoupled, rank reduced, massive and frequency-selective aspects in MIMO interfering broad-

cast channels," *in Proc. ISCCSP*, Athens, Greece, May 2014.

- Y. Lejosne, M. Bashar, D. Slock, and Y. Yuan-Wu, "MIMO interfering broadcast channels based on Local CSIT," *in Proc. EW*, Barcelona, Spain May 2014.

- Y. Lejosne, D. Slock, and Y. Yuan-Wu, "Ergodic Interference Alignment for the SIMO/MIMO Interference Channel, *in Proc. ICASSP*," Firenze, Italy, May 2014.

- M. Bashar, Y. Lejosne, D. Slock, and Y. Yuan-Wu, "MIMO Broadcast Channels with Gaussian CSIT and Application to Location based CSIT," *in Proc. ITA*, San Diego, CA, USA Feb. 2014.

- Y. Lejosne, D. Slock, and Y. Yuan-Wu, "Foresighted delayed CSIT feedback for finite rate of innovation channel models and attainable netDoFs of the MIMO interference channel," *in Proc. WD*, Valencia, Spain, Nov. 2013.

- Y. Lejosne, D. Slock, and Y. Yuan-Wu, "NetDoFs of the MISO Broadcast Channel with Delayed CSIT Feedback for Finite Rate of Innovation Channel Models," *in Proc. ISIT*, Istanbul, Turkey, Jul. 2013.

- Y. Lejosne, D. Slock, and Y. Yuan-Wu, "Space Time Interference Alignment Scheme for the MISO BC and IC with Delayed CSIT and Finite Coherence Time," *in Proc. ICASSP*, Vancouver, Canada, May 2013.

- Y. Lejosne, D. Slock, and Y. Yuan-Wu, "Net Degrees of Freedom of Recent Schemes for the MISO BC with Delayed CSIT and Finite Coherence Time," *in Proc. WCNC*, Shanghai, China, Apr. 2013.

- Y. Lejosne, D. Slock, and Y. Yuan-Wu, "Finite Rate of Innovation Channel Models and DoF of MIMO Multi-User Systems with Delayed CSIT Feedback," *in Proc. ITA*, San Diego, CA, USA, Feb. 2013.

- Y. Lejosne, D. Slock, and Y. Yuan-Wu, "Degrees of Freedom in the MISO BC with delayed-CSIT and Finite Coherence Time: Optimization of the number of users," *in Proc. NetGCooP*, Avignon, France, Nov. 2012.

- Y. Lejosne, D. Slock, and Y. Yuan-Wu, "User Selection in MIMO BC," *in Proc. EUSIPCO*, Bucharest, Romania, Aug. 2012.

- Y. Lejosne, D. Slock, and Y. Yuan-Wu, "Degrees of Freedom in the MISO BC with Delayed-CSIT and Finite Coherence Time: a Simple Optimal Scheme," *in Proc. ICSPCC*, Hong Kong, China, Aug. 2012.

- Y. Lejosne, D. Slock, and Y. Yuan-Wu, "On Greedy Stream Selection in MIMO BC," *in Proc. WCNC*, Paris, France, Apr. 2012.

Patents owned by Orange Labs

- Y. Lejosne, Y. Yuan-Wu and D. Slock, "Stratégie de transmission à deux niveaux pour certains réseaux de cellules interférées et servant chacun des utilisateurs asymétriques et pour certains réseaux hétérogènes," FR Patent FR 1 456 224, Jun. 30, 2014.

- Y. Lejosne, Y. Yuan-Wu, and D. Slock, "Procédé itératif d'évaluation de filtres numériques destinés à être utilisés dans un système de communication," FR Patent 1 462 878, Dec. 12, 2014.

Bibliography

[1] "Cisco visual networking index: Global mobile data traffic forecast update, 20132018," http://www.cisco.com/c/en/us/solutions/collateral/service-provider/visual-networking-index-vni/white_paper_c11-520862.html, Feb. 2014.

[2] G. Caire and S. Shamai, "On the achievable throughput of a multiantenna gaussian broadcast channel," *IEEE Transactions on Information Theory*, vol. 49, no. 7, pp. 1691–1706, Jul. 2003.

[3] D. Gesbert, S. Hanly, H. Huang, S. Shamai Shitz, O. Simeone, and W. Yu, "Multi-cell MIMO cooperative networks: A new look at interference," *IEEE Journal on Selected Areas in Communications*, vol. 28, no. 9, pp. 1380 – 1408, Dec. 2010.

[4] V. Cadambe and S. Jafar, "Interference alignment and degrees of freedom of the k-user interference channel," *IEEE Transactions on Information Theory*, vol. 54, no. 8, pp. 3425 –3441, Aug. 2008.

[5] M. Costa, "Writing on dirty paper (corresp.)," *Information Theory, IEEE Transactions on*, vol. 29, no. 3, pp. 439–441, May 1983.

[6] H. Wang, X. Xu, M. Zhao, W. Wu, and Y. Yao, "Robust transmission for multiuser MIMO downlink systems with imperfect csit," in *Wireless Communications and Networking Conference, 2008. WCNC 2008. IEEE*, 31 2008-April 3 2008, pp. 340–344.

[7] J. Zhang, Y. Wu, S. Zhou, and J. Wang, "Joint linear transmitter and receiver design for the downlink of multiuser MIMO systems," *Communications Letters, IEEE*, vol. 9, no. 11, pp. 991–993, Nov. 2005.

[8] M. Amara, Y. Yuan-Wu, and D. Slock, "Receiver and transmitter iterative optimization using maximum sum-rate criterion for multi-user MIMO systems," in *ISCCSP 2010. IEEE International Symposium on Communications, Control and Signal Processing*, March 2010.

[9] ——, "Optimal MU-MIMO precoder with miso decomposition approach," in *Spawc 2010. IEEE International Workshop on Signal Processing Advances for Wireless Communications*, June 2010.

[10] M. Ivrlac, R. Choi, R. Murch, and J. Nossek, "Effective use of long-term transmit channel state information in multi-user MIMO communication systems," in *Vehicular Technology Conference, 2003. VTC 2003-Fall. 2003 IEEE 58th*, vol. 1, Oct. 2003, pp. 373–377 Vol.1.

[11] M. Lee and S. K. Oh, "A per-user successive mmse precoding technique in multiuser MIMO systems," in *Vehicular Technology Conference, 2007. VTC2007-Spring. IEEE 65th*, April 2007, pp. 2374–2378.

[12] Q. Spencer, A. Swindlehurst, and M. Haardt, "Zero-forcing methods for downlink spatial multiplexing in multiuser MIMO channels," *Signal Processing, IEEE Transactions on*, vol. 52, no. 2, pp. 461–471, Feb. 2004.

[13] M. Amara, Y. Yuan-Wu, and D. Slock, "Optimized linear receivers and power allocation for two multi-user MIMO downlink schemes with linear precoding," in *ISCCSP 2010. IEEE International Symposium on Communications, Control and Signal Processing*, March 2010.

[14] M. Stojnic, H. Vikalo, and B. Hassibi, "Rate maximization in multi-antenna broadcast channels with linear preprocessing," *Wireless Communications, IEEE Transactions on*, vol. 5, no. 9, pp. 2338–2342, September 2006.

[15] L. Sun and M. Mckay, "Eigen-based transceivers for the MIMO broadcast channel with semi-orthogonal user selection," *Signal Processing, IEEE Transactions on*, vol. PP, no. 99, pp. 1 –1, 2010.

[16] B. Nazer, M. Gastpar, S. Jafar, and S. Vishwanath, "Ergodic interference alignment," *IEEE Transactions on Information Theory*, vol. 58, no. 10, pp. 6355–6371, Oct. 2012.

[17] A. Motahari, S. Oveis-Gharan, M.-A. Maddah-Ali, and A. Khandani, "Real interference alignment: Exploiting the potential of single antenna systems," *IEEE Transactions on Information Theory*, vol. 60, no. 8, pp. 4799–4810, Aug 2014.

[18] K. Gomadam, V. Cadambe, and S. Jafar, "A distributed numerical approach to interference alignment and applications to wireless interference networks," *IEEE Transactions on Information Theory*, vol. 57, no. 6, pp. 3309–3322, June 2011.

[19] D. Papailiopoulos and A. Dimakis, "Interference alignment as a rank constrained rank minimization," *IEEE Transactions on Signal Processing*, vol. 60, no. 8, pp. 4278–4288, Aug 2012.

[20] P. Mohapatra, K. E. Nissar, and C. Murthy, "Interference alignment algorithms for the k user constant MIMO interference channel," *IEEE Transactions on Signal Processing*, vol. 59, no. 11, pp. 5499–5508, Nov 2011.

[21] C. Yetis, T. Gou, S. Jafar, and A. Kayran, "On feasibility of interference alignment in mimo interference networks," *IEEE Transactions on Signal Processing*, no. 9, 2010.

[22] T. Gou and S. Jafar, "Degrees of freedom of the k user MxN MIMO interference channel," *IEEE Transactions on Information Theory*, vol. 56, no. 12, pp. 6040–6057, Dec. 2010.

[23] T. Liu and C. Yang, "Genie chain and degrees of freedom of symmetric MIMO interference broadcast channels," *[Online]*, 2013, http://arxiv.org/abs/1309.6727.

[24] ——, "On the feasibility of linear interference alignment for MIMO interference broadcast channels with constant coefficients," *IEEE Transactions on Signal Processing*, vol. 61, no. 9, pp. 2178–2191, May 2013.

[25] C. Wang, H. Sun, and S. Jafar, "Genie chains and the degrees of freedom of the k-user MIMO interference channel," in *Proc. ISIT*, Boston, MA, USA, Jun. 2012.

[26] L. Ruan and V. Lau, "Dynamic interference mitigation for generalized partially connected quasi-static mimo interference channel," *IEEE Transactions on Signal Processing*, vol. 59, no. 8, pp. 3788–3798, Aug. 2011.

[27] L. Ruan, V. Lau, and X. Rao, "Interference alignment for partially connected MIMO cellular networks," *IEEE Transactions on Signal Processing*, vol. 60, no. 7, pp. 3692–3701, July 2012.

[28] Y. Xu, Y. Tian, and C. Yang, "Interference-alignment-embedded iterative beamforming design for multi-cell MIMO broadcasting," in *Proc. ICSP*, vol. 1, Oct 2012, pp. 52–55.

[29] C. Lameiro, Ó. González, and I. Santamaría, "An interference alignment algorithm for structured channels," in *Proc. SPAWC*, Darmstadt, Germany, June 2013.

[30] A. Lapidoth, S. Shamai, and M. A. Wigger, "On the capacity of fading MIMO broadcast channels with imperfect transmitter side-information," *Arxiv preprint arxiv:0605079*, 2006.

[31] M. Maddah-Ali and D. Tse, "Completely stale transmitter channel state information is still very useful," in *Proc. Allerton*, Monticello, IL, USA, Oct. 2010.

[32] J. Xu, J. Andrews, and S. Jafar, "Miso broadcast channels with delayed finite-rate feedback: Predict or observe?" *IEEE Transactions on Wireless Communications*, vol. 11, no. 4, pp. 1456–1467, 2012.

[33] M. Kobayashi and G. Caire, "On the net DoF comparison between ZF and MAT over time-varying MISO broadcast channels," in *Proc. ISIT*, Boston, MA, USA, Jun. 2012.

[34] S. Yang, M. Kobayashi, D. Gesbert, and X. Yi, "Degrees of freedom of time correlated MISO broadcast channel with delayed CSIT," in *Proc. ISIT*, Boston, MA, USA, Jun. 2012.

[35] N. Lee and R. W. Heath Jr., "Not too delayed CSIT achieves the optimal degrees of freedom," in *Proc. Allerton*, Monticello, IL, USA, Oct. 2012.

[36] C. Suh, I.-H. Wang, and D. Tse, "Two-way interference channels," in *Proc. ISIT*, Boston, MA, USA, Jun. 2012.

[37] T. Gou and S. Jafar, "Optimal use of current and outdated channel state information: Degrees of freedom of the MISO BC with mixed CSIT," *IEEE Communications Letters*, vol. 16, no. 7, pp. 1084–1087, Jul. 2012.

[38] S. Yang, M. Kobayashi, D. Gesbert, and X. Yi, "Degrees of freedom of time correlated MISO broadcast channel with delayed CSIT," *IEEE Transactions on Information Theory*, vol. 59, no. 1, pp. 315–328, Jan. 2013.

[39] X. Yi, D. Gesbert, S. Yang, and M. Kobayashi, "On the dof of the multiple-antenna time correlated interference channel with delayed CSIT," in *Proc. Asilomar*, Pacific Grove, CA, USA, Nov. 2012.

[40] N. Lee and R. W. Heath Jr., "CSI feedback delay and degrees of freedom gain trade-off for the MISO interference channel," in *Proc. Asilomar*, Pacific Grove, CA, USA, Nov. 2012.

[41] R. Tandon, S. Jafar, S. Shamai Shitz, and H. Poor, "On the synergistic benefits of alternating CSIT for the MISO broadcast channel," *IEEE Transactions on Information Theory*, vol. 59, no. 7, pp. 4106–4128, July 2013.

[42] J. Chen, S. Yang, and P. Elia, "On the fundamental feedback-vs-performance tradeoff over the MISO-BC with imperfect and delayed CSIT," in *Proc. ISIT*, Istanbul, Turkey, Jul. 2013.

[43] H. Maleki, S. Jafar, and S. Shamai, "Retrospective interference alignment," in *Proc. ISIT*, St Petersburg, Russia, Aug. 2011.

[44] M. J. Abdoli, A. Ghasemi, and A. K. Khandani, "On the degrees of freedom of K-user SISO interference and X channels with delayed CSIT," *IEEE Trans. Inf. Theory*, vol. 59, no. 10, pp. 6542–6561, Oct. 2013.

[45] M. Kang and W. Choi, "Ergodic interference alignment with delayed feedback," *IEEE Signal Processing Letters*, vol. 20, no. 5, pp. 511–514, May 2013.

[46] C. Geng and S. Jafar, "On optimal ergodic interference alignment," in *Proc. GLOBECOM*, Anaheim, CA, USA, Dec. 2012.

[47] P. De Kerret and D. Gesbert, "Interference alignment with incomplete csit sharing," *IEEE Transactions on Wireless Communications*, vol. 13, no. 5, pp. 2563–2573, May 2014.

[48] G. Caire and S. Shamai, "On the achievable throughput of a multiantenna gaussian broadcast channel," *Information Theory, IEEE Transactions on*, vol. 49, no. 7, pp. 1691–1706, July 2003.

[49] N. Jindal, W. Rhee, S. Jafar, and Goldsmith, "Sum power iterative water-filling for multi-antenna gaussian broadcast channels," *IEEE Trans. Inform. Theory*, vol. 51, pp. 1570–1580, 2005.

[50] M. Sadek, A. Tarighat, and A. Sayed, "A leakage-based precoding scheme for downlink multi-user mimo channels," *Wireless Communications, IEEE Transactions on*, vol. 6, no. 5, pp. 1711 –1721, may. 2007.

[51] T. Yoo and A. Goldsmith, "On the optimality of multiantenna broadcast scheduling using zero-forcing beamforming," *Selected Areas in Communications, IEEE Journal on*, vol. 24, no. 3, pp. 528 – 541, mar. 2006.

[52] Z. Tu and R. Blum, "Multiuser Diversity for a Dirty Paper Approach," *IEEE Comm. Letters*, Aug. 2003.

[53] G. Dimic and N. Sidiropoulos, "On Downlink Beamforming with Greedy User Selection: Performance Analysis and a Simple New Algorithm," *IEEE Trans. Sig. Proc.*, Oct. 2005.

[54] J. Wang, D. Love, and M. Zoltowski, "User Selection with Zero-Forcig Beamforming Achieves the Asymptotically Optimal Sum Rate," *IEEE Trans. Sig. Proc.*, Aug. 2008.

[55] D. Schmidt, M. Joham, R. Hunger, and W. Utschick, "Near Maximum Sum-Rate Non-Zero-Forcing Linear Precoding with Successive User Selection," in *Asilomar Conf. Signals, Systems, Computers*, Pacific Grove, CA, USA, 2006.

[56] N. Jindal, "Antenna Combining for the MIMO Downlink Channel," *IEEE Transactions on Wireless Communications*, vol. 7, no. 10, pp. 3834 –3844, october 2008.

[57] R. Hunger and M. Joham, "An Asymptotic Analysis of the MIMO Broadcast Channel under Linear Filtering," in *Conf. Information Sciences and Systems (CISS)*, 2009.

[58] N. Jindal, "High SNR analysis of MIMO broadcast channels," in *Proc. ISIT*, sept. 2005, pp. 2310 –2314.

[59] M. Sharif and B. Hassibi, "A comparison of time-sharing, DPC, and beamforming for MIMO broadcast channels with many users," *IEEE Transactions on Communications*, vol. 55, no. 1, pp. 11 –15, jan. 2007.

[60] D. Schmidt, M. Joham, R. Hunger, and W. Utschick, "Near maximum sum-rate non-zero-forcing linear precoding with successive user selection," in *Proc. Asilomar*, 29 2006-nov. 1 2006, pp. 2092 –2096.

[61] C. Guthy, W. Utschick, and G. Dietl, "Low-Complexity Linear Zero-Forcing for the MIMO Broadcast Channel," *IEEE Trans. Sel. Topics Sig. Proc.*, Dec. 2009.

[62] C. Guthy, W. Utschick, R. Hunger, and M. Joham, "Efficient Weighted Sum Rate Maximization with Linear Precoding," *IEEE Trans. Sig. Proc.*, Apr. 2010.

[63] S. Christensen, R. Agarwal, E. Carvalho, and J. Cioffi, "Weighted sum-rate maximization using weighted MMSE for MIMO-BC beamforming design," *IEEE Trans. on Wireless Communications*, vol. 7, no. 12, pp. 4792–4799, December 2008.

[64] O. Johnson, M. Aldridge, and R. Piechocki, "Delay-rate tradeoff in ergodic interference alignment," in *Proc. ISIT*, Boston, MA, USA, Jun. 2012.

[65] S.-W. Jeon and S.-Y. Chung, "Capacity of a class of linear binary field multisource relay networks," *IEEE Trans. Information Theory*, Oct. 2013.

[66] R. Bassily and S. Ulukus, "Ergodic secret alignment for the fading multiple access wiretap channel," in *Proc. ICC*, May 2010.

[67] J. Koo, W. Wu, and J. Gill, "Delay-rate tradeoff for ergodic interference alignment in the gaussian case," in *Proc. Allerton*, Sep. 2010.

[68] M. Razaviyayn, G. Lyubeznik, and Z. Luo, "On the degrees of freedom achievable through interference alignment in a MIMO interference channel," *IEEE Transactions on Signal Processing*, vol. 60, no. 2, pp. 812–821, Feb. 2012.

[69] G. Bresler, D. Cartwright, and D. Tse, "Settling the feasibility of interference alignment for the MIMO interference channel: the symmetric square case," *Arxiv preprint*, 2011.

[70] L. Ruan, V. Lau, and M. Win, "The feasibility conditions for interference alignment in mimo networks," *IEEE Transactions on Signal Processing*, 2013.

[71] O. González, I. Santamaría, and C. Beltran, "A general test to check the feasibility of linear interference alignment," in *Proc ISIT*, July 2012.

[72] S. Peters and R. Heath, "Interference alignment via alternating minimization," in *Proc. ICASSP*, Tapei, Taiwan, April 2009.

[73] F. Negro, S. Shenoy, I. Ghauri, and D. T. M. Slock, "On the MIMO interference channel," in *Proc ITA*, San Diego, CA, USA, Jan 2010.

[74] N. Jindal, S. Vishwanath, and A. Goldsmith, "On the duality of gaussian multiple-access and broadcast channels," *IEEE Transactions on Information Theory*, vol. 50, no. 5, pp. 768–783, May 2004.

[75] C. Suh and D. Tse, "Interference alignment for cellular networks," in *Proc. Allerton*, Monticello, IL, USA, Sept. 2008.

[76] W. Shin, W. Noh, K. Jang, and H.-H. Choi, "Hierarchical interference alignment for downlink heterogeneous networks," *IEEE Transactions on Wireless Communications*, vol. 11, no. 12, pp. 4549–4559, December 2012.

[77] G. Foschini, K. Karakayali, and R. Valenzuela, "Coordinating multiple antenna cellular networks to achieve enormous spectral efficiency," *IEE Proceedings-Communications*, vol. 153, no. 4, pp. 548–555, August 2006.

[78] J. Zhang, R. Chen, J. Andrews, A. Ghosh, and R. Heath, "Networked mimo with clustered linear precoding," *IEEE Transactions on Wireless Communications*, vol. 8, no. 4, pp. 1910–1921, April 2009.

[79] M. Hong, R. Sun, H. Baligh, and Z.-Q. Luo, "Joint base station clustering and beamformer design for partial coordinated transmission in heterogeneous networks," *IEEE Journal on Selected Areas in Communications*, vol. 31, no. 2, pp. 226–240, February 2013.

[80] M. Sanjabi, M. Razaviyayn, and Z.-Q. Luo, "Optimal joint base station assignment and beamforming for heterogeneous networks," *IEEE Transactions on Signal Processing*, vol. 62, no. 8, pp. 1950–1961, April 2014.

[81] M. Guillaud and D. Gesbert, "Interference alignment in partially connected interfering multiple-access and broadcast channels," in *Proc. GLOBECOM*, Houston, TX, USA,, Dec. 2011.

[82] M. Westreicher and M. Guillaud, "Interference alignment over partially connected interference networks: Application to the cellular case," in *Proc. WCNC*, Paris, France, April 2012.

[83] V. Ntranos, M. Maddah-Ali, and G. Caire, "Cellular interference alignment," in *Proc. ISIT*, Honolulu, HI, USA, Jun. 2014.

[84] V. Chandrasekhar, J. Andrews, and A. Gatherer, "Femtocell networks: a survey," *IEEE Communications Magazine*, vol. 46, no. 9, pp. 59–67, Sept. 2008.

[85] S. W. Choi, S. Jafar, and S.-Y. Chung, "On the beamforming design for efficient interference alignment," *IEEE Communications Letters*, vol. 13, no. 11, pp. 847–849, Nov. 2009.

[86] M. Maddah-Ali and D. Tse, "Completely stale transmitter channel state information is still very useful," *IEEE Transactions on Information Theory*, vol. 58, no. 7, pp. 4418–4431, Jul.

[87] C. Vaze and M. Varanasi, "The degrees of freedom region and interference alignment for the mimo interference channel with delayed csit," *Trans. Info Theory*, july 2012.

[88] R. Etkin and D. Tse, "Degrees of Freedom in Some Underspread MIMO Fading Channels," *IEEE Trans. Inf. Theory*, Apr. 2006.

[89] L. Zheng and D. Tse, "Communication over the Grassmann Manifold: a Geometric Approach to the Noncoherent Multiple-Antenna Channel," *IEEE Trans. Inf. Theory*, Feb. 2002.

[90] A. Kannu and P. Schniter, "On the Spectral Efficiency of Noncoherent Doubly Selective Block-Fading Channels," *IEEE Trans. Inf. Theory*, Jun. 2010.

[91] P. Vaidyanathan, "On Predicting a Band-limited Signal Based on Past Values," *Proceedings of the IEEE*, Aug. 1987.

[92] A. Papoulis, *Signal Analysis*. McGraw-Hill, 1977.

[93] N. Jindal and A. Lozano, "A Unified Treatment of Optimum Pilot Overhead in Multipath Fading Channels," *IEEE Trans. Communications*, Oct. 2010.

[94] J. Chen and P. Elia, "Can Imperfect Delayed CSIT be as Useful as Perfect Delayed CSIT? DoF Analysis and Constructions for the BC," in *IEEE Allerton Conf. Comm's Control and Comput.*, Monticello, IL, USA, Sept. 2012.

[95] M. Vetterli, P. Marziliano, and T. Blu, "Sampling signals with Finite Rate of Innovation," *IEEE Trans. Signal Processing*, Jun. 2002.

[96] Y. Grenier, "Modeling of Nonstationary Signals," 1984, phD, Orsay, France.

[97] M. Tsatsanis and G. Giannakis, "Modeling and Equalization of Rapidly Fading Channels," *Int. J. Adaptive Control and Signal Proc.*, 1996.

[98] J. Uriguen, Y. Eldar, P. Dragotti, and Z. Ben-Haim, "Sampling at the Rate of Innovation: Theory and Applications," in *Compressed Sensing: Theory and Applications*, Y. Eldar and G. Kutyniok, Eds. Cambridge University Press, 2012.

[99] M. Vetterli, J. Kovačević, and V. Goyal, *Foundations of Signal Processing*. http://fourierandwavelets.org/, 2013.

[100] E. Aguerri, D. Gunduz, A. Goldsmith, and Y. Eldar, "Distortion-Rate Function for Undersampled Gaussian Processes," in *IEEE Int'l Symp. on Iformation Theory (ISIT)*, Istanbul, Turkey, Jul. 2013, submitted, also ITA2013 talk.

[101] E. Silva, M. Derpich, and J. Østergaard, "Rate-Distortion in Closed-Loop LTI Systems," in *IEEE Iformation Theory Workshop (ITA)*, San Diego, CA, USA, Feb. 2013.

[102] U. Salim and D. T. M. Slock, "How much feedback is required for TDD multi-antenna broadcast channels with user selection ?" *EURASIP Journal on Advances in Signal Processing*, May 2010.

[103] N. Jindal, "Mimo broadcast channels with finite-rate feedback," *IEEE Transactions on Information Theory*, vol. 52, no. 11, pp. 5045 –5060, nov. 2006.

[104] F. Negro, D. Slock, and I. Ghauri, "On the noisy MIMO interference channel with CSI through analog feedback," in *Proc. ISCCSP*, Rome, Italy, May 2012.

[105] C. Vaze and M. Varanasi, "The degrees of freedom region and interference alignment for the MIMO interference channel with delayed CSIT," *IEEE Transactions on Information Theory*, vol. 58, no. 7, pp. 4396 –4417, Jul 2012.

[106] J. Kovačević, V. Goyal, and M. Vetterli, *Fourier and Wavelet Signal Processing*. http://fourierandwavelets.org/, 2013.